Lithium-Lead/Water Interactions: Experiments and Analysis

J.P. Herzog

March 1989

UWFDM-791

FUSION TECHNOLOGY INSTITUTE

UNIVERSITY OF WISCONSIN

MADISON WISCONSIN

Lithium-Lead/Water Interactions: Experiments and Analysis

J.P. Herzog

Fusion Technology Institute
University of Wisconsin
1500 Engineering Drive
Madison, WI 53706

http://fti.neep.wisc.edu

March 1989

UWFDM-791

LITHIUM-LEAD/WATER INTERACTIONS: EXPERIMENTS AND ANALYSIS

James Paul Herzog

Fusion Technology Institute
Nuclear Engineering and Engineering Physics Department
University of Wisconsin-Madison
1500 Johnson Drive
Madison, WI 53706

March 1989

UWFDM-791

Table of Contents

List of Figures

List of Tables

Acknowledgements

We acknowledge the financial support of the Department of Energy and EG&G Idaho. The technical discussions with Dr. S. Piet and Mr. L. Cadwallader were quite helpful.

Nomenclature

A	- Interaction area
a_{H_2}	- Hydrogen stoichiometric coefficient
a_{H_2O}	- Water stoichiometric coefficient
a_{Li}	- Lithium stoichiometric coefficient
C_{gas}	- Molar concentration of gas in gas layer
C_i	- Molar concentration of species i
$C_{Li\ max}$	- Molar concentration of lithium in pure lithium-lead
c_{pi}	- Specific heat of species i
C_δ	- Gas layer boundary condition
D_{gas}	- Gas layer diffusion coefficient
$D_{Li\ Pb}$	- Diffusion coefficient of liquid lithium in a lead solution
$D_{l\ m}$	- Liquid metal layer diffusion coefficient
$D_{Pb\ Pb}$	- Lead self-diffusion coefficient
dP/dt	- Measured leakage rate
$D_{T\ C}$	- Thermocouple diameter
D_0	- Diffusion coefficient proportionality constant
g	- Gravitational constant
H	- Enthalpy
h	- Heat transfer coefficient
h_{film}	- Film boiling heat transfer coefficient
H_{conv}	- Heat lost by particle due to convection

H_{fi} - Heat of formation of species i

H_{rad} - Heat lost by particle due to radiation

H_{reac} - Heat gained by particle due to the chemical reaction

i_{fg} - Latent heat of vaporization

J_i - Molar flowrate of species i

k - Reaction rate coefficient

k_g - Gas layer thermal conductivity

$k_{l\,m}$ - Liquid metal layer thermal conductivity

$k_{T\,C}$ - Thermocouple thermal conductivity

k_0 - Reaction rate coefficient proportionality constant

$L_{T\,C}$ - Thermocouple length

m - Lithium concentration reaction exponent

$m_{Li_{17}Pb_{83}}$ - Mass of metal sample in grams

M_i - Molecular weight of species i

M_z - Mass of zirconium consumed by reaction

n - Water concentration reaction exponent

N_{Ar} - Total moles of argon

$N_{Ar\ sol}$ - Moles of argon in solution

N_{H_2O} - Moles of liquid water

$N_{H_2\ leak}$ - Total moles of hydrogen to have leaked from system

$N_{H_2\ sol}$ - Moles of hydrogen in solution

$N_{H_2\ tot}$ - Total moles of hydrogen generated by the reaction

Nu - Nusselt number

P - Measured system pressure

P_{Ar} - Argon partial pressure

P_{dn} - Lower gas layer pressure

P_{i} - Initial system pressure

Pr - Prandtl number

P_{vap} - Water vapor pressure

P_{H_2} - Hydrogen partial pressure

q''_{cond} - Conduction heat flux

q''_{reac} - Reaction heat flux

R - Universal gas constant

Ra - Rayleigh number

R_{H_2O} - Rate at which water is consumed by the reaction

$R_{H_2\ exp}$ - Initial experimental hydrogen generation rate

r_{ii} - Distance of minimum in atomic interaction potential curve

R_{Li} - Rate at which lithium is consumed by the reaction

s - Liquid metal layer depth

t - Time

T - Temperature

T_{dn} - Lower gas layer temperature

T_{film} - Gas layer film temperature

T_{gas} - Upper gas layer temperature

T_{ref} - Reference temperature

T_{s} - Surface temperature

T_{sat} - Water saturation temperature

$T_{T\ C}$ - Thermocouple temperature

T_{UP} - Upper plate temperature

T - Lower portion of the apparatus wall temperature

v - Velocity

V - Volume

V_{dn} - Lower gas layer volume

V_{gas} - Total gas volume

V_{up} - Upper gas layer volume

X_{Ar} - Solubility of argon in water

X_{H_2} - Solubility of hydrogen in water

z - Distance from bottom of liquid metal well

δ - Gas layer thickness

ΔE - Activation energy

ΔE_d - Diffusion coefficient activation energy

ΔE_k - Reaction rate coefficient activation energy

ΔP - Difference between measured and calculated pressures from lead tests

ΔP_{lead} - Time averaged difference between measured and calculated pressures from corresponding lead test

Δt - Calculation timestep

ΔT_{min} - Difference between liquid metal surface and water saturation temperatures

ΔT_{sub} - Difference between water saturation and water bulk temperatures

$\Delta \rho$ - Difference between saturated vapor and liquid densities

ϵ	- Emissivity of water
ϵ_{ii}	- Energy of minimum in atomic interaction potential curve
λ	- Taylor instability wavelength
μ_g	- Gas viscosity
ρ	- Density
σ	- Surface tension
σ_i	- Uncertainty in the value of quantity i
σ_{SB}	- Stefan-Boltzmann constant
τ	- Time constant

I. Introduction

It is generally assumed that the first power reactors will use deuterium and tritium as their principal fuels, and that the tritium will have to be bred by capturing neutrons from the fusion reaction in a blanket containing lithium in some form.[1] Along with its breeding capabilities, the blanket represents the primary fusion energy heat sink and heat transfer medium. Lithium breeder-blanket materials being considered in conceptual designs of fusion power reactors include liquid lithium metal, lithium-lead alloy $Li_{17}Pb_{83}$ lithium-lead compound (Li_7Pb_2), lithium oxide (Li_2O), and the ternary ceramics ($LiAlO_2$, Li_2ZrO_3, Li_2SiO_3, Li_4SiO_4, and $LiTiO_3$). The breeder-blanket coolants being considered include liquid lithium, helium, pressurized and boiling water, and flibe (lithium and beryllium fluoride molten salt).[2]

A recent study examines the comparative strengths and weaknesses of the lithium breeder-blanket materials based on the following criteria:[2]

1. adequate tritium breeding capability
2. ability for sufficient tritium recovery
3. acceptable material properties
4. demonstrated safety compatibility with associated materials.

A series of breeder-material compatibility experiments were performed by the authors to help identify the breeder that presents the least

safety risk. Using data collected from their experiments and other sources, the authors assembled their conclusions in a table which is reproduced here as Table 1.[2]

Most breeders either have a high lithium atom density, or require a neutron multiplier to insure adequate breeding.[3] Among the breeder materials being considered, lithium and lead based compounds and eutectics have received considerable attention. This is because the lithium and lead based materials, which at operating temperatures of conceptual fusion reactors can take the form of a solid (Li_7Pb_2), a liquid ($Li_{17}Pb_{83}$), or even a two-phase mixture ($Li_{62}Pb_{38}$), have the unique capability of being both a low lithium atom density breeding material and a neutron multiplier at the same time.[3] From many standpoints the most attractive of these breeder-blanket materials is $Li_{17}Pb_{83}$ (hereon designated as "lithium-lead"). At operating temperatures of many proposed fusion reactor blankets, lithium-lead is highly fluid and thermally conductive, has high cross sections for fast and thermal neutrons, is inert to radiation, and provides an adequate breeding ratio.[1] Although the eutectic reacts relatively mildly with water, the reaction does produce hydrogen. Thus engineered safeguards would be required for a lithium-lead blanket with a water coolant. The ultimate goal of current fusion designs is to incorporate not only 'active' safeguards but more importantly passive design concepts that promote inherent safety.

GENERAL CONCLUSIONS OF TEST RESULTS

PROMISING FUSION REACTOR BLANKET OR BLANKET-COOLANT MATERIALS	BREEDING RATIO	TRITIUM EXTRACTION	SAFETY RELATED CHEMICAL REACTIONS				
			WITH COOLANT			WITH SURROUNDING MATERIALS	
			HELIUM	WATER	ORGANIC	AIR	CONCRETE
Li_2O	GOOD	APPEARS ACCEPTABLE	NO * INTER-ACTION	MILD REACTION	NA	NO INTER-ACTION	TBD
$Li_{17}Pb_{83}$	ADEQUATE	APPEARS ACCEPTABLE	"	MILD REACTION	TBD	MILD REACTION	MILD REACTION
Li_7Pb_2	GOOD	APPEARS ACCEPTABLE	"	MAJOR REACTION CONCERNS	NA	TBD	TBD
Li_4SiO_4	REQUIRES ** MULTIPLIER/ REFLECTOR	APPEARS ACCEPTABLE	"	NO INTER-ACTION	"	NO INTER-ACTION	NO INTER-ACTION
$LiAlO_2$	"	APPEARS ACCEPTABLE	"	"	"	"	"
Li_2SiO_3	"	APPEARS ACCEPTABLE	"	"	"	"	"
Li_2ZrO_3	"	APPEARS ACCEPTABLE	"	"	"	"	"
$LiTiO_3$	"	APPEARS ACCEPTABLE	"	"	"	"	"
Li	GOOD	APPEARS ACCEPTABLE	"	MAJOR REACTION CONCERNS	"	MAJOR REACTION CONCERNS	MAJOR REACTION CONCERNS

* HELIUM HAS MAJOR LEAKAGE PROBLEM, AVAILABILITY CONCERN AND HIGH TEMPERATURE MATERIALS PROBLEM

** COMPATIBILITY STUDIES OF MULTIPLIERS WITH COOLANTS AND SURROUNDING MATERIALS WOULD BE NEEDED

Table 1. Breeder Material Comparison Table[2]

Much of the work described in this report was done in conjunction with the Mirror Advanced Reactor Study (MARS) and follow-up studies (e.g., MINIMARS) conceptual fusion reactor design.[4] The MARS conceptual fusion reactor design utilizes the lithium lead alloy $Li_{17}Pb_{83}$ as a liquid metal breeder and primary coolant. Lithium-lead was chosen as the breeder-coolant for the MARS design for the same reasons enunciated above; e.g., high tritium breeding ratio, good neutron multiplication, acceptable corrosion rates, and relatively benign chemical reaction rates with water and air. The main reason for choosing lithium-lead over lithium, which has similar properties, is the more benign chemical reaction potential of lithium-lead with reactor materials.

For various accident sequences one can identify four possible "contact modes" between the molten metal breeder and the water. These contact modes are important because they broadly determine how the molten metal and water will hydrodynamically mix, and the energy and mass transfer rates between the materials. The first contact mode would occur after a tube rupture in a liquid metal steam generator or in a pressurized blanket module. One could identify this contact mode as "coolant injection" due to the high pressure injection of the steam/water into the low pressure liquid metal (Figure 1). This contact mode is characterized by rapid mixing, due to the initially enormous pressure difference between the two species. Also, due to the fact that the steam is injected into what is

Figure 1. Coolant Injection Contact Mode

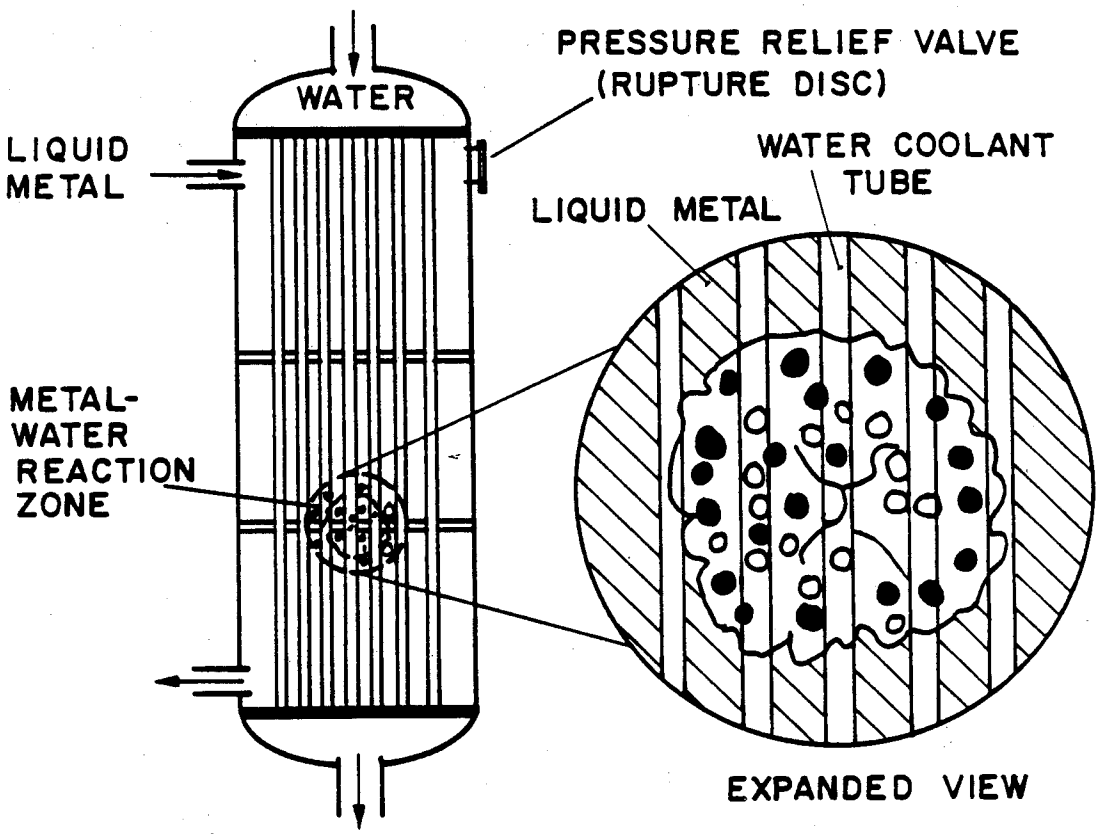

- HIGH PRESSURE TWO-PHASE BLOWDOWN
- LIQUID METAL ENTRAINED IN EXPANDING MIXING ZONE

effectively a pool of liquid metal, the steam is the limiting reagent. The second contact mode can be depicted by pouring of the liquid metal from a ruptured blanket component into a pool of water, also present due to the accident. This contact mode is identified as a "pouring contact mode". The pouring contact mode is a subset of a larger generic class of heat transfer phenomena in which one hot liquid, "melt", interacts with a more volatile cold liquid, "coolant", producing vapor and perhaps oxidizing the melt. Historically, this more general contact mode, referred to as the "Melt-Coolant" contact mode, has been considered to be of special importance to fission reactor safety. This contact mode may occur, in a fusion reactor, after a severe accident in which molten metal is poured from a ruptured component into a stagnant pool of water in the containment (Figure 2). This contact mode would be characterized by less rapid mixing than the coolant injection contact mode, because the two species are initially at the same pressure. In this case, because the liquid metal pours into a large pool of water, the liquid metal is the limiting reagent. The third contact mode would occur after the rupture of water and breeder-blanket tubes in the vacuum vessel (i.e. torus or central cell), resulting in a spray of these reactants into a common volume (Figure 3). This contact mode is of special concern in a fusion reactor because the major radioactive inventory resides within the vacuum vessel. One may consider this contact mode to be a subset of the previous two, because it is due to the simultaneous

Figure 2. Liquid Metal Pouring Contact Mode

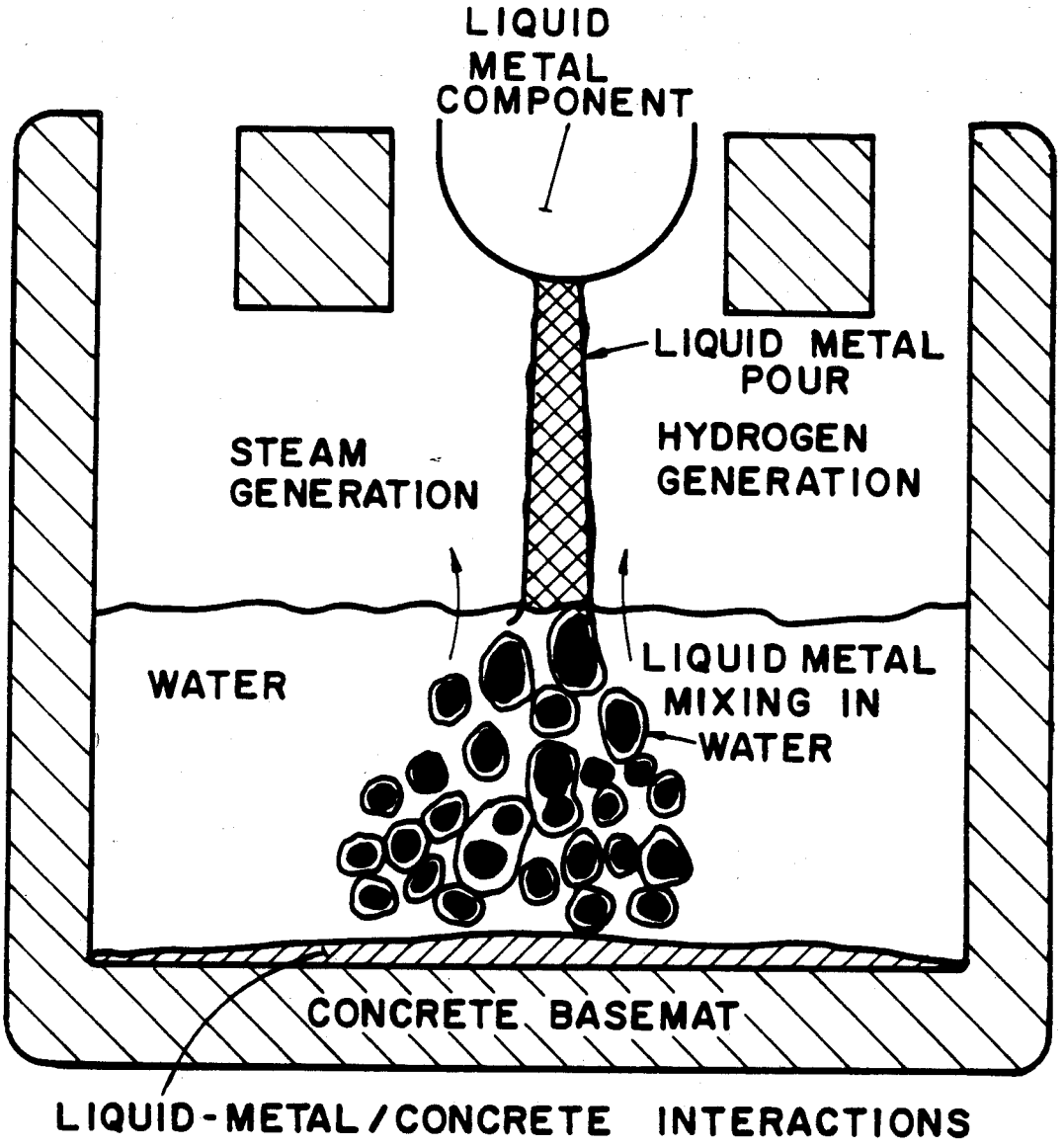

Figure 3. Breeder and Water Tube Rupture Contact Mode

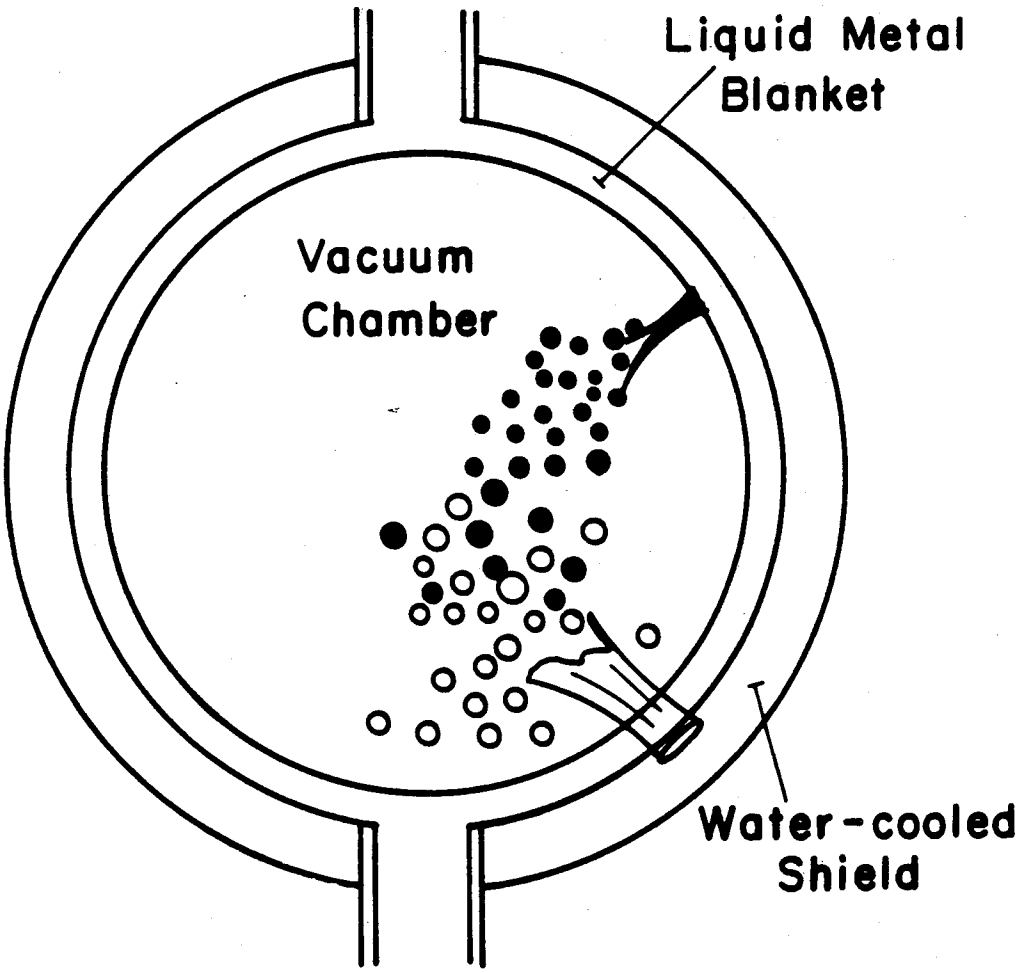

injection of the liquid metal breeder and water into a common volume. The fourth contact mode would occur if the liquid-metal and the water came into contact as stratified layers of materials with different densities (e.g. lithium pouring on water, water pouring on lithium-lead). One can expect this to be the most benign of the possible contact modes because even though the two materials are liquid, density stratification would initially limit their surface area for mixing.

As described elsewhere,[5,6] models, based on the specific accident scenario of a pressure tube rupture, have been developed. These models, parametric in nature, use a dynamic calculation to predict the consequences of a steam tube rupture. The models contain a very primitive approach to the dynamics of the lithium-lead/water reaction. They are based on the assumption that, the amount of water that flows from the broken steam tube, during each timestep of the calculation, comes in contact with unreacted lithium-lead and reacts. Although a portion of the water may not react depending upon a set parameter, the remainder of the water reacts instantaneously. Thus the lithium-lead/water reaction rate, as modeled, does not depend upon any real reaction rate but upon the rate of flow of water from the broken steam tube and a fictitious parameter. By ignoring the effects of the lithium-lead/water reaction rate and the local hydrodynamic mixing of the reactants; and concentrating instead only on the large scale interaction of high pressure steam injection from

the broken steam tube and shell side pressure relief through the steam generator pressure relief valve; these models present a worst case scenario of a steam generator accident.

This report is only indirectly concerned with the large scale accident scenarios described above. The main purpose of this report is to determine the chemical kinetics of the lithium-lead/water interaction by conducting a series of small scale experiments and to develop the theoretical groundwork to analyze the results of the experiments. Because the experiments consist of the pouring of water onto the exposed surface of a small lithium-lead pool, they are most directly related to the stratified layer contact mode. Although the other contact modes do not exhibit large scale stratified layers, they are all driven by the interaction of locally separated species. Since the experiments are small scale (e.g., the contact area is small), the results should provide the reaction rate per unit area, and can therefore be used in conjunction with large scale lithium-lead/water interaction models, provided a suitable model describing the dynamic mixing (and thus the time dependent total contact area) of the species exists.

II. Previous Investigations

For convenience, the discussion of relevant previous investigations is divided into three parts; (1) early (1960's) solid lithium/water and zirconium/water reaction experiments, (2) recent small scale liquid lithium and lithium-lead/water reaction experiments, and (3) recent large scale liquid lithium and lithium-lead/steam reaction experiments.

II.1 Early Lithium/water and Zirconium/water Experiments

Lithium and water react to form Li_2O, H_2, and LiOH by two reaction paths:[7]

$$2\ Li + H_2O \rightarrow Li_2O + H_2 + 5.6*10^5\ J/Mole\ Li \quad (1)$$

$$Li + H_2O \rightarrow LiO\,H + 1/2\ H_2 + 2.0*10^5\ J/Mole\ Li \quad (2)$$

While lithium-lead and water react by two similar reaction paths,

$$Li_{17}Pb_{83} + 0.085\ H_2O \rightarrow 0.085\ Li_2O + 0.085\ H_2 + 0.83\ Pb \quad (3)$$

$$Li_{17}Pb_{83} + 0.17\ H_2O \rightarrow 0.17\ LiO\,H + 0.085\ H_2 + 0.83\ Pb, \quad (4)$$

the extent to which Li and H_2O (or $Li_{17}Pb_{83}$ and H_2O) react by the first or second reaction path will depend upon the temperature and pressure of the system, and the relative mass of Li to H_2O (or

$Li_{17}Pb_{83}$ to H_2O). Given complete mixing and ample time, the system will reach an equilibrium. The equilibrium composition will depend only upon the initial state of the system (e.g., the initial pressure, temperature, and reactant masses).[8] But in real systems, the lithium/water (or lithium-lead/water) interaction will not be an equilibrium one. In real systems, the extent of the hydrodynamic mixing of the system components will influence the dynamic composition of the system. Thus the dynamic reaction rate will depend upon the local temperature, pressure, and composition.

For solid lithium metal and liquid water or water vapor interactions, one might expect a relatively benign reaction to take place, as long as the metal does not change phase. This has been confirmed experimentally. In reaction with liquid water (250 cm^3) at room temperature under an argon atmosphere, a 0.95 cm diameter sphere of solid lithium retained its spherical shape when immersed in the water.[7] The maximum bulk temperature of the lithium sphere reached only 98 C. The reason for this phenomenon is that the water acted as a heat sink for the heat generated by the reaction. In another experiment, a 0.95 cm sphere of lithium metal was immersed in a pool of water, of the same volume, but at 0 C. In this case, diminished activity and a maximum lithium temperature of only 40 C was reported. This proved the effectiveness of the surrounding water as a heat sink. It should be noted that the water was an effective heat sink because its volume (250 cm^3) was much

greater than the volume of the solid lithium (0.45 cm^3). For large pieces of solid lithium in restricted volumes of water one would expect the reaction to be vigorous because of the absence of an effective heat sink. But the relative insolubility of the product (LiOH) may impede the reaction.[7] This hypothesis is supported by the results of a solid lithium steam experiment. When a solid lithium sphere was suspended in a stream of flowing steam, a white coating consisting of LiOH, LiOH * H_2O and Li_2O was formed that temporarily inhibited the reaction. But within five minutes, the coating of reaction products began to crack and the reaction became quite vigorous.[7] This occurred because, although the coating lost its protective nature, it still functioned as a thermal insulator. Therefore the metal retained much of the heat from the reaction, which in turn increased the rate of reaction.

The formation of a protective reaction product coating was also observed in a second series of solid lithium metal and water vapor experiments.[9,10] Water vapor present in an argon atmosphere with partial pressures up to 100 mm Hg, reacted with solid lithium, with initial temperatures ranging from 20 C to 75 C. In the later series of tests conducted by Irving and Lund, three reaction stages were identified. In the first stage, a lithium hydroxide film, which grew at a constant rate, formed on the surface of the metal. In an intermediate stage, lithium hydroxide monohydrate began to enclose the outer surface of the hydroxide film and soon covered the outer

surface. In the third stage, the lithium hydroxide monohydrate film expanded in size, at a constant rate approximately 1.5 times greater than the rate observed in the initial stage, until the entire metal was converted into LiOH * H_2O.[10] The conversion of the lithium hydroxide film to lithium hydroxide monohydrate was accompanied with pronounced swelling of the outer surface of the metal sample. The pronounced swelling lead to the formation of cracks, at least in the outer layers of the film. In the third stage of the reaction, the reaction products were assumed to cover the metal surface with the distribution shown in **Figure** 4.[10] Irving and Lund suggested the following mechanism for the course of the reaction in the third stage. The water vapor diffuses through the porous lithium hydroxide monohydrate layer relatively easily, reaching the lithium hydroxide layer underneath. The rate of the reaction is controlled by the rate of diffusion of reactants across the lithium hydroxide layer. The thickness of the lithium hydroxide layer remains constant during this phase because the rate of lithium hydroxide formation is balanced by the rate of formation of lithium hydroxide monohydrate. In all three stages the reaction was diffusion controlled, dependent upon the diffusion of the reacting species across the developing hydroxide film.

For liquid lithium/water interactions, it has been suggested that the reaction rate can be extrapolated from analogous solid lithium/water reaction experiments.[11] The argument is made that if the rate of the reaction is determined by diffusion of reactants

Figure 4. Assumed Distribution of Reaction Products[10]

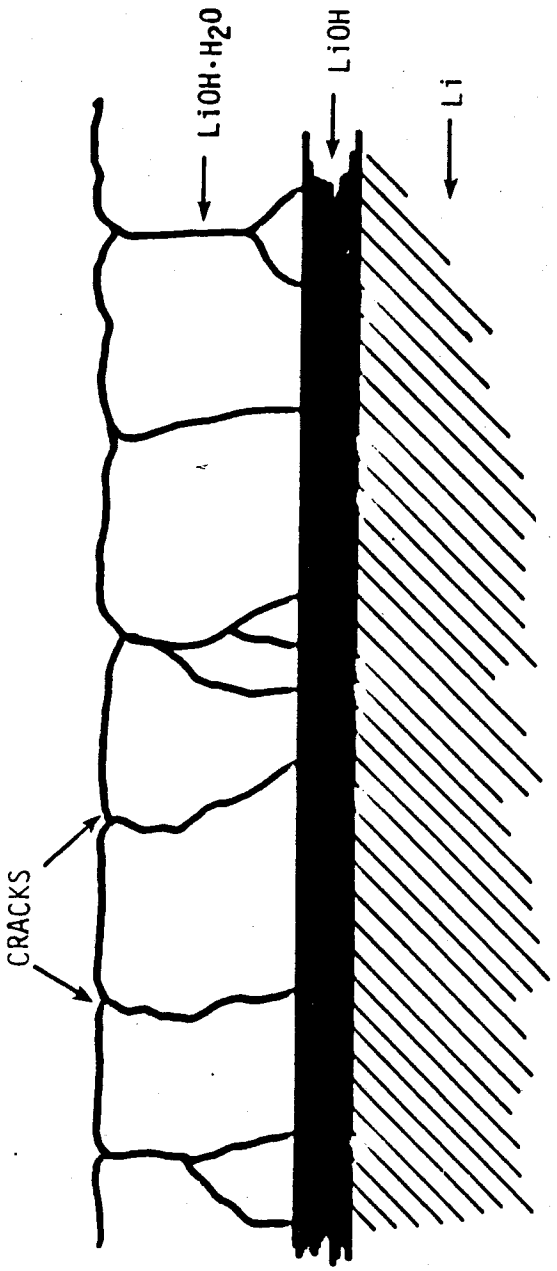

through a surface film, the nature of the substrate under this film, whether it is solid or liquid, is of minor importance.

Since there has been a lack of detailed investigations of liquid lithium/water or liquid lithium-lead/water interactions, one needs to turn to the detailed investigations of other liquid metal/water systems. In the area of fission reactor safety, a concentrated effort has been put forth to fully understand the mechanisms involved in the zirconium/water interaction. This work was prompted by the possibility that a molten metal mass, containing zirconium, could be injected into a stagnant pool of liquid water, following a severe reactor accident. Relevant to this analysis is the work of Baker and Just.[12] During the 1960's, they conducted an experimental and theoretical study of the zirconium/water reaction, that exceeds in detail and breadth any analysis of the lithium/water or lithium-lead/water reaction at this time. The experiments were initiated by passing a large current through a zirconium wire, either 0.76 mm or 1.52 mm in diameter, which was immersed in degassed water. The current caused the wire to fragment, creating a range of sizes of zirconium particles, the temperature of which could be determined from the energy deposited by the current. Two series of tests were conducted, one with the pool of water at room temperature and atmospheric pressure, and the other with the pool of water at 315 C and 10.3 MPa. The hydrogen generated by the reaction was collected and the quantity determined. From this and

the specimen weight, the percent of metal reacted in each run could be determined.

The results of the experiments are compiled in Figures 5 and 6, which contain the data from the room temperature water runs and the heated water runs, respectively[12]. Both figures show that for significantly high initial metal temperatures, an explosive pressure rise resulted. This phenomena may also be construed as a particle size phenomena, since nonexplosive runs had mean particle diameters in excess of 650 microns, whereas all but one explosive run had mean particle diameter below 500 microns.[12]

As shown in Figure 6, the runs in heated water showed markedly greater reaction. This is explained in terms of a 2 step reaction scheme in which the reaction rate is initially controlled by the rate of gas diffusion of water vapor toward the hot metal particles and of hydrogen, generated by the reaction, away from the particles.[12] The heated water runs showed a greater extent of reaction because the vapor pressure of the water, which drives diffusion, is roughly twice as great as the water vapor pressure of the room temperature runs. The explosive runs were found to be due to the stripping of the gas layer from the zirconium particles. The initial high temperature of the explosive runs caused the initial hydrogen generation rate to be relatively large. The rapidly evolving hydrogen propelled the particles through the water at high speed. The high speed particle motion, detected on motion picture film, in

Figure 5. Zirconium/water Reaction Results for Room Temperature Water[12]

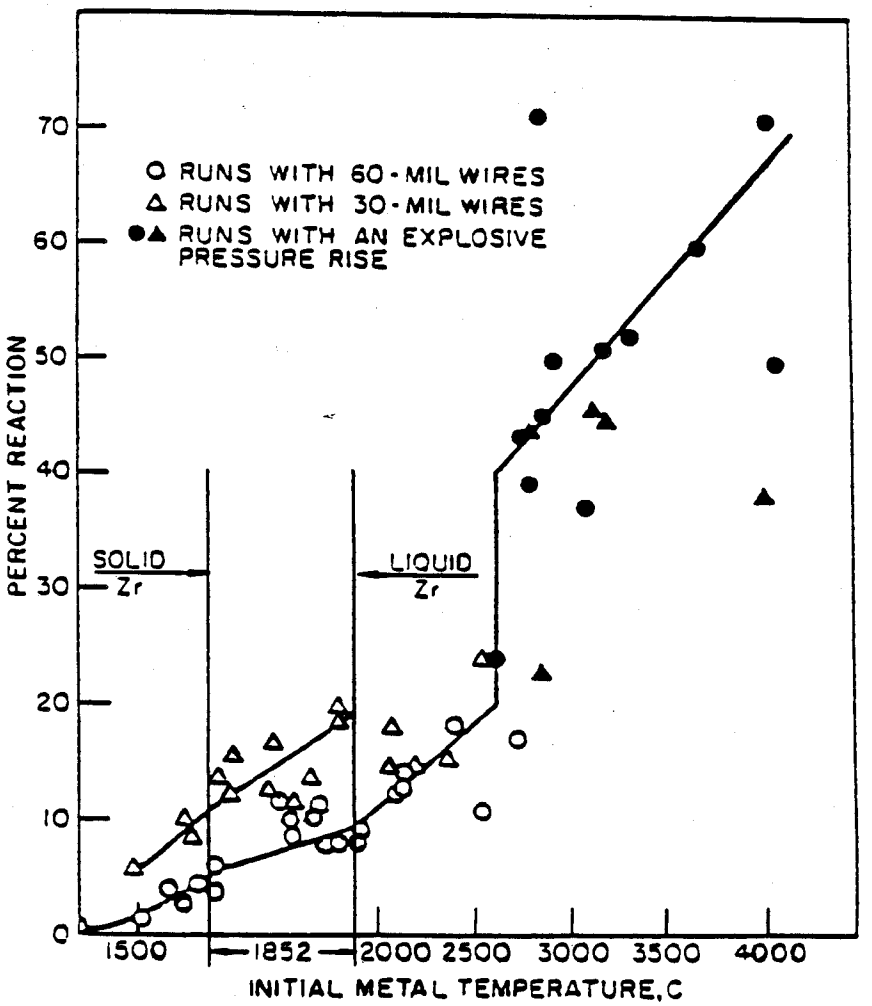

Figure 6. Zirconium/water Reaction Results for Heated Water[12]

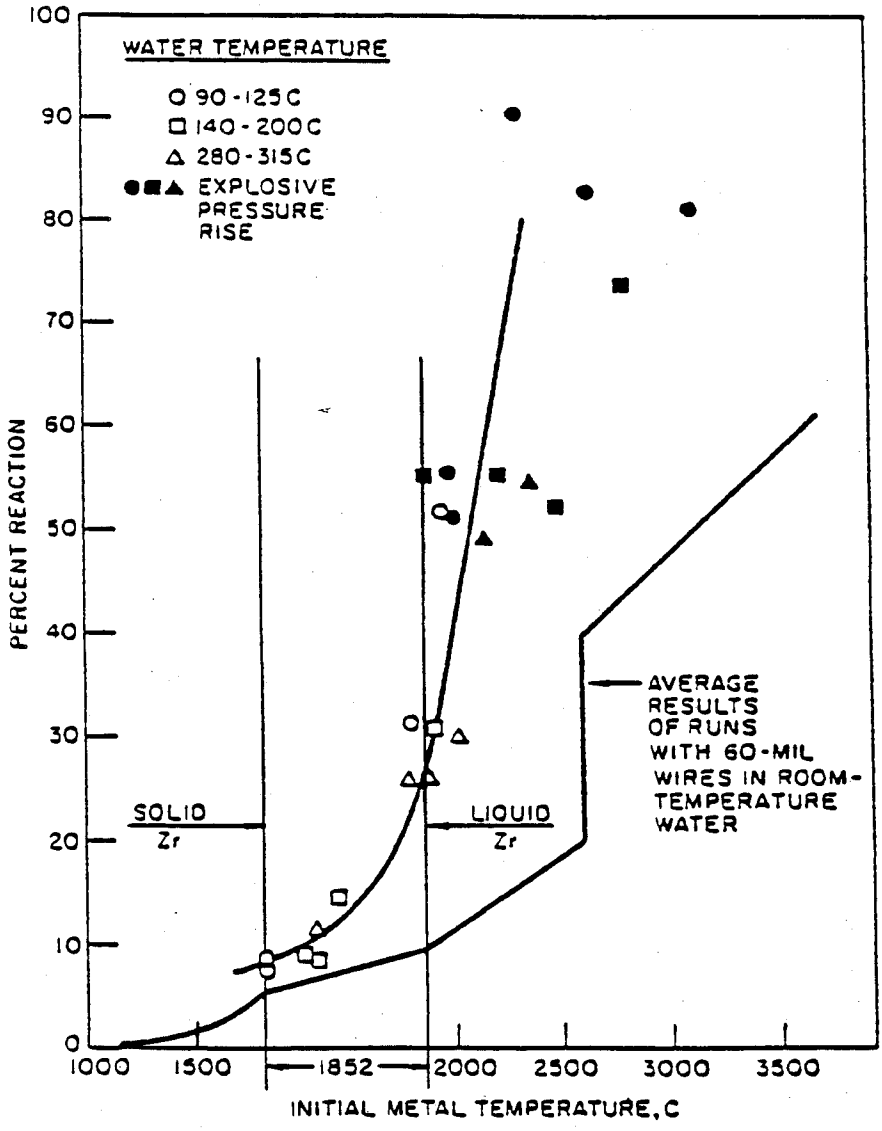

turn had the effect of removing the gas diffusion barrier, resulting in very rapid reaction. Thus the explosive runs resulted when the gas diffusion layer did not have a chance to form.

Later during the reaction sequence, the diffusion of reactants across a growing oxide film becomes the dominate rate determining process. For reaction rates controlled by solid state diffusion (i.e., the diffusion of either zirconium ions or oxide ions through the crystal lattice of the oxide film) the mass of zirconium reacted, as a function of time, can be expressed as:[12]

$$M_z^2 = k A^2 t \exp\left(-\frac{\Delta E}{R T_s}\right) \qquad (5)$$

The two unknowns in this equation, the proportionality constant k and the activation energy ΔE, were determined by matching the results of a computer model with the data. The model was based on a two stage reaction rate. At each timestep during the computation, the mass transfer resistance of the gas layer and of the oxide layer was determined. The greater of these two mass transfer resistances was then used to determine the reaction rate. Mathematically, the reaction was modeled as a single drop interaction. The zirconium drop was assumed to be spherical, and its radius was assumed to be fixed at a given initial value. At each timestep, the temperature of the drop was determined by an energy balance. After the mass of zirconium reacted was determined from the two step reaction rate model, the amount of heat generated by the reaction was calculated.

The particle could lose energy by two processes; convection and radiation. These heat generation and loss terms were balanced by the rate of change of internal energy of the particle. Therefore the energy balance could then be expressed as:[12]

$$\rho_z \, c_{pz} \, V \frac{dT}{dt} = H_{reac} - H_{conv} - H_{rad} \qquad (6)$$

The computer model results compared favorably with experimental data for $k = 3.33 * 10^3$ kg^2 / m^4 - s, and $\Delta E = 1.91 * 10^5$ J / mole.[12]

The computational model predicted that the extent of reaction depends upon the particle diameter and the water temperature, which compares favorably with experimental results. The model was not able to predict the explosive pressure rise of high initial temperature runs. This should not be surprising though, since the explosive runs resulted whenever the gas diffusion layer did not have a chance to form, a phenomenon not included in the model.

The two step reaction rate model accurately predicts the reaction rate of solid or liquid zirconium with water, as long as the initial conditions are such that an explosive pressure rise will not occur. The effect of a high melting point reaction product, such as the effect of the lithium oxide or lithium hydroxide products during the lithium/water experiments, was also present in the zirconium/water system. Computationally, as the zirconium oxide layer became the dominant mass transfer resistance, the

zirconium/water reaction was quickly quenched. As was suggested for the lithium/water interaction, the high melting point zirconium oxide shell was an effective container for molten zirconium, thus there was no sharp change in the character of the reaction rate corresponding to the melting point of the metal.[12] Although this may lead one to conclude that molten metal/water and solid metal/water interactions would be much the same, for similar initial conditions, this is not always the case. For metal/water systems with the same initial conditions except temperature, the molten metal system will have a greater reaction rate than the solid metal/water system. This temperature effect was first observed by Arrhenius, who showed that the temperature dependence of the reaction rate can be expressed as:[13]

$$\text{Reaction rate} = \text{constant} * \exp\left(-\frac{\Delta E}{R\,T}\right) \qquad (7)$$

The main cause of dissimilarity between molten metal/water and solid metal/water reactions is due to the possibility that molten metal and water can mix much more completely than solid metal and water. For solid metal/water interactions, unless the two species are brought together with great force, the area of contact (the solid surface area) will be constant throughout the course of the interaction. But for molten metal/water interactions the mixing process can cause the area of contact to increase with time. Eventually the solid oxide layer will bring this process to a halt, but for interactions with the

same initial conditions, including the same surface area, the final contact area of the molten metal/water interaction will be greater than, or at least equal to, the final contact area of the solid metal/water interaction. For the zirconium/water interaction, this means that the mass of hydrogen generated will be greater for the molten zirconium/water interaction than for the solid zirconium/water interaction, since the mass of hydrogen generated is directly proportional to the area of contact (equation 5).

II.2 Recent Small Scale Experiments

Included in the series of breeder-material compatibility experiments performed to generate Table 1 were several small scale liquid lithium/water and lithium-lead/water experiments. Two series of tests were performed in a 20 l capacity reaction chamber filled with argon at 1 atm.[2] In the first series of tests, a small amount of breeder at 600 C was dropped into 4000 gm of water at 98 C. For liquid lithium dropped into water a large chemical heat release was reported and a release of $7.2 * 10^{-2}$ moles of H_2 / gm Li was measured. This compares with a mild chemical heat release and a release of $3.7 * 10^{-2}$ moles H_2 / gm Li for liquid lithium-lead dropped in water. In the second series of tests, a small amount of water at 98 C was poured onto a larger amount of breeder at 600 C. For water poured onto excess lithium, a peak temperature increase of 300 C and a release of 0.16 mole H_2 / mole H_2O was measured. For

water poured onto excess lithium-lead, a peak temperature increase of 52 C and a release of 0.22 mole H_2 / mole H_2O was measured.[2] If one assumes that the extent of mixing of the liquid metal and water was comparable for both series of tests, then one can conclude that liquid lithium/water interactions release more heat than liquid lithium-lead/water interactions. Also one can conclude that significantly more hydrogen is generated for liquid lithium/ excess water interactions than for liquid lithium-lead/ excess water interactions, and that the hydrogen generation rate will be roughly equivalent for excess liquid lithium/water interactions and excess liquid lithium-lead/water interactions.

In another series of small scale experiments, Finn, et. al. performed lithium-lead alloy drop tests.[14] These experiments consisted of dropping small amount of breeder into excess amounts of water, under an air atmosphere. When molten lithium-lead at 500 C was dropped into room temperature water, the reaction was relatively modest producing only a very slow evolution of hydrogen bubbles. No pressurization was noted. Other tests performed included liquid lithium at 500 C dropped or injected into 95 C water. In the lithium drop test, the lithium initially floated on the surface reacting vigorously. After 1.8 sec, the hydrogen ignited and combustion occurred, producing a measured pressurization of 0.27 MPa. When lithium was injected below the surface of water, a pressure event of over 2 MPa occurred 513 msec after initial contact. In all of these

tests, the interaction had both an ignition source, the molten metal, and oxygen available to produce a hydrogen combustion event. However, hydrogen combustion only occurred in the lithium/water interactions.

In a European research program, based at the European Communities Joint Research Center, Ispra Italy, a series of small scale liquid lithium-lead alloy/water tests have been performed. One portion of the test program consisted of liquid metal drop experiments. In a preliminary test, a 100 gm sample of liquid lithium-lead was poured into excess water, but there appeared to be no difference between this test and a test in which pure lead was poured into water.[15] In two other tests, very similar in nature to the lithium-lead experiment conducted by Finn and his associates, a stream of lithium-lead was poured into a large beaker, open to air, and partially filled with water.[16] In the first test, the temperature of the lithium-lead stream was 350 C, and the water temperature was 20 C. The second test consisted of pouring a 500 C stream of lithium-lead into 90 C water. In these experiments, the lithium-lead and water interacted in an indiscernible manner. In both experiments, bubbles formed as the stream of liquid metal flowed to the bottom of the container. These bubbles consisted mostly of steam and entrained air. Any hydrogen formed in this phase of the interaction did not reach a sufficient concentration for it to be ignited above the water surface with a fine burner flame. At a later

stage, the lithium-lead lying on the bottom of the beaker, became coated with a thin bubble film which later became detached as larger bubbles. These bubbles could be ignited with a flame. Repeating the first of these two tests, but in a closed vessel, the rise in pressure measured after 12 hours, was interpreted to mean that only 16% of the lithium in the alloy had reacted during this period.[16]

Another of the small scale experiments performed by the European team consisted of spraying about 500 gm of lithium-lead over a large water surface.[16] A flame directed over the water surface during the spraying period indicated that, again, no spontaneous generation of hydrogen had occurred. But a few minutes after the alloy was sprayed into the water pool, hydrogen bubbles appeared at the surface. Chemical tests of the spray remains indicated that roughly 65% of lithium contained in the alloy had reacted during the experiment.

The quantity of hydrogen produced by the lithium-lead/water interaction is dependent upon the area of contact. The spray tests show that even when the area of contact is made exceptionally large, the liquid lithium-lead/liquid water interaction did not produce either a large spontaneous generation of hydrogen or a complete reaction of the lithium content of the alloy. A study of hydrogen ignition was not a part of this work.

In another of the experiments conducted by the European group, 500 gm of lithium-lead were reacted, in an autoclave, with a

stoichiometric amount of water necessary to react with the Li contained in the eutectic.[17] After 100 hours, all of the lithium had reacted. The product of the reaction consisted of a mixture of elemental Pb, LiOH, and LiOH * H_2O. Since the autoclave was held at 400 C during the duration of the experiment, the lithium-lead was molten throughout the test. Complete oxidation of the lithium in lithium-lead eutectic is possible, but apparently only under certain conditions.

As was observed in the zirconium/water experiments, a possible consequence of liquid metal/water interactions is the formation of an explosive pressure pulse. Recognizing this, the European team has carried out a series of small scale experiments, which were designed to produce explosive liquid metal/water interactions.[18] The experiments consisted of loading the lower portion of a shock tube with either liquid lead or liquid lithium-lead alloys, and then accelerating a water column onto the liquid metal surface. The high pressure that forced the water column into the initially evacuated upper portion of the shock tube, ranged from 0.1 to 2.5 MPa, and the subcooling of the water column was varied. The variable system pressure influenced the ambient conditions and the kinetic energy of the water column. By measuring the pressure generation and the gas formation as a function of time, the mechanical work could be calculated. These experiments are continuing with an expanded test matrix to include lithium.

The essential factor that determined the violence of the interaction was found to be the extent to which the liquid metal and water mixed.[18] Experiments show that for melt/water systems, mixing occurs in two steps; mixing of the liquid metal and water due to the kinetic energy imparted to the species as they are brought in contact with one another, and fine fragmentation caused by self or external pressure triggers. Especially in the second stage, fragmentation and mixing have to occur quickly so that freezing does not impede the process.[18] The energy for fragmentation and mixing was obtained from the variable kinetic energy of the water. In the lithium-lead/water experiments, noncondensible gas production by the chemical reaction (hydrogen) cushioned the impact, diminishing the effect of fragmentation and mixing. Only violent boiling, no explosions, were observed in the lithium-lead/water experiments. The lead/water experiments, on the other hand, did produce violent explosions. For the lithium-lead/water tests, the long term hydrogen production was found to be dependent upon the extent of the short term fragmentation and mixing, as well as the independent variables.

These experiments show that the chemical reaction attenuates high pressure peaks during the early portion of a lithium-lead/water interaction. Although the possibility of a violent explosion is diminished by the chemical reaction, the long term pressurization of the system due to the hydrogen generation and the possibility of hydrogen combustion are still major safety concerns.

Recently, the European group has begun a series of experiments which are designed to facilitate the measurement of the average rate of reaction of various breeder materials with steam.[19] The reaction was initiated by passing steam through a heated test chamber containing the breeder samples. Tests have been performed with three different breeder materials: liquid $Li_{17}Pb_{83}$, with initial temperatures from 310 C to 450 C; solid and liquid Li_7Pb_2, with initial temperatures from 550 C to 850 C; and liquid Li, with initial temperatures from 700 C to 900 C. After the steam passed over the exposed surface of a breeder sample, the resulting steam and hydrogen mixture was passed through a condenser, which separated the unreacted H_2O from the gas mixture. The free hydrogen was then collected. By measuring the amount of hydrogen collected, the average rate of reaction could be inferred. The results of these experiments are summarized in Figure 7.[19] As expected, this figure shows that the rate of reaction of steam with Li is greater than the rate of reaction of steam with Li_7Pb_2, and that the rate of reaction of steam with $Li_{17}Pb_{83}$ is the least of the three breeder/steam reactions. The figure also shows that the rates of reaction of the three breeder/steam reactions are not strong functions of the initial breeder temperatures.

The wide range of small scale lithium lead alloy/water experiments, performed here and in Europe, lead one to the following conclusions. The extent of the hydrogen generation is a weak

Figure 7. Rates of Reaction for $Li_{17}Pb_{83}$/steam, Li_7Pb_2/steam and Li/steam[19]

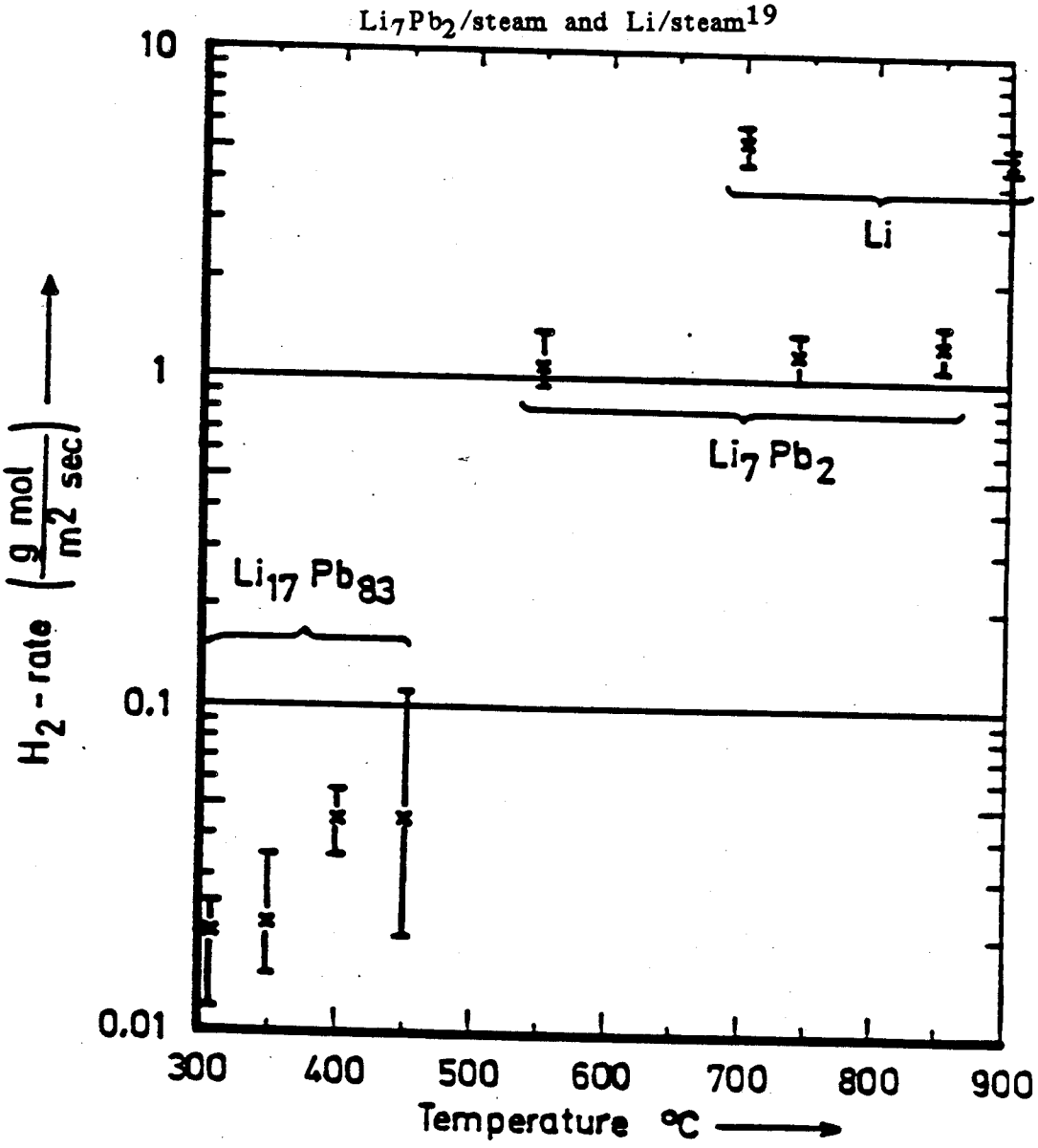

H_2-reaction rate constant as a function of Temperature for Li, Li_7Pb_2, $Li_{17}Pb_{83}$ with H_2O

function of temperature and a strong function of the contact area. The contact area is dependent upon the force with which the water and metal are brought in contact. The chemical reaction inhibits the formation of a explosive pressure rise. And in all possible contact modes, the lithium-lead/water interaction is less severe than the lithium/water interaction.

II.3 Recent Large Scale Experiments

Recently, a series of large scale lithium-lead and lithium/material compatibility experiments have been performed at the Hanford Engineering Development Laboratory (HEDL) in Richland, Washington.[20] The experimental program consisted of three liquid metal/material groups; liquid metal/atmosphere (air, nitrogen, and carbon dioxide atmospheres), liquid metal/steam, and liquid metal/concrete. The experimental conditions were chosen to reflect the conditions of postulated accident scenarios. Accident scenarios considered include rupture of breeder material lines or modules allowing breeder material spillage to containment cells, and rupture of coolant lines to allow coolant breeder material contact.[20]

The lithium-lead/steam reaction test consisted of injecting 335 C superheated steam at about 7 gm/sec into a 200 kg pool of 500 C lithium-lead for 325 seconds. A schematic of the experimental apparatus used in the test is given in Figure 8.[20] The open reaction chamber was placed in a containment vessel containing an argon

Figure 8. Large Scale Lithium-lead/steam Reaction Test Chamber[20]

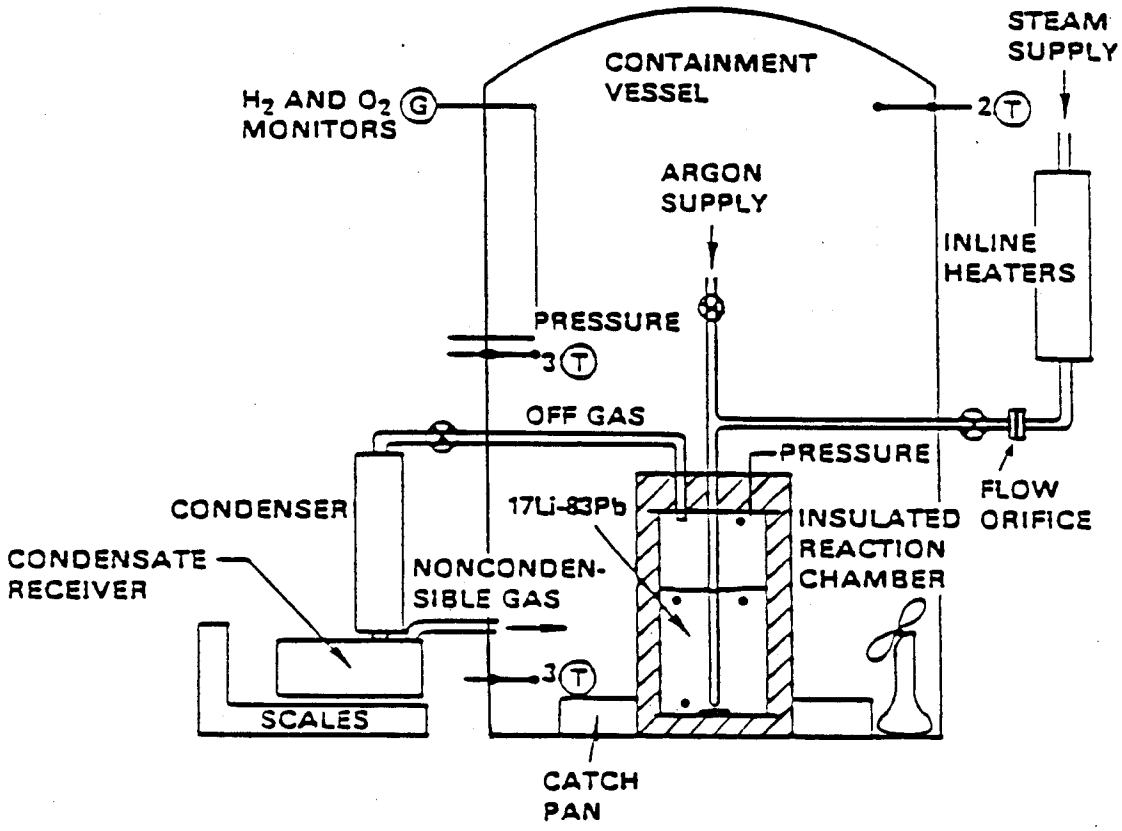

atmosphere. The reaction chamber was covered with three inches of insulation to minimize heat loss. The reaction chamber was vented by a line that passed through a condenser. The condenser was attached to the vent line to condense any exiting steam, allowing the hydrogen to pass on through to the containment vessel atmosphere. The hydrogen release was measured by a hydrogen monitor. The lithium-lead pool temperature response was measured by five thermocouples placed at throughout the alloy pool. After the test, the reaction chamber contents were chemically analyzed to determine the extent of the reaction.

The lithium-lead pool reached a maximum temperature of 870 C, 240 seconds after the steam injection began. The pool temperature remained near the maximum temperature for the remainder of the experiment. The thermocouple temperature response is shown in Figure 9.[20] Roughly all of the steam injected into the lithium-lead reacted. This conclusion was supported by the fact that only very little steam condensate was collected in the condensers during the experiment. Most of the hydrogen release occurred during the first 240 seconds of the experiment. The increased chemical activity during the first 240 seconds of the experiment was due to a two step chemical reaction sequence.[20] During the first 240 seconds of the experiment, 93 moles of H_2O entered the reaction chamber. Since the lithium-lead pool contained 195 moles of Li, the steam depleted almost the entire lithium content of the pool, during this period, by

Figure 9. Lithium-lead Alloy Pool Temperatures[20]

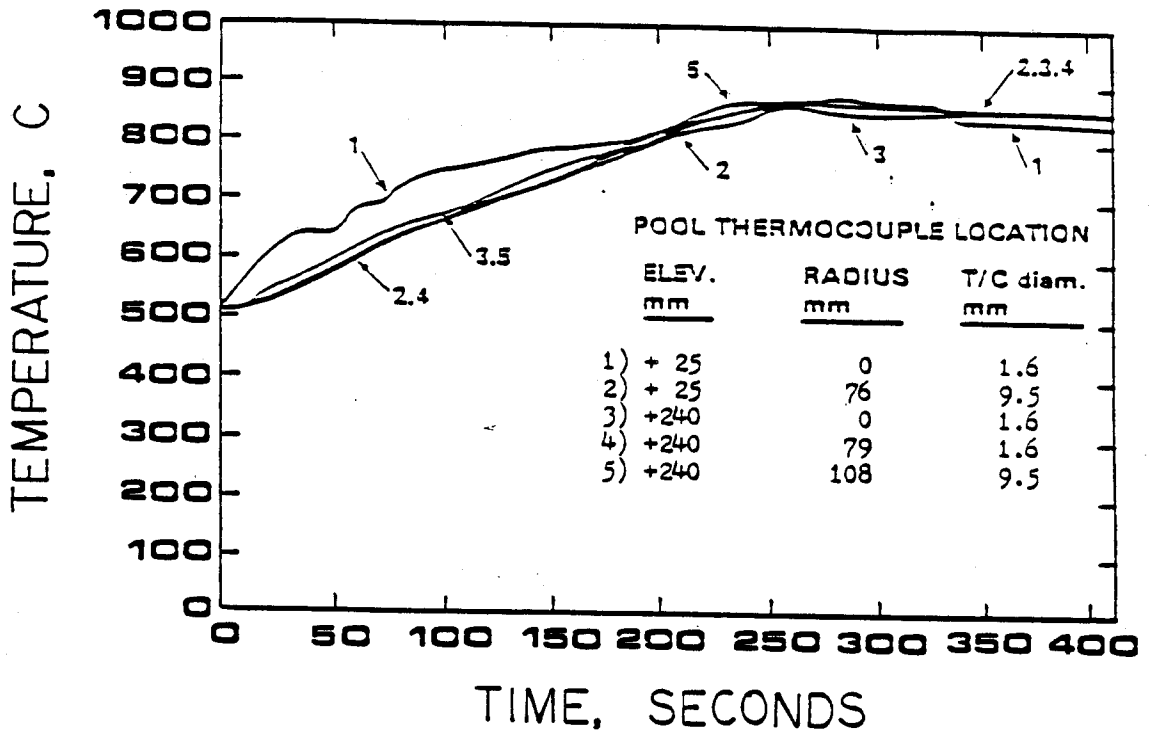

this reaction:

$$2\ Li + H_2O \rightarrow Li_2O + H_2 + 3.6*10^5\ J/Mole\ Li \qquad (8)$$

As lithium was depleted from the alloy, steam began to react with Li_2O to form LiOH, by a less energetic reaction:

$$Li_2O + H_2O \rightarrow 2\ LiOH + 6.9*10^4\ J/Mole\ Li_2O \qquad (9)$$

The heat of reaction of equation 8 is evaluated at 685 C, which is the average system temperature during the first 240 seconds of the experiment. The heat of reaction of equation 9 is evaluated at 850 C.

When lithium is still in abundance in the pool, the reason that lithium and water react to form Li_2O (by equation 8) instead of LiOH by:

$$Li + H_2O \rightarrow LiOH + 1/2\ H_2 + 2.0*10^5\ J/Mole\ Li \qquad (10)$$

is because water is the limiting reactant.[21] As water enters a system that contains an abundance of lithium, it reacts to form Li_2O instead of LiOH, since it takes only 1/2 mole of H_2O reacting with 1 mole of Li to form Li_2O and it takes 1 mole of H_2O reacting with 1 mole of Li to form LiOH. In a lithium-rich environment, any LiOH formed at these temperatures should react with excess lithium as follows:

$$LiOH + Li \rightarrow Li_2O + 1/2\ H_2 \qquad (11)$$

As lithium becomes depleted form the alloy pool, the rate of formation of LiOH will become greater than the rate of LiOH depletion and the H_2O, Li_2O reaction (equation 9) will become the dominant chemical reaction. All of this assumes that the mixing is complete enough that the reacting species are evenly mixed throughout the system. If lithium is the limiting reactant, then just the opposite occurs. The Li will react to form LiOH instead of Li_2O.

The Li_2O and LiOH reaction products accumulated on the top of the surface of the depleted alloy.[20] Chemical analysis of the reaction products showed that only 0.37% of the lithium content of the pool remained unreacted at the end of the experiment. Hydrogen released amounted to about 0.56 mole H_2 / mole of lithium reacted. Hydrogen was released from the steam/lithium reaction forming Li_2O and from the reaction of LiOH with iron from the reaction chamber. The fact that essentially all of the lithium was depleted from the alloy was supported by a measurement of the melting point of the final metal, which was 327 C (the melting point of pure lead).[20] The chemical analysis also showed that no oxide or hydroxide compounds of lead were formed during the experiment.

The chemical reaction was rapid and complete. The fact that virtually all of the water and lithium introduced to the reaction chamber had reacted meant that the reactants had mixed completely throughout the reaction chamber. The fact that the measured alloy temperatures varied less than 20 C between one another, except at

the point of steam injection, also indicated that there was good mixing in the reaction chamber.

A large scale lithium/steam test was also conducted at HEDL. In this experiment, the reaction chamber was closed to the containment vessel atmosphere.[22] In this experiment, superheated steam at 320 C was injected, at a rate of 2.6 gm/sec for 510 seconds, into a 10 kg pool of lithium with an initial temperature of 580 C. The lithium pool temperatures are shown in Figure 10.[22] These pool temperatures indicated a localized high temperature zone near the point of steam discharge, but otherwise good pool mixing throughout the test.[22]

The lithium and steam reacted to form Li_2O and LiH. Since lithium hydride has been shown to decompose at temperatures near 1000 C, releasing hydrogen gas, the steam addition to the pool was discontinued when the bulk pool temperature reached 980 C. This prevented an overpressurization of the reaction chamber due to hydrogen generation.[22] Both experiments were characterized by a complete and rapid chemical reaction. Heat balances on both systems showed that the lithium-lead/steam interaction generated $5.2 * 10^5$ J/mole of water reacted,[20] and that the lithium/steam interaction generated $1.7 * 10^6$ J/mole of water reacted.[22] Thus the lithium/steam reaction generated heat at a rate that was 3 times as great as the lithium-lead/steam heat generation rate.

Figure 10. Lithium Alloy Pool Temperatures[20]

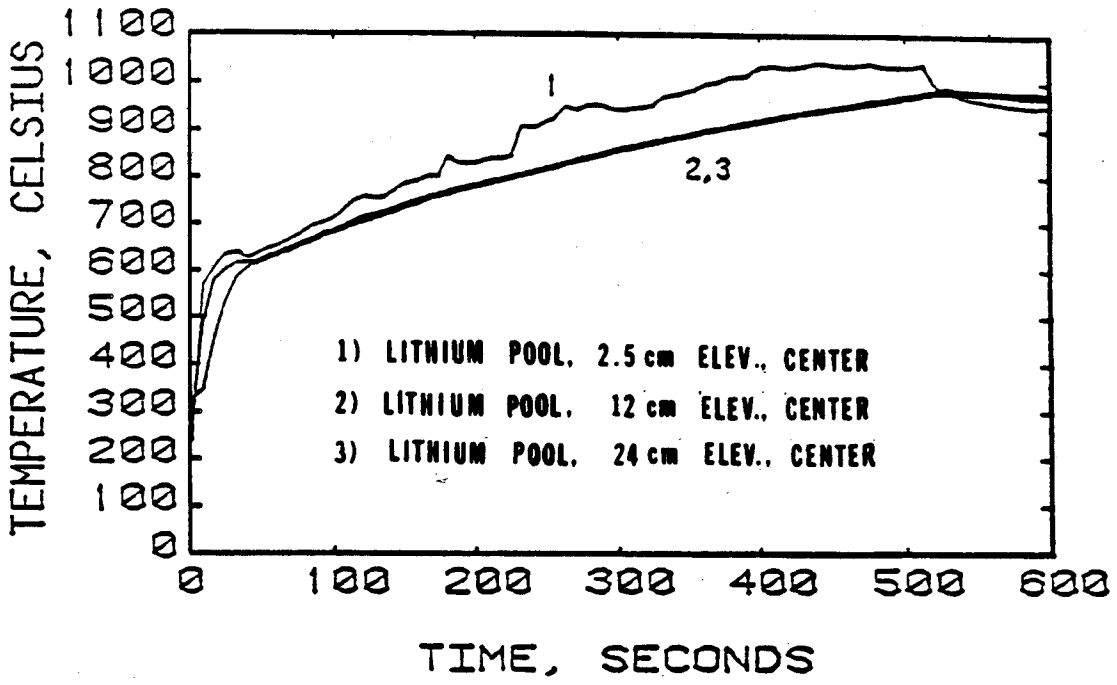

The HEDL large scale lithium-lead/steam experiment shows that for a coolant vapor injection accident scenario (i.e., the breaking of a steam tube in a lithium-lead steam generator) the steam will completely mix and react with the lithium-lead, at least for the early portion of the accident (t ~ seconds). The very self-limiting and moderate lithium-lead/water reactions observed in the small scale experiments would not be observed in a coolant vapor injection accident scenario. One should not conclude based on these observed facts that all large scale lithium-lead/water interactions will show such vigorous reactions. Large scale pouring of liquid lithium-lead into a pool of water may also lead to a self-limiting, relatively moderate reaction. The major reason for this difference resides in the hydrodynamic mixing of the water and liquid metal during the interaction. This has not been specifically addressed in any past experiments.

III. Experimental Apparatus and Procedures

III.1 Description of Experiment

As mentioned earlier, our goal in this research was to investigate the kinetics of the lithium-lead/water reaction by means of a series of small scale experiments. This task was approached by starting with the simplest apparatus conceivable. This was done so that we could obtain an idea of the scale of the reaction. After these initial scoping experiments, we were ready to design and construct the closed vessel experiment. The closed vessel experiment was designed to contain and measure the hydrogen produced by the lithium-lead/water reaction.

Our initial scoping experiments were very similar to the small scale liquid metal drop experiments preformed by Finn, et. al.,[14] and Kuhlborsch and Reiter.[16] While the experiments of these investigators consisted of pouring a stream of molten lithium-lead into water, our experiments consisted of dropping a single, controlled size, drop of molten lithium-lead into water under an argon atmosphere. The basic apparatus consisted of a heated droptube suspended over a beaker of water, all of which was placed in an argon filled glove box. The droptube was a hollow quartz cylinder, connected on one end to a high pressure argon supply. The other end of the droptube was plugged with a small quartz capillary tube. The capillary tube was pierced with a variable sized opening (the

opening sizes varied from 0.05 to 0.2 inches). By this design, we could generate reproducible drops of lithium-lead.

A high speed camera was used to film the interaction of the liquid metal drops and water. By comparing the films of runs of pure lead with those of lithium-lead, for the same drop size and temperature, we hoped to ascertain the amount of hydrogen formed by the lithium-lead/water reaction, as the lithium-lead drop fell through the water. The films showed that as the liquid metal drops entered the water, a layer of gas quickly formed and enveloped them. This gas layer was stripped away though, as the drops fell through the water. We were not able to detect any difference between the behavior of lead drops and lithium-lead drops as they passed though the beaker of water. When the drops lay on the bottom of the beaker though, we did detect evidence of a chemical reaction. Gas bubbles formed on the lithium-lead drops, but did not form on the lead drops. Over a period of minutes, a thin layer gas film formed as the bubbles coalesced on the lithium-lead drops. At no point though did the gas film reach sufficient size to form a bubble and detach from the drop. Later analysis of the drops revealed that the exposed surface of the lithium-lead drops were covered with a thin, black, porous layer. In contrast, the surface of the lithium-lead drops that contacted the bottom of the beaker retained a silvery, metallic color, which also was exhibited by the entire surface of the lead drops.

Because of the indiscernible behavior of the lead and lithium-lead drops as they entered the water, one can conclude that gas formed in this phase of the interaction consisted of mainly steam. Because of their small size and the insignificant heating from the reaction, the drops quickly lost heat and solidified soon after entering the water. Therefore, for the most part, any lithium-lead/water reaction that occurred, occurred between the solid phase of the lithium-lead and the liquid phase of the water.

The scoping tests showed us that the lithium-lead/water reaction is indeed mild and self-limiting. Conceivably, pouring large amounts of molten lithium-lead into a pool of water will produce measurable amounts of hydrogen. But the area of interaction in such a test would be time dependent and almost impossible to measure. Reducing the amount of molten metal used will allow one to keep the area of contact constant and measurable, as in the liquid metal drop experiments. But the relatively benign nature of the lithium-lead/water reaction makes the measurement of the hydrogen production rate very difficult. Because of this, we decided to alter the form of the experiment. Instead, we settled on an experimental design that was characterized by the pouring of water onto a small pool of liquid metal. By appropriate sizing of the liquid metal pool exposed surface, one can control the interaction contact area. By also insisting on a closed vessel design, one can contain and measure the hydrogen produced by the reaction. These two facts are the

primary motivation behind the design of the closed vessel experiment.

During the operation of the experiment, the apparatus is essentially a closed steel cylinder. A drawing detailing the components of the experimental apparatus is given in Figure 11. To facilitate the loading of the reactants, the apparatus consists of four separable components: the lower portion of the apparatus, a butterfly valve, the upper portion of the apparatus, and the upper plate.

The lower portion of the apparatus contains a cavity for placement of the liquid metal (16 cm^3), and a free volume (110 cm^3) for inflowing water. These cavities were formed by drilling cylindrical holes into the top of a 175 mm by 62.5 mm dia. stainless steel cylinder. The free volume cavity was formed by drilling a 37.5 mm by 50 mm dia. hole into the steel cylinder. The liquid metal cavity was formed by drilling a 32 mm by 25 mm dia. into the bottom of the free volume cavity. In the bottom of the steel cylinder, a final cavity, 100 mm by 10 mm dia., was drilled. This final cavity is a well for the placement of a thermocouple. Therefore, we are able to place a thermocouple 6.4 mm from the bottom of the liquid metal pool. The axes of these three cavities are coincident with the axis of the steel cylinder. The large mass of the lower section of the apparatus (3.4 kg) helps to maintain the temperature of the liquid metal. During the experiment, the lower portion of the apparatus is inserted into a annular, electrically heated, furnace. Therefore the entire lower portion of the apparatus can be heated to a high

Figure 11. Closed Vessel Experiment

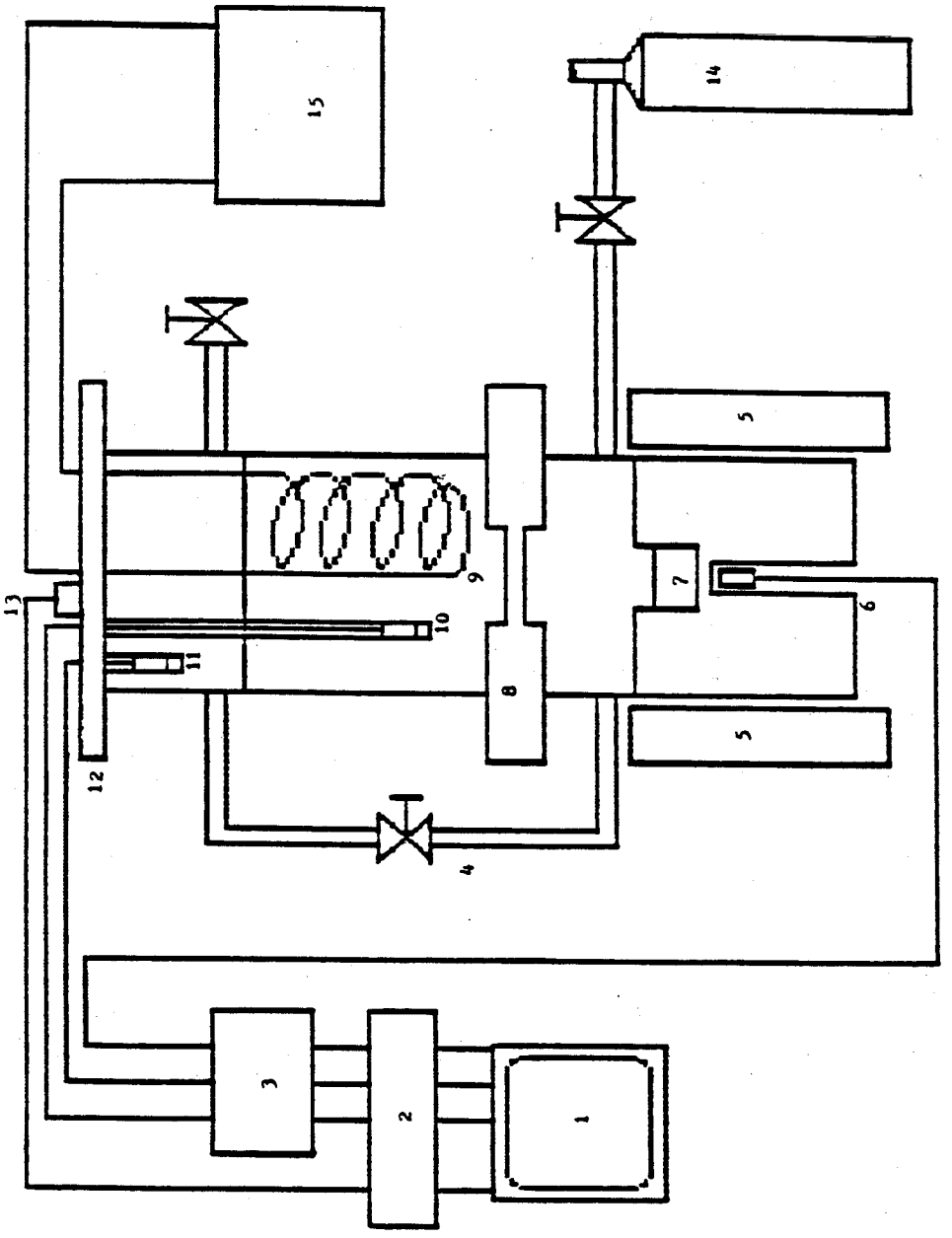

temperature before the initiation of the liquid metal/water interaction. The lower portion of the apparatus, with its large thermal inertia, helps to keep the liquid metal from freezing too rapidly.

After the lower portion of the apparatus has been loaded with a metal sample for the experiment, it is covered with a disk shaped butterfly valve. The valve keeps the water separated from the metal during the heating phase of the experiment. When both the metal sample and the water have reached the desired initial temperatures, the butterfly valve is opened, allowing the water to pour onto the surface of the liquid metal pool.

The upper portion of the apparatus, which is placed on top of the butterfly valve, contains a reservoir for the water. The volume of water used during the sequence of experiments was 1 liter. The upper portion of the apparatus also contains a convection coil connected to a constant temperature bath. By this means, the temperature of the water can be controlled during experiment runs.

The convection coil and main diagnostics for the experiment are fitted into the upper plate, which can be bolted onto the top of the upper portion of the experiment. The top plate contains two thermocouple wells. One thermocouple well reaches into the upper gas region, above the column of water. The other thermocouple well reaches into the bulk of the water column. The pressure of the upper gas region is measured by a pressure transducer, ported

through the top plate. The convection coil, and its intake and outtake lines, are connected to the upper plate by swagelock fittings. These fittings, which are also used to connect the thermocouple wells, form leak tight seals.

When bolted together, the four components of the experimental apparatus form a closed volume. By means of flanges and o-rings, the apparatus can hold most of the hydrogen produced by the reaction, for the duration of the experiment. As the pressure in the closed vessel rises, there is a small leakage of the gases from the system. But the rate of this leakage can be measured, and its effect compensated for, as described later in this report.

As mentioned earlier, the primary motivation for the closed volume design, was that it allows one to collect and measure the hydrogen produced by the reaction, and that the contact area between the water and the liquid metal could be kept constant throughout the interaction. As just shown, the first of these conditions is satisfied by the design, but we need to explain how the second of these conditions is also satisfied by the design. Because the two liquids involved in the interaction have greatly different densities, and since the lower density liquid is poured onto the higher density liquid, one would expect that the two liquids will not mix. Thus one would expect the initial contact area between the two fluids to remain constant throughout the interaction. But because of the rapid boiling of the water that ensues when the water is poured onto

the hot liquid metal, the possibility of Taylor instabilities arises. The boiling of the water can disturb the liquid metal surface, causing waves to form on the liquid metal surface. These instability waves can grow if the characteristic length of the liquid metal surface is greater the Taylor wavelength (λ).[23]

$$\lambda = 2\pi \left(\frac{3\sigma}{\Delta\rho g}\right)^{1/2} \tag{12}$$

Since, for our experiment, the Taylor wavelength equals 27 mm, we designed the liquid metal cavity so that it had a diameter of 27 mm. Thus the liquid metal surface is impervious to Taylor instabilities, which implies that the contact area will remain relatively constant throughout the duration of the experiment.

The main experimental variables, pressure and temperature, are measured by a pressure transducer, and three thermocouples. The output of these devices is automatically logged electronically. Readings from all four are taken about once a second. The pressure transducer output and the amplified output of the thermocouples are connected to a multichannel analog to digital convertor. The output of the analog to digital convertor is fed into a microcomputer allowing an electronic record of the system variables. The three thermocouples are situated in the following manner. One thermocouple is placed in the cavity drilled into the bottom of the lower portion of the apparatus. As explained above, this allowed us

to measure the temperature of the apparatus 6.4 mm below the bottom of the liquid metal pool. The other two thermocouples were placed into the thermocouple wells connected to the upper plate. These allowed us, in turn, to measure the bulk water temperature and the temperature of the gas layer above the water level. It should be noted that because the thermocouples are placed in steel thermocouple wells, the thermocouples were not able to measure rapidly varying temperatures. The consequences of this shortcoming will be described later. Unfortunately, in order to maintain a reasonably leak resistant design, the thermocouples could not be placed directly into desired locations.

Two other thermocouples are used in the experiment. These thermocouples are used to measure the temperature of the gas in the free volume above the metal sample during the heating phase of the experiment. One thermocouple is inserted radially through the lower portion of the apparatus, directly into the free volume. The other thermocouple is used to measure the temperature of the apparatus at the base of the first thermocouple. This second thermocouple is needed because the temperature measured by the first is influenced by convection from the free volume gas and conduction through the body of the thermocouple from the lower portion of the apparatus. By knowing the temperature of the apparatus at the base of the inserted thermocouple, and the temperature measured by the inserted thermocouple, the temperature of the free volume gas can be

evaluated. Since these two thermocouples are needed only during the heating phase, they are not connected to the analog to digital convertor - computer circuit. They are instead connected to digital thermocouple meters, and the data from them recorded by hand.

The lower portion of the apparatus, and an enclosed metal sample, are heated by two semi-cylindrical heating units. Pieced together, the heating units form an annulus, which has a 75 mm inner dia. and a 100 mm outer dia. The heating units, constructed of high resistance wire coils embedded in high thermal conductivity cement, are enclosed by 3 in. of insulating firebrick and glass wool. The heating units are operated at 1200 W. This furnace is capable of heating the metal to 600 C, as measured by the liquid metal well thermocouple, in about an hour. We did not attempt to heat the metal sample to higher temperatures, since a finite element analysis of the furnace and lower portion of the experiment indicated that operating the system at higher temperatures may cause the temperature of the heating units to rise to its rated maximum temperature (1200 C).

The water temperature was controlled by a separate cooling (and heating) loop. This loop consisted of a convection coil, inserted into the upper portion of the apparatus, and connected to a temperature controller. The temperature controller contains a 2 l. capacity, constant temperature bath. The temperature controller has heating and refrigeration units to control the water temperature, and has the

ability to pump the constant temperature water through the convection coil. By this means, the water in the apparatus can be heated to a desired temperature, before the initiation of the experiment. The initial water temperature in the experiment is never lower than 5 C below the temperature controller set temperature. After initiation of the experiment, the temperature control loop removes the heat generated by the interaction of the hot metal and cool water from the system. In this phase, the water temperature is never higher than 30 C above the temperature controller set temperature. The temperature control loop is able to keep the bulk of the water subcooled for the duration of the experiment. Therefore, the steam that is generated by the interaction condenses as it rises through the column of subcooled water.

To accommodate the model discussed later in this report, it is necessary to insure that the water interacting with the liquid metal boils in the film boiling regime. In film boiling, the liquid water does not completely contact the liquid metal. Therefore, the reaction, assumed by the model to occur at the liquid metal/water interface, involves only the liquid phase of the metal and the gas phase of the water. An approximate condition for the onset of film boiling is given by:[24]

$$\Delta T_{min} = 101 + 8\,\Delta T_{sub} \qquad (13)$$

This correlation states that the minimum temperature difference

between the liquid metal surface temperature and the water saturation temperature (ΔT_{min}) that will ensure film boiling is a function of the degree of subcooling (ΔT_{sub}). The units of this equation are degrees centigrade. Although this correlation was derived from experiments with water and heated metal spheres, it probably overestimates T_{min} for our experiment. This is because our reaction produces hydrogen, which helps cover the liquid metal surface with a layer of gas. Thus for a given desired initial liquid metal temperature, the initial water temperature must be chosen so that the above equation is satisfied.

The experiment has incorporated in its design an external gas line and series of valves that insures that, during the heating phase, the free volumes above the metal sample and water column are at the same pressure. Argon is allowed to flow through the free volume above the metal sample, then through a connecting line to the gas region above the water column, and then out of the system to the atmosphere. The pressure equalization line was incorporated into the design to eliminate a pressure difference that would appear between the upper and lower portions of the apparatus during the heating phase of the experiment. This pressure difference would occur because the two gas layers, originally at the same temperature and pressure, would be heated to temperatures as much as 200 C apart. The resulting pressure difference would cause the butterfly valve to leak. When the pressure equalization line is open, an argon flow, from the lower gas region to the upper gas region, must be

maintained to insure that water vapor does not diffuse from the upper gas region to the lower gas region and react with the metal. Besides equalizing the pressure, this system has the added benefit of insuring that the metal sample and the water column are covered with an inert gas.

As one might conclude, the pressure equalization line was not originally incorporated into the design of the experiment. Instead, it was incorporated after we found that the butterfly valve could not withstand the pressure differential it was subjected to. This trial and error approach was needed in other aspects of the design. We attempted to place unshielded thermocouples directly into the upper gas and water regions, but were unable to develop a leakproof fitting needed for this purpose. As described earlier, we had to settle on thermocouples placed into wells. By iteration, we were able to arrive at an experimental apparatus that functioned properly. Although some limitations in the final design led to difficulties in extracting the desired data, the apparatus is a workable design within the given constraints.

III.2 Experimental Procedure

We developed an uncomplicated and consistent procedure to operate the experiment. Applicable to all tests, a set of ordered steps were developed. The impetus behind these rules was our desire for safety and to eliminate as many extraneous variables as possible.

To achieve this goal, the apparatus was loaded and pieced together in the same manner for each test; the temperature controller and furnace controls were set, and then were not changed during the experiment; and the interaction was initiated and controlled the same way every time. By these means, we were able to reduce the experimental variables to three: the initial water temperature, the initial liquid metal temperature, and the liquid metal mass. It was found though, that the liquid metal mass had a negligible effect on the outcome of the experiment because the amount of hydrogen generated was a function of the liquid metal area, which was constant for the experiments, and not the liquid metal mass. Ultimately this meant that the tests varied from one to the other only by the choice of the initial water temperature and liquid metal temperature.

The tests were initiated by first loading a metal sample into the liquid metal well. The apparatus was then pieced together in the following manner. The lower portion of the apparatus and the liquid metal thermocouple were placed into the furnace. Then the butterfly valve and upper portion bolted onto the top of the lower portion of the apparatus. Next one liter of distilled water was poured into the upper portion of the apparatus. Then the upper plate, with its attached convection coil, gas and water thermocouple wells, and pressure transducer, was bolted onto the top of the apparatus. Lastly, the electronics were connected and checked, and an argon

feed line was connected to the apparatus.

We were then ready to begin the heating phase of the experiment. This phase consisted of simply starting the heaters and waiting then for the water and liquid metal to reach their desired temperatures. Because of the relatively low initial water temperature, the temperature controller was able to heat the water to its desired temperature before the furnace raised the liquid metal temperature to its the desired value. Since the furnace heaters were always operated at 1200 W, the liquid metal temperature as a function of time was approximately the same for each run. Therefore we could predict when the liquid metal would reach a desired temperature.

Knowing when the liquid metal temperature would reach a desired value, allowed us to start a five minute countdown phase before the initiation of the interaction. At the beginning of the countdown phase the argon flow through the system was stopped, a valve on the pressure equalization line was closed, and the automatic recording of the system variables was begun. Since the system then became a closed one, the water and covering argon gas reached an equilibrium. Closing the valve on the pressure equalization line insured that water vapor was not able to reach the liquid metal during this phase. Because we measured the initial temperatures and pressure during this phase, we were able to evaluate the mass of argon in the system.

At the end of the countdown phase all was set: the initial water and liquid metal temperatures were at desired values; the mass of argon, water, and liquid metal were known; and the system pressure was known. Therefore we were ready to open the butterfly valve and initiate the interaction. After the valve was opened, the experiment was run, without interference, for 30 minutes. After this time period, the furnace heaters were turned off. The temperature controller continued to run, for a while, at a low temperature allowing it to remove much of the residual heat from the system.

After the system had returned to room temperature, we measured the system leakage rate. This was accomplished by reconnecting the argon feed line, pressurizing the system to a high pressure, and then recording the system pressure for 10 minutes. We repeated this process six times, each time pressurizing the system to a new value. By later curvefitting the data for each of the six pressure tests, we were able to evaluate the system leakage rate at each of the six chosen pressures. In this means, we were able to measure the system leakage rate, as a function of pressure, for each of the experiments.

The last step in the experimental procedure was to prepare the apparatus for the next test. The only noteworthy part of this process was the removal of the metal sample from the lower portion of the apparatus. Because the liquid metal had frozen into the well, it had to be drilled out. Although this was relatively simple, it

meant that the lithium-lead samples had to be considerably fragmented to remove them from the apparatus. Since our facilities did not permit this to be done under an inert atmosphere, this meant that any unreacted lithium in the sample would be contaminated by air, invalidating any chemical analysis that would verify the extent of reaction.

At the beginning of the proceeding discussion we noted that the first step in the experimental procedure was to load the lower portion of the apparatus with a metal sample. While in the case of the lead tests this involved nothing more than dropping a measured amount of lead shot into the liquid metal well, the lithium-lead tests required a much more complicated procedure. Because of the chemically reactive nature of the lithium-lead with many of the atmospheric gases, the lithium-lead had to be removed from its container and placed into the lower portion of the apparatus under an argon atmosphere. We obtained our lithium-lead samples from Argonne National Laboratory. The lithium-lead was packaged in 30 cm by 10 mm dia. steel tubes. Each tube contained enough lithium-lead for two experimental runs. The lithium-lead was loaded into the apparatus with the following procedure. First the tube, the lower portion of the apparatus, the butterfly valve, and an electrical heating tape were placed into a glove bag. After the glove bag was filled with argon, the tube was cut in half and one half of the tube was wrapped with the heating tape. The wrapped tube was then

suspended an inch above the liquid metal well and the heating tape power source activated. In the meantime, a concentrated argon flow was directed onto the lower, exposed end of the tube. When the lithium-lead in the tube reached its melting point (230 C), it flowed into the liquid metal well and quickly solidified. As soon as the lithium-lead had flowed into the liquid metal well, the closed butterfly valve was bolted onto the top of the lower portion of the apparatus. The loaded lower portion of the apparatus could then be removed from the glove box and the rest of the experiment could then be pieced together. While the experiment was being pieced together, we pumped argon gas through the pressure equalization line. This allowed us to keep the gas region above the metal sample flushed with argon while the rest of the apparatus was pieced together.

III.3 Data Analysis

As we have pointed out, the main experimental variables were the initial water and liquid metal temperatures. Because of the temperature limit on the heaters, the maximum initial liquid metal temperature was 600 C in this test series. Since the melting point of the lithium-lead is 230 C, the liquid metal had to be heated to a high enough initial temperature to insure that the water would not cool the liquid metal enough to freeze it. Therefore the initial liquid metal temperature was never lower than 350 C. To insure film

boiling at the beginning of the experiment, the limits imposed by the minimum film boiling correlation (equation 13) had to be met. Given these limits on the initial water and liquid metal temperatures, we developed the following test matrix. With the initial liquid metal temperature equal to 600 C, tests were performed with the initial water temperature equal to 60 C, 70 C, 80 C, and 90 C. With the initial liquid metal temperature equal to 500 C, tests were performed with the initial water temperature equal to 70 C and 90 C. With the initial liquid metal temperature equal to 400 C, tests were performed with the initial water temperature equal to 80 C and 90 C. And with the initial liquid metal temperature equal to 350 C, tests were performed with the initial water temperature equal to 90 C. For each of these initial liquid metal and water temperature pairs, one or two lithium-lead tests and one lead test were performed.

We can now discuss the method used to analyze the raw pressure and temperature data from the experiment. A computer program was written that, using the bulk water temperature, the gas layer temperature, and the system pressure, would evaluate the pressure and mass of hydrogen in the system, for each data time point.

Because there were two gases in the system, argon and hydrogen, we had to know the mass of argon in the system to infer the hydrogen mass. The mass of argon in the system could be calculated from the system initial conditions. Before the initiation of

the interaction, argon would be found in three regions: it would fill the free volume above the liquid metal, it would occupy, along with water vapor, the region above the water, and a small amount would be dissolved in the water. Using the ideal gas law, this can mathematically be expressed as:

$$N_{Ar} = \frac{(P - P_{vap})\ V_{up}}{R\ T_{gas}} + \frac{P_{dn}\ V_{dn}}{R\ T_{dn}} + N_{Ar\ sol} \qquad (14)$$

where 'up' designates the upper portion of the apparatus and 'dn' the lower portion. The first term in this equation is the mass of argon in the region above the water. It is a function of the measured pressure (P) and gas temperature (T_{gas}) at the end of the countdown phase. It is also a function of the water vapor pressure, which is equal to the saturation pressure of water at the measured gas layer temperature. The second term in this equation is the mass of argon in the free volume above the liquid metal. Because the pressure equalization line is closed at the beginning of the countdown phase, the lower region pressure (P_{dn}) is the pressure measured by the pressure transducer at the beginning of the countdown phase. The last term in this equation is the mass of argon dissolved in the water. It can be evaluated using the following equation.

$$N_{Ar\ sol} = X_{Ar}(T,P)\ N_{H_2O} \qquad (15)$$

The solubility of argon in water (X_{Ar}) is a function of the water

temperature and the partial pressure of argon. By Henry's law, the solubility of a gas is directly proportional to the partial pressure of that gas.[25] Since at saturation temperature the solubility of a gas in a liquid equals 0, and since we know the solubility of argon in water at 25 C and 1 atm only, we assume that the solubility of argon in water can be expressed as:

$$X_{Ar}(T,P) = X_{Ar}(25\ C, 1at\ m) * \frac{(T_{sat} - T)}{(T_{sat} - 25\ C)} * \frac{P}{1\ at\ m} \qquad (16)$$

As alluded to earlier, the temperature of the argon in the free volume above the liquid metal (T_{dn}) must be measured with two thermocouples. The first thermocouple, inserted directly into the gas through the lower portion of the apparatus, is influenced by conduction through its steel sheath by the hot apparatus. By measuring the temperature of the apparatus at the base of the first thermocouple with a second thermocouple, the temperature of the gas can be calculated. For a cylinder extending at right angles from a heated wall, the temperature at the its end (T_{TC}) is related to the temperature at its base (T_w) and the gas temperature (T_{dn}) by:[26]

$$\frac{T_w - T_{dn}}{T_{TC} - T_{dn}} = \cosh\left(\left(\frac{4h}{D_{TC} k_{TC}}\right)^{1/2} L_{TC}\right) \qquad (17)$$

The heat transfer coefficient (h) in this equation is given by the correlation for the Nusselt number of free convection flow over a

heated, horizontal cylinder.[27]

$$Nu = .525 \ (Ra)^{1/4} \qquad (18)$$

With the initial mass of argon in the system known, the computer program can now move to processing the information gathered from the experiment. The first step in this process is to convert the thermocouple readings in millivolts to readings in degrees Centigrade. The data acquisition system records the output voltage from the thermocouples. The data analysis computer program then converts the voltage readings into temperature readings by using an eighth order polynomial. The polynomial was supplied by the manufacturer of the thermocouple, and converts the thermocouple reading in millivolts to a temperature reading in Centigrade with a degree of accuracy of +/- .7 C.[28]

The data analysis program achieves its goal of evaluating the hydrogen mass and pressure in the lithium-lead tests by accounting for all calculable components of the pressure. The sum of the calculable components of pressure is then compared to the measured system pressure. Because we know the mass of argon and water in the system, the gas volume, and the gas temperature; we can calculate the partial pressure of argon and water vapor in the system. Therefore the difference between the measured pressure and the calculable components of the pressure is equal to the partial pressure of hydrogen in the system.

Lead tests are run, with the same initial water and liquid metal temperatures as the lithium-lead tests, to see if we can accurately predict all of the components of pressure in the system. For the lead tests, we evaluate the difference between the measured and calculated pressure (ΔP) using the following equations.

$$\Delta P = P - P_{vap} - P_{Ar} \tag{19}$$

$$P_{Ar} = (N_{Ar} - N_{Ar\ sol}) R T_{gas} / V_{gas} \tag{20}$$

As before, the partial pressure of water vapor (P_{vap}) is equal to the water saturation pressure at the measured gas temperature. The moles of argon in solution, which is a function of the water temperature through the solubility coefficient, is given by equation 15. The total mass of argon in the system, accurately given by equation 14 at the beginning of the interaction, has to be corrected for leakage afterward. As described in the last section, the leakage rate as a function of system pressure is measured for each test. In the computer program, the leakage of gas is accounted for by updating the mass of argon in the system each timestep using:

$$N_{Ar}(t) = N_{Ar}(t-\Delta t) - \frac{\frac{dP}{dt}(P)\ \Delta t\ V_{gas}}{R\ T_{gas}} \tag{21}$$

For lithium-lead tests similar calculations are performed by the program. In this case, the difference between the measured and calculated pressure will be equal to the pressure of hydrogen in the

system. The pressure of hydrogen in the system is given by equation 19, with one correction term for the mass of hydrogen in solution.

$$P_{H_2} = P - P_{vap} - P_{Ar} - \frac{N_{H_2sol} R T_{gas}}{V_{gas}} \qquad (22)$$

The mass of hydrogen in solution is evaluated in the same manner as before:

$$N_{H_2sol} = X_{H_2}^{(T,P)} N_{H_2O} \qquad (23)$$

$$X_{H_2}^{(T,P)} = X_{H_2}^{(25\ C,1atm)} * \frac{(T_{sat} - T)}{(T_{sat} - 25\ C)} * \frac{P}{1\ atm} \qquad (24)$$

These three equations account for the hydrogen in the system at any given time. But the total amount of hydrogen generated by the reaction is not accounted for by these equations. As hydrogen is generated by the reaction, a small amount of hydrogen is lost from the system due to leakage. Therefore, at any time, the total amount of hydrogen generated by the reaction equals the sum of the hydrogen in the system at that time plus the amount of hydrogen that has leaked from the system up to that time. In the lithium-lead tests, the leakage rate affects the mass of the argon and hydrogen in the system. The dynamic mass of argon in the system is evaluated with:

$$N_{Ar}(t) = N_{Ar}(t-\Delta t) - \frac{\frac{dP}{dt}(P)\ \Delta t\ V_{gas}}{R\ T_{gas}} * \frac{P_{Ar}}{P_{Ar} + P_{H_2}} \qquad (25)$$

The accumulated mass of hydrogen to leak from the system is given by:

$$N_{H_2 leak}(t) = N_{H_2 leak}(t-\Delta t) - \frac{\frac{dP}{dt}(P)\ \Delta t\ V_{gas}}{R\ T_{gas}} * P_{H_2} / (P_{H_2} + P_{Ar}) \qquad (26)$$

Equations 22, 23, and 26 can now be combined to equation for the mass of hydrogen generated by the reaction.

$$N_{H_2 tot} = \frac{P_{H_2}\ V_{gas}}{R\ T_{gas}} + N_{H_2 sol} + N_{H_2 leak} \qquad (27)$$

The calculations for the hydrogen partial pressure and mass in the lithium-lead tests rely on the our ability to accurately evaluate the argon and water vapor partial pressures. We cannot directly measure the hydrogen partial pressure, so we must evaluate it by accounting for the other components of system pressure. Therefore, we arrive at the partial pressure of hydrogen by a process of elimination. As will be shown in the following chapter, we can accurately evaluate the hydrogen contribution to the system after about a minute into the interaction. The hydrogen production continues throughout the test, even after the sample is cooled to the

water temperature (~ 400 K). In the initial phase of the interaction we can evaluate the hydrogen production with only limited success.

IV. Results of Experiments

IV.1 General Data Trends

We can now examine the raw data from the experiments. By concentrating on the data from typical experiments, we can point out the phenomena common to all of the experiments. We will also be able to show how the readings from the pressure transducer and thermocouples are used to give us a depiction of the liquid metal water interaction.

Because of the large amount of data generated by the experiments, we will scrutinize the data from only a few experiments. A graphical library of the data from all of the experiments is given in the Appendix 4. This collection of graphs show the data from the pressure transducer, the water thermocouple, and the gas thermocouple, during the first 200 s of the interaction for each experiment. Other graphs depict the readings from the liquid metal well thermocouple during the first 1000 s of the interaction for most of the experiments. Also included in this collection, are plots of the calculated hydrogen pressure during the first 200 s of the interaction for the lithium-lead experiments. These final graphs include plots of the difference between the experimental pressure and the calculated pressure from corresponding lead tests.

Turning our attention now to a typical experiment, we will consider the data from test #16. This test, the first lithium-lead test

performed, was characterized by an initial water temperature of 60 C and an initial liquid metal temperature of 600 C. The raw data from this experiment is reproduced in the following Figures. In Figure 12, the response of the pressure transducer is shown. It illustrates trends common to the lithium-lead tests. Right after the butterfly valve is opened, and the interaction is initiated, the system pressure quickly rises to a peak. The system pressure then drops to an equilibrium value, from which it rises a relatively small amount over the duration of the experiment. The height and duration of the peak depend upon the initial conditions. The difference between the peak and equilibrium values of the pressure increases with increasing initial water temperature. The length of time to reach the equilibrium pressure also increases with increasing initial water temperature.

In Figure 13 and 14, the thermocouple data from test #16 are plotted. As revealed in Figure 13, the water and gas temperatures exhibit the same type of behavior as the system pressure. The water and gas temperatures rise to a peak soon after the initiation of the interaction and then drop to an equilibrium value. Although the water and gas temperature data from test #16 do not exhibit a definitive peak, the temperature data from experiments with higher initial water temperatures do. In Figure 14, the response of the liquid metal well thermocouple is graphed. It shows that the liquid metal temperature falls at a rapid rate from the initial liquid metal temperature until, after roughly 500 s an equilibrium temperature is

Figure 12. Lithium-lead Test #16 System Pressure

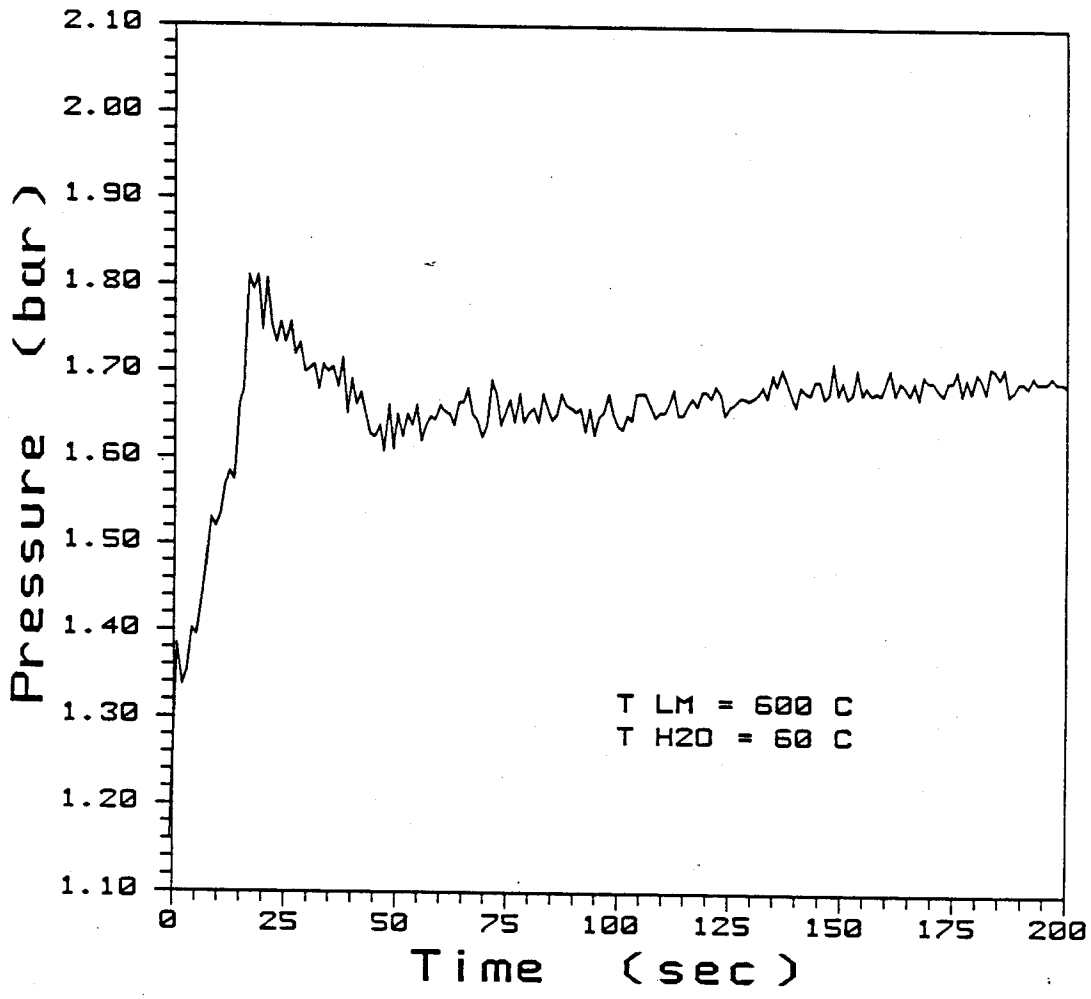

Figure 13. Lithium-lead Test #16 Gas and Water Temperatures

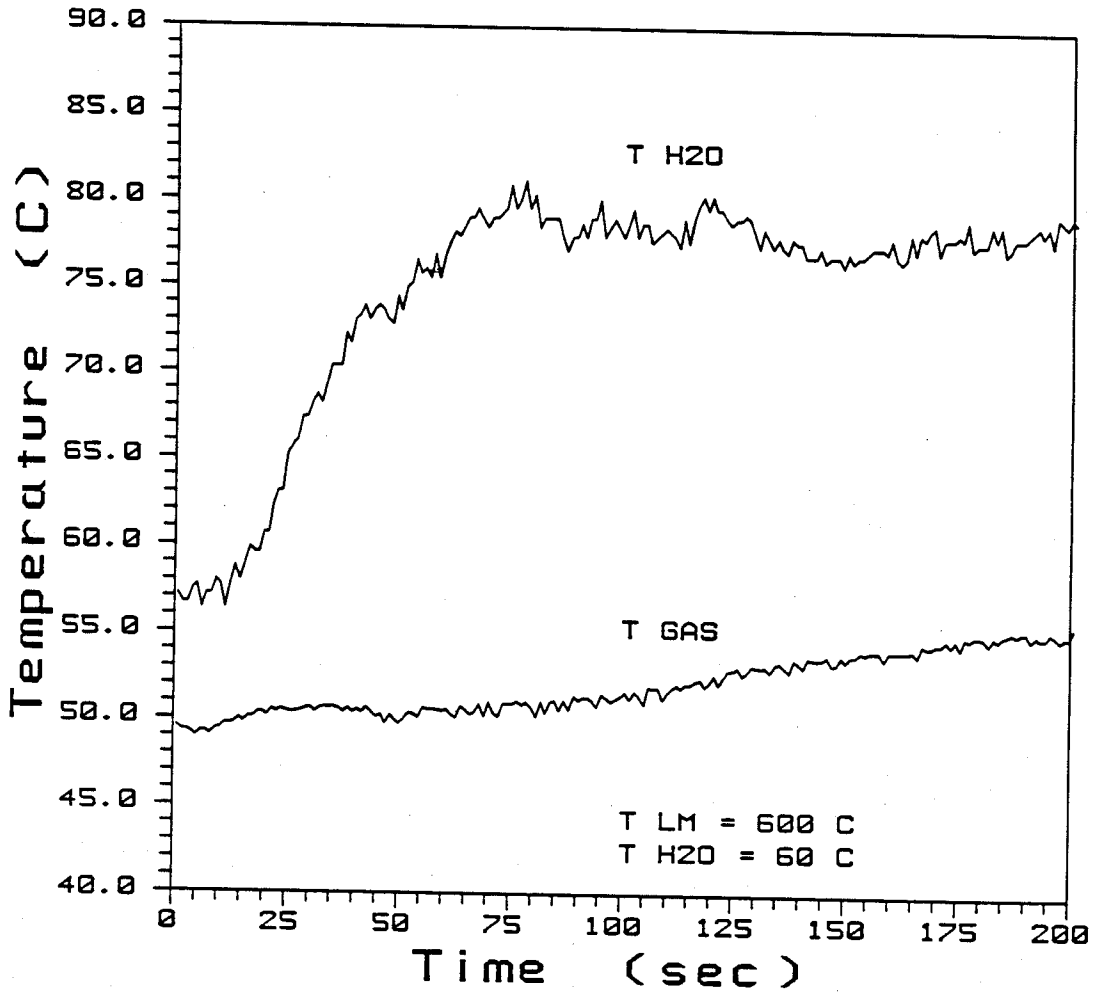

Figure 14. Lithium-lead Test #16 Liquid Metal Temperature

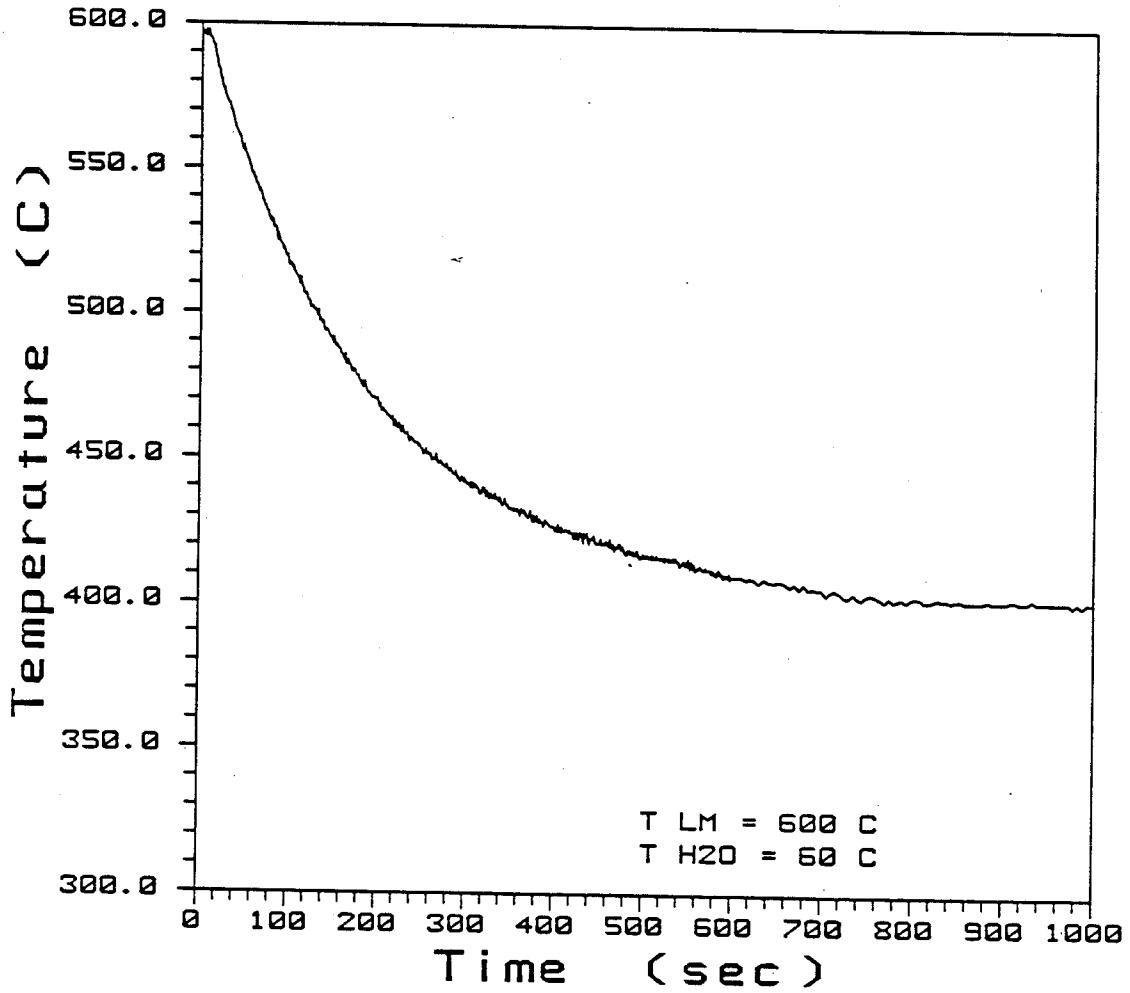

reached. The difference between the initial and equilibrium liquid metal temperatures depends upon the initial liquid metal temperature. At high initial liquid metal temperatures (600 C) the equilibrium liquid metal temperature is 150 C to 200 C lower. At low initial liquid metal temperatures (350 C) the equilibrium liquid metal temperature is from 0 C to 25 C lower.

The typical system pressure, gas, water and liquid metal temperatures from test #16 are interpreted in the following manner. As the water pours into the lower portion of the apparatus and onto the liquid metal surface, the hot metal causes the water to boil rapidly, which in turn causes the system pressure and water temperature to rise. In the meantime, the convection coil begins to remove heat from the water, since the temperature of the water in the coil is kept constant. Because the system is closed and insulated, it eventually reaches thermodynamic equilibrium. In this state, the rate of heat addition to the system from the resistance heaters is balanced by the rate of heat removal from the system due to heat losses to the surroundings and through the convection coil. The equilibrium pressure, gas temperature, and water temperature are functions of the temperature of the water in the convection coil and the power level of the resistance heaters. For the lithium-lead tests, the system pressure gradually rises a small amount above the equilibrium pressure, due to hydrogen generation. The rate at which the system pressure rises in the later stages of the experiment is

much less than the initial rate of pressure increase, because the rate of reaction has decreased significantly by the time thermodynamic equilibrium is reached.

The system pressure increase shown in Figure 12 is primarily due to hydrogen generation from the lithium-lead/water reaction. Because the gas temperature increases as the pressure increases, the amount of pressure increase due to the reaction is not clear. And because one would expect the partial pressure of hydrogen to increase monotonically, the peak in the early pressure response must be due, in part, to another phenomena. The pressure peak is due to the combination of two effects. During the countdown phase of the experiment, the gas region above the high temperature liquid metal is separated from the gas region above the lower temperature water by the butterfly and pressure equalization line valves. Therefore the pressure and temperature of the gas above the liquid metal are greater than the temperature and pressure of the gas above the water. Thus when the butterfly valve is opened and the higher temperature and pressure gas from the lower portion of the apparatus bubbles through the water column and rises to the top of the apparatus, the pressure recorded by the transducer, which is located in the top of the apparatus, increases. Secondly, as the butterfly valve is opened, a large burst of water vapor is formed as the water quenches the lower portion of the apparatus. Eventually, the burst of vapor condenses, and the hot gas is cooled, causing the pressure

to fall.

Before we discuss the calculation of the hydrogen mass and partial pressure from the raw data, we compare the data graphs of lithium-lead test #16 to the data graphs from the corresponding lead test. Test #15 was a lead test with the same initial conditions as test #16 - 60 C water and 600 C liquid metal. Comparing Figure 15, the system pressure for test #15, to the system pressure graph of test #16, one notices the consistently greater system pressure of the lithium-lead test. Because the gas and water temperature response is the same for both tests (compare the gas and water temperature plots of lead test #15 (Figure 16) to the gas and water temperature plots of lithium-lead test #16 (Figure 13)), the difference in the system pressure response of the two tests is a direct indication of the partial pressure of hydrogen present in the lithium-lead test.

With the pressure transducer and thermocouple data from a typical lithium-lead test and corresponding lead test in hand, we can now examine how the equations developed in the last chapter are used to calculate the partial pressure and mass of hydrogen generated by the reaction. For lithium-lead tests, the partial pressure of hydrogen is evaluated by equation 22:

$$P_{H_2} = P - P_{vap} - P_{Ar} - \frac{N_{H_2 sol} R T_{gas}}{V_{gas}} \qquad (22)$$

In Figure 17 the partial pressure of hydrogen for lithium-lead test

Figure 15. Lead Test #15 System Pressure

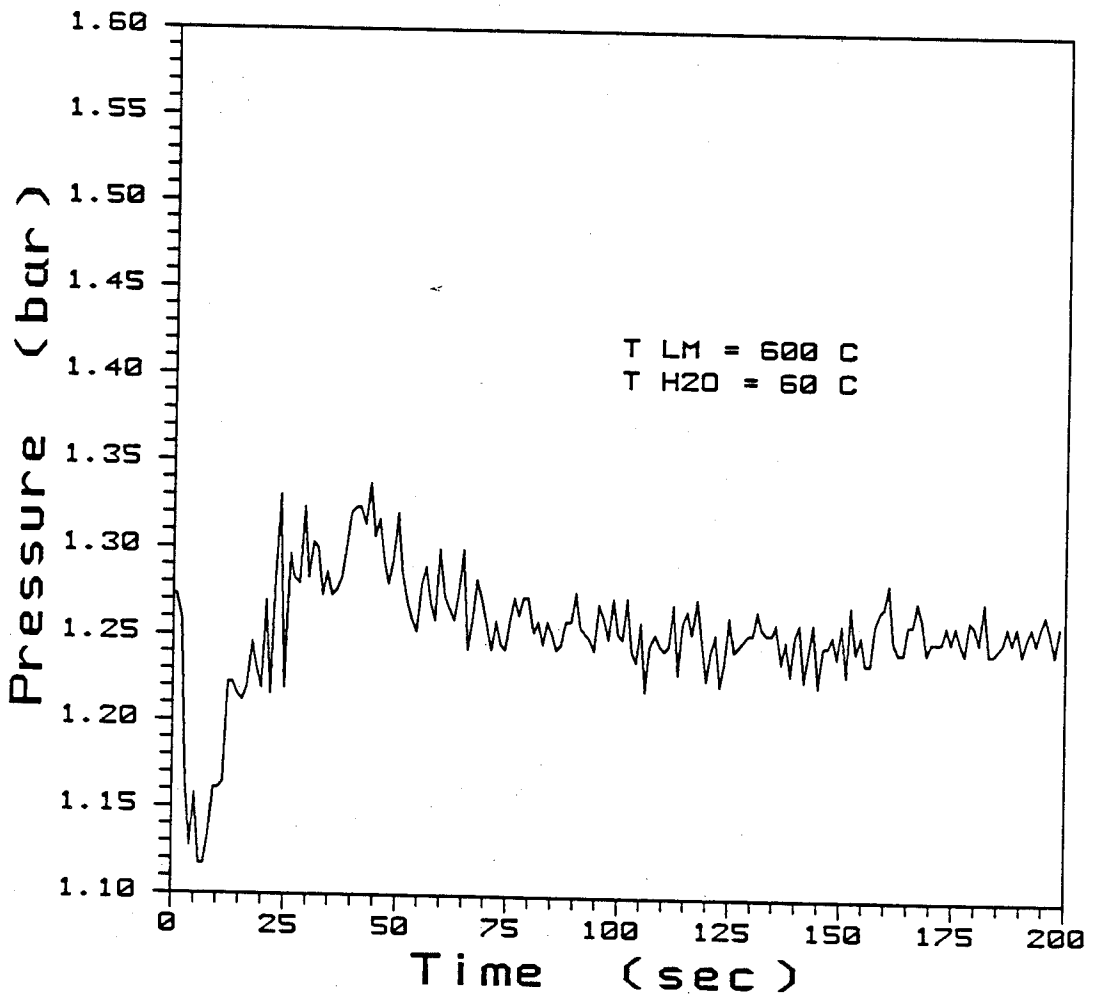

Figure 16. Lead Test #15 Gas and Water Temperatures

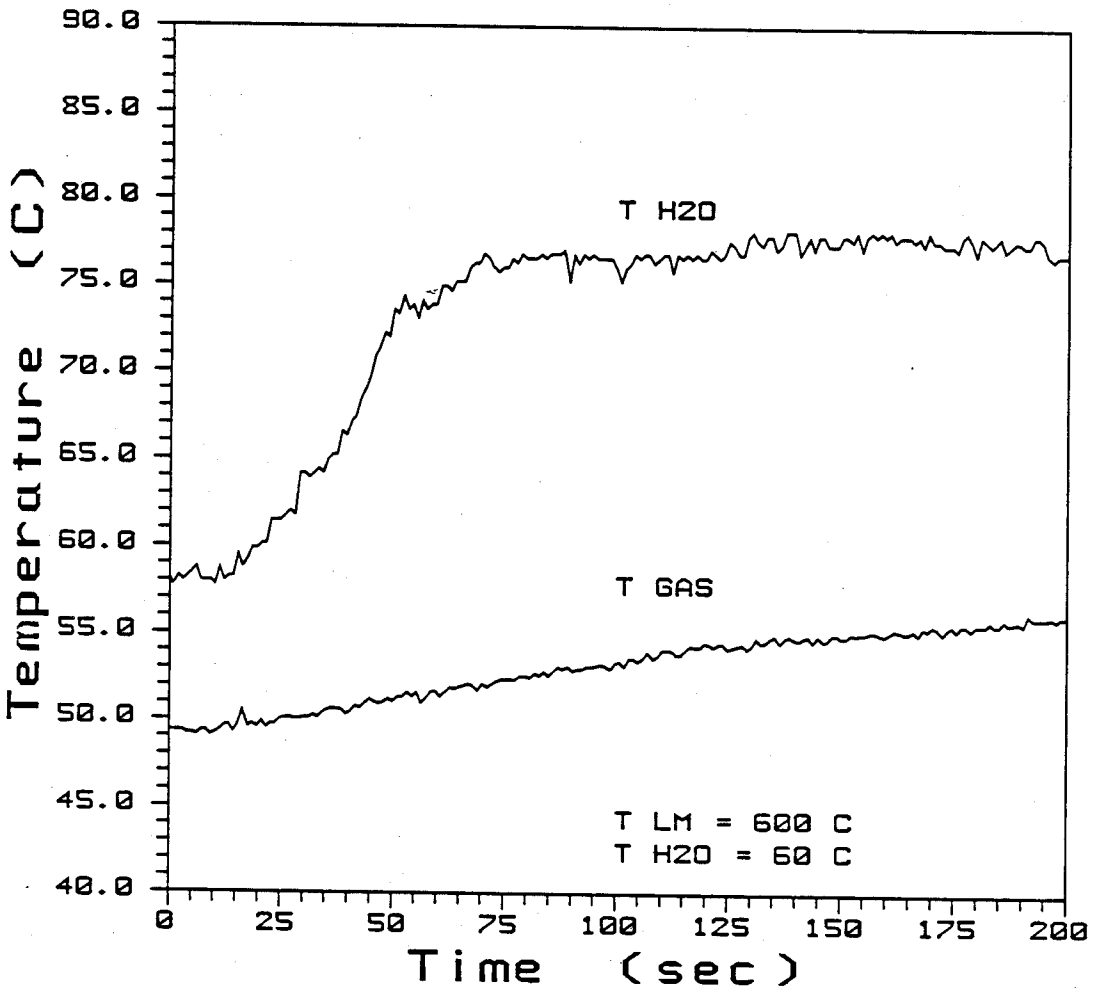

#16, evaluated with equation 22, is plotted. Also shown in this Figure is the difference between the experimental and calculated pressure (ΔP) for lead test #15. This function given by equation 19,

$$\Delta P = P - P_{vap} - P_{Ar} \qquad (19)$$

is evaluated in essentially the same manner as the hydrogen pressure is for the lithium-lead tests. The partial pressure of hydrogen in the system is equal to the difference between the experimental pressure and the calculable components of the pressure. As mentioned before, the accuracy of this method of calculating the hydrogen pressure is dependent upon how precisely we can evaluate the other components of the system pressure. Because we have no way of telling how accurate our method is when it is applied only to lithium-lead tests, we use corresponding lead tests to benchmark the accuracy of the lithium-lead tests. If our method was perfectly precise, ΔP for the corresponding lead test would be equal to 0 at all times. As shown in Figure 17, the method is reasonably accurate for lithium-lead test #16 because ΔP for the corresponding lead test (#15) is relatively small compared to the difference between the experimental and calculated pressure (P_{H2}) of test #16.

With the partial pressure of hydrogen in the system determined, we can finally proceed to evaluate the mass of hydrogen generated by the reaction. The mass of hydrogen is determined by applying the ideal gas law to the hydrogen partial pressure, combined with correction terms for the mass of hydrogen remaining in solution and

Figure 17. Hydrogen Partial Pressure for Lithium-lead test #16 and Δ P for Lead test #15

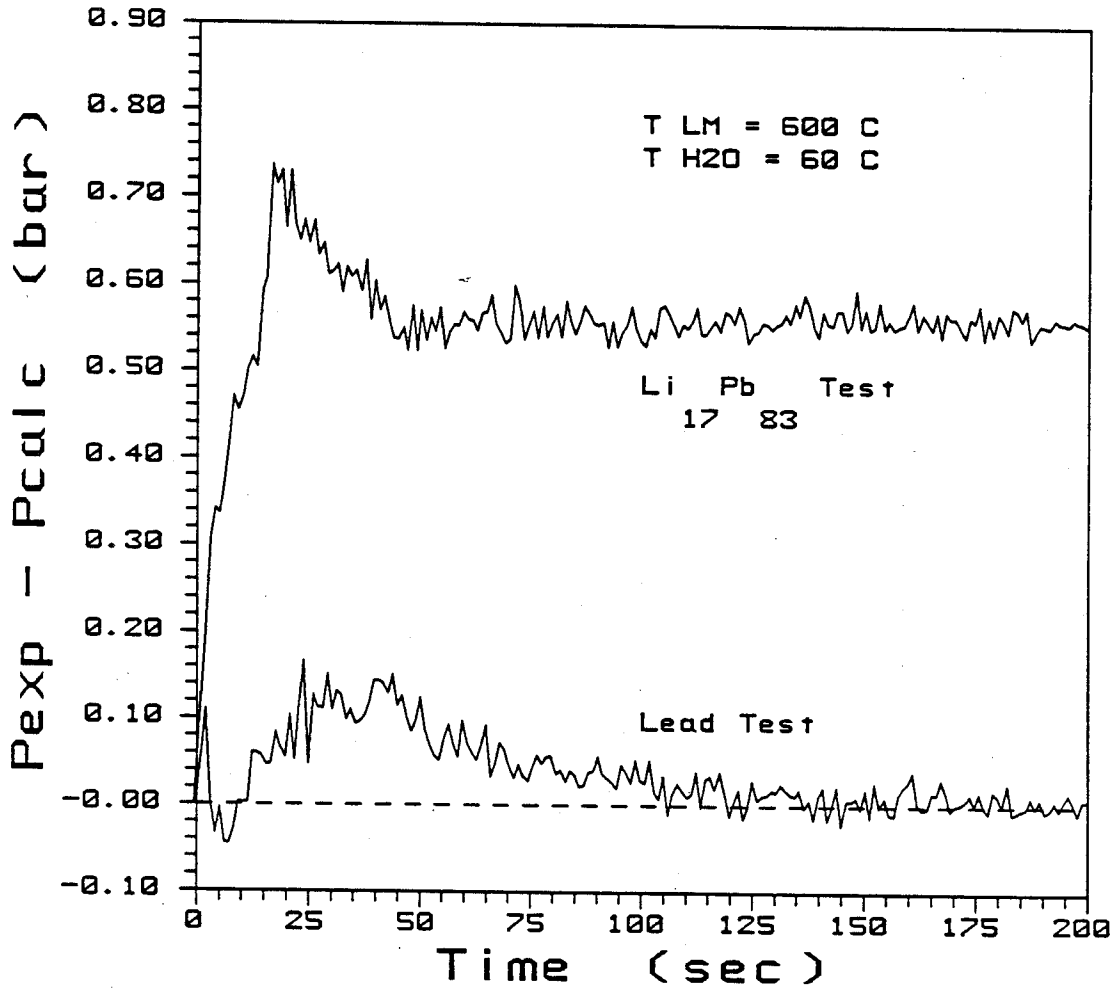

leaking from the system (equation 27).

$$N_{H_2 tot} = \frac{P_{H_2} V_{gas}}{R T_{gas}} + N_{H_2 sol} + N_{H_2 leak} \qquad (27)$$

With this method, the mass of hydrogen for lithium-lead test #16 was calculated (Figure 18). The shape of the mass of hydrogen plot is nearly identical to the hydrogen partial pressure plot. The only difference being due to the last two terms in the above equation. The effect of these terms is relatively small. At 200 s, 97% of the mass of hydrogen generated by the reaction is due to the partial pressure of hydrogen, while only 2.5% is due to hydrogen in solution, and only .5% is accounted for by leakage from the system.

IV.2 Problems with the Experimental Method

Examination of Figure 18 reveals a deficiency in our method of calculating the mass of hydrogen generated by the reaction. Because our method accounts for the total mass of hydrogen generated by the reaction at any time, one would expect this quantity to increase monotonically with time. This is not the case. The calculated mass of hydrogen increases at a great rate, after initiation of the interaction, it then reaches a peak, and ultimately declines to a nearly constant value. This peak in the mass of hydrogen curve corresponds to the peak in the system pressure curve. It should be noted though, that the gas temperature curve for test #16 does not

Figure 18. Mass of Hydrogen for Lithium-lead test #16

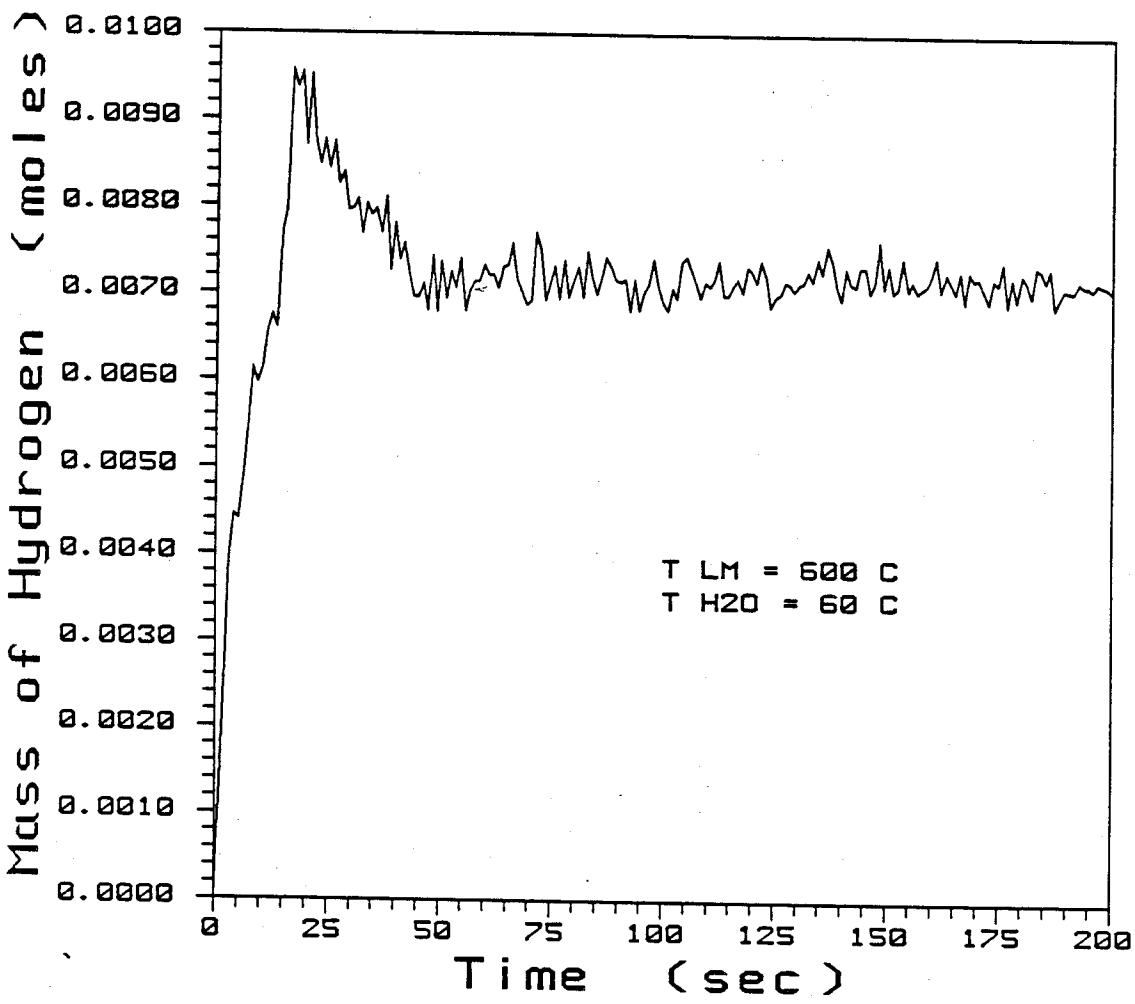

exhibit a corresponding peak. As discussed before, there is an influx of high temperature gas from the lower portion to the upper portion of the apparatus in the initial phase of the interaction. Thus one would expect to see a peak in the gas temperature. This expectation is reinforced by initial state data from test #16. The temperature and mass of gas in the lower portion of the apparatus at the beginning of the experiment was found to be 241.8 C and $3.24 * 10^{-3}$ moles, respectively. While the temperature and mass of gas in the upper portion of the apparatus was found to be 49.3 C and $9.44 * 10^{-3}$ moles. Thus, although the mass of gas in the lower region was only about a third of the mass in the upper region, the greater lower region gas temperature should have caused the mixture gas temperature to increase noticeably. Because our gas temperature measurements did not show this, we suspect that the peak observed in our calculated curves of the partial pressure and mass of hydrogen is due, in part, to inexact measurement of the gas temperature during the initial phase of the interaction. This deficiency in gas thermocouple response is caused by the fact that the gas thermocouple is placed in a thick-walled 3 mm steel thermocouple well, which prevents the thermocouple from accurately reading the quickly varying gas temperature. This is established by the following analysis. Because the Biot number (hD/k) of the thermocouple well is on the order of 10^{-3}, the thermocouple well can be thermodynamically treated as a lumped parameter.[29] This means that the conductive resistance of

resistance of the thermocouple well is negligibly small compared to the convective resistance to heat transfer between the thermocouple well and the surrounding fluid. Thus if the temperature of the surrounding fluid increases suddenly from an initial temperature (T_i) to some constant, final temperature (T_f), the thermocouple well temperature will also increase from T_i to T_f, but as a function of time:[29]

$$T_{TC} = T_i + (T_f - T_i) \exp(- t / \tau) \qquad (28)$$

where $$\tau = \frac{c_{p\,TC}\, \rho_{TC}\, D_{TC}}{2\, h} \qquad (29)$$

The time constant (τ) for the thermocouple well is on the order of 100 s, which implies that the thermocouple would not notice the effect of temperature fluctuations in the surrounding fluid that have periods less than 100 s. Because the system pressure peak occurs within the first 100 s of the interaction, the suspected peak in the actual gas temperature would also occur within the first 100 s of the reaction. Therefore, the gas layer thermocouple is unable to measure the peak in gas temperature in the initial phase of the interaction.

We attempt to correct for the deficiency in the thermocouple response of lithium-lead tests by using the data from corresponding lead tests. This is justified by the fact that tests with the same initial conditions should have similar temperature and pressure responses during the initial phase of the interaction. Thus we

attempt to negate the detrimental effect of the gas thermocouple form the lithium-lead tests by using:

$$P_{H_2\ \text{corrected}} = P - \Delta P_{\text{lead}} - P_{\text{vap}} - P_{Ar} - \frac{N_{H_2 \text{sol}}\, R\, T_{\text{gas}}}{V_{\text{gas}}} \qquad (30)$$

The corrected partial pressure of hydrogen is evaluated in the same manner as before (equation 22) except for the presence of a correction term (ΔP_{lead}), which is equal to the difference between the experimental and calculated pressures from the corresponding lead test. This correction term is evaluated by applying a least-squares curvefit to the ΔP curve (equation 19) of the corresponding lead test.

The corrected partial pressure of hydrogen is then used to evaluate a corrected form of the hydrogen mass using equation 27. Applying the pressure correction technique to the data from lithium-lead test #16, we see limited improvement (Figure 19). Comparing Figures 18 and 19, one notices that the pressure correction method diminishes, but does not eliminate, the peak. Figures 20 and 21 show the effect of applying the pressure correction method to data from two other lithium-lead tests, tests #21 and #25. Figure 20 contains data from test #21, which was a test characterized by an initial water temperature equal to 70 C and an initial liquid metal

Figure 19. Corrected Mass of Hydrogen for Lithium-lead Test #16

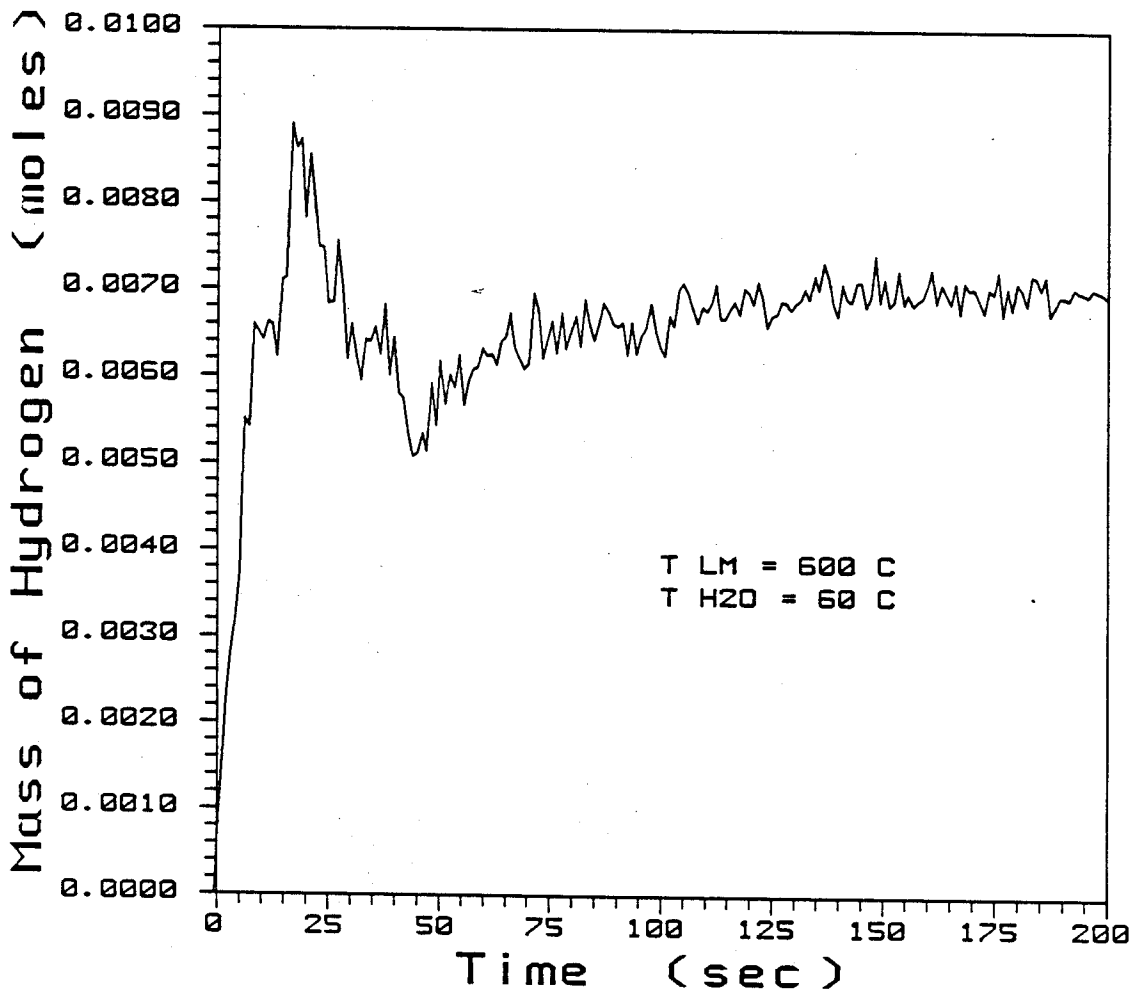

Figure 20. Mass of Hydrogen for Lithium-lead Test #21

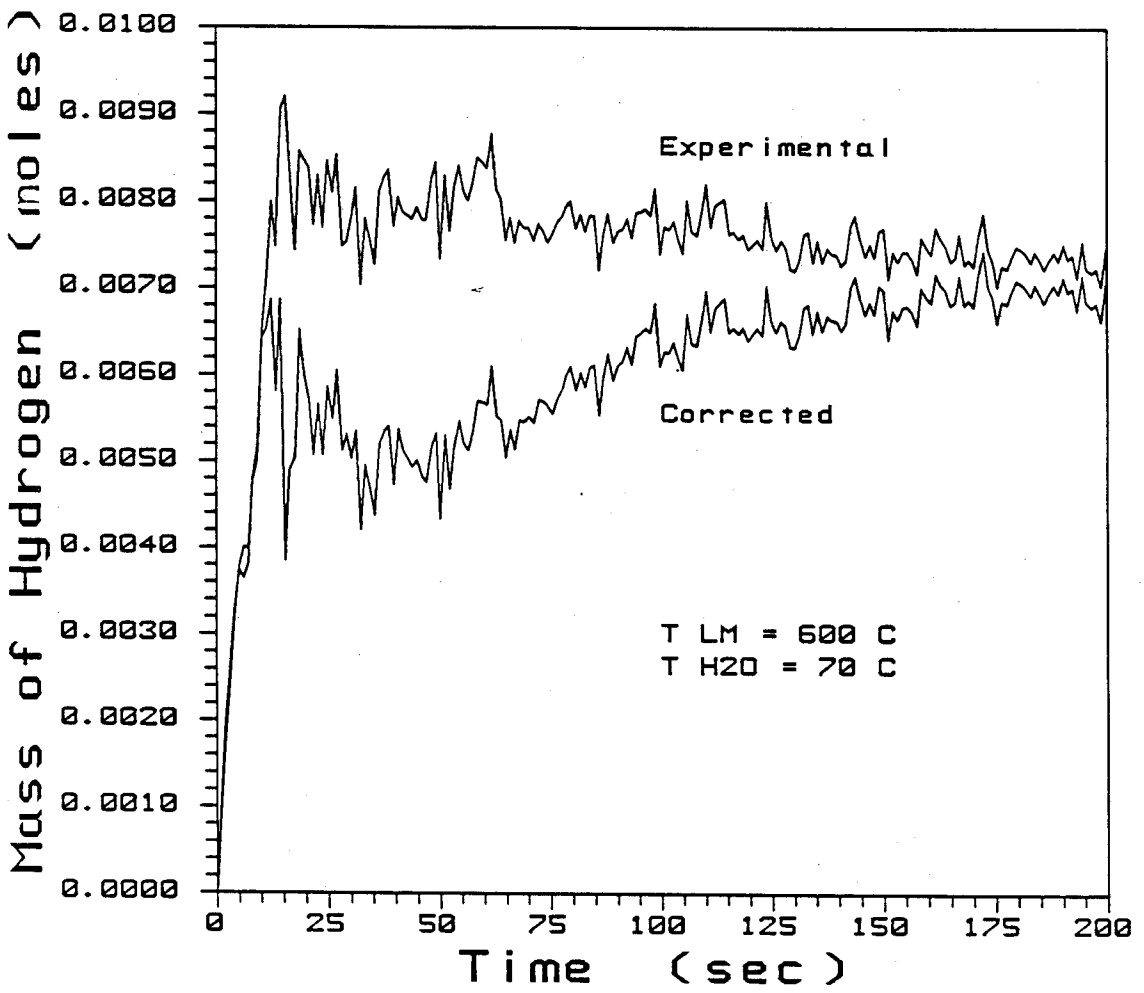

Figure 21. Mass of Hydrogen for Lithium-lead Test #25

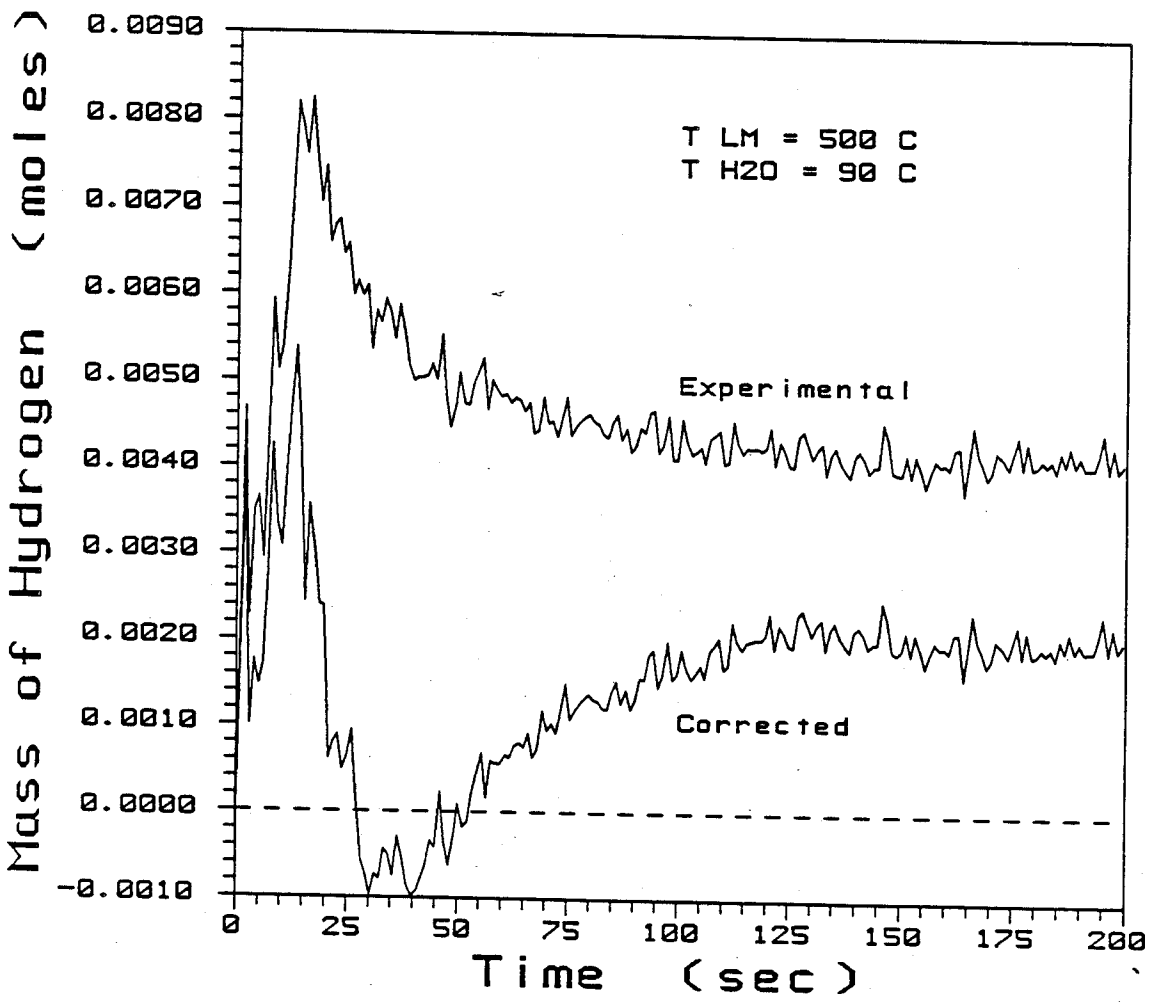

temperature equal to 600 C. Figure 21 contains data from test #25, which was a test characterized by initial water temperature equal to 90 C and initial liquid metal equal to 500 C. These Figures contain plots of the mass of hydrogen as calculated using only the experimental data (equation 27) and as calculated by using the pressure correction method (equation 29). The three preceding figures show that the pressure correction method has limited utility. For tests with low initial water temperature (Figures 19 and 20), the corrected mass of hydrogen curve is relatively close to the anticipated response curve (a monotonically increasing function). For high initial water tests (Figure 21), the correction method does a very poor job at correcting for the peak. The reason for this can be more readily found by examining the partial pressure of hydrogen curve for lithium-lead test #25 and its companion lead test ΔP curve (Figure 22). This figure shows that the pressure peak of the lead test is comparable to the size of the lithium-lead pressure peak. For high initial water temperature tests, the effect of the rapid boiling in the initial phase of the interaction is considerably greater than its effect on low initial water temperature tests. In high initial water temperature tests, the water is only slightly subcooled. Therefore the initial boiling rate will be greater. Also the initial condensation rate will be smaller. Thus the time at which the boiling rate becomes equalized by the condensation rate will be delayed. Because the calculated vapor pressure in equation 19, 22, and 30 are valid

Figure 22. Hydrogen Partial Pressure for Lithium-lead test #25 and Δ P for Lead test #38

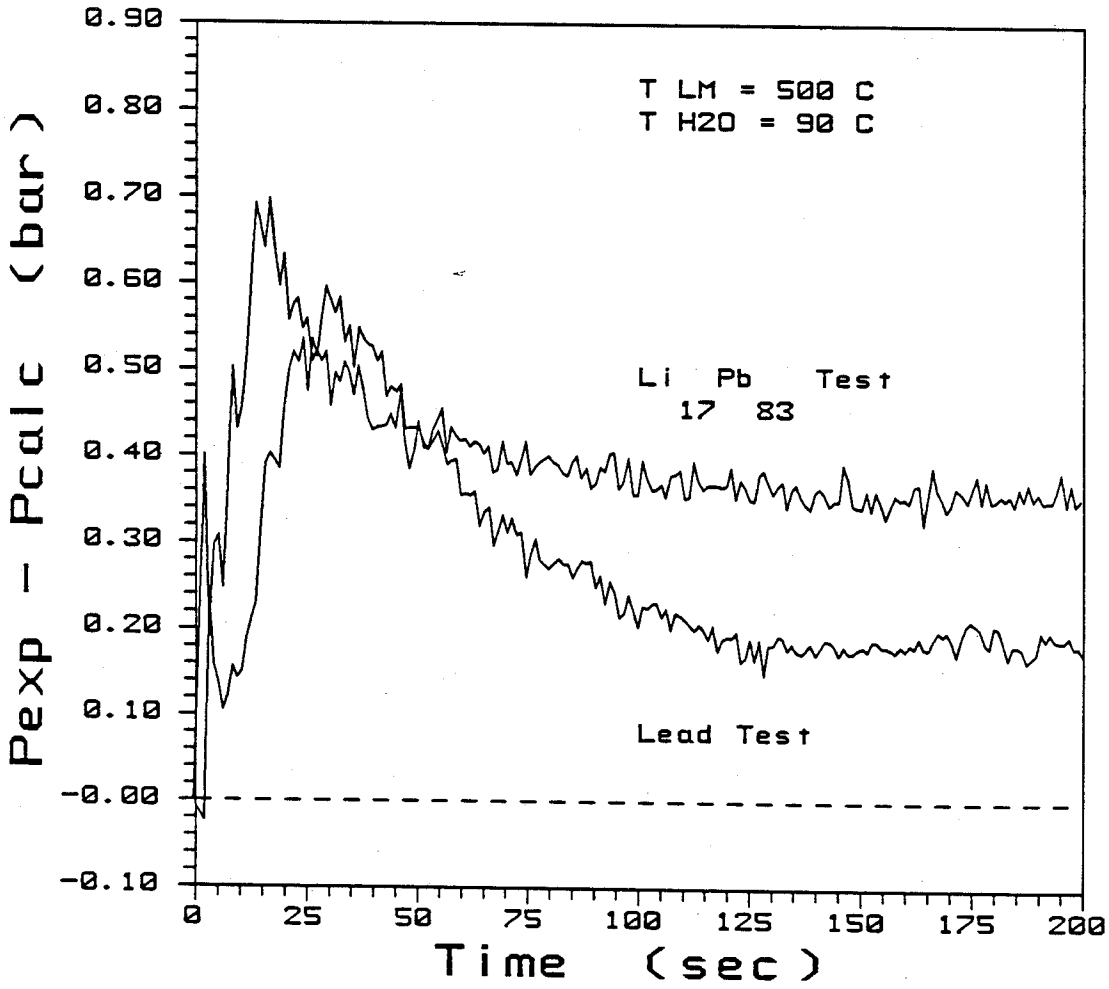

only at equilibrium, the actual vapor pressure in the system during the initial phase of the interaction will be greater than the values used in these equations. The vapor pressure of water increases drastically with increasing temperature. Thus for tests with higher initial water temperatures the effect of unequal boiling and condensation rates on the accuracy of the calculated vapor pressure will be greater than its effect on lower initial water temperature tests.

The error induced by unequal boiling and condensation rates and the deficiency in the time response of the gas layer thermocouple make the accurate evaluation of the partial pressure of hydrogen during the initial phase of the interaction impossible. Although we can attempt to correct for this problem by using the data from corresponding lead tests, this technique provides mixed results in correcting the early time behavior. Therefore we can satisfactorily determine the mass of hydrogen in the system only after thermodynamic equilibrium has been reached. Since our data indicate that the system pressure, gas temperature, and water temperature reach equilibrium values only after 100 - 150 s into the interaction, we are confident in our calculated values of the mass of hydrogen generated by the reaction only for times greater than 150 s.

Because of the limited utility of the pressure correction technique in determining the initial phase partial pressure of hydrogen, one may wonder why it is used at all. But it is needed to

correct a different problem. Returning our attention to Figure 22, one should notice that, even after equilibrium has been reached, the Δ P curve of lead test #38 does not converge to zero as it should. This is due to a deficiency in the response of the gas layer thermocouple not related to the one mentioned earlier. Because the gas layer thermocouple well is bolted into the upper plate, the temperature measured by a thermocouple placed in it will be influenced by the temperature of the upper plate, if upper plate temperature is significantly different than the gas layer temperature. For high initial water temperature tests (90 C), the temperature of the upper plate is as much as 10 C lower than the measured gas layer temperature. For low initial water temperature tests (60 C), this temperature difference is virtually nonexistent. When the upper plate temperature is less than the gas temperature, the thermocouple well is cooled by conduction to the upper plate. This in turn causes the gas layer thermocouple to report a temperature which is lower than the actual gas layer temperature. This is the same phenomenon that affected the thermocouple used to measure the argon temperature in the lower gas region (see page 59). Therefore the actual gas temperature (T_{gas}) is related to the measured gas temperature (T_{TC}) and the upper plate temperature (T_{UP}) by:

$$\frac{T_{UP} - T_{gas}}{T_{TC} - T_{gas}} = \cosh\left(\left(\frac{4\,h}{D_{TC}\,k_{TC}} \right)^{1/2} L_{TC} \right) \qquad (31)$$

For lead test #38, we placed, on the upper plate, a thermocouple at the base of the gas layer thermocouple well. As shown in Figure 23, the temperature of the upper plate was consistently lower than the measured gas temperature. We then added a subroutine to our experimental analysis program that calculated the gas layer temperature using the experimentally measured gas layer and upper plate temperatures and equation 31. As shown in Figure 24, this change has a significant effect on ΔP for lead test #38. The upper plot in this figure shows ΔP as evaluated using the measured gas temperature, the lower plot shows ΔP as evaluated with the gas temperature calculated with equation 31. As established by this figure, a portion of the initial phase pressure peak is due to the effect of the gas layer thermocouple being cooled by the upper plate. But more importantly, this figure shows that with the actual gas layer temperature, the ΔP curve for high initial water temperature lead tests will indeed converge to zero.

Unfortunately, we did not know that this problem existed because the high initial water temperature lead tests were not performed until late in the test series. Thus we have to rely on the pressure correction method to give us the mass of hydrogen during the equilibrium phase of the high initial temperature tests. For low initial water temperature tests, the upper plate temperature is equal to the measured gas temperature. For these tests, the measured equilibrium gas temperature is correct. This is established by the

Figure 23. Gas Layer and Upper Plate Temperatures for Lead Test #38

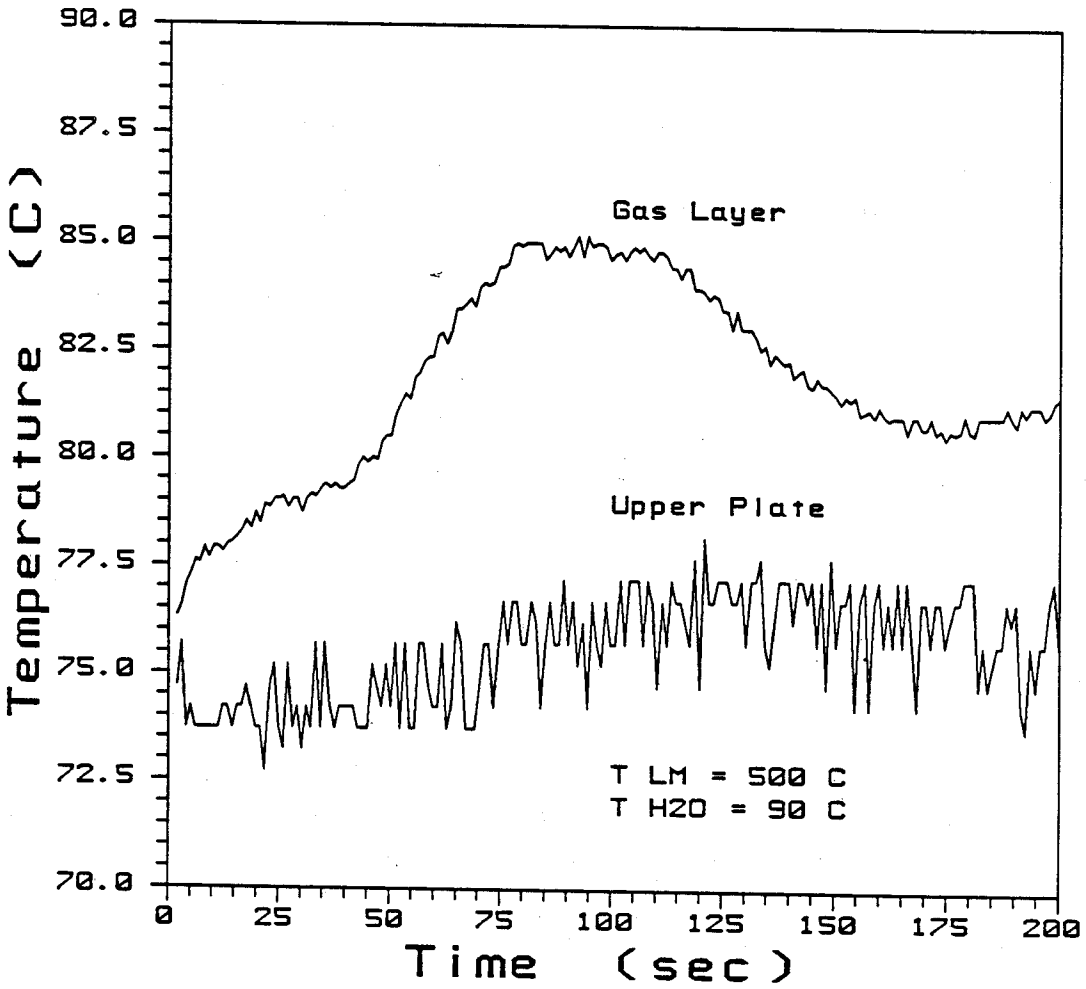

Figure 24. Δ P for Lead Test #38

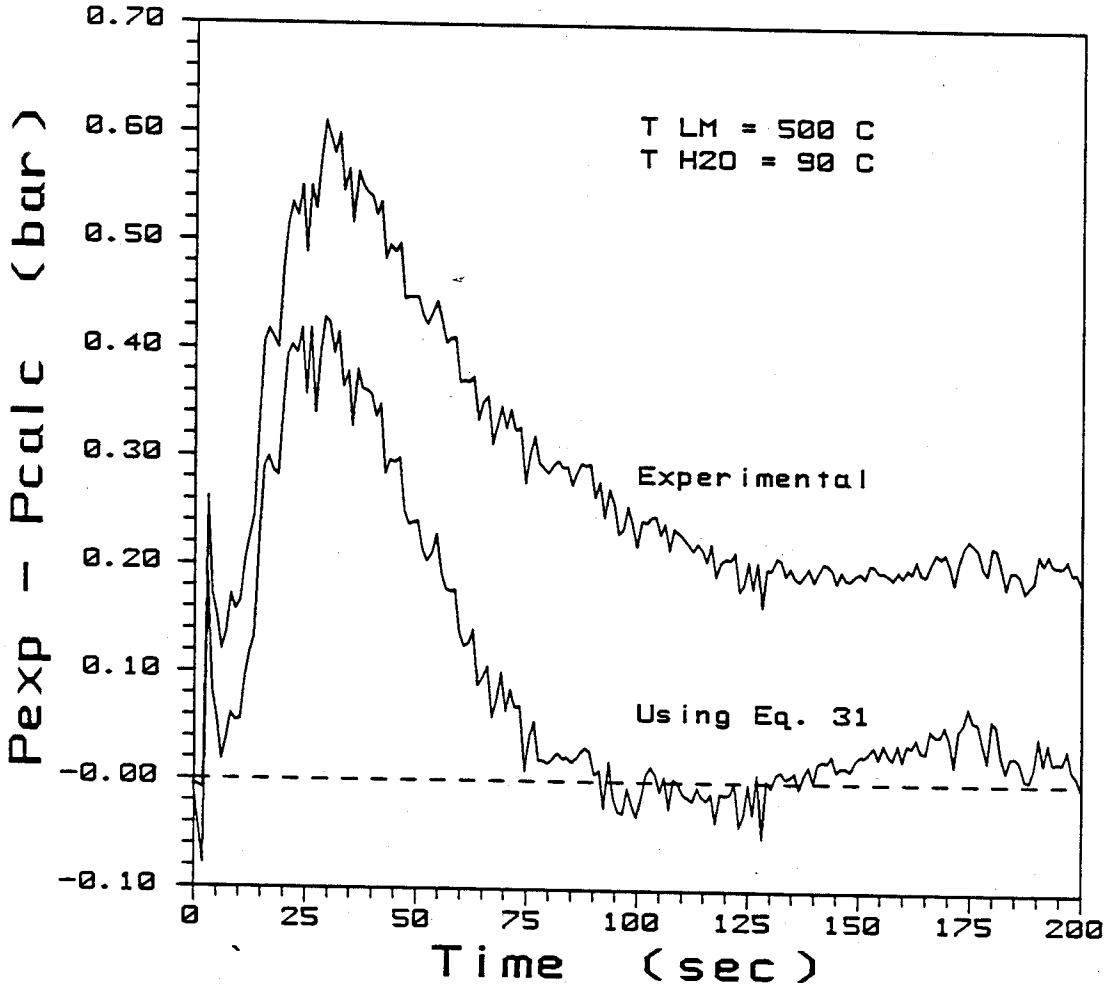

fact that ΔP for low initial water temperature tests converges to zero. This also means that the hydrogen partial pressure of low initial water temperature lithium-lead tests evaluated with the pressure correction method will approximately equal the hydrogen partial pressure evaluated with the data from the lithium-lead test alone, after equilibrium has been reached.

IV.3 Collected Results

After having described the application of thermodynamic principles to the raw data from specific experiments, which provided us with a means of determining the mass of hydrogen generated by the reaction during these experiments, we are now ready to proceed to analyze the results obtained by applying this process to the whole range of experiments. As described in the last section, difficulties attributed to the nature of the experiment prevented us from accurately determining the mass of hydrogen generated by the reaction during the first 150 s of the experiment. Since we are interested in investigating how variations in the two main system variables (initial water temperature and initial liquid metal temperature) affect the extent of the reaction, we concentrate on the mass of hydrogen generated by the reaction at some time during the equilibrium phase of the interaction. We have chosen to concentrate on the mass of hydrogen generated by the reaction 200 s into the interaction. On the following page we have tabulated the collected

Table 2. Collected Data from the Lithium-lead Tests

$Li_{17}Pb_{83}$ Test Number	T_i LM (C)	T_i H_2O (C)	Mass $Li_{17}Pb_{83}$ (gr)	Pb Test Number	N_{H_2} (200 s) (* 10^3 mole)	N_{H_2} (200 s) Corrected (* 10^3 mole)
16	600	60	47.0	15	7.12 +/- .65	7.01 +/- .83
17	600	60	56.3	15	6.62 +/- .64	6.48 +/- .82
20	600	90	39.8	34	9.78 +/- .89	7.47 +/- 1.2
21	600	70	67.9	35	7.33 +/- .68	6.97 +/- .86
22	600	80	51.3	37	6.95 +/- .69	4.84 +/- .94
23	350	90	64.3	39	1.94 +/- .62	0.98 +/- .86
24	400	90	61.7	36	8.28 +/- .76	6.73 +/- .98
25	500	90	56.4	38	4.08 +/- .66	2.04 +/- .92
26	350	90	16.9	39	1.18 +/- .60	0.84 +/- .82
27	400	90	30.0	36	7.32 +/- .73	5.77 +/- .96
28	500	90	25.2	38	2.95 +/- .61	0.94 +/- .92
29	600	90	25.9	34	8.47 +/- .81	6.94 +/- 1.2
30	600	70	19.0	35	6.49 +/- .66	6.12 +/- .85
31	500	70	19.2	40	2.96 +/- .56	2.74 +/- .75
32	400	80	31.5	41	3.76 +/- .63	3.75 +/- .83
42	600	60	35.5	15	8.81 +/- .73	8.68 +/- .89
43	600	60	32.8	15	6.53 +/- .60	6.40 +/- .79

results of the lithium-lead experiments. For each lithium-lead test, the table has listed: the initial liquid metal temperature, the initial water temperature, the mass of lithium-lead used in the test, the number of the corresponding lead test, the mass of hydrogen at 200 s evaluated with the experimental data alone (equation 27), and the mass of hydrogen evaluated using the pressure correction method (equation 30). This table shows that we were able to perform only a limited number of lithium-lead tests (seventeen). The distribution of these tests are as follows. Two tests, both with initial water temperatures of 90 C, were performed with initial liquid metal temperatures of 350 C. Three tests, one with initial water temperatures at 80 C, the other two with initial water temperatures at 90 C, were performed with initial liquid metal temperatures of 400 C. Three tests, one with initial water temperatures at 70 C, the other two with initial water temperatures at 90 C, were performed with initial liquid metal temperatures of 500 C. The other nine tests had initial liquid metal temperatures of 600 C, with this distribution of initial water temperatures; four tests at 60 C, two tests at 70 C, one test at 80 C, and two tests at 90 C. The great number of tests with initial liquid metal temperatures of 600 C were performed for the following reasons. First, as mentioned earlier, the 600 C initial liquid metal temperature tests could withstand up to 45 C subcooling in the initial water temperature, with film boiling at the interaction surface still insured. This meant that the 600 C initial liquid metal

tests afforded us with the greatest range of initial water temperatures to investigate the effect of initial water temperature on the reaction. Secondly, we found that the 600 C initial liquid metal temperature tests provided the greatest extent of reaction, which meant that their results would be the least ambiguous.

The trends contained in the collected data are most fully appreciated when presented in graphical form. The first relationship we will discuss is the effect of initial water temperature on the reaction. In Figure 25, the mass of hydrogen at 200 s, evaluated using equation 27, is graphed as a function of initial water temperature. The data presented in this figure are for tests with initial liquid metal temperatures equal to 600 C. The straight line in this figure is the least-squares curvefit of the 11 data points. Although this figure seems to indicate that the extent of the reaction is proportional to initial water temperature, Figure 26 shows that extent of reaction, in fact, is not a function of initial water temperature. Figure 26 graphically presents the mass of hydrogen at 200 s, evaluated with the pressure correction method (equation 30), again for the tests with initial liquid metal temperatures of 600 C. The least-squares curvefit of the data in this graph establishes that the extent of reaction is not a function of the initial water temperature. Analysis of these two figures reveals that the pressure correction method lowers the calculated values of the mass of hydrogen at 200 s for high initial water temperature tests. But the

Figure 25. Mass of Hydrogen (200 s) as a Function of Initial Water Temperature

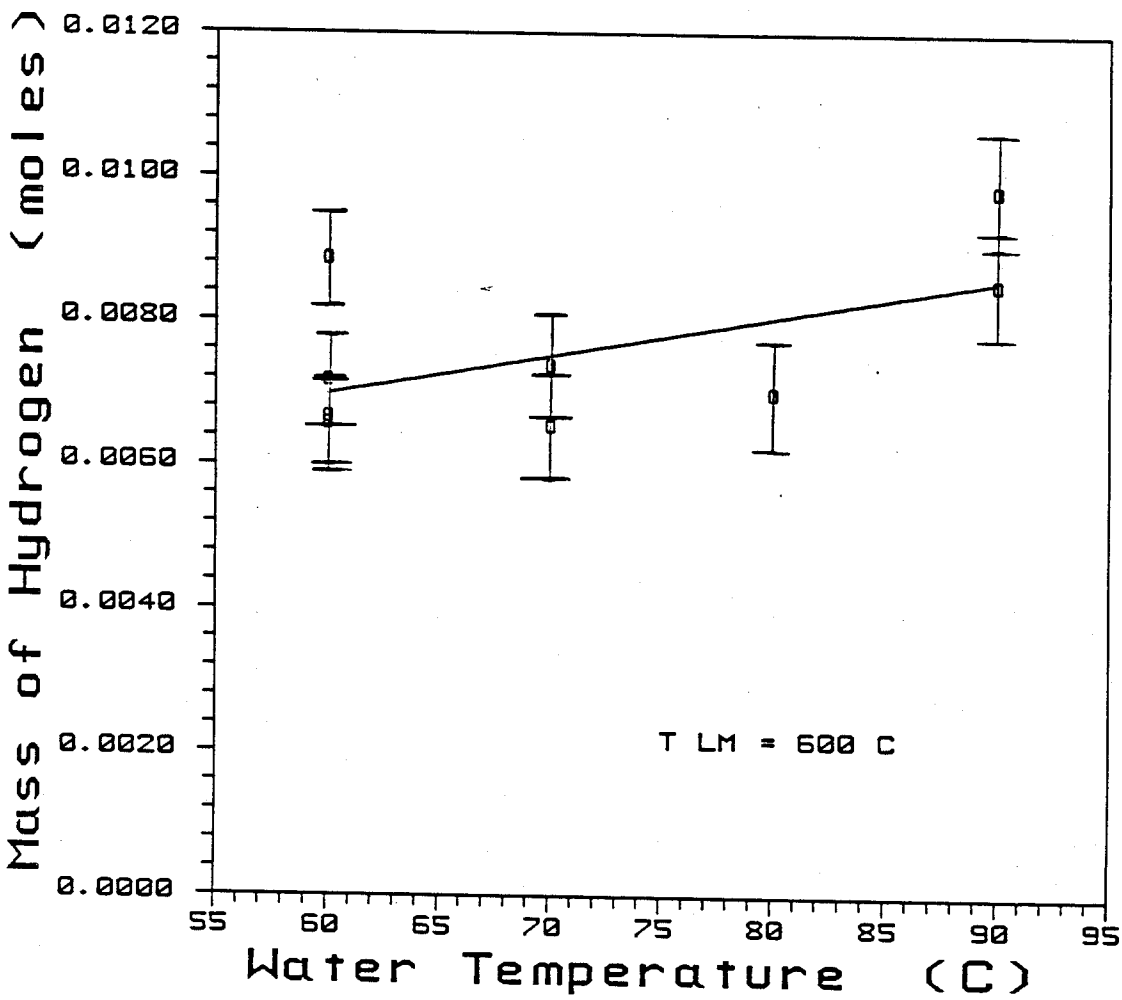

Figure 26. Mass of Hydrogen (200 s) as a Function of Initial Water Temperature Using the Pressure Correction Method

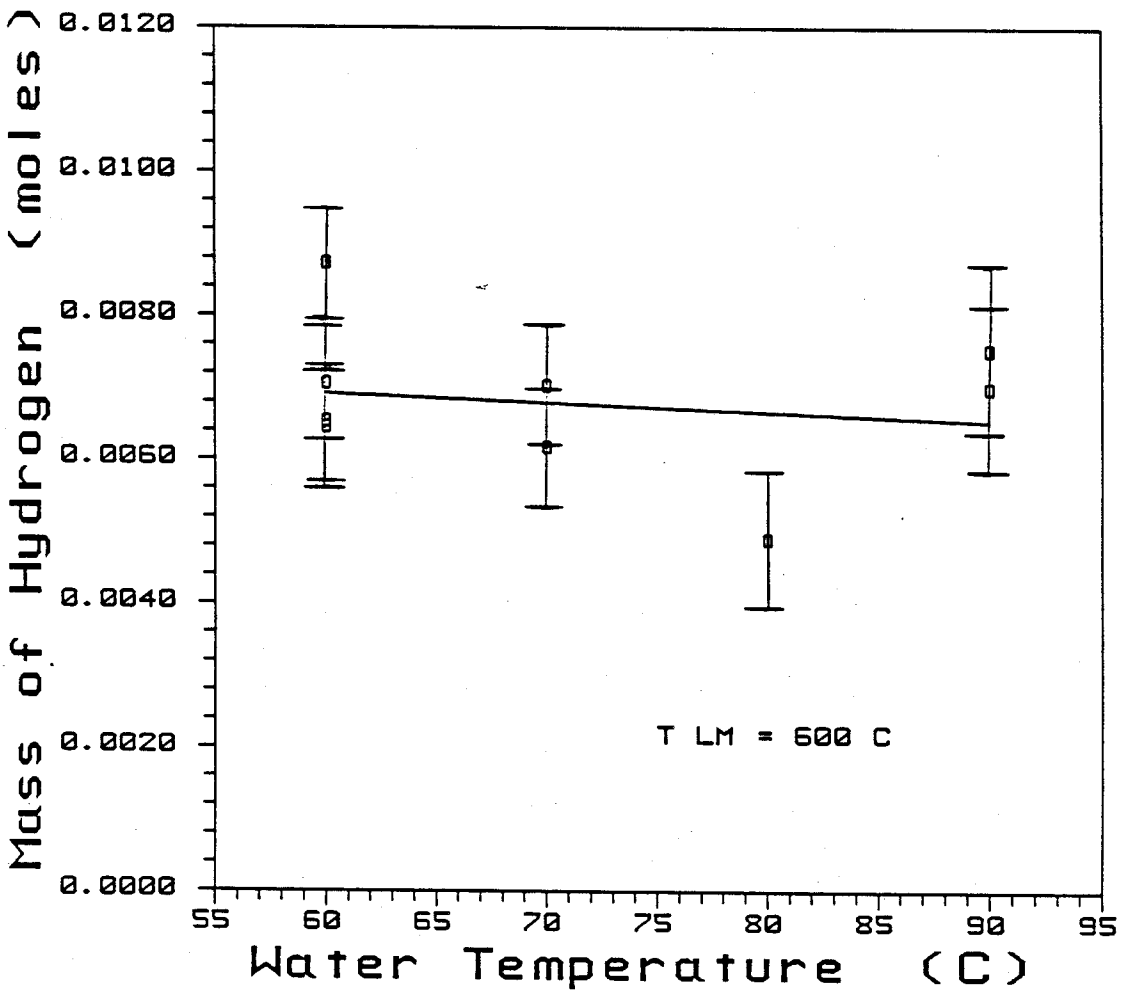

pressure correction method has little effect on the calculated values of the mass of hydrogen at 200 s for low initial water temperature tests. As described above, the pressure correction method rectifies the error in the measured gas temperature induced by conduction through the thermocouple well to a cool upper plate. Since the effect of the pressure correction method is proportional to the initial water temperature, this implies that the size of the error in the measured gas temperature due to conduction through the thermocouple well is also proportional to the initial water temperature. This of course is no surprise since the rate of heat loss to the surroundings is proportional to the difference in temperature between the system and the surroundings. Increasing the initial water temperature increases the rate of heat loss by conduction through the thermocouple well, and its effect on the measured gas temperature.

Because the mass of hydrogen produced during the experiments is a function of the area of interaction, one can generalize the results of the experiments by expressing the mass of hydrogen generated during the experiments as a function of unit area. In Figure 27 the corrected mass of hydrogen per unit area is shown as a function of the initial water temperature. The data in this graph is derived by dividing the corrected mass of hydrogen at 200 s by the area of interaction for the experiments ($5.067 * 10^{-4}$ m^2).

Generally speaking, the reaction consumed only a modest portion of the total inventory of lithium in the metal samples. This is

Figure 27. Mass of Hydrogen per Unit Area as a Function of Initial Water Temperature

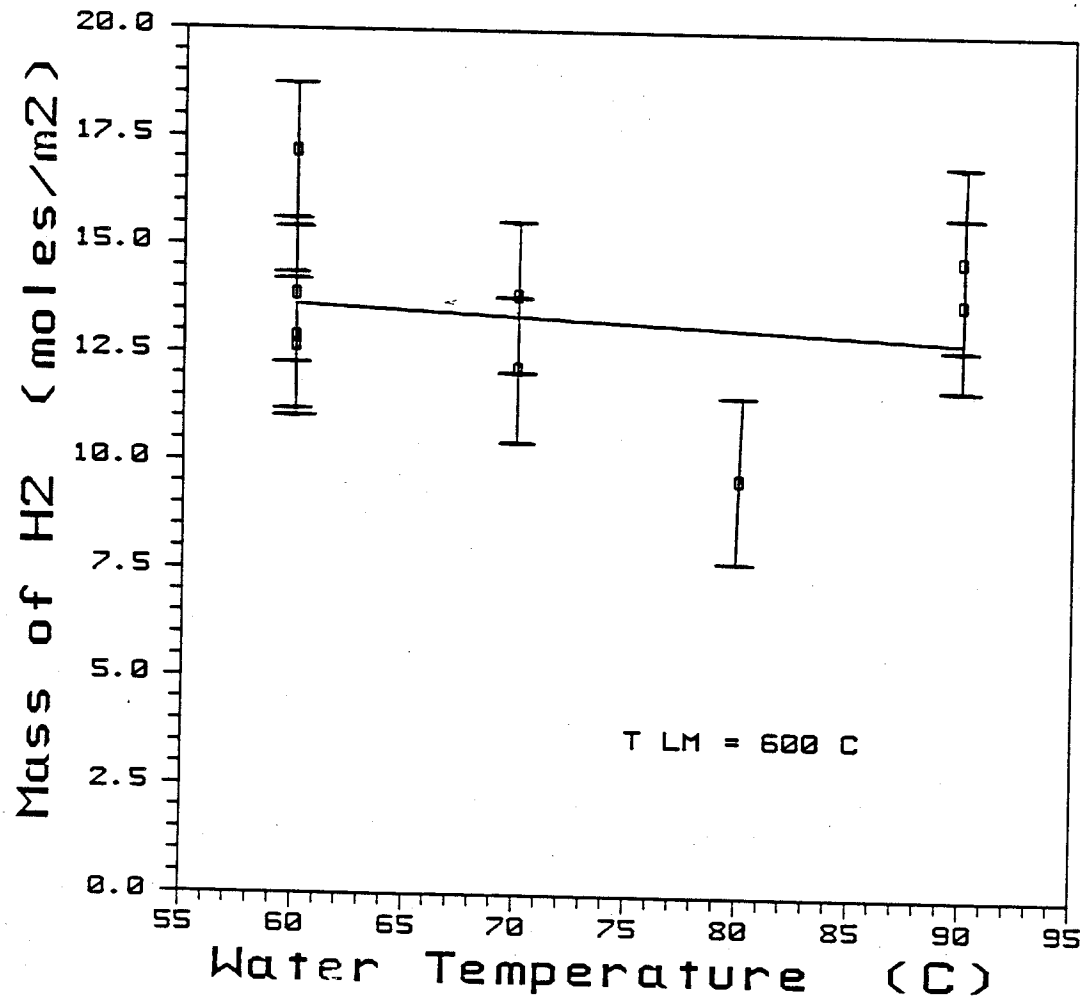

established by Figure 28. This figure shows the percentage of the lithium inventory consumed by the reaction as a function of initial water temperature. The moles of hydrogen generated during the reaction equal one half of the number of moles of lithium consumed during the reaction, regardless of the reaction path (see equations 1 and 2). Thus the percentage of the lithium inventory consumed by the reaction can be estimated by:

$$\% \text{ Li reacted} = \frac{2\, N_{H_2}(200\text{ s})\; M_{Li_{17}Pb_{83}}}{.17\; m_{Li_{17}Pb_{83}}} \qquad (32)$$

The corrected mass of hydrogen produced by the reaction at 200 s is used in the above equation because it represents at least 95 % of the mass of hydrogen generated over the entire course of the experiments (30 minutes). The great spread of the data in Figure 28 is due to the fact that the extent of the reaction is not a function of mass of the metal sample ($m_{Li17Pb83}$). This can be shown by examining the mass of hydrogen data from lithium-lead tests 21 and 30, which were characterized by initial water temperatures of 70 C and initial liquid metal temperatures of 600 C. The corrected mass of hydrogen at 200 s for test 30 is only 12% less than the mass of hydrogen at 200 s for test 21, this difference is less than the uncertainty of the data (roughly 13%). But the percentage of lithium consumed by the reaction for test 30 is 65.6% while the percentage of lithium consumed by the reaction for test 21 is only 20.8%. This divergence

Figure 28. Percentage of Lithium Consumed by the Reaction as a Function of Initial Water Temperature

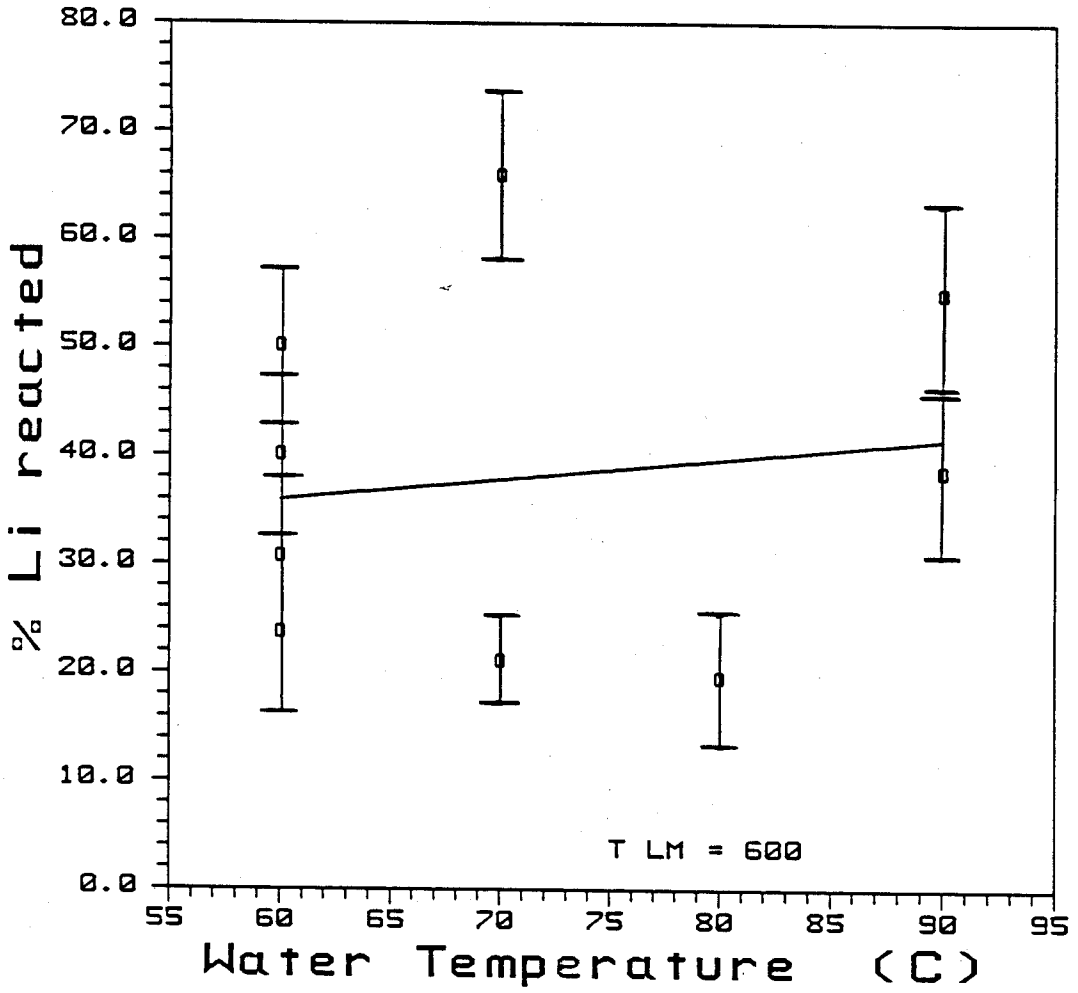

in the percentage of lithium consumed by the reaction is accounted for by the great difference in the mass of metal samples used in the two tests (67.9 gm in test 21, 19.0 gm in test 30). This mass variation was caused by the available liquid metal inventory for our tests. Thus, although the mass of metal used in the two tests varies by almost a factor of four, the extent of the reaction varies within the range of uncertainty of the data.

We have seen that the extent of the reaction is not a function of the initial water temperature. Next we consider how the extent of reaction varies as a function of initial liquid metal temperature. Figure 29 contains a graphical representation of the mass of hydrogen at 200 s as a function of the initial liquid metal temperature. Because we have shown that the pressure correction method negates the effect of conduction through the thermocouple well, the data points in Figure 29 were derived with the pressure correction method. The lines in the graph are connected to the mean of the distribution of data points at each of the four values of initial liquid metal temperatures. The mean values of the mass of hydrogen at each initial liquid metal temperature are; 6.77 +/- .31 * 10^{-3} moles at $T_{i\ LM}$ = 600 C, 1.91 +/- .51 * 10^{-3} moles at $T_{i\ LM}$ = 500 C, 5.42 +/- .53 * 10^{-2} moles at $T_{i\ LM}$ = 400 C, and 0.91 +/- .59 * 10^{-3} moles at $T_{i\ LM}$ = 350 C. The behavior of the extent of reaction as a function of initial liquid metal temperature as illustrated in this figure is difficult to interpret, especially given the sparse distribution

Figure 29. Mass of Hydrogen at 200 s

As a Function of Initial Liquid Metal Temperature

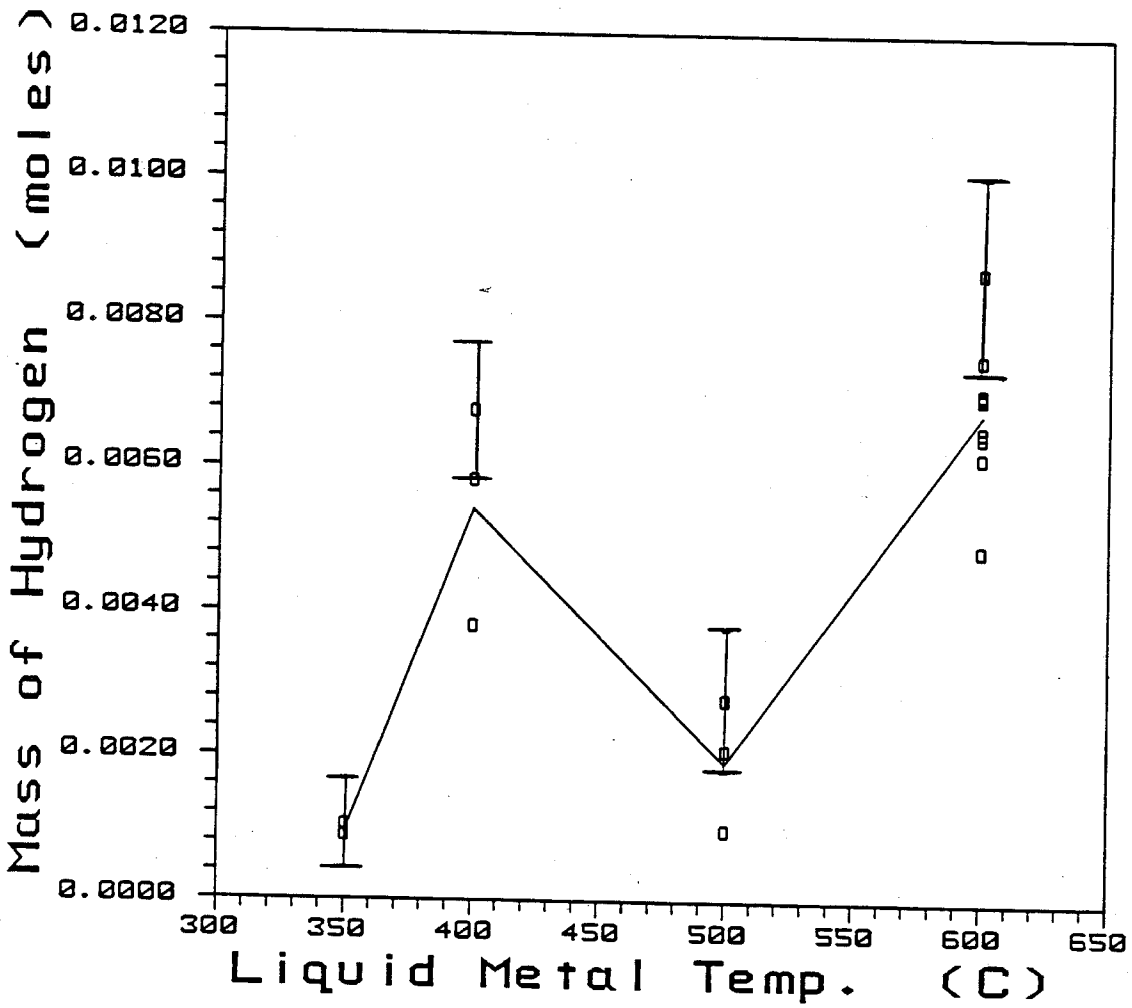

of tests - only 17 lithium-lead tests were conducted, spread across 4 values of initial liquid metal temperature. Yet the following facts can be gathered from this Figure. The extent of reaction as a function of initial liquid metal temperature increases with increasing initial liquid metal temperature, at low values of the initial liquid metal temperature. For initial liquid metal temperatures varying between 400 C and 500 C, the reaction appears to go through some sort of transition. For initial liquid metal temperatures above 500 C, the extent of reaction again increases with increasing initial liquid metal temperature.

As before, we can generalize the trends in the corrected mass of hydrogen data by dividing it by the area of interaction. In Figure 30 the corrected mass of hydrogen at 200 s per unit area is shown as a function of the initial liquid metal temperature. We also include a figure showing the percentage of lithium consumed by the reaction as a function of initial liquid metal temperature (Figure 31). As before, the great spread of the data in this figure is mainly accounted for by the variation in the mass of the metal used in the tests.

Referring to the work of other investigators, as described in the second chapter, Baker and Just[12] found that the extent of the zirconium/water reaction increased with increasing metal temperature. Arrhenius[13] showed that the rate at which a particular reaction proceeds can be expressed as a function of the exponential of the reactant temperature (equation 7). Baker and Just found that the

Figure 30. Mass of Hydrogen per Unit Area as a Function of Initial Liquid Metal Temperature

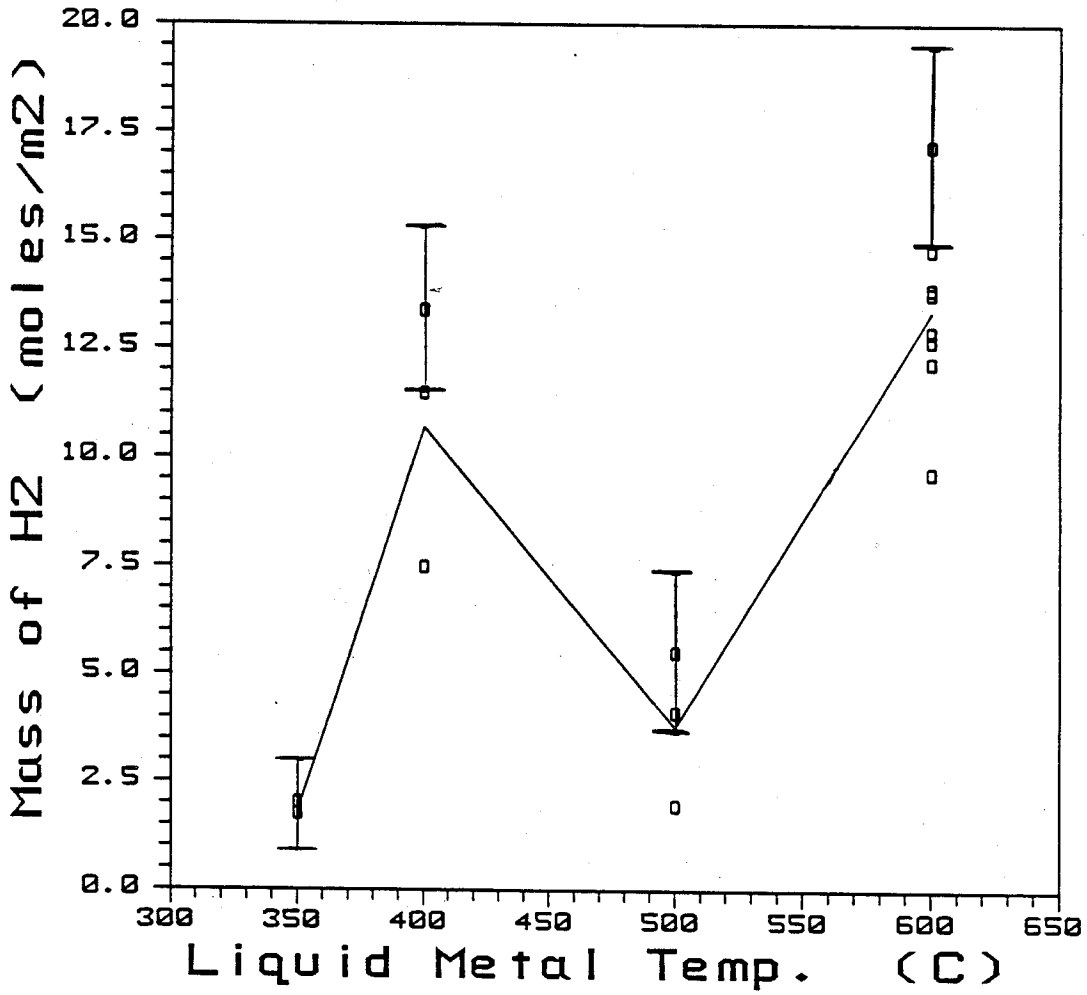

Figure 31. Percentage of Lithium Consumed by the Reaction as a Function of Initial Liquid Metal Temperature

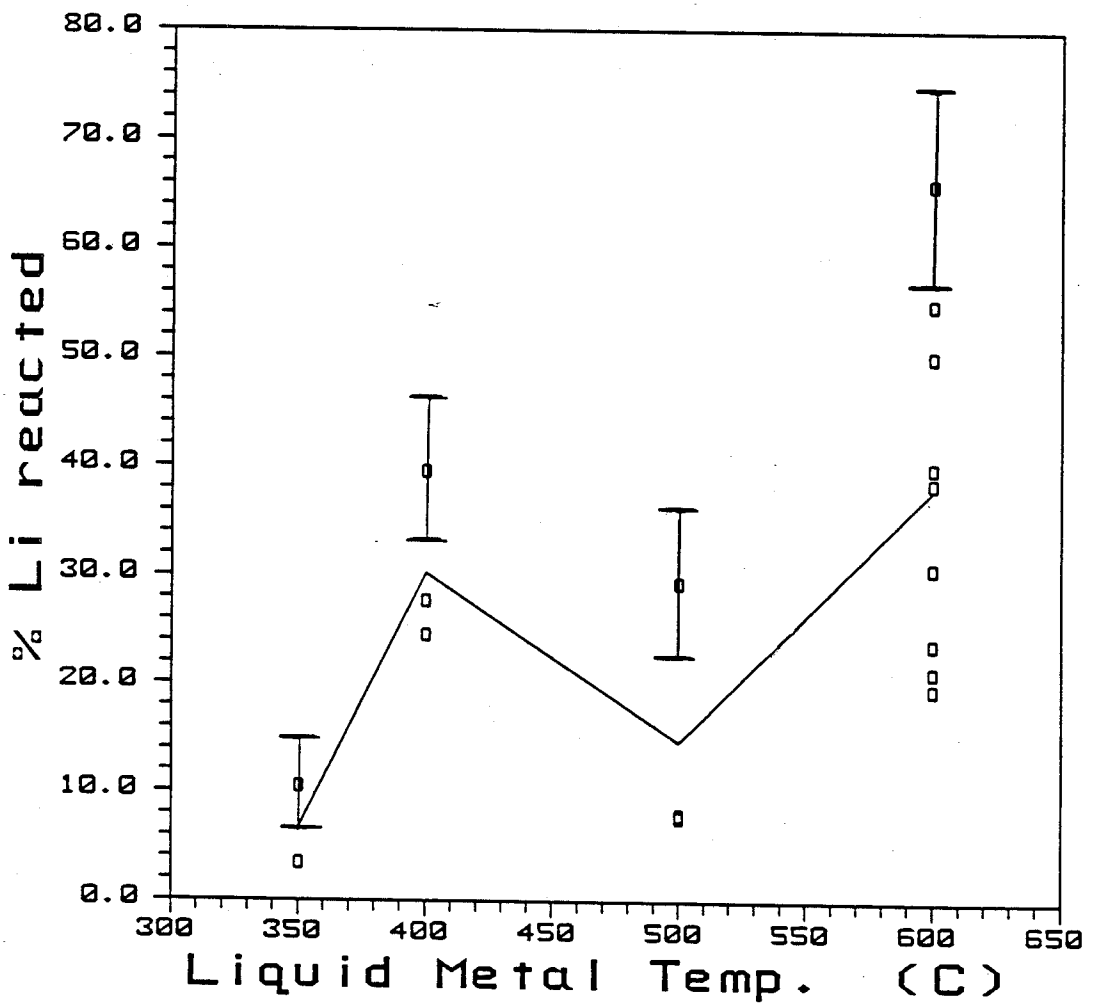

zirconium/water reaction was also dependent upon an Arrhenius form of the reaction rate (equation 5). One would thus expect the extent of the lithium/water reaction to increase with increasing liquid metal temperature. The transition that the reaction goes through between 400 C and 500 C indicates that the lithium/water reaction must either rely upon a mechanism completely different from the Arrhenius form of reaction temperature dependency, or it must rely on some hybrid of the Arrhenius form of reaction temperature dependency.

The idea that a hybrid of the Arrhenius form of reaction temperature dependency controls the lithium/water reaction becomes apparent if one remembers that the lithium/water reaction can proceed by one of two reaction paths.

$$2\,Li + H_2O \rightarrow Li_2O + H_2 \qquad (1)$$

$$2\,Li + 2\,H_2O \rightarrow 2\,LiO\,H + H_2 \qquad (2)$$

It is possible that one of these reaction paths dominates for initial liquid metal temperatures below 400 C, and that the other dominates for initial liquid metal temperatures greater than 500 C. If these two reactions proceed at greatly different rates, the observed experimental behavior could then result.

Another possibility arises when one considers that one of the reaction products (LiOH) goes through a phase change (melting) as its temperature increases from 400 C to 500 C. The melting point of pure lithium hydroxide is 470 C. It is possible that the presence of

the solid phase of the reaction product provides less resistance to diffusion than the liquid phase of the reaction product. At first, this may seem like a contradiction, because it has generally been found that the atomic diffusivity of the solid phase of a metal is considerably lower than the atomic diffusivity of the liquid phase.[30] If, at low temperatures, the solid phase of the lithium hydroxide forms in the liquid metal solution, it will accumulate at the top of the liquid metal because its density is less than that of the liquid metal. And since lithium hydroxide is soluble in water,[31] a portion of the lithium hydroxide at the top of the metal pool may dissolve into the water. At 80 C, a saturated solution of water and lithium hydroxide will contain .166 gm LiOH / gm H_2O.[31] Therefore any lithium hydroxide that reaches the top of the metal pool and mixes with the water will dissolve into the water. If a portion of the lithium hydroxide formed in the reaction dissolves into the water during the experiment, the rate of diffusion in the liquid metal will be enhanced.

At this point, we only have a pair of hypotheses to explain the aberrant behavior of the extent of reaction to changes in the initial liquid metal temperature. In the next chapter we will present an analytical model for the reaction that can be used to predict the course of the reaction, given data drawn from the experiments. After discussing the significance of the model, we will formulate a possible explanation for the observed aberrant behavior.

IV.4 Error Analysis

Before we proceed to the description of our reaction model, we want to present a few notes on the error involved with our experiment. Our analysis of the experiment depended upon the data from four diagnostic devices and their supporting electronics; the pressure transducer, the liquid metal well thermocouple, the water thermocouple, and the gas layer thermocouple. We measured the error inherent to these devices and their supporting electronics by calculating the standard deviation of the signal from these devices, when they were given constant, known inputs. For the pressure transducer, we simply recorded its response, for an hour, at atmospheric pressure. The three thermocouples were placed in the constant temperature bath for an hour. The standard deviation of the pressure transducer is $6.2 * 10^{-3}$ bar. The standard deviation of the liquid metal well thermocouple is .70 C. The standard deviation of the water thermocouple is .64 C. And the standard deviation of the gas layer thermocouple is .43 C.

Knowing the uncertainty in the system variables, the uncertainty in the calculated mass of hydrogen can be found by applying the error propagation formula to equation 27, which is used to evaluate the mass of hydrogen generated by the reaction. The error propagation formula expresses the standard deviation of any derived quantity as a function of the standard deviations of the variables used in the evaluation of that quantity.[32] In particular, the standard

deviation of the mass of hydrogen (σ_{NH2}) is given by:

$$\sigma_{N_{H_2}}^2 = \left(\frac{d\,T_{gas}}{d\,N_{H_2}}\right)^2 \sigma_{T_{gas}}^2 + \left(\frac{d\,P}{d\,N_{H_2}}\right)^2 \sigma_P^2 + \left(\frac{d\,V_{gas}}{d\,N_{H_2}}\right)^2 \sigma_{V_{gas}}^2 \qquad (33)$$

The uncertainty in the calculated mass of hydrogen is a function of the uncertainty in the measured gas temperature, the measured system pressure, and the gas layer volume. We include a factor for the uncertainty in the total gas volume. The total system volume, measured on three separate occasions, is 1.345 +/- .005 l. The gas volume is given by the difference between the total volume and the water and liquid metal volumes. The water volume used in the experiments was 1.000 +/- .005 l. Since the uncertainty in the liquid metal volume is much less than .005 l (the total metal volume was never greater than .008 l), the uncertainty in the gas volume is .007 l. There is a possibility that a small amount of argon gets trapped in the lower portion of the gas feed line after the interaction has started. The calculation of the mass hydrogen is based on the assumption that all of the gas in the system accumulates at the top of the apparatus. Thus any gas that remains in the lower portion of the pressure equalization line will have a temperature which is different from the gas temperature. But since the volume of the

lower portion of the pressure equalization line is roughly .004 cm^3, and since the temperature of this region is strongly influenced by the bulk water temperature the uncertainty this introduces into the calculated pressure is negligible.

The error propagation formula was used to calculate the uncertainties in the mass of hydrogen at 200 s data points listed in Table 2. The use of this formula gives us an estimate of the experimental error. Another means of estimating the error inherent in the experiment is to evaluate the standard deviation from the mean of the a series of tests performed with the same initial conditions. To help us in this task, we conducted four experiments with initial liquid metal temperatures of 600 C and the initial water temperatures of 60 C. This set of initial conditions was chosen because the extent of reaction is greatest at 600 C, and the effect of conduction through the thermocouple well is smallest at 60 C. The mean mass of hydrogen at 200 s for these four tests, evaluated with the lithium-lead test data alone, is 7.27 +/- .83 * 10^{-3} moles. And the mean mass of hydrogen at 200 s for these four tests, using the pressure correction method, is 7.14 +/-0.94 * 10^{-3} mole. For these tests the standard deviation is 11% of the mean hydrogen mass at 200 s, as evaluated with either method.

We can use the error propagation formula[31] to evaluate the uncertainty in the mean mass of hydrogen from these four tests. The uncertainty in the mean mass of hydrogen ($\sigma_{H2\ mean}$) is related to

the uncertainties in the mass of hydrogen from each of the four tests ($\sigma_{H2\ i}$) by:

$$\sigma_{H_2\ mean} = \frac{1}{N} \left(\sum_{i=1}^{N=4} \sigma_{H_2\ i}^2 \right)^{1/2} \qquad (34)$$

Referring to table 2, the uncertainty in the calculated value of the mean mass of hydrogen from these four tests, using the data from the tests alone, is roughly 8% of the mean mass of hydrogen. And the uncertainty in the calculated value of the mean mass of hydrogen from these four tests, using the pressure correction method, is roughly 10% of the mean mass of hydrogen.

Because the extent of the reaction is not a function of the initial water temperature, we can evaluate the error in the mean mass of hydrogen at 200 s for the group of tests at each initial liquid metal temperature value by using equation 34. For the 600 C initial liquid metal temperature tests, the average mass of hydrogen at 200 s was 13.4 +/- 0.61 mole/m^2. For the 500 C initial liquid metal temperature tests, the average mass of hydrogen at 200 s was 3.77 +/- 1.01 mole/m^2. For the 400 C initial liquid metal temperature tests, the average mass of hydrogen at 200 s was 10.7 +/- 1.05 mole/m^2. And for the 350 C initial liquid metal temperature tests, the average mass of hydrogen at 200 s was 1.80 +/- 1.16 mole/m^2. The error in the mean mass of hydrogen at 200 s, as given by the standard deviation from the mean, varies slightly from the estimate

of the error, as evaluated with equation 24. For the 600 C initial liquid metal temperature tests, the standard deviation from the mean is .71 mole/m^2. For the 500 C initial liquid metal temperature tests, the standard deviation from the mean is 1.26 mole/m^2. For the 400 C initial liquid metal temperature tests, standard deviation from the mean is 2.13 mole/m^2. For the 350 C initial liquid metal temperature tests, standard deviation from the mean is .19 mole/m^2.

V. The Surface Reaction Model

V.1 The Kinetic Reaction Rate and Liquid Metal Transport Reaction Models

To help us understand the mechanisms involved in the lithium-lead/water reaction we developed two models which predict the mass of hydrogen generated by the reaction as a function of time. The models are based on the premise that the reaction occurs at the interaction surface. The point of departure between the two models is that one is controlled by the kinetic rate of reaction at the interaction surface, while the second model is controlled by the rate of diffusion of reactants to the interaction surface and products in the liquid metal pool.

In the kinetic reaction rate model, the course of the reaction is controlled by the kinetic rate of reaction. This means that the rate of diffusion of the reactants towards the interaction surface and the rate of diffusion of the products away from the interaction surface is greater than the rate at which the reactants at the surface mix and react. For the kinetic reaction rate model, the rate at which the reactants are consumed by the reaction is a function of the concentrations of the reactants at the surface, the reaction rate coefficient k, and the reaction rate exponents n and m:[33]

$$R_{Li} = \frac{a_{H_2O}}{a_{Li}} R_{H_2O} = k C_{H_2O}^{n} C_{Li}^{m} \qquad (35)$$

ecause the temperature of the liquid metal surface drops after the water is poured onto it, we need to consider the effect of temperature on the rate of reaction. As alluded to in the last chapter, the reaction rate is assumed to have an Arrhenius form of temperature dependency. Therefore, the reaction coefficient is modeled with the following formula.

$$k(T) = k_0 \exp\left(- \frac{\Delta E_k}{R T} \right) \qquad (36)$$

The equation of continuity in the gas layer above the surface and in the liquid metal pool, along with the equation of energy in the liquid metal pool, are used to solve for the concentrations of the reactants. Using information from the experiments, the kinetic reaction rate model solves for the values of the reaction coefficient parameters (ΔE_k and k_0) which best match the mass of hydrogen as calculated by the kinetic reaction rate model to the mass of hydrogen from the experiments. The model must also be supplied with values for the reaction exponents n and m, and a specified, constant, liquid metal diffusion coefficient.

In the liquid metal transport reaction model, the rate of the reaction is controlled by the rate of diffusion of reactants and products in the liquid metal pool. This means that the rate at which the reactants at the interaction surface react will be greater than the rate at which the liquid metal reactant diffuses to the interaction

surface. Thus the reaction at the surface will be an equilibrium reaction. This means that the unreacted lithium atoms that manage to diffuse to the surface will be in local equilibrium with the other reactants (H_2O) and the products (LiOH or Li_2O, and H_2). Since either path of the reaction is highly exothermic,[7] the equilibrium concentration of unreacted lithium at the interaction surface will be negligible. For the liquid metal transport reaction model, the rate at which the reactants are consumed by the reaction depends upon the rate at which unreacted lithium diffuses to the interaction surface:

$$R_{Li} = \frac{a_{H_2O}}{a_{Li}} R_{H_2O} = - D_{lm} \frac{d C_{Li}}{d z} \qquad (37)$$

As in the kinetic reaction rate model we need to consider the effect of temperature variation on the reaction rate. In the liquid metal transport reaction model, we assume that the liquid metal diffusion coefficient has an Arrhenius form of temperature dependency.

$$D_{lm} = D_0 \exp\left(- \frac{\Delta E_d}{R T} \right) \qquad (38)$$

The equation of continuity in the liquid metal pool, along with the equation of energy in the liquid metal pool, are used to solve for the concentration of the lithium. Using information from the experiments, the transport reaction model solves for the value of the

diffusion coefficient parameters (ΔE_d and D_0) which best match the mass of hydrogen as calculated by the transport reaction model to the mass of hydrogen from the experiments.

The liquid metal transport reaction model is essentially a simplification of the more general kinetic reaction rate model. The diffusion equation is an integral part of the kinetic reaction rate model. In fact the kinetic reaction rate becomes a boundary condition to the diffusion equations in the liquid metal pool and the gas layer. If the kinetic rate of reaction is much greater than the rate of transport in the liquid metal pool though, it can be ignored. In the liquid metal transport reaction model, the kinetic reaction rate is assumed to be so great that any unreacted lithium that reaches the interaction surface reacts instantaneously.

V.2 Basic Equations

We can now discuss the basic equations on which the models are based. For the kinetic reaction rate model, we must solve the equation of continuity in both the gas layer and the liquid metal pool, and the equation of energy in the liquid metal pool. For the liquid metal transport reaction model, we must solve the equation of continuity and the equation of energy in the liquid metal pool.

Besides the assumption that the reaction occurs only at the interaction surface, the models incorporate a number of other assumptions. First, as alluded to above, the equation of energy is

not solved in the gas layer. This is justified on the grounds that the model used to describe the nature of the gas layer is dependent upon the water temperature and the liquid metal surface temperature. Therefore we do not need to solve for the flow of energy within the gas layer itself, but only how gas layer affects the flow of energy from the surface of the liquid metal. Next, the system is assumed to be one dimensional, with the independent variable (z) normal to the interaction surface. Since the reaction is assumed to occur at the surface, the driving force of diffusion will cause the molar concentrations to vary axially. The assumption that the liquid metal temperature varies axially, is justified by the fact that the water is significantly cooler than the liquid metal and surrounding apparatus. Therefore heat flow will be directed axially, from the hot liquid metal to the cool water above it. Thirdly, the concentration of lead is assumed to be constant throughout the interaction. This is justified by the facts that there are only 17 atoms of lithium for every 83 atoms of lead, and that there is no diffusive driving force for the lead - it does not react. The other assumptions are that the liquid metal is incompressible, the gas is ideal, thermodynamic properties are constant, and there is no convective motion in either gas or liquid metal layers. Although the violent nature of the boiling process will undoubtedly cause the liquid metal surface to vibrate, we assume that since the diameter of the liquid metal surface is smaller than the Taylor wavelength, the vibrational motion will not be great

enough to cause bulk mixing within the liquid metal pool.

The reference coordinate system for the models is presented in Figure 32. The origin of the coordinate system is the lower surface of the liquid metal well. The interaction surface is a distance S above the bottom of the liquid metal well. For the set of lithium-lead experiments performed, the liquid metal layer thickness (s) roughly varied from .4 to 1.2 cm. Because the concentration of lead is assumed to be constant, the transport problem in the liquid metal layer reduces to simple counter-diffusion - the diffusion of unreacted lithium towards the interaction surface, and the diffusion of the liquid metal product (Li_2O or LiOH) away from the interaction surface. In the gas layer, the transport problem is also one of simple counterdiffusion. Here the reacting water vapor diffuses toward the interaction surface, and the hydrogen produced diffuses away. The thickness of the gas layer (δ), derived from film boiling theory, is on the order of .01 cm.

For a multicomponent system the equation of continuity for each species is[34]

$$\frac{d}{dt}(C_i) = -\frac{d}{dz}(C_i v + J_i) \qquad (39)$$

The velocity term in this equation refers to the overall movement of the components relative to a fixed coordinate system. In our models, this movement is possible because the density of pure lithium is different than the density of pure LiOH or Li_2O. But the relative

Figure 32. Model Coordinate System

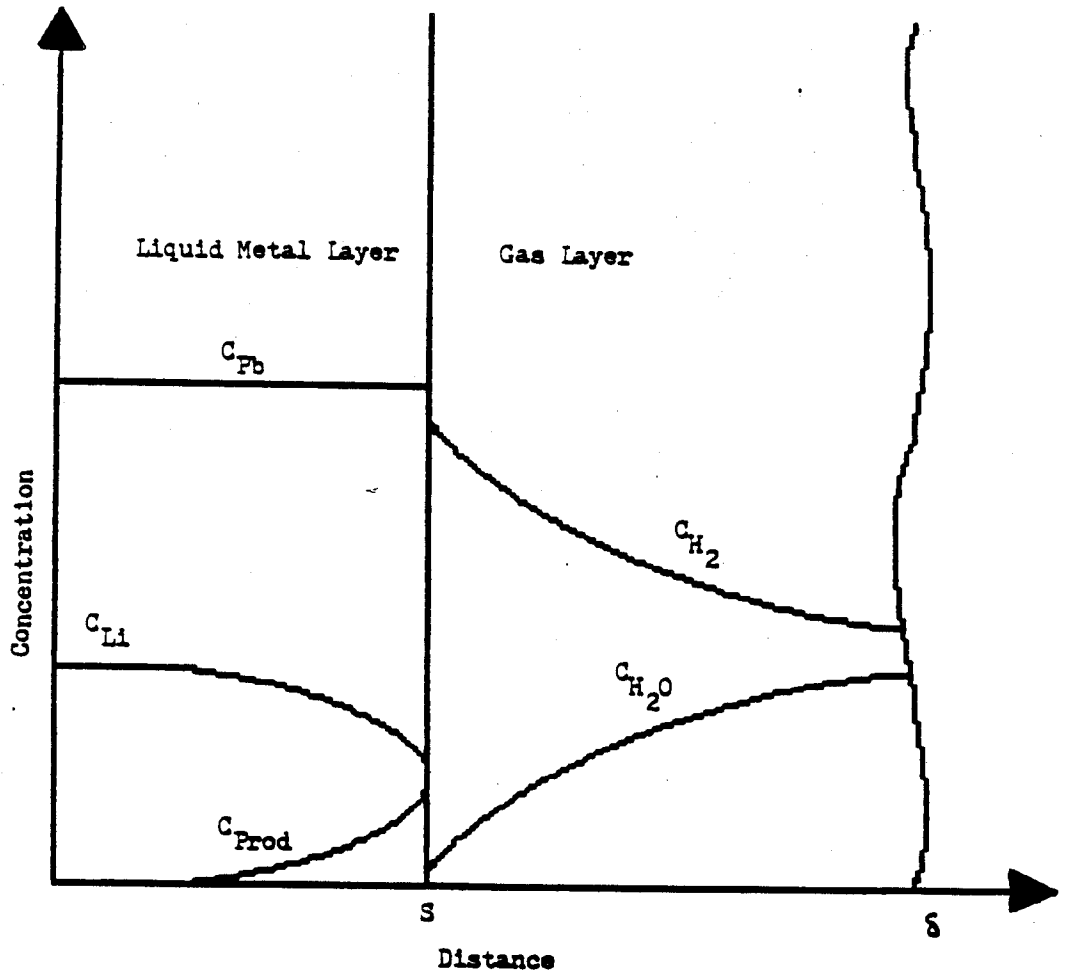

atomic abundance and mass of lithium or the liquid metal product is very small compared to lead. Thus, even if the complete inventory of lithium in the liquid metal well reacted, the final volume of the liquid metal mixture would only increase 2.2%, if LiOH was the product, and only 1.0%, if Li_2O was the product. Because the maximum volume change is so small, we can ignore its effect, which implies that the velocity term in equation 39 can be ignored.

Using the assumptions that the liquid metal is incompressible, and that the bulk liquid is motionless, the equation of energy for the liquid metal layer can be expressed as:[34]

$$\rho \frac{DH}{Dt} = -\frac{d}{dz}\left(-k_{lm}\frac{dT}{dz} + \sum_i M_i H_i J_i \right) + \frac{DP}{Dt} \qquad (40)$$

For an incompressible liquid, the mixture enthalpy is related to temperature and pressure by:[35]

$$dH = c_p\, dT + \frac{dP}{\rho} \qquad (41)$$

Given the assumption of constant properties, the last two equations can be combined to reduce the equation of energy.

$$\rho\, c_p \frac{dT}{dt} = k_{lm}\frac{d^2T}{dz^2} - \sum_i \left(J_i M_i c_p \frac{dT}{dz} + M_i H_i \frac{dJ_i}{dz} \right) \qquad (42)$$

Next we show how the system equations (39 and 42) are applied to the two models. For the kinetic reaction rate model we need to solve the equation of continuity in the gas region. Assuming that the gases are ideal, we can use the equation of state to express the total concentration of gas as a function of the system pressure and the water film temperature (the water film temperature is equal to the average of the water saturation temperature and the liquid metal surface temperature).

$$C_{gas}(t) = \frac{P(t)}{R\ T_{film}} = C_{H_2}(z,t) + C_{H_2O}(z,t) \quad (43)$$

We evaluate the system pressure by adding the partial pressure of hydrogen to the initial, constant, system pressure. Because the hydrogen generated by the experiment accumulates at the top of the experiment, we use the total mass of hydrogen generated as calculated by the kinetic reaction rate model, the equilibrium gas temperature from the experiment, and the volume of the upper gas layer to evaluate the partial pressure of hydrogen. The initial system pressure, the equilibrium gas temperature, and the upper gas layer volume are supplied as inputs to the computer model, and are taken from experimental data.

$$P(t) = P_i + \frac{N_{H_2}(t)\ R\ T_{gas}}{V_{gas}} \quad (44)$$

Finally, using Fick's first law of diffusion, we can use the continuity

equation to determine the concentration of water vapor.

$$\frac{d\,C_{H_2O}}{d\,t} = D_{gas}\,\frac{d^{\,2}\,C_{H_2O}}{d\,z^{\,2}} \qquad (45)$$

These last three equations are used to evaluate the hydrogen and water vapor concentrations in the gas layer. To complete the gas layer formulation of the kinetic reaction rate model, we must specify boundary conditions at the interaction surface and at the edge of the gas layer, and the gas layer initial condition. The first boundary condition gives the water vapor concentration at the edge of the gas layer. At the edge of the gas and water vapor film, bubbles continually form, grow to a certain size, then detach. The transitory nature of the edge of the gas and vapor film makes it difficult to specify a boundary condition at this location. To simplify matters, we assume that the concentration of water vapor at the gas film edge is a some constant fraction of the total gas concentration. The value of this fraction is an input parameter in the computer model. The other gas layer boundary condition is given by the surface reaction equation (35). Since this equation specifies the molar flowrate of reactants at the surface, we can use it and Fick's law to provide the other gas layer boundary condition. The initial condition is set by the fact that at the initiation of the interaction, no hydrogen has been formed. Therefore, initially, the concentration of water vapor throughout the gas layer equals the total molar

concentration of gas. The two gas layer boundary conditions and the initial condition can then be expressed as:

$$C_{H_2O} = C_{\delta} \qquad \text{at } z = \delta \qquad (46)$$

$$D_{gas} \frac{d\, C_{H_2O}}{d\, z} = \frac{a_{H_2O}{}^{k}\, C_{H_2O}{}^{n}\, C_{Li}{}^{m}}{a_{H_2}} \qquad \text{at } z = s \qquad (47)$$

$$C_{H_2O}(z,0) = C_{gas} \qquad (48)$$

Next we describe the derivation of the liquid metal layer system equations from the mass and energy balances for both models. As above, we first relate the concentration of the liquid metal product to the concentration of the liquid metal reactant. From the assumption that the lead concentration does not vary, and since the volume change in the liquid metal due to the reaction is negligible, a mass balance in the liquid metal region shows that the molar flowrates of the liquid metal product and the liquid metal reactant must be equal in magnitude and opposite in direction.

$$J_{Li} = - J_{Prod} \qquad (49)$$

This implies that the sum of the molar concentrations of lithium and the liquid metal product must equal a constant. This constant is the concentration of lithium in pure lithium-lead ($C_{Li\ max}$).

$$C_{Prod}(z,t) + C_{Li}(z,t) = C_{Li\ max} \qquad (50)$$

We then need only solve one of the continuity equations to complete the liquid metal mass transfer formulation. This is done again by applying Fick's law of diffusion.

$$\frac{d C_{Li}}{d t} = D_{l m} \frac{d^2 C_{Li}}{d z^2} \qquad (51)$$

The first of the boundary conditions for the liquid metal mass transfer equations is based on the fact that molar flowrate of lithium at the origin, which is the also the bottom of the liquid metal well, must be equal to zero. The initial condition is that the concentration of lithium equals the concentration of lithium in pure lithium-lead. The second boundary condition depends upon the model used. For the kinetic reaction rate model the second boundary condition is again given by the surface reaction equation. As mentioned before for the liquid metal transport reaction model, any lithium that reaches the interaction surface reacts instantaneously. Therefore the second boundary condition for the liquid metal transport reaction model is that the concentration of unreacted lithium at the interaction surface is negligible. Therefore the diffusion equation boundary conditions are:

for both models,

$$\frac{d C_{Li}}{d z} = 0 \qquad \text{at } z = 0 \qquad (52)$$

$$C_{Li}(z,0) = C_{Li\,max} \qquad (53)$$

for the kinetic reaction rate model,

$$D_{l\,m}\frac{d\,C_{Li}}{d\,z} = k\,C_{H_2O}{}^{n}\,C_{Li}{}^{m} \qquad at\ z = s \qquad (54)$$

and for the liquid metal transport reaction model,

$$C_{H_2O}\,(s,t) = 0. \qquad (55)$$

The equation of energy is solved in the same manner for both reaction models. Expressing the enthalpy of the liquid metal components as the product of their specific heat and the difference between the local temperature and a reference temperature, and by once again using Fick's law of diffusion, we can express the equation of energy in a more usable form. And by using equation 50 to express the concentration of the liquid metal product as a function of the the concentration of liquid lithium, we can eliminate the liquid metal product concentration from the energy balance. In this manner, we can relate the liquid metal temperature profile to the liquid lithium concentration profile.

$$\rho\ c_p\frac{d\,T}{d\,t} = k_{l\,m}\frac{d^{\,2}T}{d\,z^{\,2}} + D_{l\,m}\,(M_{Li}\,c_{p\,Li} - M_{Prod}$$

$$c_{p\,Prod})\left[\frac{d\,T}{d\,z} * \frac{d\,C_{Li}}{d\,z} + \frac{d^{\,2}C_{Li}}{d\,z^{\,2}}(T - T_{ref})\right] \qquad (56)$$

The first of the boundary conditions for the energy balance specifies the temperature at the origin. Since the origin refers to the bottom of the liquid metal pool, which is 1/4 in. above the location of the liquid metal well thermocouple, we use the temperature measured by the liquid metal thermocouple as the energy balance boundary condition at z = 0. The second boundary condition is set by specifying the heat flux at the interaction surface. This heat flux has two components. The first component reflects the heat gained from the reaction. The other component is a measure of the heat lost from the liquid metal by conduction to the gas and water vapor film. The initial condition for the energy balance is set by the temperature measured by the liquid metal thermocouple at the initiation of the interaction ($T_{TC}(0)$).

$$T = T_{TC}(t) \qquad \text{at } z = 0 \qquad (57)$$

$$-k_{lm}\frac{dT}{dz} = q''_{Reac} + q''_{Cond} \qquad \text{at } z = s \qquad (58)$$

$$T(0,z) = T_{TC}(0) \qquad (59)$$

The two heat flux terms in equation (58) need to be specified. The reaction heat flux is equal to the amount of heat produced per mole of lithium reacted multiplied by the rate of reaction.

$$q''_{Reac} = R_{Li}\left(\sum_i \left(a_i\left(H_{fi} + c_{pi}\left(T - T_{ref}\right)\right)\right)_{prod} - \sum_i \left(a_i\left(H_{fi} + c_{pi}\left(T - T_{ref}\right)\right)\right)_{reac}\right) \qquad (60)$$

The conduction heat flux is given by the product of the film boiling heat transfer coefficient and the temperature difference across the gas and vapor film. Since the edge of the film is a boundary between saturated vapor and saturated liquid, its temperature is the saturation temperature. Therefore the temperature difference across the vapor film is equal to the difference between the liquid metal surface temperature and the water saturation temperature.

$$q''_{Cond} = h_{film} (T(s,t) - T_{sat}) \qquad (61)$$

To complete the surface reaction model formulation, we must refer to standard film boiling theory to specify the gas layer parameters h_{film} and δ. For nonflow film boiling on a horizontal surface the heat transfer coefficient is specified by the following set of equations.[36]

$$h_{film} = h_{conv} + 0.75\, h_{rad} \qquad (62)$$

where h_{conv} is the heat transfer coefficient for the effect of convection:

$$h_{conv} = .62 \left(\frac{g\, \Delta\rho\, \rho_g\, k_g^3\, i_{fg}'}{\lambda_c\, \mu_g\, \Delta T} \right)^{1/4} \qquad (63)$$

where $$\lambda_c = 2\pi \left(\frac{\sigma}{g\, \Delta\rho} \right)^{1/2} \qquad (64)$$

and where i_{fg}' is an effective latent heat of vaporization, allowing

for the effect of superheat.

$$i_{fg}' = i_{fg}\left(1 + .68\left(\frac{c_{pg}\,\Delta T}{i_{fg}}\right)\right) \qquad (65)$$

The second term in equation 61 reflects the effect of radiation from the hot surface to the bulk of the water.[36]

$$h_{rad} = \sigma_{SB}\,\epsilon\left(\frac{T_s^4 - T_{H_2O}^4}{T_s - T_{H_2O}}\right) \qquad (66)$$

Finally, the thickness of the gas layer can be approximated by relating it to the heat transfer coefficient.[36]

$$\delta = \frac{k_g}{h_{film}} \qquad (67)$$

These equations form a complete closed set. The assumptions reduce a very complex problem to a simpler system of three partial, nonlinear, differential equations (equations 45, 51, and 56). In the kinetic reaction rate model, these three equations are used to solve for the concentrations of the reactants in their respective layers, and the liquid metal temperature in the liquid metal layer. In the liquid metal transport reaction model only the diffusion equation and the equation of energy are needed (equations 51 and 56). These two equations are used to solve for the concentration of lithium and the

temperature of the liquid metal.

By using information from the experiments, wherever possible, the models are designed so that their calculation of the mass of hydrogen can be compared to the mass of hydrogen calculated from the experimental data. In the kinetic reaction rate model, we have shown that the initial pressure, the upper gas layer equilibrium temperature, and gas layer volume are used to evaluate the molar concentration of the gas layer (equations 43 and 44). For both models, by equating the temperature at the origin to the liquid metal thermocouple temperature, the liquid metal temperature as evaluated by the models can be tied to the temperature response of specific experiments. And finally, the mass of liquid metal from the experiments is used to set the liquid metal layer thickness.

Although many of the model parameters can be tied to experimental data, other parameters remain that must be specified before the models can be used. In the kinetic reaction rate model six parameters remain. The parameters that must be specified are: the liquid metal diffusion coefficient, the water vapor boundary value at the edge of the gas and vapor film, the reaction rate exponents m and n, and the reaction rate coefficient parameters (ΔE_k and k_0). In the liquid metal transport reaction model only two remaining parameters must be specified - the liquid metal diffusion coefficient parameters (ΔE_d and D_0).

For both reaction models, the main rate controlling coefficients (the reaction rate coefficient for the kinetic reaction rate model and the liquid metal diffusion coefficient for the liquid metal transport reaction model) are assumed to have an Arrhenius form of temperature dependency. The Arrhenius temperature dependency is specified by two parameters - a proportionality constant (k_0 for the kinetic reaction rate model and D_0 for the liquid metal transport reaction model) and an activation energy parameter (ΔE_k for the kinetic reaction rate model and ΔE_d for the liquid metal transport reaction model). By using data from the experiments the values of these parameters can be determined. By this process, the rate of reaction as determined by the models can be tied to data from the experiments.

In the kinetic reaction rate model, data from the experiments are used to evaluate the reaction rate coefficient parameters in the following manner. By using the initial hydrogen generation rate from a specific experiment, we can set the initial reaction rate of the model. Because the initial concentrations of the reactants are specified by the model initial conditions, the initial value of the temperature dependent reaction rate coefficient can be determined.

$$k\,(\,T(s,0)\,) \;=\; \frac{R_{H_2\,exp}\;{}^{a}H_2}{{}^{a}Li\;\;C_{gas}{}^{n}\;C_{Li\,max}{}^{m}} \qquad (68)$$

This equation states that the initial value of the reaction rate coefficient, which is a function of the liquid metal surface temperature (T(s,0)), can be determined from the initial experimental hydrogen generation rate (R_{H2exp}) in moles of hydrogen per unit area and time. The initial experimental hydrogen generation rate is estimated from the slope of the experimental mass of hydrogen curve at beginning of the interaction. For given values of n and m, this equation can only specify one of the two parameters in the Arrhenius reaction rate coefficient equation (equation 36). The other one is found by requiring that the mass of hydrogen at 200 s calculated with the model equal (within a specified tolerance) the experimentally determined mass of hydrogen at 200 s.

We can now summarize the workings of the kinetic reaction rate model. The partial differential equations were cast in a finite difference form. A computer program was then written to solve the finite difference form of the equations. The needed experimental data are provided as inputs to the program. Also included in the input deck are chosen values of the undetermined parameters - the reaction rate coefficients (n and m), the boundary value of the water vapor concentration at the edge of the gas layer (C_δ), and the liquid metal diffusivity. The program determines the proper value of the reaction rate coefficient parameters (ΔE_k and k_0) by an iterative procedure. At the beginning of the first pass through the main body of the program, initial values of ΔE_k and k_0 are chosen. These

parameters are chosen such that the initial reaction rate coefficient equation (68) is satisfied. The program then calculates the total mass of hydrogen generated as a function of time. At each timestep in the calculation, the mass of hydrogen generated by the reaction during the timestep is given by:

$$\Delta N_{H_2}(t) = \frac{a_{H_2}}{a_{Li}} A \Delta t k(T(s,t)) * C_{H_2O}(s,t)^n C_{Li}(s,t)^m \quad (69)$$

When 200 s of calculation time has passed, the total mass of hydrogen is compared to the experimental mass of hydrogen at 200 s. If these two quantities differ, new values of the reaction rate coefficient parameters are determined, such that they satisfy equations 36 and 68, and the program reiterates. Eventually values of the reaction rate coefficients are found which satisfy both of the experimental constraints.

In the liquid metal transport reaction model, data from the experiments are used, in a similar manner as in the kinetic reaction rate model, to evaluate the diffusion coefficient parameters. Before we used data from the experiments to determine the values of the reaction rate parameters (ΔE_k and k_0), we now use data from the experiments to determine the values of the diffusion coefficient parameters (ΔE_d and D_0).

The liquid metal transport reaction rate model contains only two undetermined parameters, the diffusion coefficient parameters. Since we can use the measured values of the initial hydrogen generation rate and the mass of hydrogen at 200 s from the experiments, we can determine all of the unknown parameters in the transport controlled reaction model. The computer program for the liquid metal transport reaction model operates in much the same manner as before. After the needed experimental data has been supplied to the program, it can determine the proper values of the diffusion coefficient parameters (ΔE_d and D_0) by an iterative procedure. At the beginning of the first pass through the main body of the program, initial values of ΔE_d and D_0 are chosen. The constraint imposed by the initial hydrogen generation rate means that the initial value of the diffusion coefficient is given by:

$$D_{lm}(T(s,0)) = \frac{R_{H_2} \exp a_{H_2}}{a_{Li} \left(- \frac{d C_{Li}(s,0)}{d z} \right)} \qquad (69)$$

The initial values of the diffusion coefficient parameters must satisfy this constraint. The program then calculates the total mass of hydrogen generated as a function of time. At each timestep in the calculation, the mass of hydrogen generated by the reaction during the timestep is given by:

$$\Delta N_{H_2}(t) = \frac{a_{H_2}}{a_{Li}} \; A \; \Delta t \; D_{l\,m}(T(z,t)) \; \frac{d\,C_{Li}(s,t)}{d\,z} \qquad (70)$$

When 200 s of calculation time has passed, the total mass of hydrogen is compared to the experimental mass of hydrogen at 200 s. If these two quantities differ, new values of the reaction rate coefficient parameters are determined, such that they satisfy equations 62 and 68, and the program reiterates. Eventually values of the diffusion coefficient parameters are found which satisfy both of the experimental constraints.

The kinetic reaction rate model uses data from experiments to predict the kinetic reaction rate of the experiment, based on an assumed values for the liquid metal diffusion coefficient, the reaction rate exponents, and the concentration of water at the edge of the gas and water vapor film. In contrast, the liquid metal transport reaction model uses data from the experiments to predict the liquid metal diffusion coefficient. At this point we can not determine which of these two models provides the more accurate description of the lithium-lead/water reaction. This is because the kinetic reaction rate model uses, up to now, an unspecified liquid metal diffusion coefficient, and the liquid metal transport reaction model attempts to predict the liquid metal diffusion coefficient. To determine which of these models provides a more accurate description of the lithium-lead/water reaction we refer to theories of liquid metal diffusivities

to supply us with an estimate of the liquid metal diffusion coefficient.

V.3 Liquid Metal Diffusivity Model

Very little data exists for liquid metal diffusivity coefficients. But there have been some papers written that attempt to predict diffusivity coefficient values of general liquid metal systems. The models developed in these papers are based on various atomic theories and measurements of self-diffusivity coefficients of a range of pure metals.

Glasstone[37] developed a theory of diffusion that gives an Arrhenius form of temperature dependency for the diffusivity coefficient. Measured values of liquid metal self-diffusivities show that this form of temperature dependency is upheld experimentally.[30]

$$D_{ii} = D_0 \exp\left(- \frac{\Delta E_d}{R T} \right) \qquad (71)$$

For lead, the liquid metal self-diffusivity parameters are $D_0 = 9.15 * 10^{-8}$ m^2/s and $\Delta E_d = 1.86 * 10^4$ J/mole.

Pasternak and Olander[38] developed a theory that can be used to predict the diffusivity of a dilute liquid metal in a liquid metal solvent. Their work was based on the theory of corresponding states developed by Thomaes and Van Itterbeek.[39] The theory of corresponding states is based on the principle that reduced viscosity or diffusivity of similar substances should be universal functions of

reduced temperature and pressure. This theory can be applied to simple (monatomic or spherical) atoms. By applying the theory of corresponding states, Pasternak and Olander derived a formula that relates the diffusivity of the dilute liquid metal to the self-diffusivity of the pure solvent and three parameters mi, r_{ij}, and ϵ_{ij}. The first parameter is the molecular weight of species i. The last two of these parameters (r_{ij} and ϵ_{ij}) are the distance and energy coordinates of the minimum in the potential energy of interaction curve, for the interaction of atoms i and j. For various pure metals, Chapman[40] tabulates the interaction parameters for collisions between like atoms (r_{ii} and ϵ_{ii}). For interactions between unlike atoms, the interaction parameters are approximately given by:

$$r_{ij} = \frac{1}{2} (r_{ii} + r_{jj}) \qquad (72)$$

$$\epsilon_{ij} = (\epsilon_{ii} \epsilon_{jj})^{1/2} \qquad (73)$$

For lithium-lead the diffusivity of lithium atoms in the lead solution, as evaluated with the theory of Pasternak and Olander, is given by:

$$D_{Li\ Pb}\left(T \frac{\epsilon_{Li\ Pb}}{\epsilon_{Pb\ Pb}} \right) = D_{Pb\ Pb}(T) * \left(\frac{\epsilon_{Li\ Pb}\ M_{Pb}}{\epsilon_{Pb\ Pb}\ M_{Li}} \right)^{1/2} * \left(\frac{r_{Li\ Pb}}{r_{Pb\ Pb}} \right) \qquad (74)$$

Using data from Chapman for the like atom interaction parameters ($\epsilon_{Li\ Li}$, $\epsilon_{Pb\ Pb}$, $r_{Li\ Li}$, and $r_{Pb\ Pb}$), and the last three equations, the diffusivity parameters for lithium atoms in lead can be determined. These parameters are $D_0 = 5.0 * 10^{-7}\ m^2/s$ and $\Delta E_d = 1.7 * 10^4$ J/mole. Therefore the temperature dependant liquid lithium-lead diffusivity, as based on the theory of corresponding states, is:

$$D_{Li\ Pb}\left(\frac{m^2}{s}\right) = 5 * 10^{-7} \exp\left(-\frac{2.04 * 10^3}{T(K)}\right) \qquad (75)$$

V.4 Application of the Liquid Metal Transport Reaction Model

We found that the kinetic reaction rate model would only work with certain values of the liquid metal diffusion coefficients. When the kinetic reaction rate program was given input values of liquid metal diffusivities which were greater than $10^{-7}\ m^2/s$, the kinetic reaction rate model appeared to do a fine job at matching the calculated mass hydrogen, as a function of time, to the mass of hydrogen derived from experimental data. But when given input liquid metal diffusivities smaller than $10^{-7}\ m^2/s$, the program could not reach a stable solution. The mass of hydrogen at 200 s calculated by the program would not converge to the experimentally determined mass of hydrogen at 200 s. There were no values of the reaction rate coefficient parameters (ΔE_k and k_0) that would satisfy the experimental constraints. The theoretical value of the liquid

metal diffusivity given by equation 66 varies from 1.4 * 10^{-8} m^2/s to 4.8 * 10^{-8} m^2/s for the range of experimental temperatures (300 C to 600 C). Thus the kinetic reaction rate model could not reach a stable solution with values of the liquid metal diffusivity as determined with liquid metal diffusivity model presented above.

In contrast, we found that the values of the liquid metal diffusion coefficient as predicted by the liquid metal transport reaction model was comparable to the values of the liquid metal diffusion coefficient as determined with the liquid metal diffusivity model. Therefore unless the liquid metal diffusivity model greatly underestimates the actual value of the liquid metal diffusion coefficient, the lithium-lead/water reaction is more accurately portrayed by the liquid metal transport reaction model than by the kinetic reaction rate model. It seems unlikely that the liquid metal diffusivity model greatly underestimates the liquid metal diffusion coefficient of our system. The liquid metal diffusivity from the model is based on the diffusion of relatively small lithium atoms through a lead solution. In the reacting metal, the actual diffusion process may be one in which ions (O^- for the first reaction path (equation 1) or OH^- for the second reaction path (equation 2)) diffuse through a relatively stationary liquid lithium and liquid lead mixture.[41] In this case, the actual diffusion coefficient for the reacting metal would be either smaller than or equal to the theoretical liquid lithium-lead diffusivity. This is because the

diffusing species is of greater atomic diameter than lithium.

We can now elaborate on the performance of the liquid metal transport reaction model by examining the results of the application of the model to data from lithium-lead test #16. In Figure 33, we have graphed the mass of hydrogen as a function of time as calculated with the liquid metal transport reaction model. Also included in this figure is the mass of hydrogen as evaluated with test #16 data using the pressure correction method. The model reproduces the general shape of the test data, except for the initial peak.

Looking closely, one will notice that the model derived mass of hydrogen curve drawn in this figure is actually composed of two lines, with one nearly drawn on top of the other. This dual curve represents the results from two runs of the program. The two computer runs differ only in the assumed reaction path. The reaction path used to derive the lower of these two curves was:

$$2\ Li + H_2O \rightarrow Li_2O + H_2 \qquad (1)$$

The other curve was derived based on the this reaction path:

$$Li + H_2O \rightarrow LiOH + 1/2\ H_2 \qquad (2)$$

As established in this figure, the extent of reaction is the same regardless of the reaction path. This is due to the fact that for each mole of lithium reacting, 1/2 mole of hydrogen is generated, regardless of the reaction path.

The program solves for the values of the diffusivity coefficient parameters which will give the best match between the model

Figure 33. Model Derived Mass of Hydrogen for Test #16

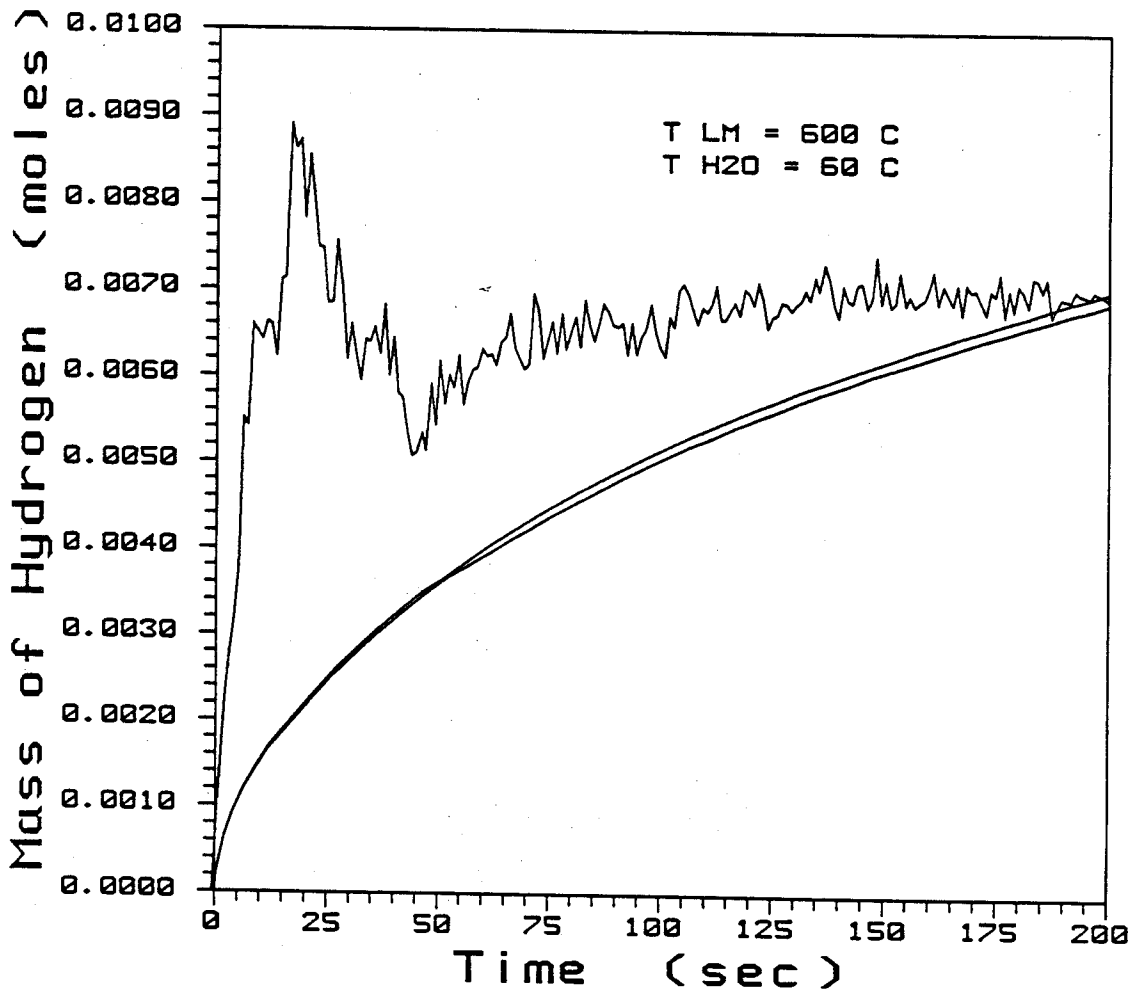

calculated hydrogen response and the experimentally determined hydrogen response. A measure of the worth of the liquid metal transport reaction model can be gathered by comparing the model derived liquid metal diffusivity coefficient to the theoretical liquid lithium-lead diffusivity coefficient (equation 75). Figure 34 graphically shows the comparison of the model diffusivity to the theoretical diffusivity. This figure shows the time varying liquid metal diffusivity as derived by applying the model to lithium-lead test#16. The derived liquid metal diffusivity decreases with time due to the dropping liquid metal temperature. By using the liquid metal temperature, we can calculate the theoretical liquid lithium-lead diffusivity for test #16. This is represented by the lower of the two curves drawn in Figure 34. As one can see, the correspondence between the model derived and theoretical diffusivities is good for test #16. We found that correspondence between model derived liquid metal diffusivity and the theoretical lithium-lead diffusivity is good for all of the tests that had 600 C initial liquid metal temperatures. Therefore it is apparent that, at high temperatures, the liquid metal diffusion coefficient can accurately be represented by a model based on the diffusion of unreacted liquid lithium through a liquid lead solution.

The liquid metal diffusivity varies with time because it is dependent upon the liquid metal temperature. The boundary condition for the energy balance at bottom of the liquid metal pool is given by

Figure 34. Model Derived and Theoretical Diffusivities for Test #16

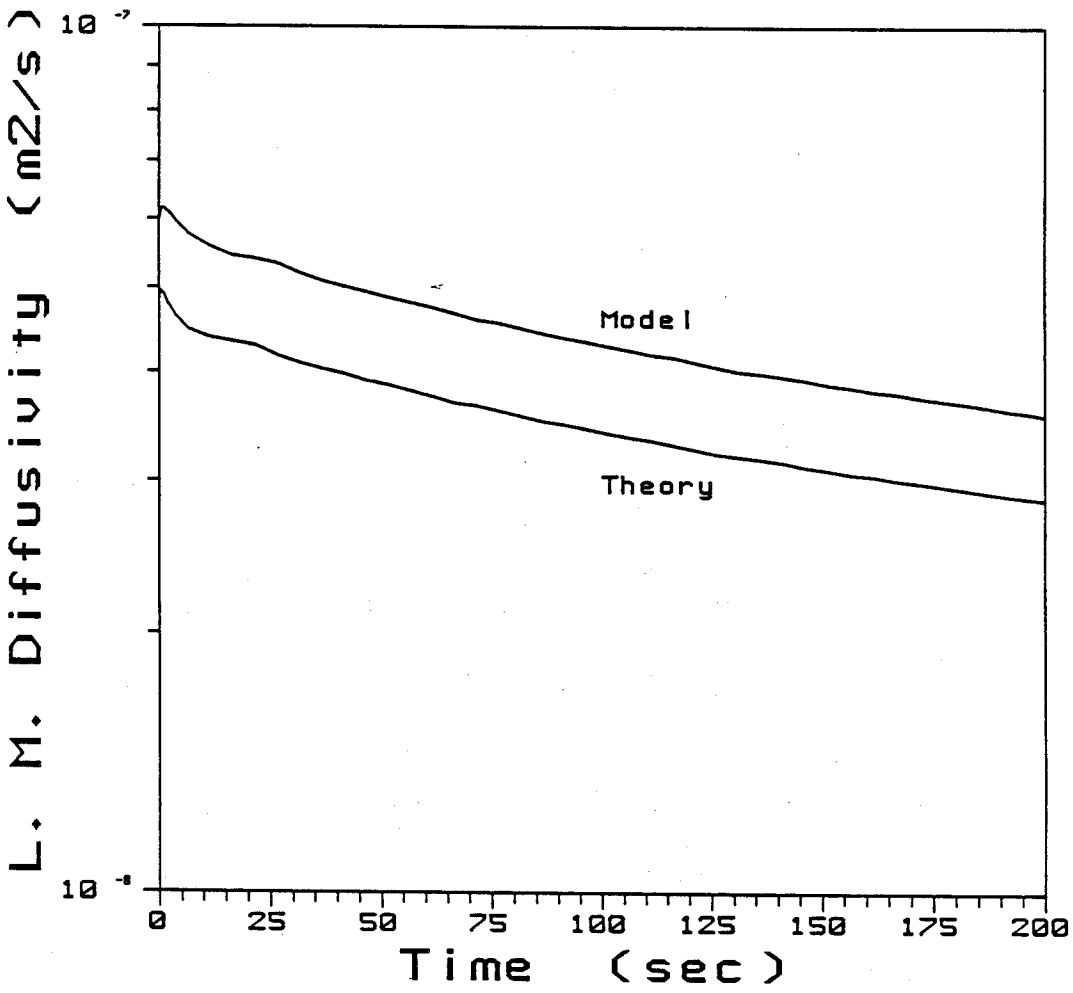

the temperature response of the liquid metal well thermocouple. Therefore the model derived liquid metal temperature should be an accurate representation of the experimental liquid metal temperature. The calculated liquid metal surface temperature from the application of the model to test #16 is presented in Figure 35. Also shown in this figure is the liquid metal thermocouple response from test #16. The model predicts that the liquid metal surface temperature will be roughly 30 C lower than the measured liquid metal thermocouple temperature for most of the experiment. This figure also shows that at the initiation of the experiment, the liquid metal surface temperature is momentarily greater than the measured temperature. This is due to the fact that the heat generated by the initially rapid reaction is greater than the heat lost by conduction to the gas layer. Because the rate of reaction decreases rapidly with time as the liquid metal reaction product accumulates, the heat generated by the reaction also decreases rapidly with time. The liquid metal transport reaction model predicts that the heat generated by the reaction decreases to one fourth of the amount of heat lost by conduction to the gas layer within 10 seconds of initiation of the interaction. To help verify the heat transfer portion of the liquid metal transport reaction model, we performed a separate finite element analysis of the system, the results of which are described in appendix 2.

The model can also be used to estimate the hydrogen generation rate from the experiment as a function of time. The hydrogen

Figure 35. Liquid Metal Surface Temperature for Test #16

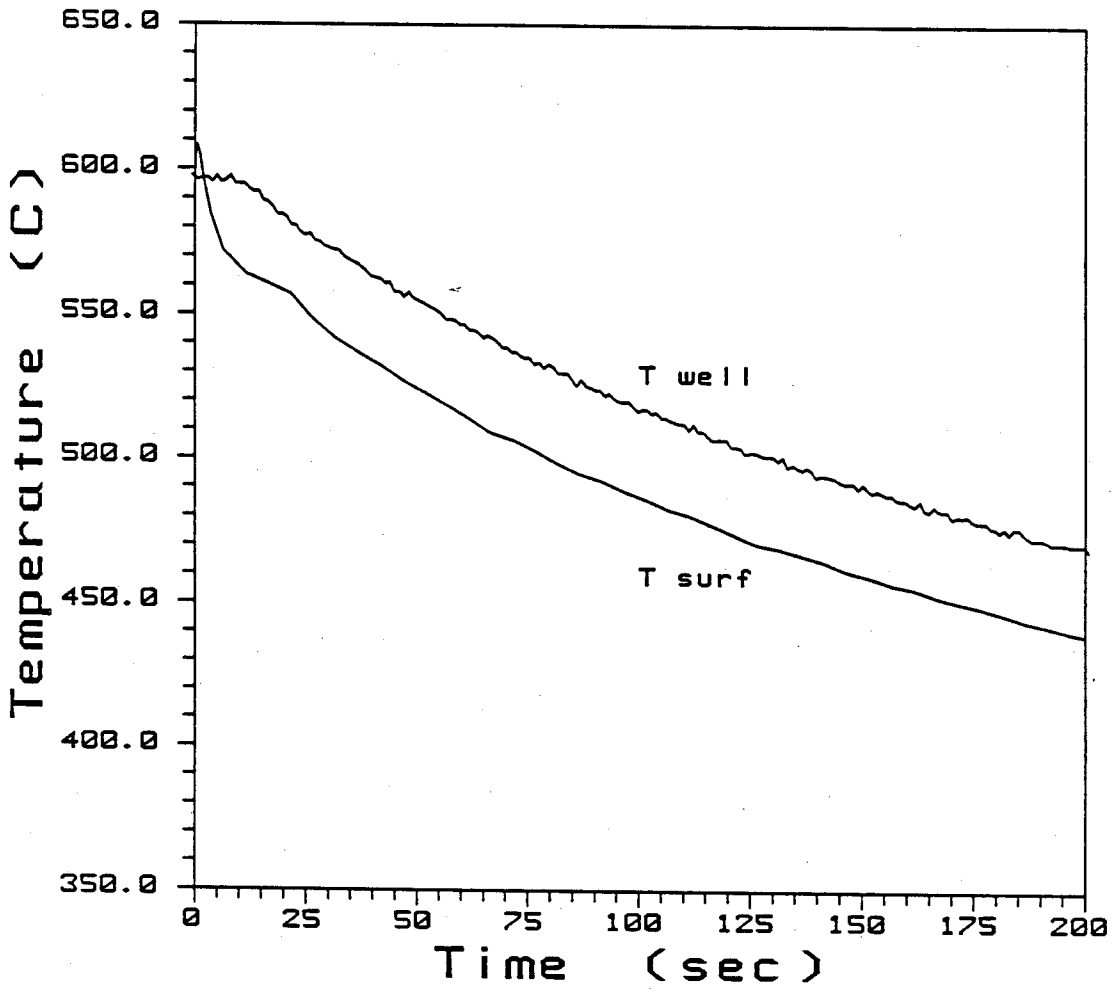

generation rate derived by the application of the model to test #16 is presented in Figure 36. This figure shows that the hydrogen generation rate decreases rapidly with time. This is due to the combination of two effects. As the reaction proceeds, the accumulation of the liquid metal reaction product increases. Thus the unreacted liquid metal has to diffuse across an increasingly greater distance to reach the liquid metal surface. At the same time, the liquid metal diffusivity decreases with time due to the falling liquid metal temperature.

As mentioned in the last chapter, we suspect that the presence of a frozen lithium hydroxide layer has an effect on the course of the reaction. This suspicion is strengthened when one examines the application of the model to data from tests with low initial liquid metal temperatures. When the model is applied to the results of lithium-lead test #24, a test characterized by an initial liquid metal temperature of 400 C, the model appears to do a good job at matching calculated hydrogen response to the experimentally determined hydrogen response. This is illustrated in Figure 37, which shows the model derived mass of hydrogen and the mass of hydrogen for test #24 as evaluated with the pressure correction method. What is more interesting though, is the comparison of the calculated liquid metal diffusivity from test #24 and the theoretical liquid metal diffusivity, as derived with the temperature response of test #24. This comparison is illustrated in Figure 38. It shows that the liquid

Figure 36. Model Derived Hydrogen Generation Rate for Test #16

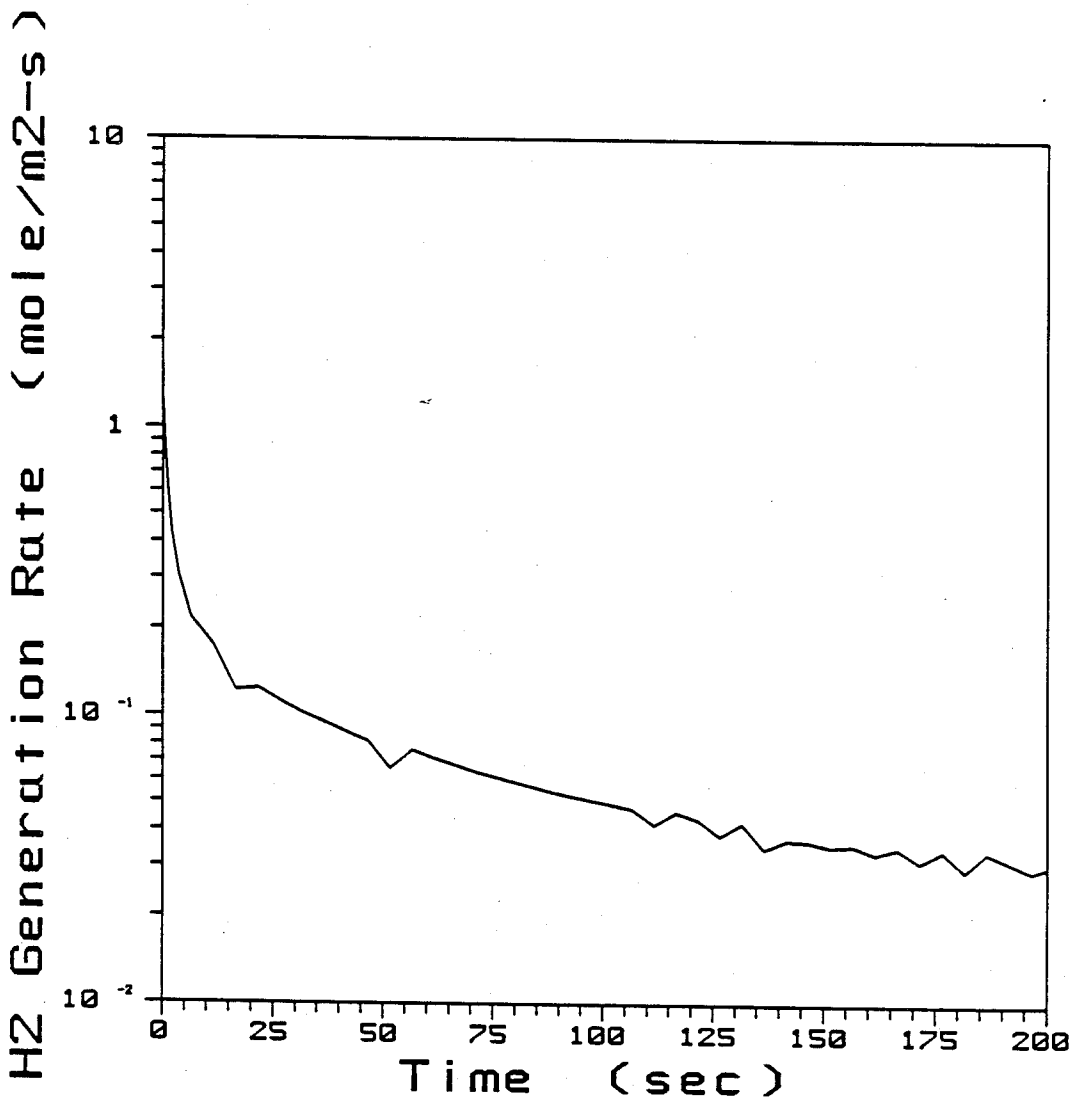

Figure 37. Model Derived Mass of Hydrogen for Test #24

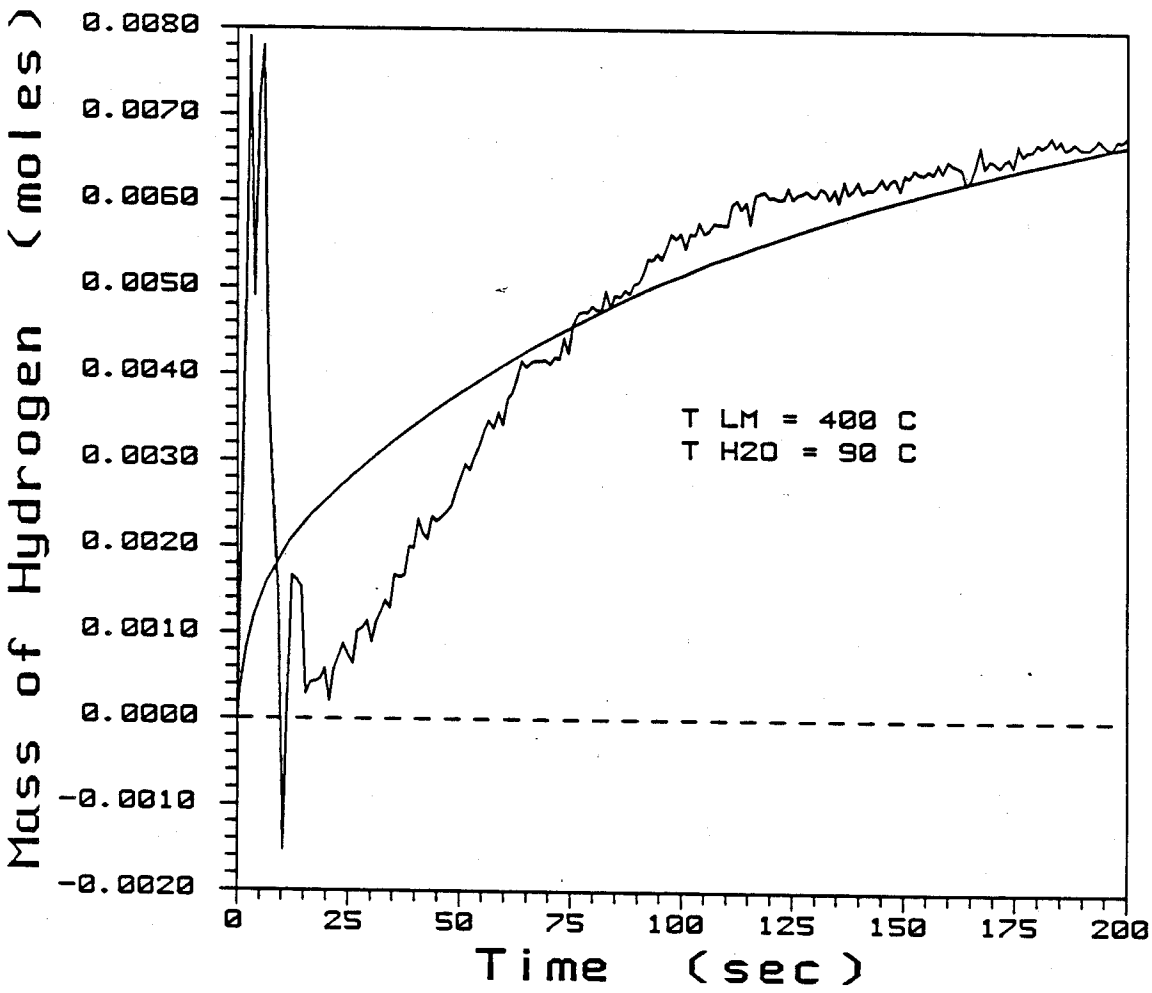

Figure 38. Model Derived and Theoretical Diffusivities for Test #24

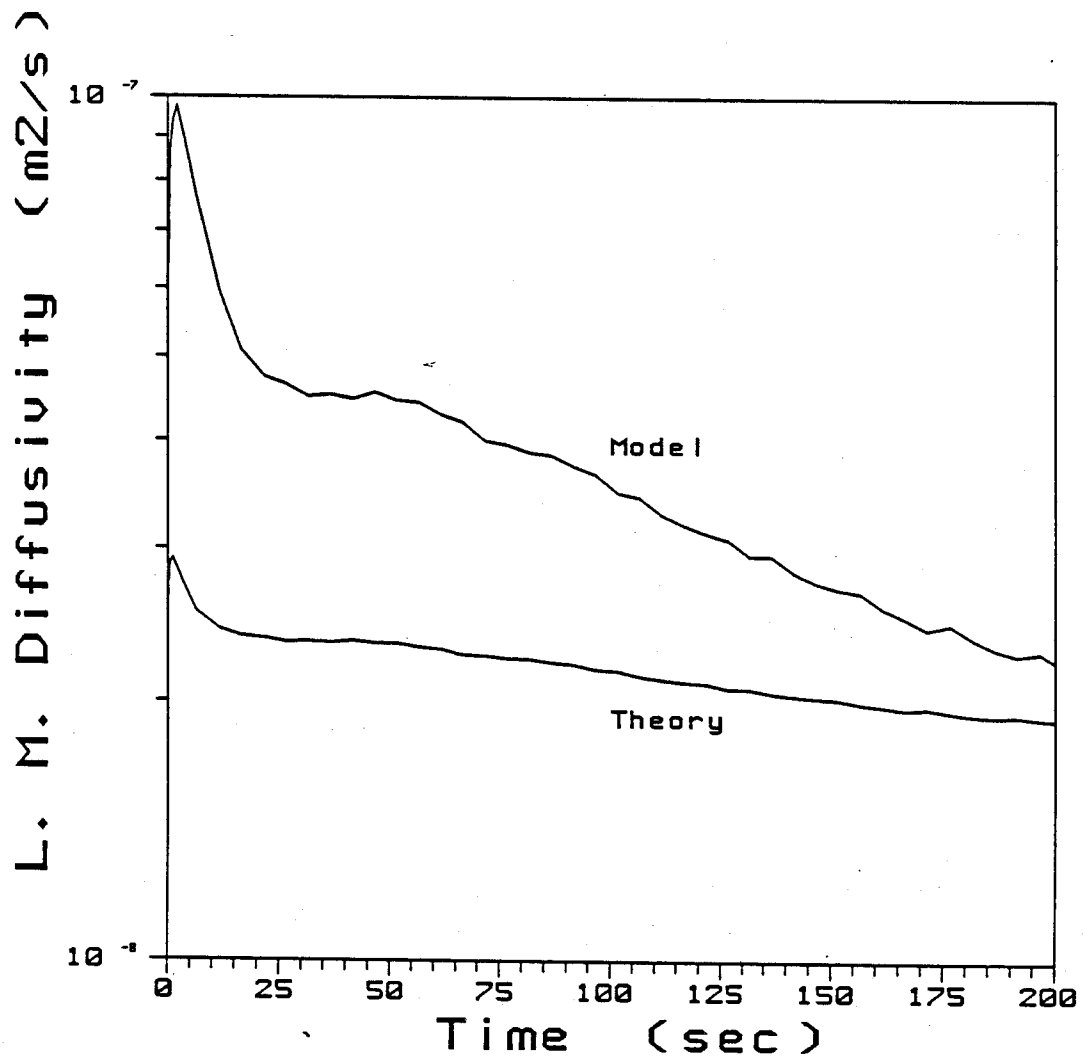

metal transport reaction model derived liquid metal diffusivity is, initially, significantly greater than the expected liquid metal diffusivity at these lower temperatures. It is apparent then, that as the initial liquid metal temperature is lowered below the melting point of lithium-hydroxide, the diffusion process in the metal sample can no longer be modeled as the diffusion of unreacted liquid lithium towards the interaction surface, through a liquid lead solution. Instead, some process enhances diffusion leading to a greater reaction rate.

Because the reaction rate is controlled by rate of diffusion of lithium and its liquid or solid reaction product through the liquid lead solution, the reaction can be considered to be lithium starved. This means that at the interaction surface, there is an abundance of water vapor, but a deficiency of lithium. Therefore, the reaction will proceed by the second reaction path (equation 2). That is because it only takes one mole of lithium to react with one mole of water to form LiOH. However, the first reaction path (equation 1) requires that two moles of lithium be present to react with one mole of water to form Li_2O. Besides, any lithium oxide that might form will react with the excess water to form lithium hydroxide.

$$Li_2O + H_2O \rightarrow 2\ LiO\,H \qquad (9)$$

Thus the predominant metal reaction product will be lithium hydroxide.

We are now ready to return to the question posed in the last chapter. As was shown in the last chapter, the extent of reaction

goes through a transition as the initial liquid metal temperature increases from 400 C to 500 C. We theorized that this transition could be caused by one of two effects. The transition could be accounted for if one reaction path was the dominant reaction for liquid metal temperatures below the transition range and the other was the dominant reaction for liquid metal temperatures above the transition range. But because our model showed that the extent of reaction was independent of the reaction path, the transition in the extent of reaction cannot be caused by changing reaction paths. In addition, the fact that the reaction is lithium starved implies that the reaction will predominantly proceed by the second reaction path (equation 2).

Therefore we surmise that the transition in the extent of reaction is likely due to the change in phase of the metal reaction product lithium hydroxide. Because the melting point of lithium hydroxide is 470 C, it is possible that the reaction product will form a solid precipitate at liquid metal surface temperatures below 470 C. Because the density of solid lithium hydroxide is less than the density of liquid lithium lead, any solid lithium hydroxide precipitate that forms will accumulate at the interaction surface.

At temperatures above the melting point of lithium hydroxide, the reaction appears to be dominated by the process of liquid metal diffusion. In this case, the rate determining process will be the counterdiffusion of liquid lithium and liquid lithium hydroxide in a

liquid lead solution. By this we mean that much of the lithium hydroxide is likely to remain in the liquid metal solution and provide a resistance to mass transfer in the liquid metal solution.

With these ideas in mind, we will now suggest a mechanism for the observed behavior of the extent of reaction as a function liquid metal temperature. At liquid metal temperatures below 470 C, the lithium hydroxide begins to come out of solution. Because it is less dense than the surrounding liquid metal, the solid lithium hydroxide accumulates at the top of the liquid metal layer. Because lithium hydroxide is soluble in water, a portion of this solid product layer may sufficiently mix with the overlying water layer and dissolve in the water. This would tend to enhance the rate of diffusion over the system where the lithium hydroxide remains in solution by removing a portion of the overall mass transfer resistance.

VI. Conclusions and Recommendations

Conclusions:

1. With a closed vessel experiment, one can determine the extent of the lithium-lead/water reaction by evaluating the mass of hydrogen generated in the reaction. Because of nonequilibrium effects during the first 100 - 150 seconds of the interaction, the extent of reaction, as measured by the hydrogen mass, can only be effectively determined after this time.

2. Analysis of the mass of hydrogen data at 200 s from the lithium-lead tests showed that the extent of reaction was not a function of the water temperature over a range of 60-90 C.

3. The extent of reaction was found to vary over the range of initial liquid metal temperatures investigated (see Table 2, p. 94). The data indicated that the hydrogen generated (lithium oxidized) passed through an apparent maximum between 350 C and 500 C. Because the data scatter is on the order of the difference in hydrogen produced from 350 C - 500 C, one should not draw any definitive outcome from this current data set. Further experiments are needed to verify this dependency and to minimize the experimental scatter. For the 600 C initial liquid metal temperature tests, the average mass of hydrogen at 200 s was 13.4 +/- 0.61 mole/m^2. For the 500 C initial liquid metal temperature tests, the average mass of hydrogen at 200 s was 3.77 +/- 1.01 mole/m^2. For

the 400 C initial liquid metal temperature tests, the average mass of hydrogen at 200 s was 10.7 +/- 1.05 mole/m^2. And for the 350 C initial liquid metal temperature tests, the average mass of hydrogen at 200 s was 1.80 +/- 1.16 mole/m^2.

4. The model of the reaction showed that diffusion in the metal sample is the rate controlling process in the lithium-lead/water reaction. It also showed that the rate of reaction is a strong function of the liquid metal temperature. One can use the model developed in Chapter V to determine the diffusion rate of lithium through the Li17Pb83 matrix or to check more theoretical models for diffusion. Both approaches were done here. One must be careful in applying the proposed mass transport and consider the time varying boundary conditions of any real situation.

Recommendations:

1. It is recommended that further experiments be done to verify the observed dependency of the extent of reaction on the initial liquid metal temperature particularly in the range of 400-500 C.

2. Beyond continued experimentation with these variables, it is recommended that the experiment be modified to investigate the effect of varying the initial system pressure from 1-10 bars. This range is chosen based on the capability of the present apparatus.

3. It is recommended that the experiment be modified to investigate the effect of varying the volume of water by a factor of two in the system, to minimize any early pressure oscillations.

4. The experiment can be improved by replacing the gas and water thermocouple wells with thermocouples that allow direct contact with the gas and water regions.

5. It is recommended that the butterfly valve be replaced with motor driven valve to maximize reproducibility in valve opening.

6. It is recommended that the entire experiment be placed in an inert atmosphere glove box, to facilitate ease of initial material preparation.

It should be recognized that the final two recommendations are made to make the experiment easier to prepare and operate. The first four are made to verify the observed behavior (#1), begin investigating a new variable (#2) that could be important, and to minimize experimental error (#3 and #4).

Appendix 1. Chemical Analysis of Samples

After five of the lithium-lead tests, the reacted metal samples were sent to an independent laboratory for a wet chemical analysis. Because we had to completely fragment the metal sample in air, in order to remove the metal sample from the liquid metal well, the chemical analysis could not provide us with a direct measurement of the extent of reaction in the metal sample caused by the experiment. Because we had to completely fragment the metal sample to remove it from the apparatus, we could not perform a separate analysis on the surface layer of the reacted metal sample. The wet chemical analysis did provide us though, with a measurement of the amount of lithium and lead in the complete reacted metal samples.

The lithium-lead samples used in the experiments were obtained from Argonne National Laboratory. The lithium-lead was packaged in eleven stainless steel sampling tubes. The tubes were twelve in. long and could hold up to 12 cm^3 of lithium-lead. The sampling tubes were filled by lowering one end of the tube into a 2 l capacity liquid lithium-lead corrosion test loop and by then connecting the other end of the tube to a vacuum pump. When the lithium-lead in the tube solidified, the tube could then be removed from the test loop. The amount of lithium-lead that could be pumped into the sample tube varied from 30 to 120 gr. The experimenters at Argonne used this method to retrieve samples from their loop for chemical analysis.

Their chemical analyses indicate that the atom percentage of lithium in the lithium-lead loop is 16.7 +/- 1.0 a%.[42] Their chemical analyses also indicate that they can retrieve lithium-lead from the loop in this manner without contaminating the metal.[42]

The results of the wet chemical analysis are summarized in Table 3. For each metal sample analyzed this table lists: the test from which sample was taken, the initial liquid metal temperature of the test, the initial water temperature, the moles of lithium in the sample, the moles of lead in the sample, and the ratio of lithium to lithium and lead in the sample. Although we did not run a chemical analysis on an unused portion of a lithium-lead sampling tube, we did have an unreacted lithium-lead sample analyzed. The first entry in this table is for an unreacted metal sample from a failed test. In one of our test runs, a lithium-lead sample was loaded into the apparatus, and the apparatus was pieced together as usual. We then pressurized the closed apparatus to insure that it was reasonably leakproof. We found through, that one of the fittings had failed and leaked profusely, forcing us to abandon the test. The unreacted metal sample from this failed test was analyzed for lithium content. As Table 3 shows, the measured atom percentage of lithium in this sample is equivalent to the atom percentage of lithium in pure lithium-lead, as it should be. This table also shows that the ratio of the moles of lithium to the moles of lithium and lead for reacted samples is less than the atom percentage of lithiumin pure lithium-

Table 3. Results of Chemical Analysis

Sample Number	Test Number	$T_{i\ LM}$ (C)	$T_{i\ H_2O}$ (C)	N_{Li} (mole)	N_{Pb} (mole)	$\frac{N_{Li}}{N_{Li} + N_{Pb}}$
1	-	-	-	0.0223	0.115	.162 +/- .019
2	23	350	90	0.0491	0.298	.141 +/- .018
3	27	600	90	0.0138	0.139	.090 +/- .012
4	28	500	90	0.016	0.112	.125 +/- .016
5	31	500	70	0.0116	0.0819	.126 +/- .016

-lead. In fact, the ratio of the moles of lithium to the moles of lithium and lead in the reacted samples is smaller for the tests which showed a greater amount of hydrogen produced. Thus the tests that exhibited the greatest amount of reaction had the least measured amount of lithium in the reacted metal samples. This is consistent with the idea that a portion of the lithium hydroxide produced by the reaction accumulates at the top of the metal sample and dissolves into the water.

Appendix 2. Finite Element Analysis

To help verify the heat transfer portion of the surface reaction model, we performed a separate finite element analysis on the experiment. To perform this analysis we used a general finite element conduction heat transfer computer code named FEM2D.[43] This code can be used to solve the equation of energy in a multi-component solid body. We used FEM2D to solve the equation of energy in the system that included the resistance heater, the surrounding insulation, the lower portion of the apparatus, and the butterfly valve. Since this region is axially symmetric, we needed only to apply the finite elements code to a cross section of the system. We divided the cross section into 130 triangular elements, which connected at 86 nodal points. The input deck to the computer code consisted of the thermal properties of each of the elements, the coordinates of the each of the nodal points relative to a fixed coordinate system, and boundary conditions for each element at the edge of the system. The elements superimposed onto the resistance heater have a specified volumetric heat generation rate given by the heater power level divided by the heater volume. The system boundaries are cooled by convection to either the surrounding air or the water in the apparatus. The code must be supplied with the heat transfer coefficients of the system boundaries and the temperature of the ambient fluid to evaluate the convective heat loss rate from the

system boundaries. The heat transfer coefficients take three forms. For regions of the system that have vertical boundaries we use a correlation which gives the Nusselt number for natural convection flow from a heated vertical wall.[44]

$$Nu = 0.6 \left(Ra\ Pr \right)^{1/4} \tag{76}$$

For regions of the system that have horizontal boundaries we use a correlation which gives the Nusselt number for natural convection flow above a heated horizontal surface.[48]

$$Nu = 0.069\ Ra^{1/3}\ Pr^{0.074} \tag{77}$$

The last heat transfer coefficient used is the film boiling heat transfer coefficient for the hot regions of the system which come in contact with water (the liquid metal surface for instance). This heat transfer coefficient is evaluated with equations 62-66.

The finite element program solves the equation of energy in the system to give the temperature at the nodal points as a function of time. Because the experiment consisted of two distinct phases - the heating phase during which the water was kept separated from the lower portion of the apparatus, and the interaction phase during which the water was allowed to pour into the lower portion of the apparatus and onto the liquid metal surface - the finite element analysis consisted of two phases. In the first phase, the code was used to evaluate the temperature of the nodal points during the heating phase of the experiment. The temperature distribution in the

nodal points at the end of this calculation could then be used as initial temperature values for the interaction phase of the analysis. In the heating phase of the calculation, the region of the apparatus above the liquid metal and below the valve is filled with argon at a constant temperature. In the interaction phase of the calculation, this region was filled with water at a constant temperature. The main point of variation between the two phases of the calculation is the difference in the rate of convective heat loss from the system to the fluid in the region between the liquid metal and the butterfly valve.

The accuracy of the heating phase finite element analysis can be gauged by examining Figure 39. This figure shows the temperature of the nodal point which corresponds to the location of the liquid metal well thermocouple as a function of time. Also included in this figure are temperature readings as measured by the liquid metal well thermocouple at intervals of five minutes during the heating phase. For each experiment, the temperature of the liquid metal well thermocouple was recorded at the end of five minute intervals during the heating phase of the experiment. The data in this figure represent the average of the five minute interval readings from all of the experiments. 58 minutes after the resistance heater is turned on, the temperature as read by the liquid metal thermocouple reaches 600 C. At this point the butterfly valve is opened and the interaction is initiated. Lower initial liquid metal temperature tests

Figure 39. Liquid Metal Well Temperature during the Heating Phase of the Finite Element Analysis

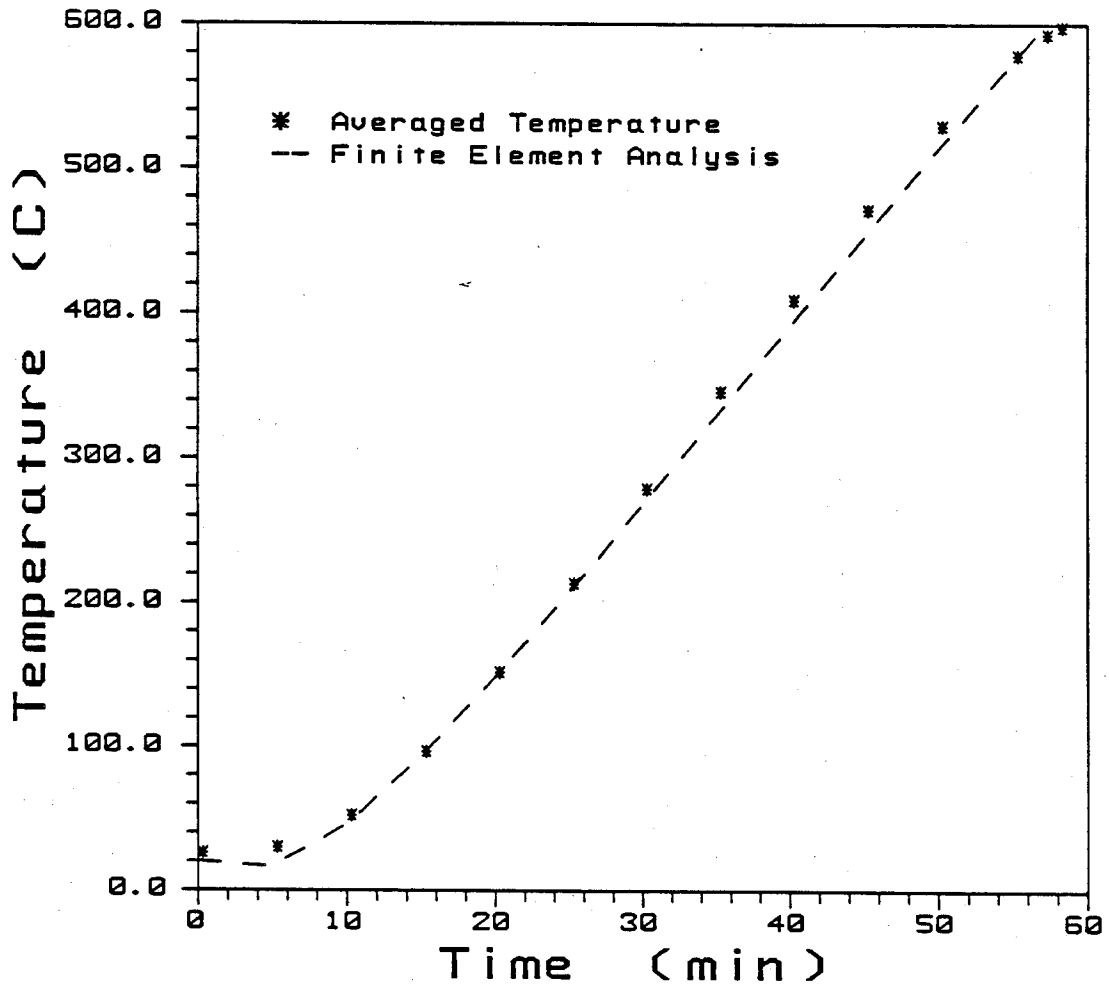

are initiated at earlier times (at 40 minutes into the heating phase for the 400 C initial liquid metal temperature tests, for instance).

The temperature distribution of the elements at the end of the heating phase are used as the initial element temperature values for the interaction portion of the calculation. In this phase of the calculation, the heat transfer coefficient for the horizontal surfaces of the lower portion of the apparatus which are covered with water (the liquid metal surface) is the heat transfer coefficient for film boiling. The following figure shows that the finite element calculation again does a good job of predicting the temperature of the system. Figure 40 shows the temperature of the nodal point that corresponds to the location of the liquid metal well thermocouple as a function of time. Also plotted on this figure, nearly overlapping the first curve, is a plot of the liquid metal well thermocouple response from lithium-lead test #16. The liquid metal well temperature evaluated by the finite element analysis (the upper curve) varies less than 5 C from the measured liquid metal well temperature of test #16. This figure shows that the finite element analysis accurately models the temperature response of the system during the interaction phase of the experiment. In Figure 41 we compare the liquid metal surface temperature as evaluated with the surface reaction model and the surface temperature as evaluated with the finite element analysis. As shown in this figure, the liquid metal surface temperature as evaluated by these models exhibit good

Figure 40. Thermocouple Well Temperature during the Interaction Phase of the Finite Element Analysis

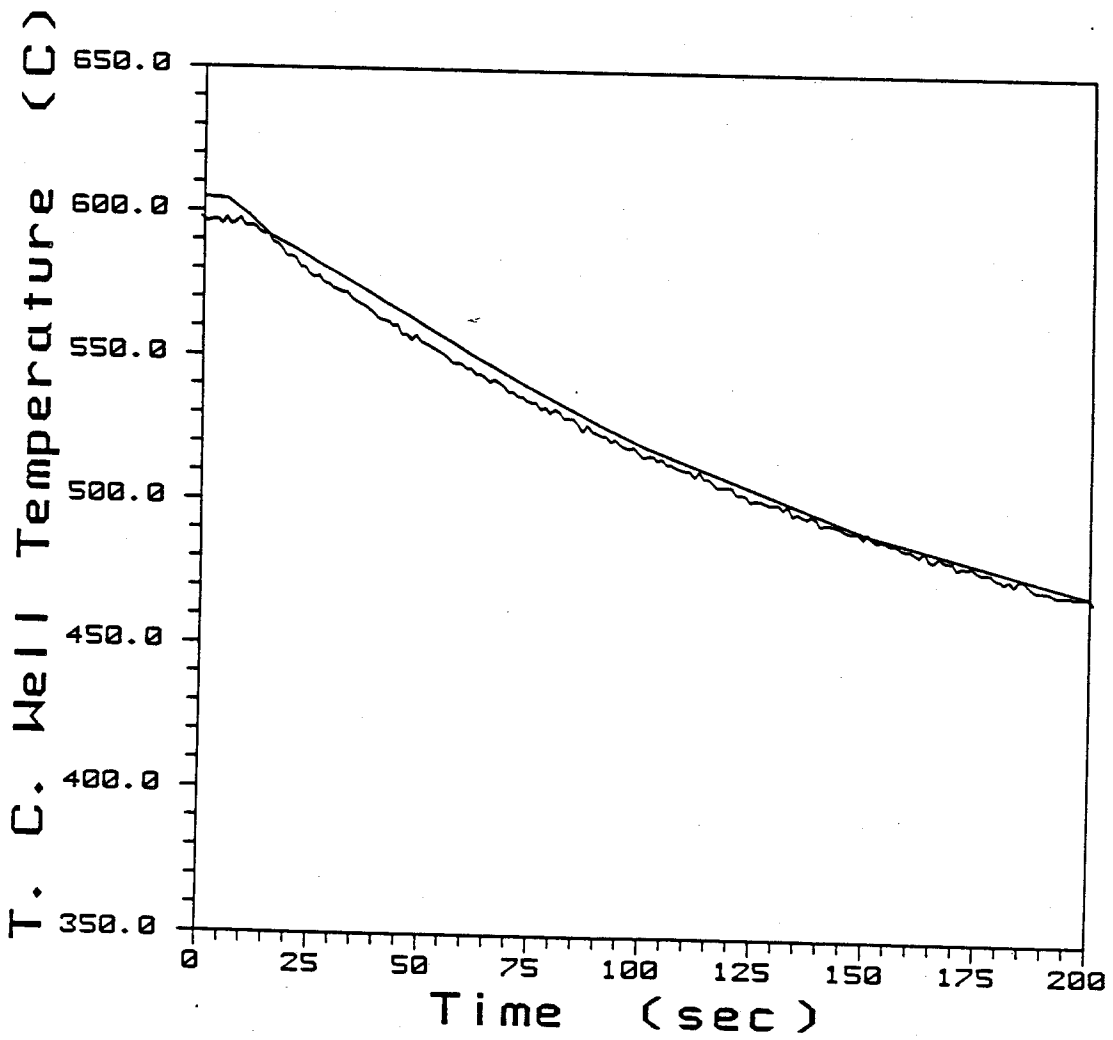

Figure 41. Liquid Metal Surface Temperature during the Interaction Phase of the Finite Element Analysis

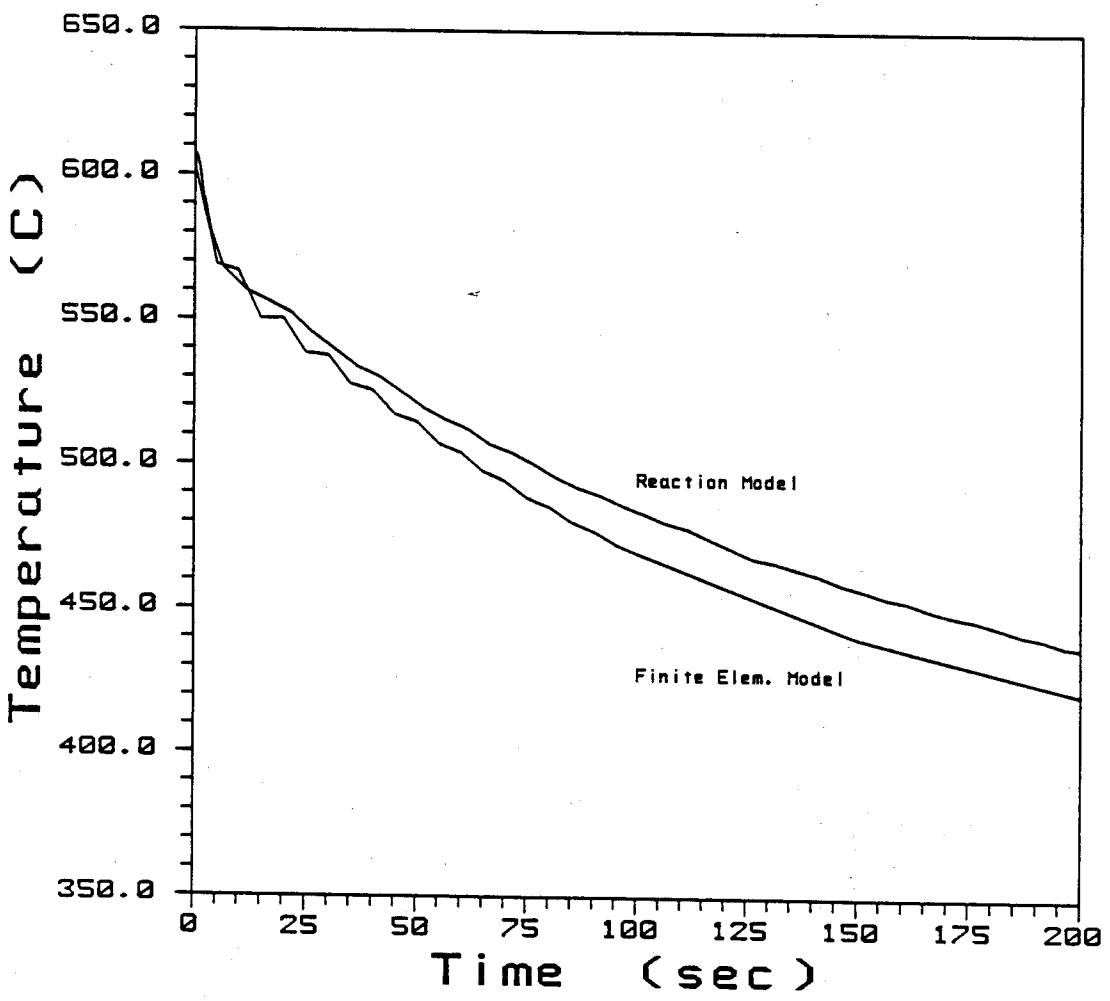

correspondence during the initial minute of the interaction. At later times though, the surface reaction model predicts a greater liquid metal surface temperature than the finite element analysis does. At 200 s into the interaction, the liquid metal surface temperature as evaluated with the surface reaction model is 16 C greater than the liquid metal surface temperature as evaluated with the finite element analysis. The reason for this is the fact that the finite element analysis allows for conductive heat loss in the radial direction away from the liquid metal well. The one-dimensional surface reaction model does not allow for the effect of radial cooling. But because most of the reaction occurs during the first minute of the interaction, the effect of neglecting radial conduction on the surface reaction model is insignificant.

Appendix 3. Source Listing for Liquid Metal Transport Reaction Program

In this appendix we provide a source listing for the transport controlled reaction model computer program (TRANREAC). This program, written in FORTRAN solves the system of equations for the transport controlled reaction model, as described in chapter V. The program was designed to be run on a personal computer.

In its present form, the program works interactively with the user. For each input parameter, the program reports the default value of the parameter to the user. The user is given the opportunity to change the value of the parameter or keep the default value of the parameter. The default program values are derived from lithium-lead test #16 data.

After the program has been supplied with the desired inputs, it proceeds to determine the values of the liquid metal diffusion coefficient parameters (ΔE_d and D_0) which satisfy the experimental constraints. It accomplishes this task by an iterative procedure. At the end of each pass through the program, the calculated mass of hydrogen at 200 s is compared to the experimentally determined mass of hydrogen at 200 s. If the calculated mass of hydrogen varies by more than 2% from the experimentally determined mass of hydrogen, the program reiterates. At the end of each iteration, the program reports the calculated mass of hydrogen and the current values of the

liquid metal diffusion coefficient parameters to the screen. The program then chooses new values for the liquid metal diffusion coefficient parameters based on previous values of these parameters. This process continues until a solution is found. Once the solution is found, the program passes through the main loop one more time in order to output data to the disk.

The program creates two output data files. At each timestep during the final pass through the main loop of the program, the program writes to the first data file the following information: the time (sec), the mass of hydrogen (mole), the liquid metal diffusion coefficient at the liquid metal surface (m^2/s), and the liquid metal diffusion coefficient at the bottom of the liquid metal pool (m^2/s). At each timestep during the final pass through the main loop of the program, the program writes to the second data file the following information: the time (sec), the hydrogen generation rate (mole/m^2-s), the temperature of the liquid metal surface (C), and the temperature at the bottom of the liquid metal pool (C).

```
      C                                                                      TREAC
      C                        PROGRAM TRANREAC                              TREAC
      C                                                                      TREAC
      C                                          By Jim Herzog       1987    TREAC
      C                                                                      TREAC
      C     This program evaluates the hydrogen production rate from the     TREAC
      C  lithium-lead/water reaction experiment, as a function of diffusion  TREAC
      C  coefficient parameters.  The reaction is transport controlled.      TREAC
      C                                                                      TREAC
      C**********************************************************************TREAC
      C                                                                      TREAC
            IMPLICIT DOUBLE PRECISION  ( A-H, M-Z )                          TREAC
            IMPLICIT INTEGER  ( I-L )                                        TREAC
      C                                                                      TREAC
            DIMENSION  DLIQ(50), CLI(51,2), CPLI(50), CDPLI(50), CLSTR(51),  TREAC
           1           CPSTR(50), CDPSTR(50)                                 TREAC
            DIMENSION  T(51,2), TP(50), TDP(50), TSTR(51), TPSTR(50)         TREAC
            DIMENSION  NLI(2), NPROD(2), NTOT(2)                             TREAC
            DIMENSION  AL(2,50), BL(2,50), CL(2,50), DL(2,50), ALPHAL(2,50), TREAC
           1           SL(2,50)                                              TREAC
            DIMENSION  TIMTLM(200), TLM(200), ITSNO(17)                      TREAC
      C*****  COMMON BLOCKS  *****                                           TREAC
            COMMON  / PROP /                                                 TREAC
           1  DENLI, DENPRO, DENPB,                                         TREAC
           2  MWLI, MWPROD, MWPB,                                           TREAC
           3  TCGAS, TCLIQ, TDLIQ,                                          TREAC
           4  ALI, AH2O, APROD, AH2,                                        TREAC
           5  CLIQ                                                          TREAC
      C                                                                      TREAC
            COMMON  / FLAG /  IPROD, IEPS, IDEB, IPALL                       TREAC
      C                                                                      TREAC
      C*****  I/O UNIT NUMBERS  *****                                        TREAC
            IWRITE = 0                                                       TREAC
            IREAD = 0                                                        TREAC
            IDATA = 20                                                       TREAC
            ISURF = 21                                                       TREAC
            IDEBUG = 30                                                      TREAC
      C                                                                      TREAC
            OPEN ( IDATA, FILE = 'TEST.DAT', STATUS = 'NEW' )                TREAC
            OPEN ( ISURF, FILE = 'TSURF.DAT', STATUS = 'NEW' )               TREAC
      C                                                                      TREAC
      C*****  FINITE DIFFERENCE POINT TOTALS  *****                          TREAC
            ILSTEP = 50                                                      TREAC
            JLSTEP = ILSTEP - 1                                              TREAC
      C                                                                      TREAC
      C     First we call the variable setting routine.                      TREAC
            CALL  INVAR (                                                    TREAC
           1                                                                 TREAC
           2                                                                 TREAC
           3  VFREE, TFREE, MASLIQ, AREA, SDEPTH, TZERO, PZERO, NH2DOT, TSTOP,TREAC
           3  NTSTOP, ACTENG, TIMTLM, TLM, ITLM, ITEST, EPSC, EPST )        TREAC
      C                                                                      TREAC
      C                                                                      TREAC
      C*****  PROGRAM CONSTANTS EVALUATION  *****                           TREAC
            RGAS = 8.314                                                     TREAC
```

```
      CLIMAX = .17 * CLIQ                                                TREAC
      NAR = VFREE * PZERO / ( TFREE * RGAS )                             TREAC
      TREF = 373.15                                                      TREAC
C                                                                        TREAC
C*****  INITIAL VALUES OF PROGRAM VARIABLES  *****                       TREAC
      NTOTAL = SDEPTH * AREA * CLIQ                                      TREAC
      HCONV =  256. + 1.631D3 * ((.5*(TZERO-TREF))**(-.25))              TREAC
      HRAD = 5.48D-8 * ( ( TZERO**4. - TREF**4. ) / ( TZERO - TREF ) )   TREAC
      HTOT = HCONV + .75 * HRAD                                          TREAC
      DELTA = TCGAS / HTOT                                               TREAC
      ATH = 1.7D4                                                        TREAC
      D0TH = 5.04D-7                                                     TREAC
C*****  INITIAL LITHIUM FLOWRATE AND LIQUID METAL DIFFUSIVITY  *****     TREAC
      NLDOT0 = ALI * NH2DOT / ( AH2 *  AREA )                            TREAC
      DLIQ0 = NLDOT0 * SDEPTH  / ( CLIMAX * DBLE( JLSTEP ) )             TREAC
C*****  INITIAL TEMPERATURE DEPENDANT REACTION RATE PARAMETERS  *****    TREAC
C                                                                        TREAC
C     Here we guess the initial activation energy and temperature depen-TREAC
C  dant reaction rate parameter.                                         TREAC
      DTEMP = DLIQ0 * DEXP( ACTENG / ( RGAS * TZERO ) )                  TREAC
C                                                                        TREAC
      ITER = 0                                                           TREAC
      JFLAG = 1                                                          TREAC
      IHIGH = 0                                                          TREAC
      ILOW = 0                                                           TREAC
      NLOW = 0.                                                          TREAC
      NHIGH = 1.                                                         TREAC
      NEPS = .02 * NTSTOP                                                TREAC
      NTLOW = NTSTOP - NEPS                                              TREAC
      NTHIGH = NTSTOP + NEPS                                             TREAC
C                                                                        TREAC
C*************************************************************************TREAC
C     RECALCULATION BRANCH POINT                                         TREAC
C*************************************************************************TREAC
C                                                                        TREAC
 9999 CONTINUE                                                           TREAC
C                                                                        TREAC
      ITER = ITER + 1                                                    TREAC
C*****  PROGRAM VARIABLE INITIATION  *****                               TREAC
      DO 20  I = 1, ILSTEP                                               TREAC
        CLI(I,1) = 1.                                                    TREAC
        CLSTR(I) = 1.                                                    TREAC
        T(I,1) = 1.                                                      TREAC
        TSTR(I) = 1.                                                     TREAC
 20   CONTINUE                                                           TREAC
C                                                                        TREAC
      CLI(1,1) = 0.                                                      TREAC
      CLSTR(1) = 0.                                                      TREAC
      NLDOT1 = NLDOT0                                                    TREAC
      NLDOT2 = NLDOT1                                                    TREAC
C                                                                        TREAC
      DO 30  J = 1, JLSTEP                                               TREAC
        TP(J) = 0.                                                       TREAC
        TDP(J) = 0.                                                      TREAC
        TPSTR(J) = 0.                                                    TREAC
```

```
111           DLIQ(J) = DLIQ0                                                  TREAC
112     30    CONTINUE                                                         TREAC
113     C                                                                      TREAC
114           XLSTEP = 1. / DBLE( JLSTEP )                                     TREAC
115           XLSTP2 = XLSTEP * XLSTEP                                         TREAC
116           CPSTR(1) = ( -21.*CLI(1,1) + 13.*CLI(2,1) + 17.*CLI(3,1) -       TREAC
117          1            9.*CLI(4,1) ) / ( 20. * XLSTEP )                    TREAC
118           CDPSTR(1) = 2. * ( CLI(2,1) - CLI(1,1) - XLSTEP*CPSTR(1) ) /     TREAC
119          1             XLSTP2                                             TREAC
120           CPLI(1) = CPSTR(1)                                               TREAC
121           CDPLI(1) = CDPSTR(1)                                             TREAC
122     C                                                                      TREAC
123           DO 35  I = 2, JLSTEP                                             TREAC
124             CPSTR(I) = .5 * ( CLSTR(I+1) - CLSTR(I-1) ) / XLSTEP           TREAC
125             CDPSTR(I) = ( CLSTR(I+1) - 2.*CLSTR(I) + CLSTR(I-1) ) /        TREAC
126          1               XLSTP2                                            TREAC
127             CPLI(I) = CPSTR(I)                                             TREAC
128             CDPLI(I) = CDPSTR(I)                                           TREAC
129     35    CONTINUE                                                         TREAC
130     C*****  INITIAL MOLAR MASSES  *****                                    TREAC
131           NTOT(1) = NTOTAL                                                 TREAC
132           NTOT(2) = NTOT(1)                                                TREAC
133           NPB = .83 * NTOTAL                                               TREAC
134           NLI(1) = .17 * NTOTAL                                            TREAC
135           NLI(2) = NLI(1)                                                  TREAC
136           NPROD(1) = 0.                                                    TREAC
137           NPROD(2) = NPROD(1)                                              TREAC
138           NGAS = NAR                                                       TREAC
139           NH2 = 0.                                                         TREAC
140           NREAC = 0.                                                       TREAC
141     C                                                                      TREAC
142           SOFTIM = SDEPTH                                                  TREAC
143           IPRINT = 0                                                       TREAC
144     C*****  INITIAL PRESSURE AND TOTAL HEATFLUX  *****                     TREAC
145           P = PZERO                                                        TREAC
146           QTOT1 = 0.                                                       TREAC
147     C*****  INITIAL TIMESTEP  *****                                        TREAC
148           TCONL = SDEPTH * SDEPTH / DLIQ0                                  TREAC
149           TSTEPL = .1                                                      TREAC
150           ITIME = 0                                                        TREAC
151           TIME = 0.                                                        TREAC
152     C*****  OUTPUT PROBLEM PARAMETERS  *****                               TREAC
153     C                                                                      TREAC
154           IF  ( JFLAG .EQ. 0 )  THEN                                       TREAC
155             TSURF = T(1,1) * ( TZERO - TREF )  +  TREF  -  273.15          TREAC
156             DTH = D0TH * DEXP( -1. * ATH / ( RGAS * TZERO ) )              TREAC
157             RRH2 = NLDOT0 * AH2 / ALI                                      TREAC
158     C                                                                      TREAC
159             WRITE (IDATA,40)  TIME, NH2, DLIQ0, DTH                        TREAC
160             WRITE (ISURF,40)  TIME, RRH2, TSURF, TSURF                     TREAC
161     40        FORMAT ( 4( 2X, 1P1G11.4 ) )                                 TREAC
162           END IF                                                           TREAC
163     C                                                                      TREAC
164     C-----  DEBUG DATA  -----                                             TREAC
165           IF  ( IDEB .EQ. 1 )  THEN                                        TREAC
```

```
      OPEN  ( IDEBUG, FILE = 'DEBUG.DAT', STATUS = 'NEW' )                TREAC
      WRITE (IDEBUG,51)  VFREE, TFREE, AREA, SDEPTH, TZERO                TREAC
 51     FORMAT ( '   VFREE       TFREE       AREA        SDEPTH' /        TREAC
     1          1P4G11.4 / '   TZERO  ' / 1P1G11.4 )                      TREAC
      WRITE (IDEBUG,52)  CLIMAX, NAR, NTOTAL, DELTA, TCONL                TREAC
 52     FORMAT ( '  CLIMAX      NAR         NTOTAL       ',               TREAC
     1          '  DELTA       TCONL  '/ 1P5G11.4 / '*****',              TREAC
     2          '*******************************************' )            TREAC
       END IF                                                             TREAC
C-------------------------                                                TREAC
C                                                                          TREAC
C**************************************************************************TREAC
C     MAIN CALCULATIONAL LOOP                                              TREAC
C**************************************************************************TREAC
C                                                                          TREAC
 1000 CONTINUE                                                             TREAC
C                                                                          TREAC
C     The first step is to evaluate the loop values of the slowly time     TREAC
C  varying variables ( i.e. DELTAS, DELTAC,... ).  These variables         TREAC
C  are evaluated at the beginning of each timestep.                        TREAC
C                                                                          TREAC
      CALL  VCALL (                                                        TREAC
     1    T, NTOT, NLI(1), NPROD(1), NREAC, TSTEPL, TZERO, TREF,          TREAC
     1    CLIMAX, AREA, SOFTIM, DTEMP, ACTENG, JLSTEP,                    TREAC
     2                                                                    TREAC
     3    VLIQ, DELTAS, DELTAC, DLIQ, DELTA )                             TREAC
C                                                                          TREAC
C     Next we update the spatial step sizes.                               TREAC
      XLSTEP = SOFTIM / ( SDEPTH * DBLE( JLSTEP ) )                        TREAC
C                                                                          TREAC
C-----  DEBUG DATA  -----                                                  TREAC
      IF  ( IDEB .EQ. 1 )  THEN                                            TREAC
        WRITE (IDEBUG,100)  VLIQ, DELTAS, DELTAC, DLIQ(1),                 TREAC
     1                      DLIQ(JLSTEP), DELTA                           TREAC
 100      FORMAT ( '   VLIQ       DELTAS     DELTAC     DLIQ1    ',      TREAC
     1            '   DLIQN      DELTA ' / 1P6G11.4 )                     TREAC
        WRITE (IDEBUG,115)  TSTEPL, XLSTEP                                 TREAC
 115      FORMAT ( '   TSTEPL   XLSTEP' / 1P2G11.4 / '**********' )       TREAC
      END IF                                                               TREAC
C-------------------------                                                TREAC
C                                                                          TREAC
C*****  LIQUID METAL SIDE FINITE DIFFERENCE FORMULATION  *****              TREAC
C                                                                          TREAC
C     First we evaluate the nondimensional value of the conduction and     TREAC
C  reaction heat fluxes from the liquid metal surface.  Since these heat   TREAC
C  fluxes are evaluated with starred values of the surface temperature     TREAC
C  and lithium concentration along with the updated surface water vapor    TREAC
C  concentration, the total heat flux will be equal to the end of time-    TREAC
C  step value when the end of timestep lithium concentration and temper-   TREAC
C  ature are found.                                                        TREAC
      CALL  HEATFX (                                                       TREAC
     1    TSTR(1), SOFTIM, DELTA, TZERO, TREF, TIMTLM, TLM, ITLM,         TREAC
     1    TIME, NLDOT2,                                                   TREAC
     2                                                                    TREAC
     3    QREAC, QCOND, TBOUND )                                          TREAC
```

```
      C                                                                 TREAC
            QTOT2 = QCOND - QREAC                                       TREAC
      C                                                                 TREAC
            XLSTP2 = XLSTEP * XLSTEP                                    TREAC
            XTFACT = XLSTP2 * SDEPTH * SDEPTH / TSTEPL                  TREAC
      C                                                                 TREAC
      C-----  DEBUG DATA  -----                                        TREAC
            IF  ( IDEB .EQ. 1 )  THEN                                   TREAC
              WRITE (IDEBUG,200)  QREAC, QCOND, TBOUND, QTOT2           TREAC
       200    FORMAT ( '   QREAC       QCOND       TBOUND      QTOT2  '/  TREAC
           1               1P6G11.4 )                                   TREAC
              WRITE (IDEBUG,205)  XLSTP2, XTFACT, TDLIQ, NLDOT1, NLDOT2 TREAC
       205    FORMAT ( '   XLSTP2      XTFACT      TDLIQ       NLDOT1 ',  TREAC
           1               '   NLDOT2  ' / 1P5G11.4 )                   TREAC
            END IF                                                      TREAC
      C-------------------------                                        TREAC
      C                                                                 TREAC
      C                                                                 TREAC
      C     Next we evaluate the coefficient vectors A, B, C, and D.    TREAC
            XL = XLSTEP                                                 TREAC
            DO 300  I = 2, JLSTEP                                       TREAC
              AL(1,I) = 4.  +  2. * VLIQ * XLSTEP * ( 1. - XL )  -      TREAC
           1              XLSTEP * DELTAC * ( TPSTR(I) + TP(I) )  +     TREAC
           2              2. * DELTAC * ( TSTR(I) + T(I,1) )            TREAC
              AL(2,I) = 4. * TDLIQ / DLIQ(I)  -  2. * VLIQ * XLSTEP *   TREAC
           1              ( 1. - XL )  -  XLSTEP * DELTAC * ( CPSTR(I) + TREAC
           2              CPLI(I) )                                     TREAC
              BL(1,I) = 8. * ( XTFACT/DLIQ(I) + 1. )  +  4. * XLSTP2 *  TREAC
           1              VLIQ  +  4. * DELTAC * ( TSTR(I) + T(I,1) )   TREAC
              BL(2,I) = 8. * ( XTFACT + TDLIQ ) / DLIQ(I)  -  2. * DELTAC TREAC
           1              * XLSTP2 * ( CDPSTR(I) + CDPLI(I) )           TREAC
              CL(1,I) = 4.  +  2. * VLIQ * XLSTEP * ( 1. - XL )  +      TREAC
           1              XLSTEP * DELTAC * ( TPSTR(I) + TP(I) )  +     TREAC
           2              2. * DELTAC * ( TSTR(I) + T(I,1) )            TREAC
              CL(2,I) = 4. * TDLIQ / DLIQ(I)  +  2. * VLIQ * XLSTEP *  TREAC
           1              ( 1. - XL )  +  XLSTEP * DELTAC * ( CPSTR(I) + TREAC
           2              CPLI(I) )                                     TREAC
              DL(1,I) = 8. * XTFACT * CLI(I,1) / DLIQ(I)  +  4. * XLSTP2 *TREAC
           1              VLIQ * ( 1. - XL ) * CPLI(I)  +  4. * XLSTP2 *  TREAC
           2              ( CDPLI(I) - VLIQ*CLI(I,1) )  +  2. * XLSTP2 *  TREAC
           3              DELTAC * ( TP(I)*CPLI(I) - TPSTR(I)*CPSTR(I) )  TREAC
              DL(2,I) = 8. * XTFACT * T(I,1) / DLIQ(I)  +  4. * XLSTP2 *  TREAC
           1              VLIQ * ( 1. - XL ) * TP(I)  +  4. * XLSTP2 * TDLIQTREAC
           2              * TDP(I) / DLIQ(I)  +  2. * XLSTP2 * DELTAC *   TREAC
           3              ( CDPLI(I)*T(I,1) - CDPSTR(I)*TSTR(I) )       TREAC
              XL = XL + XLSTEP                                          TREAC
       300    CONTINUE                                                  TREAC
      C                                                                 TREAC
      C     Next we evaluate the coefficients at the interface, which are TREAC
      C  functions of the reaction boundary conditions.                 TREAC
            BL(1,1) = 4. * ( XTFACT/DLIQ(1) + 1. )  +  2. * XLSTP2 * VLIQ TREAC
           1            +  2. * DELTAC * ( TSTR(1) + T(1,1) )           TREAC
            BL(2,1) = 4. * ( XTFACT + TDLIQ ) / DLIQ(1)  -  DELTAC *    TREAC
           1            XLSTP2 * ( CDPSTR(1) + CDPLI(1) )               TREAC
            CL(1,1) = 4.  +  2. * DELTAC * ( TSTR(1) + T(1,1) )         TREAC
```

```
276             CL(2,1) = 4. * TDLIQ / DLIQ(1)                                  TREAC
277             DL(1,1) = CLI(2,1) * ( 4. + 2.*DELTAC*( TSTR(1)+T(1,1) ) )      TREAC
278         1             + CLI(1,1) * ( 4.*( XTFACT/DLIQ(1)-1. ) - 2.*XLSTP2TREAC
279         2             *VLIQ - 2.*DELTAC*( TSTR(1)+T(1,1) ) ) + ( SDEPTH TREAC
280         3             * ( NLDOT2 + NLDOT1 ) / ( DLIQ(1) * CLIMAX ) ) *   TREAC
281         4             ( 2.*XLSTP2*VLIQ - 4.*XLSTEP                       TREAC
282         5             + DELTAC*XLSTP2*( TPSTR(1)+TP(1) ) - 2.*DELTAC*    TREAC
283         6             XLSTEP*( TSTR(1)+T(1,1) ) ) - DELTAC*XLSTP2*       TREAC
284         7             ( TPSTR(1)+TP(1) )*( CPSTR(1)+CPLI(1) )            TREAC
285             DL(2,1) = 4. * T(2,1) * TDLIQ / DLIQ(1) + T(1,1) * ( 4. *    TREAC
286         1             ( XTFACT - TDLIQ ) / DLIQ(1) + DELTAC*XLSTP2*(     TREAC
287         2             CDPSTR(1)+CDPLI(1) ) ) + ( QTOT1 + QTOT2 ) * ( 2. TREAC
288         2             *XLSTP2*VLIQ - 4.*XLSTEP*TDLIQ/DLIQ(1) + DELTAC*   TREAC
289         3             XLSTP2*( CPSTR(1)+CPLI(1) ) ) - DELTAC * XLSTP2 *  TREAC
290         4             ( CDPSTR(1)+CDPLI(1) ) * ( TSTR(1)+T(1,1) )        TREAC
291     C                                                                      TREAC
292     C-----  DEBUG DATA  -----                                             TREAC
293               IF  ( IDEB .EQ. 1 ) THEN                                     TREAC
294                 WRITE (IDEBUG,305)                                         TREAC
295      305          FORMAT ( 10X, '    ALI         BLI         CLI     ',  TREAC
296          1                       '    DLI     ' )                       TREAC
297                 DO 307  I = 1, JLSTEP                                      TREAC
298                   WRITE (IDEBUG,309)  AL(1,I), BL(1,I), CL(1,I), DL(1,I)   TREAC
299      309            FORMAT ( 10X, 1P5G11.4 )                              TREAC
300      307          CONTINUE                                                 TREAC
301                 WRITE (IDEBUG,310)                                         TREAC
302      310          FORMAT ( 10X, '    AT          BT          CT      ',  TREAC
303          1                       '    DT      ' )                       TREAC
304                 DO 312  I = 1, JLSTEP                                      TREAC
305                   WRITE (IDEBUG,314)  AL(2,I), BL(2,I), CL(2,I), DL(2,I)   TREAC
306      314            FORMAT ( 10X, 1P5G11.4 )                              TREAC
307      312          CONTINUE                                                 TREAC
308               END IF                                                       TREAC
309     C-------------------------                                            TREAC
310     C                                                                      TREAC
311     C     Now we determine the Gaussian elimination factors ALPHAL and SL. TREAC
312               ALPHAL(1,1) = BL(1,1)                                        TREAC
313               ALPHAL(2,1) = BL(2,1)                                        TREAC
314               SL(1,1) = DL(1,1)                                            TREAC
315               SL(2,1) = DL(2,1)                                            TREAC
316               DO 315  I = 2, JLSTEP                                        TREAC
317                 DO 320  J = 1, 2                                           TREAC
318                   ALPHAL(J,I) = BL(J,I)  - AL(J,I) * CL(J,I-1) /           TREAC
319          1                      ALPHAL(J,I-1)                             TREAC
320                   SL(J,I) = DL(J,I)  + AL(J,I) * SL(J,I-1) / ALPHAL(J,I-1) TREAC
321      320          CONTINUE                                                 TREAC
322      315        CONTINUE                                                   TREAC
323     C                                                                      TREAC
324     C-----  DEBUG DATA  -----                                             TREAC
325               IF  ( IDEB .EQ. 1 )  THEN                                    TREAC
326                 WRITE (IDEBUG,322)                                         TREAC
327      322          FORMAT ( 10X, '  ALPHAL1    ALPHAL2      SL1     ',   TREAC
328          1                       '    SL2     ' )                       TREAC
329                 DO 324  I = 1, JLSTEP                                      TREAC
330                   WRITE (IDEBUG,326)  ALPHAL(1,I), ALPHAL(2,I), SL(1,I),   TREAC
```

```
331        1                              SL(2,I)                                    TREAC
332     326           FORMAT ( 10X, 1P5G11.4 )                                     TREAC
333     324         CONTINUE                                                       TREAC
334               END IF                                                           TREAC
335     C-------------------------                                                 TREAC
336     C                                                                          TREAC
337     C     Now we can evaluate the updated values of CLI and T.  But first      TREAC
338     C  we evaluate the CLI and T at the outer boundary.                        TREAC
339               CLI(ILSTEP,2) = SL(1,JLSTEP) / ( ALPHAL(1,JLSTEP) -              TREAC
340          1                    CL(1,JLSTEP) )                                   TREAC
341               T(ILSTEP,2) = TBOUND                                             TREAC
342     C                                                                          TREAC
343               DO 330  I = 1, JLSTEP                                            TREAC
344                 J = ILSTEP - I                                                 TREAC
345                 CLI(J,2) = ( CL(1,J) * CLI(J+1,2)  +  SL(1,J) )  /             TREAC
346          1                   ALPHAL(1,J)                                      TREAC
347                 T(J,2) = ( CL(2,J) * T(J+1,2)  +  SL(2,J) )  /  ALPHAL(2,J)    TREAC
348     330         CONTINUE                                                       TREAC
349     C                                                                          TREAC
350     C-----  DEBUG DATA  -----                                                  TREAC
351               IF  ( IDEB .EQ. 1 )  THEN                                        TREAC
352                 WRITE (IDEBUG,331)                                             TREAC
353     331           FORMAT ( 10X, '  CL          T         ' )                   TREAC
354                 DO 332  I = 1, ILSTEP                                          TREAC
355                   WRITE (IDEBUG,333)  CLI(I,2), T(I,2)                         TREAC
356     333             FORMAT ( 10X, 1P2G11.4 )                                   TREAC
357     332         CONTINUE                                                       TREAC
358               END IF                                                           TREAC
359     C-------------------------                                                 TREAC
360     C                                                                          TREAC
361     C*****  LIQUID METAL BOUNDARY CONDITION AT SURFACE  *****                  TREAC
362               CLI(1,2) = 0.                                                    TREAC
363     C                                                                          TREAC
364     C     Next we must check to see if any value of CLI or T is negative.      TREAC
365               INEG = 0                                                         TREAC
366               DO 335  I = 1, ILSTEP                                            TREAC
367                 IF  ( ( CLI(I,2) .LT. 0. ) .OR. ( T(I,2) .LT. 0. ) )           TREAC
368          1          INEG = 1                                                   TREAC
369     335         CONTINUE                                                       TREAC
370     C                                                                          TREAC
371     C*****  READJUST TIMESTEP AND REEVALUATE LOOP  *****                       TREAC
372     C                                                                          TREAC
373     C     In this case, a negative value of CLSTR(1) can lead to a divergentTREAC
374     C  loop, or a convergence to unphysical negative Lithium concentrations.TREAC
375     C  To avoid this problem, we decrease the current value of the timestep,TREAC
376     C  reinitialize the loop inputs, and return to the beginning of the      TREAC
377     C  loop.  The quantities that must be reinitialized are all of the star-TREAC
378     C  red variables.                                                          TREAC
379     C                                                                          TREAC
380               IF  ( INEG .EQ. 1 )  THEN                                        TREAC
381                 TSTEPL = .66667 * TSTEPL                                       TREAC
382                 DO 340  I = 1, ILSTEP                                          TREAC
383                   CLSTR(I) = CLI(I,1)                                          TREAC
384                   TSTR(I) = T(I,1)                                             TREAC
385     340         CONTINUE                                                       TREAC
```

```
C                                                                       TREAC
            CPSTR(1) = ( -21.*CLI(1,1) + 13.*CLI(2,1) + 17.*CLI(3,1) -  TREAC
     1                  9.*CLI(4,1) ) / ( 20. * XLSTEP )                TREAC
            CDPSTR(1) = 2. * ( CLI(2,1) - CLI(1,1) - XLSTEP*CPSTR(1) ) /TREAC
     1                  XLSTP2                                          TREAC
            TPSTR(1) = QTOT1                                            TREAC
            NLDOT2 = NLDOT1                                             TREAC
C                                                                       TREAC
            DO 345  I = 2, JLSTEP                                       TREAC
              CPSTR(I) = .5 * ( CLSTR(I+1) - CLSTR(I-1) ) / XLSTEP      TREAC
              CDPSTR(I) = ( CLSTR(I+1) - 2.*CLSTR(I) + CLSTR(I-1) ) /   TREAC
     1                    XLSTP2                                        TREAC
              TPSTR(I) = .5 * ( TSTR(I+1) - TSTR(I-1) ) / XLSTEP        TREAC
 345        CONTINUE                                                    TREAC
C                                                                       TREAC
C                                                                       TREAC
C-----  DEBUG DATA  -----                                               TREAC
            IF  ( IDEB .EQ. 1 )  THEN                                   TREAC
              WRITE (IDEBUG,350)  TSTEPL                                TREAC
 350            FORMAT ( '***** TIMESTEP CHANGED IN L M SECTION *****'  TREAC
     1                 / '     NEW TIMESTEP =     '  1P1G11.4 /        TREAC
     2                 '*****************************************' )TREAC
            END IF                                                      TREAC
C-----------------------                                                TREAC
C                                                                       TREAC
            GO TO 1000                                                  TREAC
          END IF                                                        TREAC
C                                                                       TREAC
C************************                                               TREAC
C                                                                       TREAC
C                                                                       TREAC
C     We now check to see if the guessed terms ( starred terms ) are    TREAC
C  equal to the new updated values of CLI and T.                        TREAC
          ICONV = 0                                                     TREAC
          DO 360  I = 1, ILSTEP                                         TREAC
            IF  ( DABS( CLI(I,2) - CLSTR(I) ) .GT. EPSC )  ICONV = 1    TREAC
            IF  ( DABS( T(I,2) - TSTR(I) ) .GT. EPST )  ICONV = 1       TREAC
 360      CONTINUE                                                      TREAC
C                                                                       TREAC
C     Now we can begin to set up the program for either an iteration    TREAC
C  on the liquid metal differential equation loop or for the next time- TREAC
C  step.  First we evaluate the new nonlinear terms guesses.            TREAC
          DO 365  I = 1, ILSTEP                                         TREAC
            CLSTR(I) = .5 * ( CLI(I,2) + CLSTR(I) )                     TREAC
            TSTR(I) = .5 * ( T(I,2) + TSTR(I) )                         TREAC
 365      CONTINUE                                                      TREAC
C                                                                       TREAC
          CPSTR(1) = ( -21.*CLI(1,2) + 13.*CLI(2,2) + 17.*CLI(3,2) -    TREAC
     1              9.*CLI(4,2) ) / ( 20. * XLSTEP )                    TREAC
          CDPSTR(1) = 2. * ( CLSTR(2) - CLSTR(1) - XLSTEP*CPSTR(1) ) /  TREAC
     1              XLSTP2                                              TREAC
          TPSTR(1) = .5 * ( QTOT1 + QTOT2 )                             TREAC
          NLDOT2 = DLIQ(1) * CLIMAX * CPSTR(1) / SDEPTH                 TREAC
C                                                                       TREAC
          DO 370  I = 2, JLSTEP                                         TREAC
```

```
441               CPSTR(I) = .5 * ( CLSTR(I+1) - CLSTR(I-1) ) / XLSTEP        TREAC
442               CDPSTR(I) = ( CLSTR(I+1) - 2.*CLSTR(I) + CLSTR(I-1) ) /     TREAC
443         1                   XLSTP2                                        TREAC
444               TPSTR(I) = .5 * ( TSTR(I+1) - TSTR(I-1) ) / XLSTEP          TREAC
445      370    CONTINUE                                                      TREAC
446     C                                                                     TREAC
447     C-----  DEBUG DATA  -----                                             TREAC
448               IF  ( IDEB .EQ. 1 )  THEN                                   TREAC
449                 WRITE (IDEBUG,375)                                        TREAC
450      375        FORMAT ( 10X, '    CLI          T         CPSTR    ',    TREAC
451         1                    ' CDPSTR      TPSTR    ' )                  TREAC
452               DO 380  I = 1, JLSTEP                                       TREAC
453                 WRITE (IDEBUG,385)  CLI(I,2), T(I,2), CPSTR(I), CDPSTR(I),TREAC
454         1                           TPSTR(I)                              TREAC
455      385          FORMAT ( 10X, 1P5G11.4 )                               TREAC
456      380        CONTINUE                                                 TREAC
457               WRITE (IDEBUG,390)  CLI(ILSTEP,2), T(ILSTEP,2)              TREAC
458      390        FORMAT ( 10X, 1P2G11.4 )                                 TREAC
459               WRITE (IDEBUG,395)  QCOND, QREAC                            TREAC
460      395        FORMAT ( '   QCOND      QREAC ' / 1P2G11.4 )             TREAC
461             END IF                                                        TREAC
462     C-----------------------                                             TREAC
463     C                                                                     TREAC
464     C     If the guesses have not converged to the solutions (ICONV=1), we TREAC
465     C  must reiterate the finite difference loops.                        TREAC
466               IF  ( ICONV .EQ. 1 )  GO TO 1000                            TREAC
467     C                                                                     TREAC
468     C*****  RESETTING LOOP VALUES  *****                                  TREAC
469     C                                                                     TREAC
470     C     Now we reset the CLI and T.                                     TREAC
471             DO 410  I = 1, ILSTEP                                         TREAC
472               CLI(I,1) = CLI(I,2)                                         TREAC
473               T(I,1) = T(I,2)                                             TREAC
474      410    CONTINUE                                                      TREAC
475     C                                                                     TREAC
476     C     Next we set reset the concentration and temperature first and   TREAC
477     C  second derivatives.                                                TREAC
478             DO 415  I = 1, ILSTEP                                         TREAC
479               CLSTR(I) = CLI(I,2)                                         TREAC
480               TSTR(I) =  T(I,2)                                           TREAC
481      415    CONTINUE                                                      TREAC
482     C                                                                     TREAC
483             CPLI(1) = ( -21.*CLI(1,2) + 13.*CLI(2,2) + 17.*CLI(3,2) -     TREAC
484         1           9.*CLI(4,2) ) / ( 20. * XLSTEP )                      TREAC
485             CPSTR(1) = CPLI(1)                                            TREAC
486             CDPLI(1) = 2. * ( CLI(2,2) - CLI(1,2) - XLSTEP*CPLI(1) ) /    TREAC
487         1               XLSTP2                                            TREAC
488             CDPSTR(1) = CDPLI(1)                                          TREAC
489             TP(1) = .5 * ( QTOT1 + QTOT2 )                                TREAC
490             TPSTR(1) = TP(1)                                              TREAC
491             TDP(1) = 2. * ( T(2,2) - T(1,2) - XLSTEP*TP(1) ) / XLSTP2     TREAC
492             NLDOT2 = DLIQ(1) * CLIMAX * CPSTR(1) / SDEPTH                 TREAC
493             NLDOT1 = NLDOT2                                               TREAC
494     C                                                                     TREAC
495             DO 420  I = 2, JLSTEP                                         TREAC
```

```
496              CPLI(I) = .5 * ( CLI(I+1,2) - CLI(I-1,2) ) / XLSTEP          TREAC
497              CPSTR(I) = CPLI(I)                                           TREAC
498              CDPLI(I) = ( CLI(I+1,2) - 2.*CLI(I,2) + CLI(I-1,2) ) /       TREAC
499         1                    XLSTP2                                       TREAC
500              CDPSTR(I) = CDPLI(1)                                         TREAC
501              TP(I) = .5 * ( T(I+1,2) - T(I-1,2) ) / XLSTEP                TREAC
502              TPSTR(I) = TP(I)                                             TREAC
503              TDP(I) = ( T(I+1,2) - 2.*T(I,2) + T(I-1,2) ) / XLSTP2        TREAC
504     420    CONTINUE                                                       TREAC
505     C                                                                     TREAC
506     C     Next we update the values of the molar masses.                  TREAC
507           NLI(1) = NLI(2)                                                 TREAC
508           NPROD(1) = NPROD(2)                                             TREAC
509           NTOT(1) = NTOT(2)                                               TREAC
510           NREAC = NLDOT2 * AREA * TSTEPL                                  TREAC
511           NLI(2) = NLI(1) - NREAC                                         TREAC
512           NPROD(2) = NPROD(1)  +  APROD * NREAC / ALI                     TREAC
513           NTOT(2) = NLI(2) + NPROD(2) + NPB                               TREAC
514           NH2 = NH2  +  AH2 * NREAC / ALI                                 TREAC
515           NGAS = NGAS  +  AH2 * NREAC / ALI                               TREAC
516           RRH2 = AH2 * NLDOT2 / ALI                                       TREAC
517     C                                                                     TREAC
518     C     Next we reset the pressure, liquid metal depth, and total heat  TREAC
519     C  flux.                                                              TREAC
520           P = RGAS * NGAS * TFREE / VFREE                                 TREAC
521           SOFTIM = SOFTIM + DELTAS                                        TREAC
522           QTOT1 = QTOT2                                                   TREAC
523     C                                                                     TREAC
524     C-----  DEBUG OUTPUT  -----                                           TREAC
525           IF  ( IDEB .EQ. 1 )  THEN                                       TREAC
526             WRITE (IDEBUG,425)                                            TREAC
527     425       FORMAT ( '**********************************************' /TREAC
528         1              '  LOOP COMPLETED ' / '                TDP ' )    TREAC
529             DO 426  I = 1, JLSTEP                                         TREAC
530               WRITE (IDEBUG,427)  TDP(I)                                  TREAC
531     427         FORMAT ( 10X, 1P1G11.4 )                                  TREAC
532     426       CONTINUE                                                    TREAC
533             WRITE (IDEBUG,428)  NREAC, NLI(2), NPROD(2), NTOT(2), NH2, P  TREAC
534     428       FORMAT ( 5X, '   NREAC       NLI         NPROD       NTOT     ',TREAC
535         1              '   NH2         P    ' / 5X, 1P6G11.4 )            TREAC
536           END IF                                                          TREAC
537     C-----------------------                                              TREAC
538     C                                                                     TREAC
539     C*****  EVALUATING THE NEW TIMESTEP AND UPDATING THE TIME  *****      TREAC
540     C                                                                     TREAC
541           TIME = TIME + TSTEPL                                            TREAC
542     C                                                                     TREAC
543           IF  ( TIME .LT. TCONL )  TSTEPL = 1.75 * TSTEPL                 TREAC
544           IF  ( TSTEPL .GT. ( .025 * TSTOP ) )  TSTEPL = .025 * TSTOP     TREAC
545           IF  ( ( TIME + TSTEPL ) .GT. TSTOP )  TSTEPL = TSTOP - TIME     TREAC
546     C                                                                     TREAC
547     C*****  OUTPUT CURRENT LOOP VALUES  *****                             TREAC
548     C                                                                     TREAC
549           IPRINT = IPRINT + 1                                             TREAC
550     C                                                                     TREAC
```

```
551           IF  ( JFLAG .EQ. 0 )  THEN                                        TREAC
552             TSURF = T(1,1) * ( TZERO - TREF )  +  TREF  -  273.15           TREAC
553             TBOT = TBOUND * ( TZERO - TREF )  +  TREF  -  273.15            TREAC
554             TLIQK = TSURF + 273.15                                          TREAC
555             DTH = D0TH * DEXP( -1. * ATH / ( RGAS * TLIQK ) )               TREAC
556     C                                                                       TREAC
557             WRITE (IDATA,40)  TIME, NH2, DLIQ(1), DTH                       TREAC
558             WRITE (ISURF,40)  TIME, RRH2, TSURF, TBOT                       TREAC
559           END IF                                                            TREAC
560     C                                                                       TREAC
561     C*****  CALCULATION CONTINUATION CONDITION  *****                       TREAC
562     C                                                                       TREAC
563     C     This section contains the main continuation conditions.  If the   TREAC
564     C  mass of hydrogen is less than the target value and the time is less  TREAC
565     C  than the stop time we return to the beginning of the main loop.      TREAC
566           IF  ( TIME .LT. TSTOP )  GO TO 1000                               TREAC
567     C                                                                       TREAC
568     C    Next we take the appropriate action because the time has reached   TREAC
569     C  the stoptime.  If the mass of hydrogen is below the target value, we TREAC
570     C  increase the nondimensional reaction rate and return to the beginningTREAC
571     C  of the program.                                                      TREAC
572           IF  ( ( NH2 .LT. NTLOW ) .OR. ( NH2 .GT. NTHIGH ) )  THEN         TREAC
573     C                                                                       TREAC
574             IF  ( NH2 .LT. NTLOW )  THEN                                    TREAC
575               ILOW = 1                                                      TREAC
576               IF  ( NH2 .GT. NLOW )  THEN                                   TREAC
577                 ACTLOW = ACTENG                                             TREAC
578                 NLOW = NH2                                                  TREAC
579               END IF                                                        TREAC
580             END IF                                                          TREAC
581             IF  ( NH2 .GT. NTHIGH )  THEN                                   TREAC
582               IHIGH = 1                                                     TREAC
583               IF  ( NH2 .LT. NHIGH )  THEN                                  TREAC
584                 ACTHIG = ACTENG                                             TREAC
585                 NHIGH = NH2                                                 TREAC
586               END IF                                                        TREAC
587             END IF                                                          TREAC
588     C                                                                       TREAC
589             IF  ( ( IHIGH .EQ. 0 ) .OR. ( ILOW .EQ. 0 ) )  THEN             TREAC
590               IF  ( NH2 .LT. NTLOW )  ACTENG = .5    * ACTENG               TREAC
591               IF  ( NH2 .GT. NTHIGH )  ACTENG = 2.   * ACTENG               TREAC
592             ELSE                                                            TREAC
593               ACTENG = ACTLOW + ( ACTHIG - ACTLOW ) * ( NTSTOP - NLOW ) /   TREAC
594          1                          ( NHIGH - NLOW )                        TREAC
595             END IF                                                          TREAC
596     C                                                                       TREAC
597             DTEMP = DLIQ0 * DEXP( ACTENG / ( RGAS * TZERO ) )               TREAC
598             WRITE (IWRITE,450)  ITER                                        TREAC
599             WRITE (IWRITE,460)  TIME, NH2, ACTENG, DTEMP                    TREAC
600      450      FORMAT ( 5X, ' Iteration number = ', I2 )                     TREAC
601      460      FORMAT ( 5X, 'At time = ', 1P1G11.4, ' sec' /                 TREAC
602          1            10X, 'NH2    = ', 1P1G11.4, ' mole' /                TREAC
603          2            10X, 'ACTENG = ', 1P1G11.4, ' J/mole '/              TREAC
604          3            10X, 'DTEMP  = ', 1P1G11.4, ' m2/s ' /// )           TREAC
605             WRITE (IWRITE,461)  NLOW, ACTLOW, NHIGH, ACTHIG                 TREAC
```

```
      461        FORMAT ( 5X, '   NLOW       ACTLOW      NHIGH       ACTHIG'/TREAC
     1               5X, 4( 1X, 1P1G11.4 ) )                                TREAC
            GO TO 9999                                                      TREAC
          END IF                                                            TREAC
C     We have found the right nondimensional reaction rate and must         TREAC
C  run through the program one more time to generate the output.            TREAC
          IF  ( JFLAG .EQ. 1 )  THEN                                        TREAC
            JFLAG = 0                                                       TREAC
            WRITE (IWRITE,450)  ITER                                        TREAC
            WRITE (IWRITE,465)  TIME, NH2, ACTENG, DTEMP, DLIQ0, DLIQ(1)    TREAC
      465     FORMAT ( 5X, 'A solution has been found.' /                   TREAC
     1               5X, 'At time = ', 1P1G11.4, ' sec' /                   TREAC
     1              10X, 'NH2    = ', 1P1G11.4, ' mole' /                   TREAC
     2              10X, 'ACTENG = ', 1P1G11.4, ' J/mole ' /                TREAC
     3              10X, 'DTEMP  = ', 1P1G11.4, ' m2/s '   /                TREAC
     4              10X, 'DLIQ0  = ', 1P1G11.4, ' m2/s '   /                TREAC
     5              10X, 'DLIQN  = ', 1P1G11.4, ' m2/s '   /                TREAC
     6              2X,  '****************************************' )        TREAC
            GO TO 9999                                                      TREAC
          END IF                                                            TREAC
C                                                                           TREAC
C                                                                           TREAC
C     That's all folks!                                                     TREAC
       END                                                                  TREAC
C                                                                           TREAC
C*************************************************************************TREAC
C*************************************************************************INVAR
C                                                                           INVAR
      SUBROUTINE  INVAR (                                                   INVAR
     1                                                                      INVAR
     2                                                                      INVAR
     3  VFREE, TFREE, MASLIQ, AREA, SDEPTH, TZERO, PZERO, NH2DOT, TSTOP,INVAR
     3  NTSTOP, ACTENG, TIMTLM, TLM, ITLM, ITEST, EPSC, EPST )             INVAR
C                                                                           INVAR
C     This subroutine prompts the user for the problem definition para- INVAR
C  meters.                                                                  INVAR
C                                                                           INVAR
      IMPLICIT DOUBLE PRECISION  ( A-H, M-Z )                               INVAR
      IMPLICIT INTEGER  ( I-L )                                             INVAR
      DOUBLE PRECISION  TIMTLM(250), TLM(250)                               INVAR
      INTEGER  ITSTNO(17)                                                   INVAR
C*****  COMMON BLOCKS  *****                                               INVAR
      COMMON  / PROP /                                                      INVAR
     1  DENLI, DENPRO, DENPB,                                              INVAR
     2  MWLI, MWPROD, MWPB,                                                INVAR
     3  TCGAS, TCLIQ, TDLIQ,                                               INVAR
     4  ALI, AH2O, APROD, AH2,                                             INVAR
     5  CLIQ                                                               INVAR
C                                                                           INVAR
      COMMON  / FLAG /  IPROD, IEPS, IDEB, IPALL                            INVAR
C*****  CHARACTER DATA  *****                                              INVAR
      CHARACTER*1  RESPON                                                   INVAR
      CHARACTER*8  UNIT(10)                                                 INVAR
      CHARACTER*6  VAR(5)                                                   INVAR
      CHARACTER*4  CPROD(2)                                                 INVAR
```

```
      CHARACTER*15 FILENM                                                INVAR
      CHARACTER*9  TLMTIT(17)                                            INVAR
C*****  TEST DATA  *****                                                 INVAR
      DATA  ITSTNO  / 16, 17, 20, 21, 22, 23, 24, 25, 26, 27,            INVAR
     1                28, 29, 30, 31, 32, 42, 43              /          INVAR
C                                                                        INVAR
      UNIT(1) = ' CM3     '                                              INVAR
      UNIT(2) = ' C       '                                              INVAR
      UNIT(3) = ' CM2     '                                              INVAR
      UNIT(4) = ' GM      '                                              INVAR
      UNIT(5) = ' BAR     '                                              INVAR
      UNIT(6) = ' SEC     '                                              INVAR
      UNIT(7) = ' MOLE    '                                              INVAR
      UNIT(8) = ' M2/S    '                                              INVAR
      UNIT(9) = ' MOLE/S  '                                              INVAR
      UNIT(10) = ' J/MOLE '                                              INVAR
C                                                                        INVAR
      CPROD(1) = 'LIOH'                                                  INVAR
      CPROD(2) = 'LI2O'                                                  INVAR
C                                                                        INVAR
      VAR(1)  = 'NH2DOT'                                                 INVAR
      VAR(2)  = 'MASLIQ'                                                 INVAR
      VAR(3)  = 'NTSTOP'                                                 INVAR
      VAR(4)  = 'TSTOP '                                                 INVAR
      VAR(5)  = 'ACTENG'                                                 INVAR
C                                                                        INVAR
      TLMTIT(1) = 'TLM16.DAT'                                            INVAR
      TLMTIT(2) = 'TLM17.DAT'                                            INVAR
      TLMTIT(3) = 'TLM20.DAT'                                            INVAR
      TLMTIT(4) = 'TLM21.DAT'                                            INVAR
      TLMTIT(5) = 'TLM22.DAT'                                            INVAR
      TLMTIT(6) = 'TLM23.DAT'                                            INVAR
      TLMTIT(7) = 'TLM24.DAT'                                            INVAR
      TLMTIT(8) = 'TLM25.DAT'                                            INVAR
      TLMTIT(9) = 'TLM26.DAT'                                            INVAR
      TLMTIT(10) = 'TLM27.DAT'                                           INVAR
      TLMTIT(11) = 'TLM28.DAT'                                           INVAR
      TLMTIT(12) = 'TLM29.DAT'                                           INVAR
      TLMTIT(13) = 'TLM30.DAT'                                           INVAR
      TLMTIT(14) = 'TLM31.DAT'                                           INVAR
      TLMTIT(15) = 'TLM32.DAT'                                           INVAR
      TLMTIT(16) = 'T500.DAT'                                            INVAR
      TLMTIT(17) = 'T500.DAT'                                            INVAR
C*****  I/O UNIT NUMBERS  *****                                          INVAR
      IWRITE = 0                                                         INVAR
      IREAD = 0                                                          INVAR
      IINPUT = 5                                                         INVAR
      IINTLM = 10                                                        INVAR
C*****  PROPERTY SETUP  *****                                            INVAR
      DENLI = 480.                                                       INVAR
      MWLI = 6.94D-3                                                     INVAR
      DENPB = 1.07D4                                                     INVAR
      MWPB = .20721                                                      INVAR
      TCGAS = 4.361D-2                                                   INVAR
      TCLIQ = 35.                                                        INVAR
```

```
716           TDLIQ = 2.27D-5                                                  INVAR
717     C*****  VARIABLE DEFAULTS  *****                                       INVAR
718           NH2DOT = 6.33D-4                                                 INVAR
719           IPROD = 0                                                        INVAR
720           ACTENG = 1.7D4                                                   INVAR
721           MASLIQ = 47.                                                     INVAR
722           VFREE = 343.                                                     INVAR
723           PZERO = 1.1                                                      INVAR
724           TFREE = 90.                                                      INVAR
725           TSTOP = 200.                                                     INVAR
726           NTSTOP = 7.001D-3                                                INVAR
727           AREA = 5.067                                                     INVAR
728           EPSC = .01                                                       INVAR
729           EPST = .01                                                       INVAR
730           IEPS = 0                                                         INVAR
731           IDEB = 0                                                         INVAR
732           IPALL = 1                                                        INVAR
733     C                                                                      INVAR
734     C*************************************************************************INVAR
735     C     INTERACTIVE INPUT                                                INVAR
736     C*************************************************************************INVAR
737     C                                                                      INVAR
738     C*****  NONDIMENSIONAL REACTION COEFFICIENT  *****                     INVAR
739           WRITE (IWRITE,200)  NH2DOT, UNIT(9)                              INVAR
740      200    FORMAT ( ' The initial hydrogen mass generation rate is ',     INVAR
741          1           1P1G11.4, A8 )                                       INVAR
742           WRITE (IWRITE,210)                                               INVAR
743      210    FORMAT ( 5X, ' Do you want to change it? (y/n)' )              INVAR
744           READ (IREAD,105)  RESPON                                         INVAR
745      105    FORMAT ( A )                                                   INVAR
746     C                                                                      INVAR
747           IF  ( ( RESPON .EQ. 'Y' ) .OR. ( RESPON .EQ. 'y' ) )  THEN       INVAR
748             WRITE (IWRITE,215)  VAR(1), UNIT(9)                            INVAR
749      215      FORMAT ( 10X, ' Enter new value of ', A8, ' in ', A8 )       INVAR
750             READ (IREAD,*)  NH2DOT                                         INVAR
751           END IF                                                           INVAR
752     C*****  MAIN PROGRAM VARIABLES  *****                                  INVAR
753           WRITE (IWRITE,220)  CPROD(IPROD+1)                               INVAR
754      220    FORMAT ( ' The default reaction product = ', A4 /  )           INVAR
755           WRITE (IWRITE,210)                                               INVAR
756      230    FORMAT ( 5X, ' Do you want to change any of these? (y/n) ' )   INVAR
757           READ (IREAD,105)  RESPON                                         INVAR
758     C                                                                      INVAR
759           IF  ( ( RESPON .EQ. 'Y' ) .OR. ( RESPON .EQ. 'y' ) )  THEN       INVAR
760             WRITE (IWRITE,240)  CPROD(1), CPROD(2)                         INVAR
761      240      FORMAT ( 10X, ' Enter a 0 for ', A4, ' Enter a 1 for ', A4 )  INVAR
762             READ (IREAD,*)  IPROD                                          INVAR
763             IF  ( IPROD .NE. 0 )  IPROD = 1                                INVAR
764           END IF                                                           INVAR
765     C                                                                      INVAR
766     C*****  EXPERIMENTAL RESULT VARIABLES  *****                           INVAR
767           WRITE (IWRITE,300)  TSTOP, UNIT(6), NTSTOP, UNIT(7)              INVAR
768      300    FORMAT ( ' The experimental result variables are:' /           INVAR
769          1           5X, ' At time = ', 1P1G11.4, A8 /                    INVAR
770          2           5X, ' The mass of hydrogen = ', 1P1G11.4, A8 /)      INVAR
```

```
771         WRITE (IWRITE,230)                                                  INVAR
772         READ (IREAD,105)  RESPON                                            INVAR
773   C                                                                         INVAR
774         IF  ( ( RESPON .EQ. 'Y' ) .OR. ( RESPON .EQ. 'y' ) )  THEN          INVAR
775           WRITE (IWRITE,215)  VAR(3), UNIT(6)                               INVAR
776           READ (IREAD,*)  TSTOP                                             INVAR
777           WRITE (IWRITE,215)  VAR(4), UNIT(7)                               INVAR
778           READ (IREAD,*)  NTSTOP                                            INVAR
779         END IF                                                              INVAR
780   C                                                                         INVAR
781   C*****  LIQUID METAL BOUNDARY VALUE  *****                                INVAR
782         WRITE (IWRITE,310)                                                  INVAR
783    310    FORMAT ( 5X, ' Enter    for test no. ' )                          INVAR
784         DO 312  I = 1, 17                                                   INVAR
785           WRITE (IWRITE,315)  I, TLMTIT(I)                                  INVAR
786    315      FORMAT ( 5X, I4, 5X, A15 )                                      INVAR
787    312  CONTINUE                                                           INVAR
788         READ (IREAD,*)  ILIPB                                               INVAR
789         ITEST = ITSTNO(ILIPB)                                               INVAR
790   C                                                                         INVAR
791         WRITE (IWRITE,340)  ACTENG                                          INVAR
792    340    FORMAT ( 5X, ' The default activation energy = ', 1P1G11.4, A8/)INVAR
793         WRITE (IWRITE,230)                                                  INVAR
794         READ (IREAD,105)  RESPON                                            INVAR
795   C                                                                         INVAR
796         IF  ( ( RESPON .EQ. 'Y' ) .OR. ( RESPON .EQ. 'y' ) )  THEN          INVAR
797           WRITE (IWRITE,215)  VAR(5), UNIT(10)                              INVAR
798           READ (IREAD,*)  ACTENG                                            INVAR
799         END IF                                                              INVAR
800   C                                                                         INVAR
801   C                                                                         INVAR
802   C*****  MAIN EXPERIMENTAL PARAMETERS  *****                               INVAR
803         WRITE (IWRITE,400)  MASLIQ                                          INVAR
804    400    FORMAT ( 5X, ' The liquid metal mass = ', 1P1G11.4, A8 / )       INVAR
805         WRITE (IWRITE,210)                                                  INVAR
806         READ (IREAD,105)  RESPON                                            INVAR
807   C                                                                         INVAR
808         IF  ( ( RESPON .EQ. 'Y' ) .OR. ( RESPON .EQ. 'y' ) )  THEN          INVAR
809           WRITE (IWRITE,215)  VAR(2), UNIT(4)                               INVAR
810           READ (IREAD,*)  MASLIQ                                            INVAR
811         END IF                                                              INVAR
812   C                                                                         INVAR
813   C*************************************************************************INVAR
814   C     PROGRAM VARIABLE EVALUATION                                         INVAR
815   C*************************************************************************INVAR
816   C                                                                         INVAR
817   C                                                                         INVAR
818         OPEN ( IINTLM, FILE = TLMTIT(ILIPB) )                               INVAR
819         I = 1                                                               INVAR
820    720  CONTINUE                                                           INVAR
821           READ (IINTLM,*,END=725)  TIMTLM(I), TLM(I)                        INVAR
822           I = I + 1                                                         INVAR
823           GO TO 720                                                         INVAR
824    725  CONTINUE                                                           INVAR
825         ITLM = I - 1                                                        INVAR
```

```
826         TZERO = TLM(1)                                                  INVAR
827   C*****  CONVERTING VARIABLES TO MKS UNITS  *****                      INVAR
828         VFREE = VFREE - MASLIQ / 9.                                     INVAR
829         TZERO = TZERO  +  273.15                                        INVAR
830         MASLIQ = 1.D-3 * MASLIQ                                         INVAR
831         VFREE = 1.D-6 * VFREE                                           INVAR
832         PZERO = 1.D5 * PZERO                                            INVAR
833         TFREE = TFREE  +  273.15                                        INVAR
834         AREA = 1.D-4 * AREA                                             INVAR
835   C*****  PRODUCT PROPERTIES SETUP  *****                               INVAR
836         IF  ( IPROD .EQ. 0 ) THEN                                       INVAR
837   C       In this case the product is LIOH.                             INVAR
838           DENPRO = 1.63D3                                               INVAR
839           MWPROD = 2.988D-2                                             INVAR
840           ALI = 1.                                                      INVAR
841           AH2O = 1.                                                     INVAR
842           APROD = 1.                                                    INVAR
843           AH2 = .5                                                      INVAR
844         ELSE                                                            INVAR
845   C       In this case the product is LI2O.                             INVAR
846           DENPRO = 2.01D3                                               INVAR
847           MWPROD = 2.395D-2                                             INVAR
848           ALI = 1.                                                      INVAR
849           AH2O = .5                                                     INVAR
850           APROD = .5                                                    INVAR
851           AH2 = .5                                                      INVAR
852         END IF                                                          INVAR
853   C                                                                     INVAR
854         CLIQ = ( .17*DENLI + .83*DENPB ) / ( .17*MWLI + .83*MWPB )      INVAR
855   C                                                                     INVAR
856         SDEPTH = MASLIQ / ( ( .17*DENLI + .83*DENPB ) * AREA )          INVAR
857   C                                                                     INVAR
858   C     That's all folks!                                               INVAR
859         RETURN                                                          INVAR
860         END                                                             INVAR
861   C                                                                     INVAR
862   C*********************************************************************INVAR
863   C*********************************************************************VCALL
864   C                                                                     VCALL
865   C                                                                     VCALL
866         SUBROUTINE  VCALL (                                             VCALL
867        1  T, NTOT, NLI, NPROD, NREAC, TSTEPL, TZERO, TREF,             VCALL
868        1  CLIMAX, AREA, SDEPTH, DTEMP, ACTENG, JLSTEP,                 VCALL
869        2                                                               VCALL
870        3  VLIQ, DELTAS, DELTAC, DLIQ, DELTA )                          VCALL
871   C                                                                     VCALL
872   C     This subroutine evaluates the slowly time varying variables used VCALL
873   C  in the main loop of the program.                                   VCALL
874         IMPLICIT DOUBLE PRECISION  ( A-H, M-Z )                         VCALL
875         IMPLICIT INTEGER  ( I-L )                                       VCALL
876         DOUBLE PRECISION  NTOT(2), DLIQ(50), T(51,2)                    VCALL
877   C                                                                     VCALL
878         COMMON  / PROP /                                                VCALL
879        1  DENLI, DENPRO, DENPB,                                        VCALL
880        2  MWLI, MWPROD, MWPB,                                          VCALL
```

```
881         3  TCGAS, TCLIQ, TDLIQ,                                          VCALL
882         4  ALI, AH2O, APROD, AH2,                                        VCALL
883         5  CLIQ                                                          VCALL
884     C                                                                     VCALL
885           COMMON  / FLAG /  IPROD, IEPS, IDEB, IPALL                      VCALL
886     C                                                                     VCALL
887     C*****  MAXIMUM PRODUCT CONCENTRATION  *****                          VCALL
888           RATLIQ = APROD / ALI                                            VCALL
889           CPRODM = .17  *  RATLIQ  *  ( ( .17*RATLIQ*DENPRO + .83*DENPB ) / VCALL
890          1          ( .17*RATLIQ*MWPROD + .83*MWPB ) )                    VCALL
891     C                                                                     VCALL
892     C*****  LIQUID METAL DIFFUSIVITY COEFFICIENT  *****                   VCALL
893           TLIQK1 = ( TZERO - TREF ) * T(1,1)  +  TREF                     VCALL
894           RGAS = 8.314                                                    VCALL
895           DO 100  I = 1, JLSTEP                                           VCALL
896             TLIQK = ( TZERO - TREF ) * T(I,1)  +  TREF                    VCALL
897             DLIQ(I) = DTEMP * DEXP( -1. * ACTENG / ( RGAS * TLIQK ) )     VCALL
898      100  CONTINUE                                                        VCALL
899     C                                                                     VCALL
900     C*****  CHANGE IN LIQUID METAL DEPTH  *****                           VCALL
901     C                                                                     VCALL
902           FACTOR = ( 1. - RATLIQ ) * NREAC / ( NTOT(1) * NTOT(2) )        VCALL
903           FPROD = ( FACTOR*NPROD*NPROD + RATLIQ*NREAC*(2.*NPROD + RATLIQ* VCALL
904          1          NREAC)/NTOT(2) )  *  MWPROD  /  DENPRO                VCALL
905           FLI = ( FACTOR*NLI*NLI + NREAC*(NREAC - 2.*NLI)/NTOT(2) )  *    VCALL
906          1        MWLI  /  DENLI                                          VCALL
907           DELTAS = ( FPROD + FLI )  /  AREA                               VCALL
908     C                                                                     VCALL
909     C*****  DIFFERENCE IN WEIGHTED SPECIFIC HEATS  *****                  VCALL
910     C                                                                     VCALL
911     C     First we need to call the subroutine that evaluates the tempera- VCALL
912     C  ture dependant properties.                                         VCALL
913           CALL  SPHEAT (                                                  VCALL
914          1  TLIQK1,                                                      VCALL
915          2                                                               VCALL
916          3  SHLI, SHH2O, SHH2, SHPROD, SHPB,                             VCALL
917          3  HFH2O, HFPROD, HFLIPB )                                      VCALL
918     C                                                                     VCALL
919           DELTAC = ( SHLI*MWLI*CLIMAX  -  SHPROD*MWPROD*CPRODM ) /        VCALL
920          1          ( SHPB*DENPB )                                       VCALL
921     C                                                                     VCALL
922     C*****  NONDIMENSIONAL VELOCITY  *****                                VCALL
923           VLIQ = DELTAS * SDEPTH / ( DLIQ(1) * TSTEPL )                   VCALL
924     C                                                                     VCALL
925     C*****  GAS LAYER THICKNESS  *****                                    VCALL
926           HCONV = 256. + 1.631D3 * ((.5*(TLIQK1-TREF))**(-.25))           VCALL
927           HRAD = 5.46D-8 * ( ( TLIQK1**4. - TREF**4. ) / ( TLIQK1 - TREF ) )VCALL
928           HTOT = HCONV + HRAD                                             VCALL
929           DELTA = TCGAS / HTOT                                            VCALL
930     C                                                                     VCALL
931     C     That's all folks!                                               VCALL
932           RETURN                                                          VCALL
933           END                                                             VCALL
934     C                                                                     VCALL
935     C*************************************************************************VCALL
```

```
C*****************************************************************************HEATFX
C                                                                               HEATFX
C                                                                               HEATFX
      SUBROUTINE  HEATFX (                                                      HEATFX
     1  TLIQ, SDEPTH, DELTA, TZERO, TREF, TIMTLM, TLM, ITLM, TIME,             HEATFX
     1  NLDOT,                                                                 HEATFX
     2                                                                         HEATFX
     3  QREAC, QCOND, TBOUND )                                                 HEATFX
C                                                                               HEATFX
C     This subroutine evaluates the heat fluxes from the liquid metal           HEATFX
C  surface due to conduction and the reaction.                                  HEATFX
      IMPLICIT DOUBLE PRECISION  ( A-H, M-Z )                                   HEATFX
      IMPLICIT INTEGER  ( I-L )                                                 HEATFX
      DOUBLE PRECISION  TIMTLM(250), TLM(250)                                   HEATFX
C                                                                               HEATFX
      COMMON  / PROP /                                                          INVAR
     1  DENLI, DENPRO, DENPB,                                                  INVAR
     2  MWLI, MWPROD, MWPB,                                                    INVAR
     3  TCGAS, TCLIQ, TDLIQ,                                                   INVAR
     4  ALI, AH2O, APROD, AH2,                                                 INVAR
     5  CLIQ                                                                   INVAR
C                                                                               HEATFX
      COMMON  / FLAG /  IPROD, IEPS, IDEB, IPALL                                HEATFX
C                                                                               HEATFX
C*****  LIQUID SURFACE TEMPERATURE IN DEG K  *****                              HEATFX
      TLIQK = ( TZERO - TREF ) * TLIQ  +  TREF                                  HEATFX
C*****  CURVEFIT LIQUID METAL TEMPERATURE  *****                                HEATFX
C                                                                               HEATFX
C     In this section we evaluate the curvefit liquid metal temperature.        HEATFX
C  This is the temperature at the bottom of the liquid metal well.  The         HEATFX
C  nondimensional value of this (TBOUND) is the temperature boundary            HEATFX
C  value.                                                                       HEATFX
      IFLAG = 0                                                                 HEATFX
      DO 100  I = 1, ITLM                                                       HEATFX
        IF  ( IFLAG .EQ. 0 )  THEN                                              HEATFX
          IF  ( TIME .LE. TIMTLM(I) )  THEN                                     HEATFX
            J = I                                                               HEATFX
            IFLAG = 1                                                           HEATFX
          END IF                                                                HEATFX
        END IF                                                                  HEATFX
 100  CONTINUE                                                                  HEATFX
C                                                                               HEATFX
      TTC = ( TLM(J) - TLM(J-1) ) * ( TIME - TIMTLM(J-1) ) /                    HEATFX
     1      ( TIMTLM(J) - TIMTLM(J-1) )    +    TLM(J-1)                       HEATFX
      TBOUND = ( TTC - TREF + 273.15 )  /  ( TZERO - TREF )                     HEATFX
C                                                                               HEATFX
C*****  REACTION AND CONVECTION HEAT FLUXES  *****                              HEATFX
C                                                                               HEATFX
C     First we need to call the subroutine that evaluates the tempera-          HEATFX
C  ture dependant properties.                                                   HEATFX
      CALL  SPHEAT (                                                            HEATFX
     1  TLIQK,                                                                 HEATFX
     2                                                                         HEATFX
     3  SHLI, SHH2O, SHH2, SHPROD, SHPB,                                       HEATFX
     3  HFH2O, HFPROD, HFLIPB )                                                HEATFX
```

```
      C
            QCOND = .5 * TCGAS * SDEPTH * TLIQ / ( TCLIQ * DELTA )                HEATFX
      C                                                                           HEATFX
            FACTOR = SDEPTH * NLDOT / TCLIQ                                       HEATFX
      C                                                                           HEATFX
            IF  ( IPROD .EQ. 0 )  THEN                                            HEATFX
              QREAC = FACTOR  *  ( ( HFH2O + HFLIPB - HFPROD ) /                  HEATFX
           1          ( TZERO - TREF )  +  ( SHH2O + SHLI - SHPROD - .5*SHH2 )HEATFX
           2          * TLIQ )
            ELSE                                                                  HEATFX
              QREAC = FACTOR * ( ( .5*HFH2O + HFLIPB - .5*HFPROD ) /              HEATFX
           1          ( TZERO - TREF )  +  ( .5*SHH2O + SHLI - .5*SHPROD -       HEATFX
           2          .5*SHH2 ) * TLIQ )
            END IF                                                                HEATFX
      C                                                                           HEATFX
      C                                                                           HEATFX
      C     That's all folks!                                                     HEATFX
            RETURN                                                                HEATFX
            END                                                                   HEATFX
      C                                                                           HEATFX
      C*************************************************************************HEATFX
      C*************************************************************************HEATFX
      C                                                                          SPHEAT
      C                                                                          SPHEAT
            SUBROUTINE  SPHEAT (                                                 SPHEAT
           1  TK,                                                                SPHEAT
           2                                                                     SPHEAT
           3  SHLI, SHH2O, SHH2, SHPROD, SHPB,                                   SPHEAT
           3  HFH2O, HFPROD, HFLIPB )                                            SPHEAT
      C                                                                          SPHEAT
      C    This subroutine evaluates the specific heats and heats of formationSPHEAT
      C  of the reactants and products.  The specific heats are assumed to be SPHEAT
      C  linear functions of temperature for the range of 373K to 900K.  The  SPHEAT
            IMPLICIT DOUBLE PRECISION  ( A-H, M-Z )                           SPHEAT
            IMPLICIT INTEGER  ( I-L )                                         SPHEAT
            COMMON  / FLAG /  IPROD, IEPS, IDEB, IPALL                        SPHEAT
      C                                                                       SPHEAT
      C*****  LI  *****                                                       SPHEAT
            IF  ( TK .LT. 373. )  THEN                                        SPHEAT
              SHLI = 26.82                                                    SPHEAT
            ELSE IF  ( ( TK .GE. 373. ) .AND. ( TK .LT. 454. ) )  THEN        SPHEAT
              SHLI = 2.941D-2 * TK  +  15.84                                  SPHEAT
            ELSE IF  ( ( TK .GE. 454. ) .AND. ( TK .LT. 900. ) )  THEN        SPHEAT
              SHLI = -3.000D-3 * TK  +  31.67                                 SPHEAT
            ELSE                                                              SPHEAT
              SHLI = 28.88                                                    SPHEAT
            END IF                                                            SPHEAT
      C                                                                       SPHEAT
      C*****  H2O  *****                                                      SPHEAT
            IF  ( TK .LT. 373. )  THEN                                        SPHEAT
              SHH2O = 33.943                                                  SPHEAT
            ELSE IF  ( ( TK .GE. 373. ) .AND. ( TK .LT. 900. ) )  THEN        SPHEAT
              SHH2O = 1.1389D-2 * TK  +  29.695                               SPHEAT
            ELSE                                                              SPHEAT
                                                                              SPHEAT
```

```
1046            SHH2O = 39.94                                                   SPHEAT
1047          END IF                                                            SPHEAT
1048          HFH2O = -2.42D5                                                   SPHEAT
1049    C                                                                       SPHEAT
1050    C*****  H2  *****                                                      SPHEAT
1051          IF  ( TK .LT. 373. )  THEN                                        SPHEAT
1052            SHH2 = 29.14                                                    SPHEAT
1053          ELSE IF  ( ( TK .GE. 373. ) .AND. ( TK .LT. 900. ) )  THEN        SPHEAT
1054            SHH2 = 1.448D-3 * TK  +  28.684                                 SPHEAT
1055          ELSE                                                              SPHEAT
1056            SHH2 = 29.907                                                   SPHEAT
1057          END IF                                                            SPHEAT
1058    C                                                                       SPHEAT
1059    C     Now for the product.                                              SPHEAT
1060          IF  ( IPROD .EQ. 0 )  THEN                                        SPHEAT
1061    C                                                                       SPHEAT
1062    C*****  LIOH  *****                                                    SPHEAT
1063            IF  ( TK .LT. 373. )  THEN                                      SPHEAT
1064              SHPROD = 56.85                                                SPHEAT
1065              HFPROD = -4.8467D5                                            SPHEAT
1066            ELSE IF  ( ( TK .GE. 373. ) .AND. ( TK .LT. 744. ) )  THEN      SPHEAT
1067              SHPROD = 4.839D-2 * TK  +  38.8                               SPHEAT
1068              HFPROD = -4.8467D5                                            SPHEAT
1069            ELSE                                                            SPHEAT
1070              SHPROD = 86.78                                                SPHEAT
1071              HFPROD = -4.7388D5                                            SPHEAT
1072            END IF                                                          SPHEAT
1073    C                                                                       SPHEAT
1074          ELSE                                                              SPHEAT
1075    C                                                                       SPHEAT
1076    C*****  LI2O  *****                                                    SPHEAT
1077            IF  ( TK .LT. 373. )  THEN                                      SPHEAT
1078              SHPROD = 62.954                                               SPHEAT
1079            ELSE IF  ( ( TK .GE. 373. ) .AND. ( TK .LT. 900. ) )  THEN      SPHEAT
1080              SHPROD = 3.885D-2 * TK  + 48.462                              SPHEAT
1081            ELSE                                                            SPHEAT
1082              SHPROD = 83.429                                               SPHEAT
1083            END IF                                                          SPHEAT
1084            HFPROD = -5.9873D5                                              SPHEAT
1085    C                                                                       SPHEAT
1086          END IF                                                            SPHEAT
1087    C                                                                       SPHEAT
1088    C*****  PB  *****                                                      SPHEAT
1089          IF  ( TK .LT. 373. )  THEN                                        SPHEAT
1090            SHPB = 27.5                                                     SPHEAT
1091          ELSE IF  ( ( TK .GE. 373. ) .AND. ( TK .LT. 600. ) )  THEN        SPHEAT
1092            SHPB = 8.41D-3 * TK  +  24.36                                   SPHEAT
1093          ELSE IF  ( ( TK .GE. 600. ) .AND. ( TK .LT. 900. ) )  THEN        SPHEAT
1094            SHPB = -3.124D-3 * TK  +  32.51                                 SPHEAT
1095          ELSE                                                              SPHEAT
1096            SHPB = 29.698                                                   SPHEAT
1097          END IF                                                            SPHEAT
1098    C                                                                       SPHEAT
1099    C*****  LIPB  *****                                                    SPHEAT
1100          HFLIPB = -8.364D4                                                 SPHEAT
```

```
1101    C                                                                      SPHEAT
1102    C     That's all folks!                                                SPHEAT
1103          RETURN                                                           SPHEAT
1104          END                                                              SPHEAT
1105    C                                                                      SPHEAT
1106    C**********************************************************************SPHEAT
```

Appendix 4. Data Graphs

The following 88 graphs contain a complete representation of the data drawn from the experiments. The graphs are grouped in the following manner. First the data from the 600 C initial liquid metal temperature tests are presented, starting with the 60 C initial water temperature tests and ending with the 90 C initial water temperature test. Next the data from the 500 C initial liquid metal temperature tests are presented, with the 70 C initial water temperature tests preceding the 90 C initial water temperature tests. The next set of graphs are drawn from the 400 C initial liquid metal temperature tests, with the 80 C initial water temperature tests preceding the 90 C initial water temperature tests. The last group of graphs contain the data from the 350 C initial liquid metal temperature and 90 C initial water temperature tests.

Within each group of tests with same initial water temperatures and initial liquid metal temperatures, are the data graphs presented in the following manner. The first graphs show the calculated partial pressure of hydrogen for the lithium-lead tests. These graphs also contain a plot of ΔP from the corresponding lead test. Next the pressure transducer response from the lithium-lead tests and the corresponding lead test is shown. This is followed by graphs showing the water and gas thermocouple responses from the lithium-lead and lead tests. The final set of graphs present the liquid metal

thermocouple response from the tests. It should be noted that for a few of the later tests we did not record the liquid metal thermocouple response.

The table on the following page gives the page numbers of each set of graphs.

If the interested reader requires more than just a graphical representation of the data from the experiments, he can obtain access to the raw data from the experiments by contacting Professor Michael Corradini of the University of Wisconsin Nuclear Engineering Department.

Table 4. Data Graph Key

Initial Liquid Metal Temperature	Initial Water Temperature	$Li_{17}Pb_{83}$ Test Numbers	Corresponding Pb Test Number	Page Numbers
600 C	60 C	16, 17, 42, 43	15	195 - 211
600 C	70 C	21, 30	35	212 - 222
600 C	80 C	22	37	223 - 229
600 C	90 C	20, 29	34	230 - 240
500 C	70 C	31	40	241 - 246
500 C	90 C	25, 28	38	247 - 256
400 C	80 C	32	41	257 - 262
400 C	90 C	24, 27	36	263 - 272
350 C	90 C	23, 26	39	273 - 282

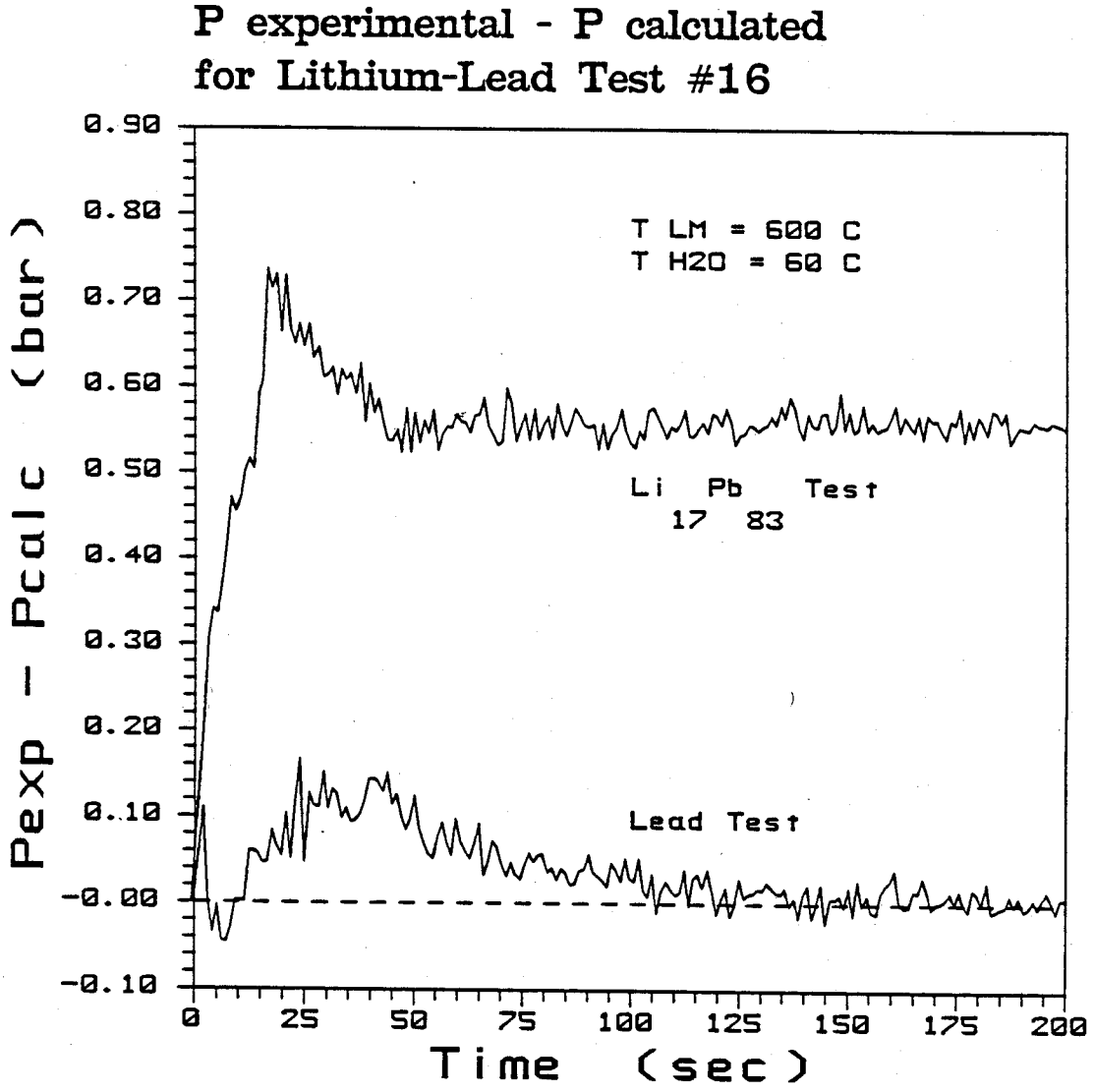
P experimental - P calculated
for Lithium-Lead Test #16
T LM = 600 C
T H2O = 60 C
Li Pb Test
17 83
Lead Test
Pexp - Pcalc (bar)
Time (sec)
0.90
0.80
0.70
0.60
0.50
0.40
0.30
0.20
0.10
-0.00
-0.10
0
25
50
75
100
125
150
175
200

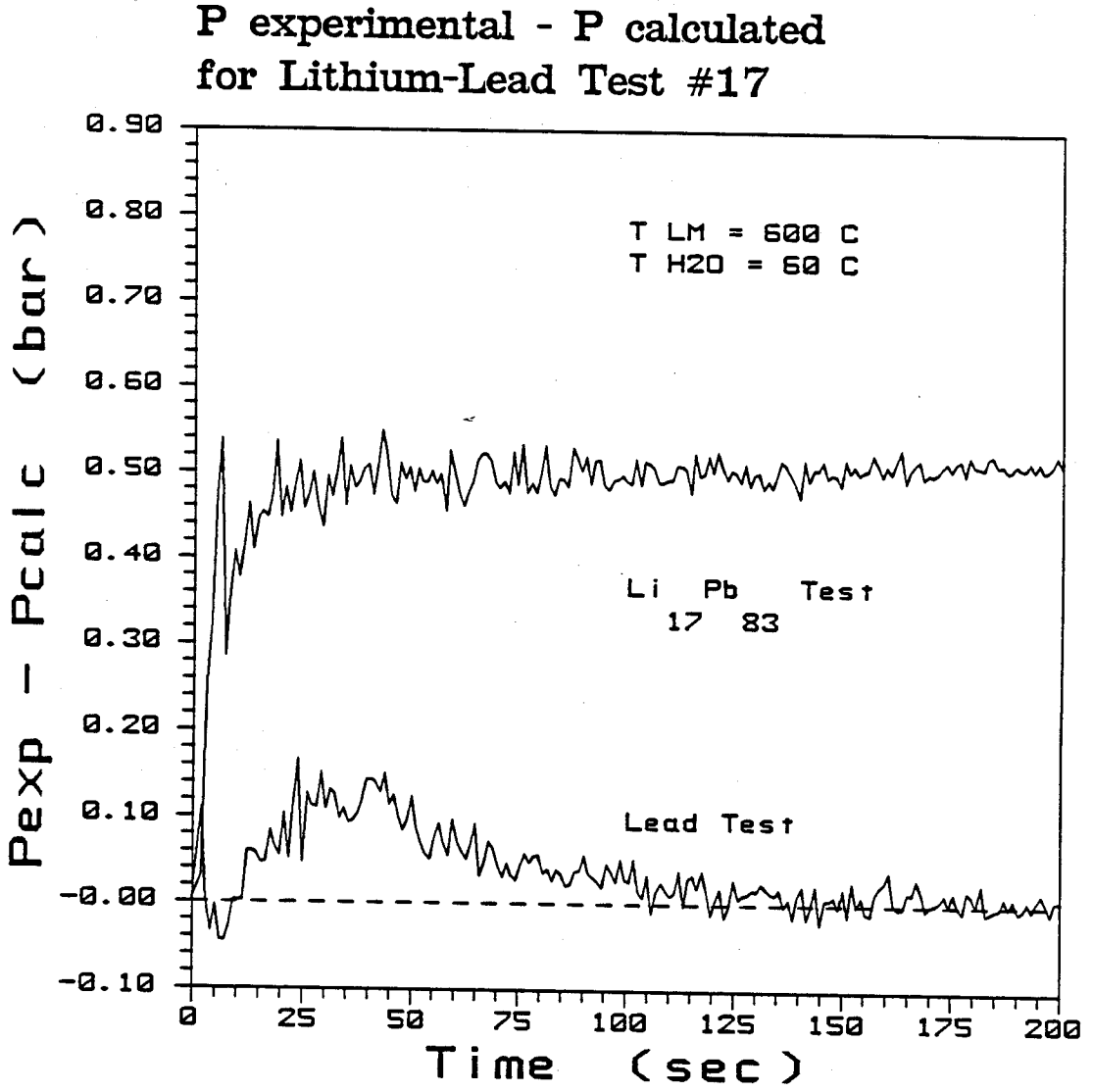
P experimental - P calculated
for Lithium-Lead Test #17
T LM = 600 C
T H2O = 60 C
Li Pb Test
17 83
Lead Test
Pexp - Pcalc (bar)
0.90
0.80
0.70
0.60
0.50
0.40
0.30
0.20
0.10
-0.00
-0.10
0
25
50
75
100
125
150
175
200
Time (sec)

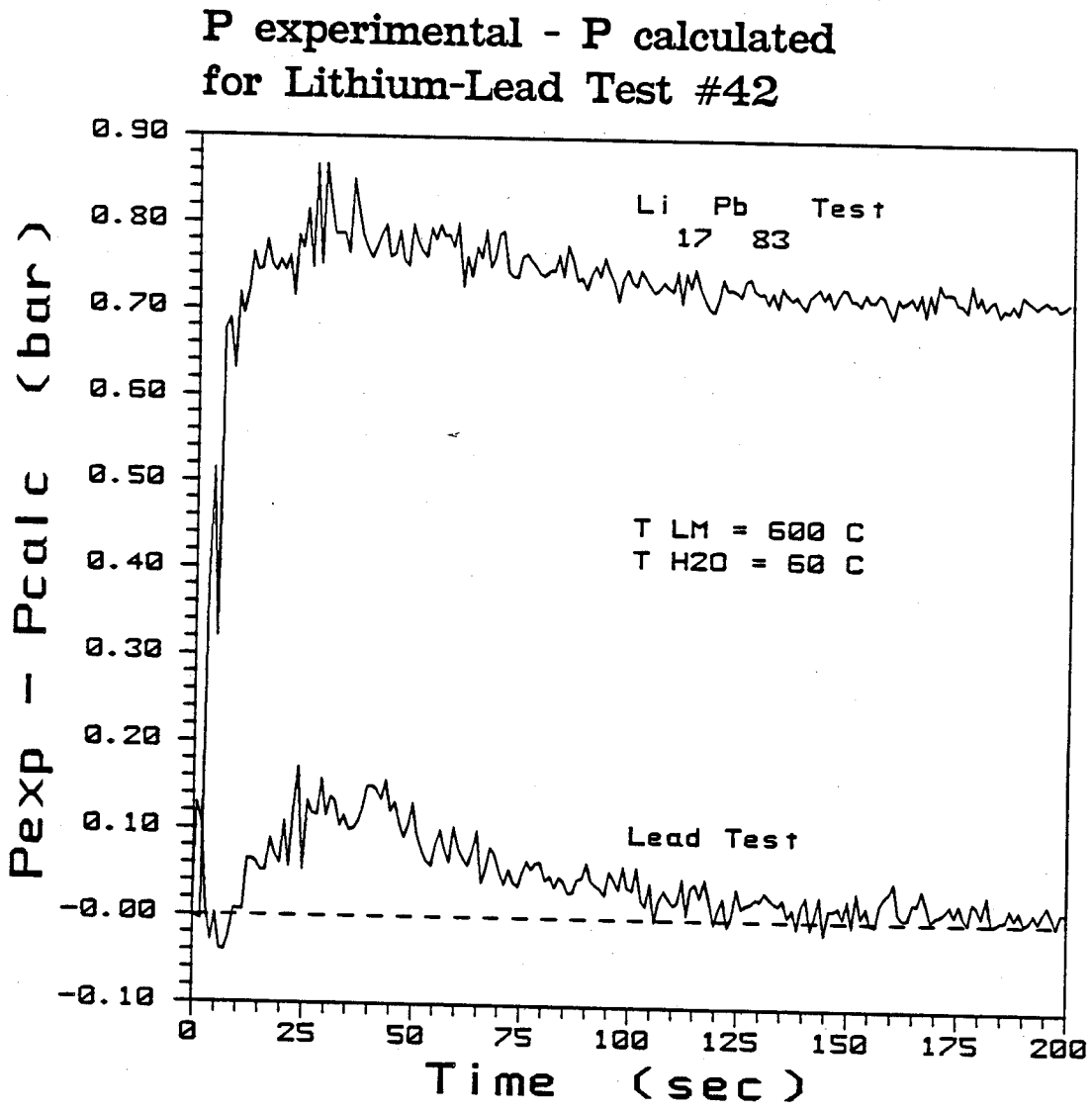
P experimental - P calculated
for Lithium-Lead Test #42
Li Pb Test
17 83
T LM = 600 C
T H2O = 60 C
Lead Test
Pexp - Pcalc (bar)
0.90
0.80
0.70
0.60
0.50
0.40
0.30
0.20
0.10
-0.00
-0.10
0
25
50
75
100
125
150
175
200
Time (sec)

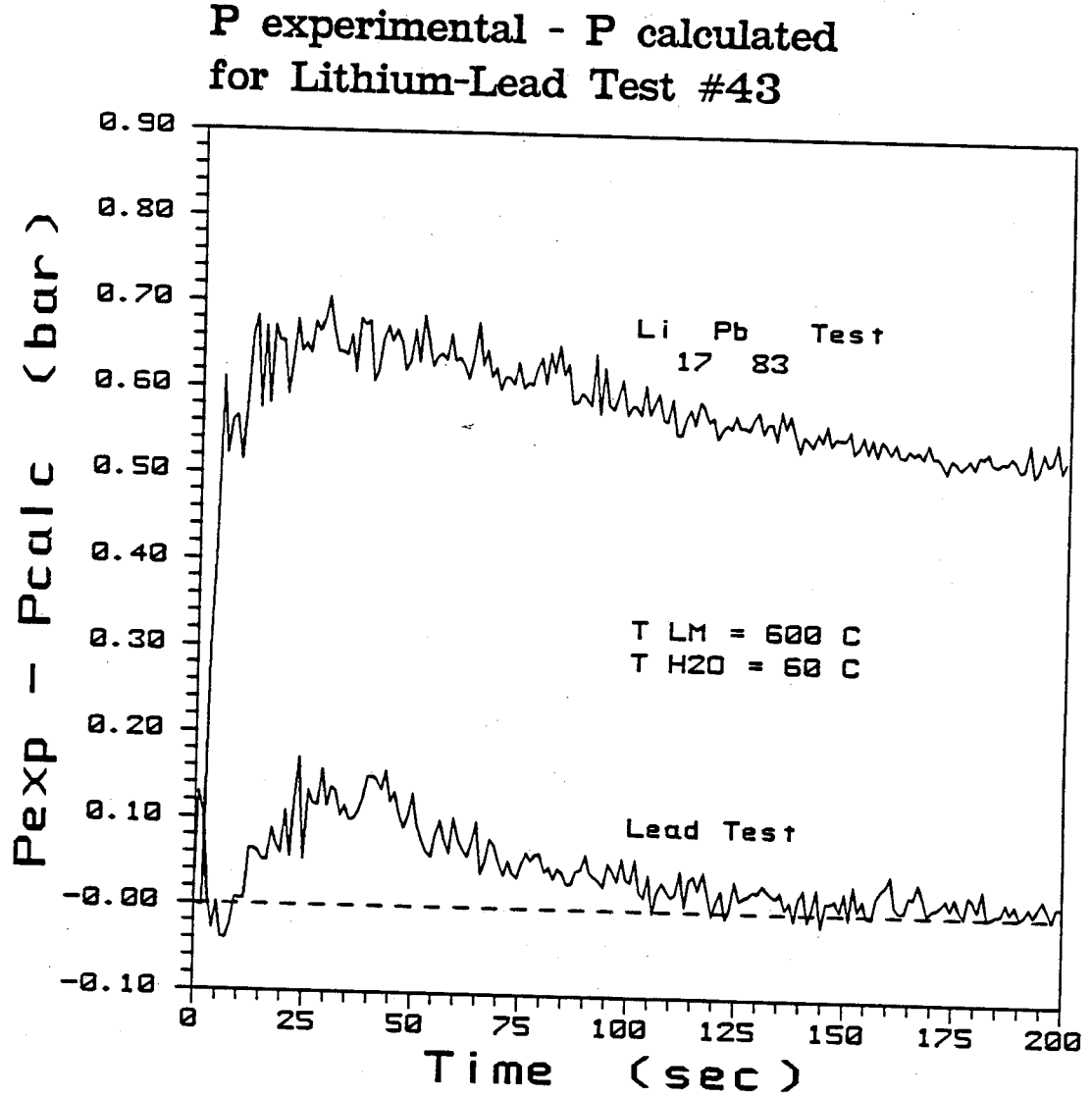
P experimental - P calculated
for Lithium-Lead Test #43
Pexp - Pcalc (bar)
0.90
0.80
0.70
0.60
0.50
0.40
0.30
0.20
0.10
-0.00
-0.10
0
25
50
75
100
125
150
175
200
Time (sec)
Li Pb Test
17 83
T LM = 600 C
T H2O = 60 C
Lead Test

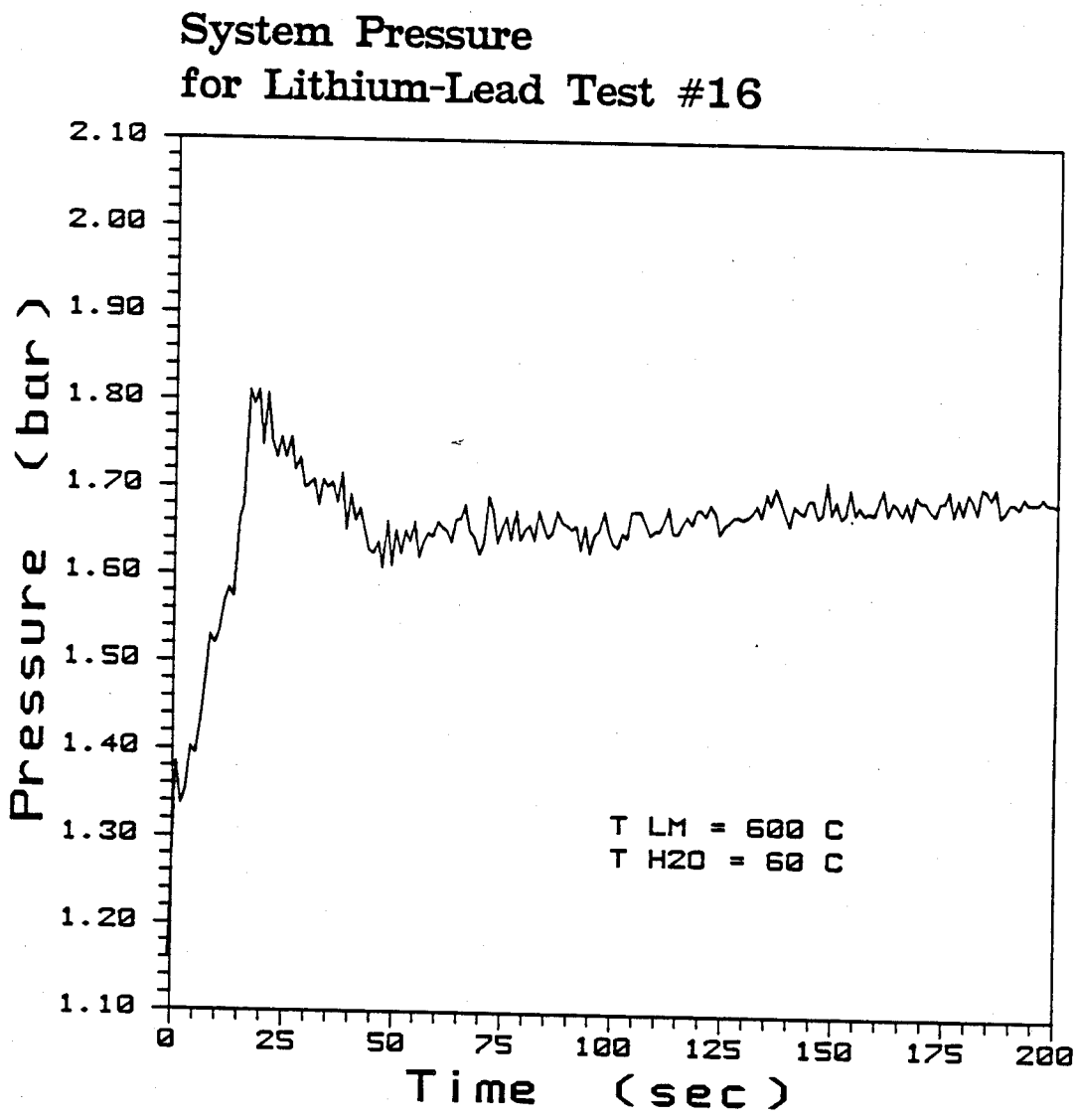
System Pressure
for Lithium-Lead Test #16
Pressure (bar)
2.10
2.00
1.90
1.80
1.70
1.60
1.50
1.40
1.30
1.20
1.10
0
25
50
75
100
125
150
175
200
Time (sec)
T LM = 600 C
T H2O = 60 C

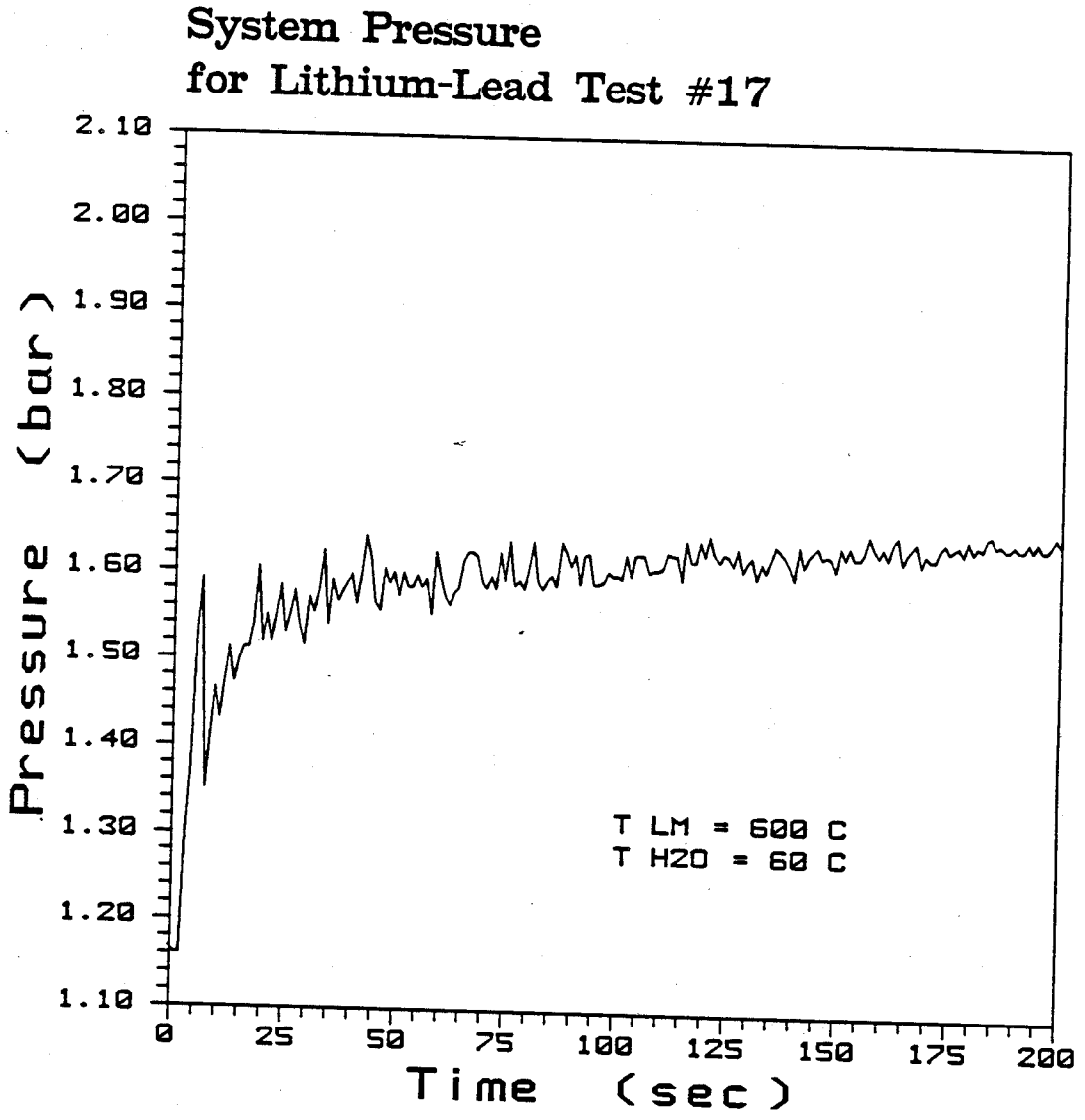
System Pressure
for Lithium-Lead Test #17
Pressure (bar)
2.10
2.00
1.90
1.80
1.70
1.60
1.50
1.40
1.30
1.20
1.10
0
25
50
75
100
125
150
175
200
Time (sec)
T LM = 600 C
T H2O = 60 C

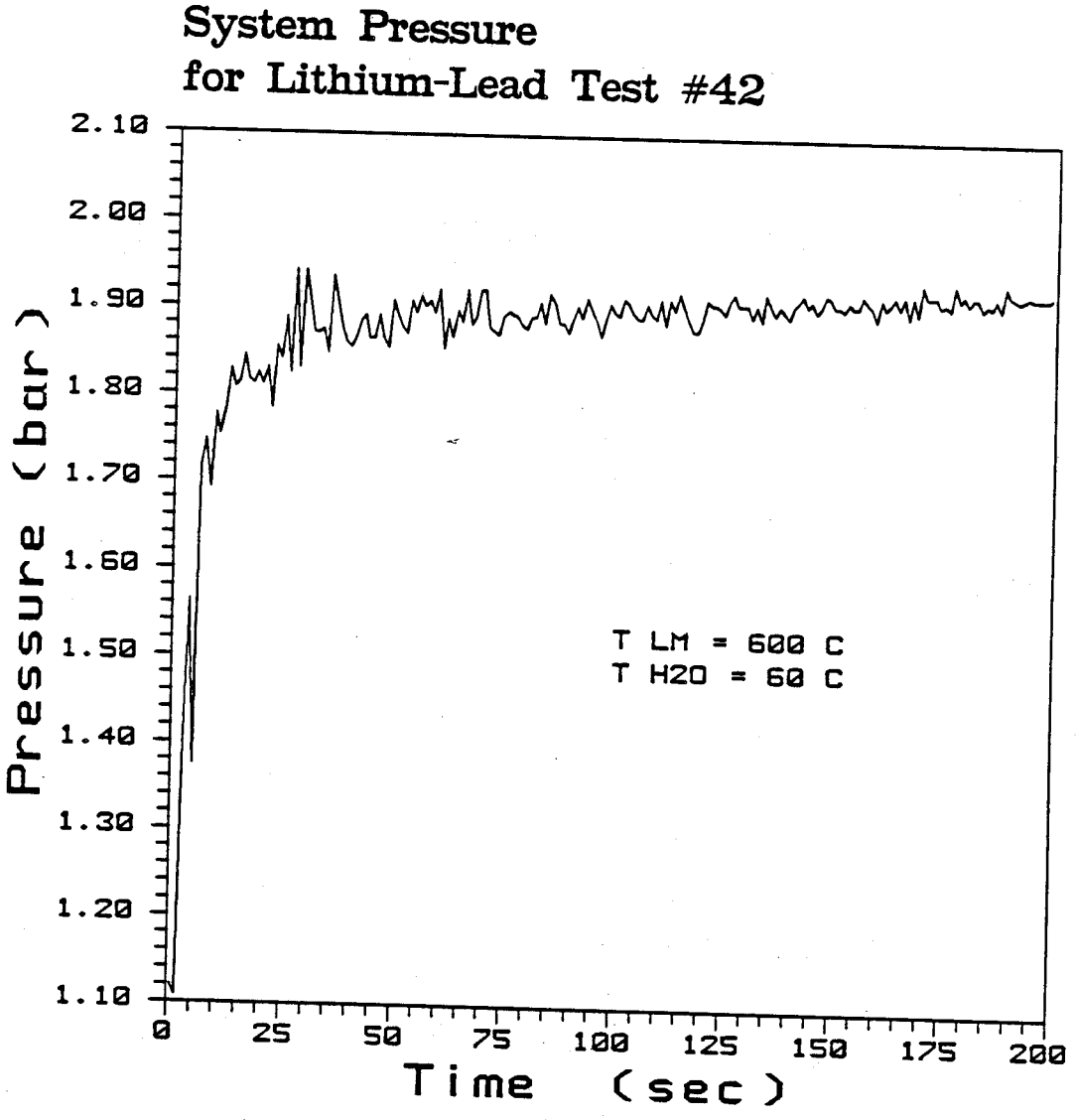
System Pressure
for Lithium-Lead Test #42
Pressure (bar)
2.10
2.00
1.90
1.80
1.70
1.60
1.50
1.40
1.30
1.20
1.10
0
25
50
75
100
125
150
175
200
Time (sec)
T LM = 600 C
T H2O = 60 C

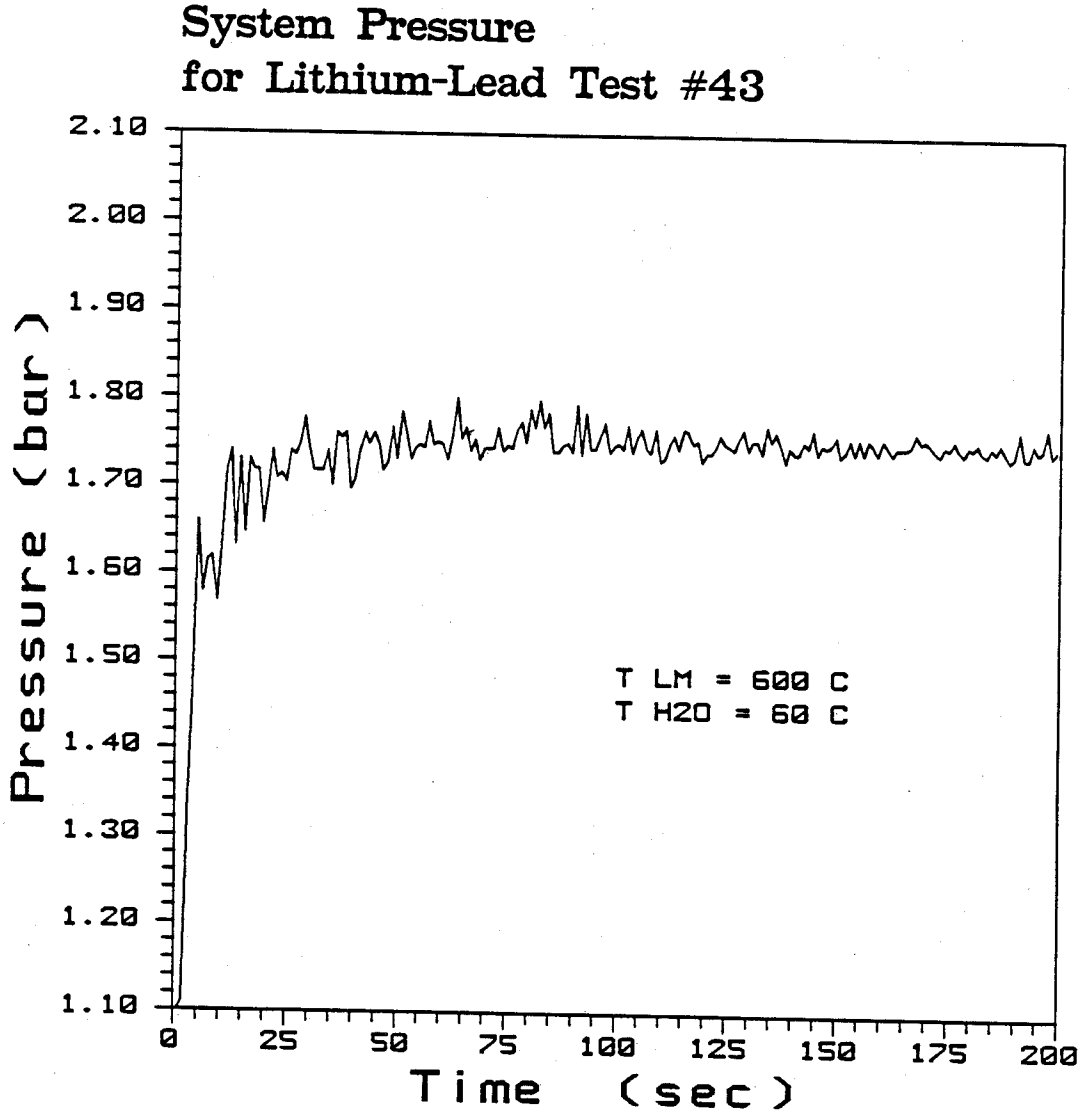
System Pressure
for Lithium-Lead Test #43
Pressure (bar)
2.10
2.00
1.90
1.80
1.70
1.60
1.50
1.40
1.30
1.20
1.10
0
25
50
75
100
125
150
175
200
Time (sec)
T LM = 600 C
T H2O = 60 C

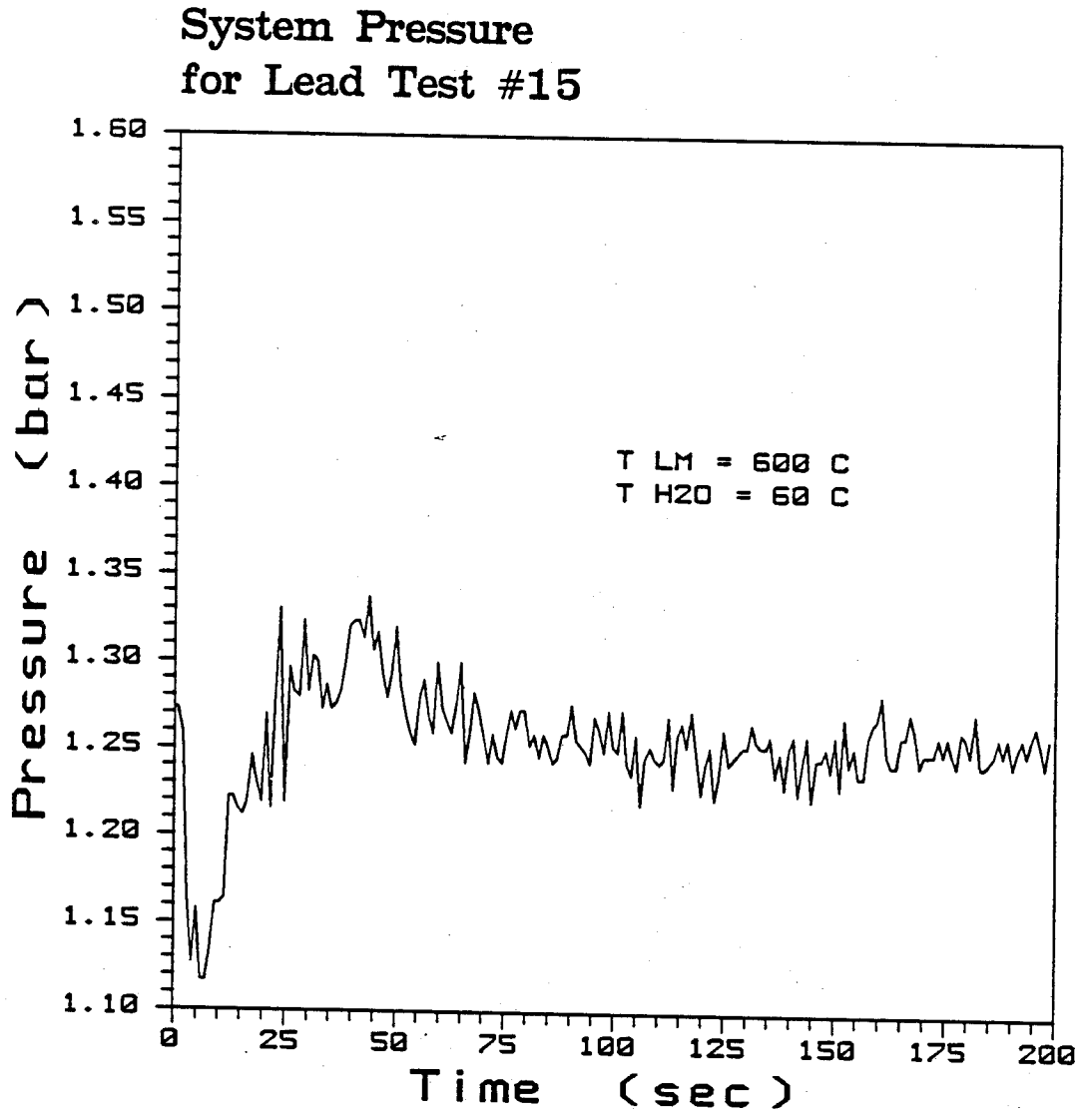
System Pressure
for Lead Test #15
T LM = 600 C
T H2O = 60 C
Pressure (bar)
1.60
1.55
1.50
1.45
1.40
1.35
1.30
1.25
1.20
1.15
1.10
0
25
50
75
100
125
150
175
200
Time (sec)

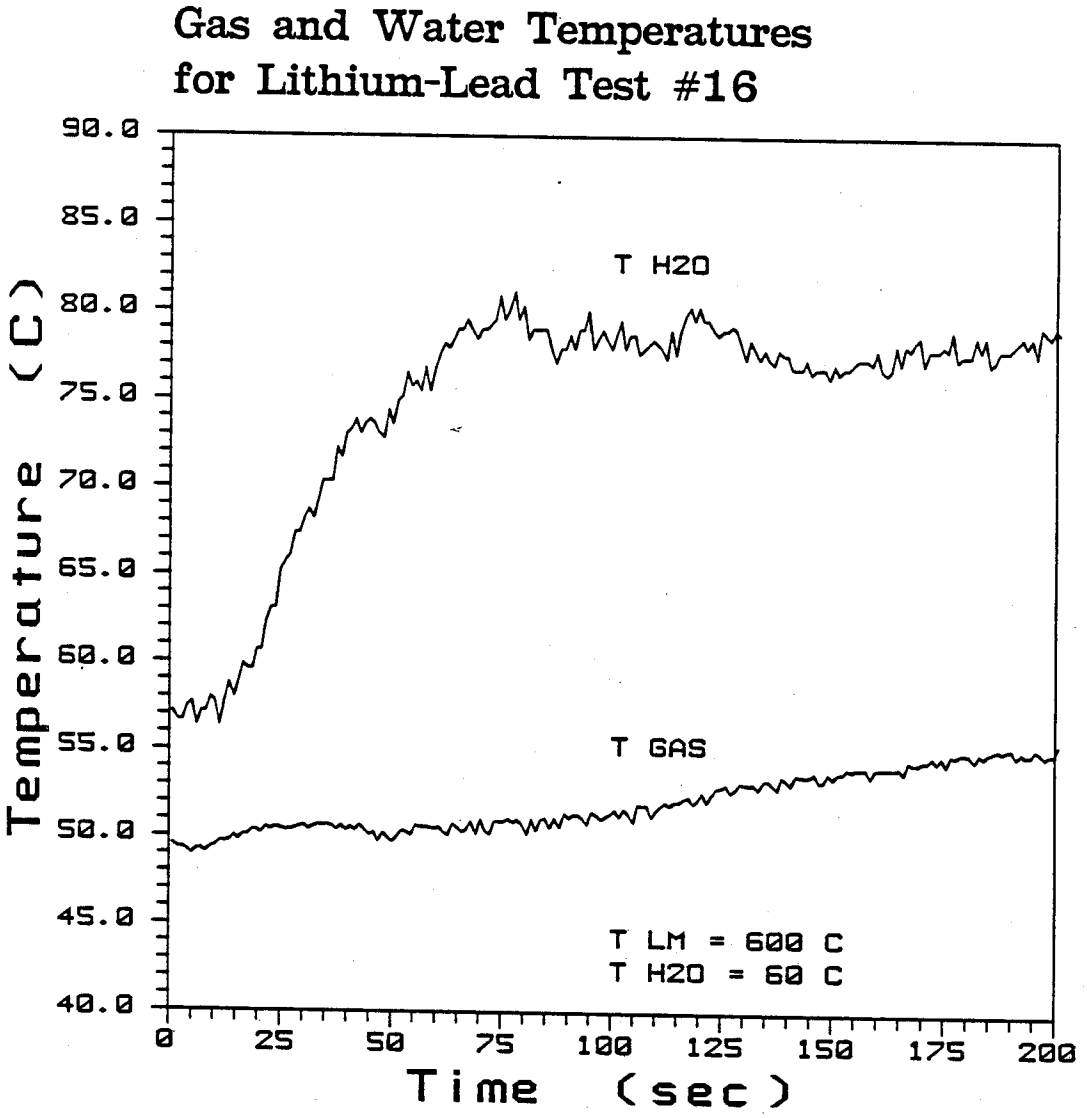
Gas and Water Temperatures
for Lithium-Lead Test #16
90.0
85.0
80.0
75.0
70.0
65.0
60.0
55.0
50.0
45.0
40.0
Temperature (C)
T H2O
T GAS
T LM = 600 C
T H2O = 60 C
0
25
50
75
100
125
150
175
200
Time (sec)

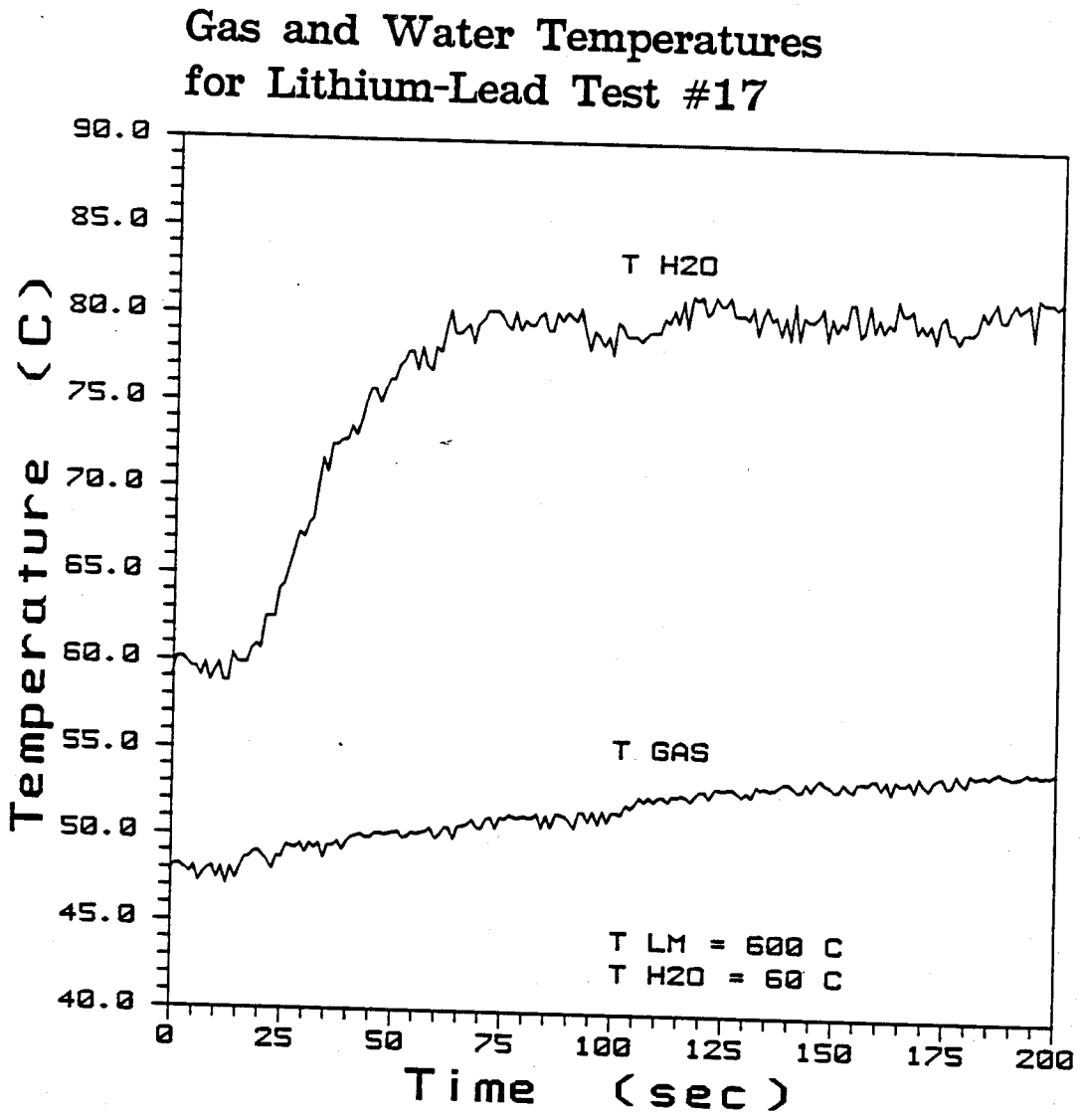
Gas and Water Temperatures
for Lithium-Lead Test #17
90.0
85.0
80.0
75.0
70.0
65.0
60.0
55.0
50.0
45.0
40.0
Temperature (C)
T H2O
T GAS
T LM = 600 C
T H2O = 60 C
0
25
50
75
100
125
150
175
200
Time (sec)

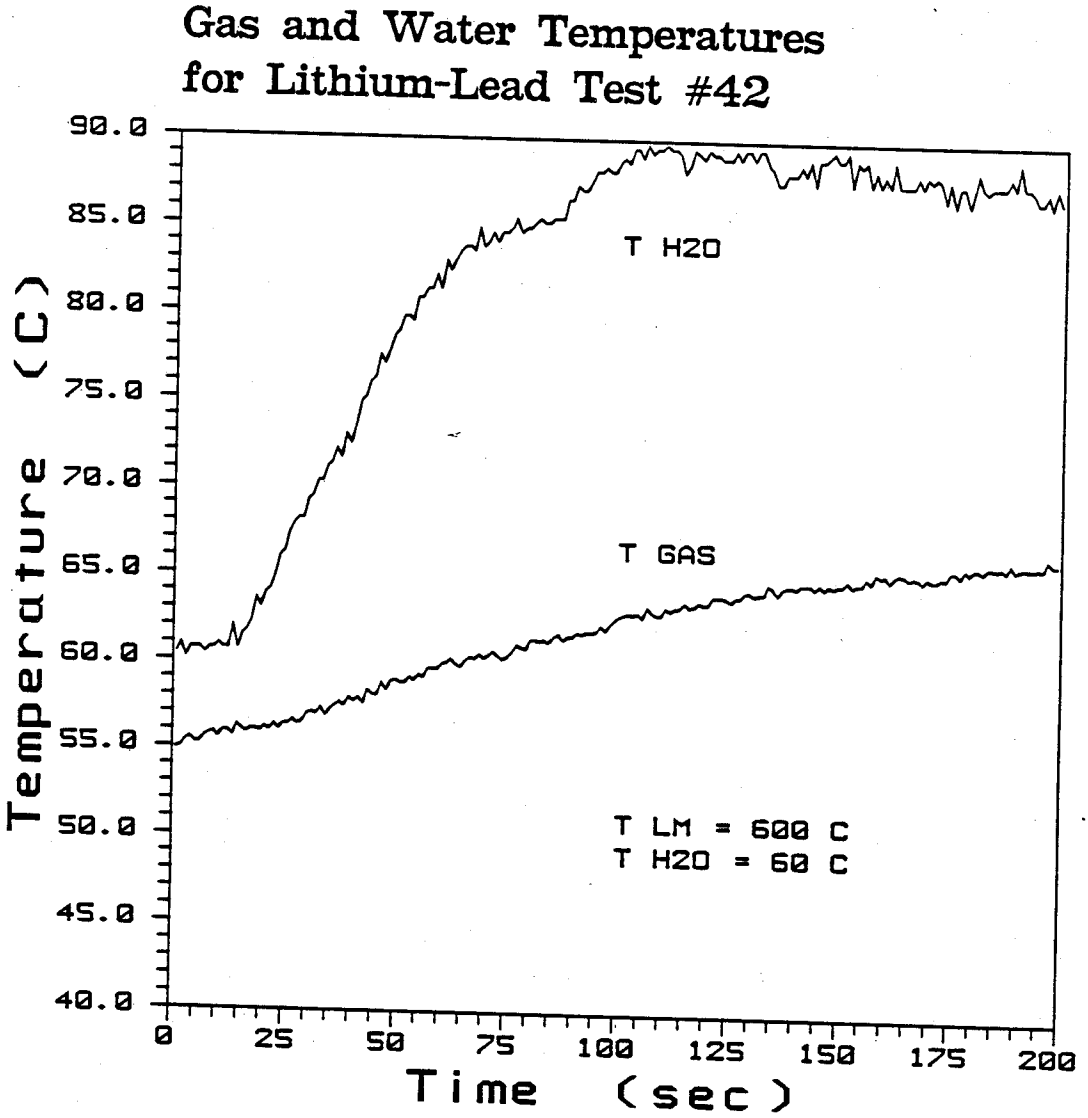
Gas and Water Temperatures
for Lithium-Lead Test #42
90.0
85.0
80.0
75.0
70.0
65.0
60.0
55.0
50.0
45.0
40.0
Temperature (C)
T H2O
T GAS
T LM = 600 C
T H2O = 60 C
0
25
50
75
100
125
150
175
200
Time (sec)

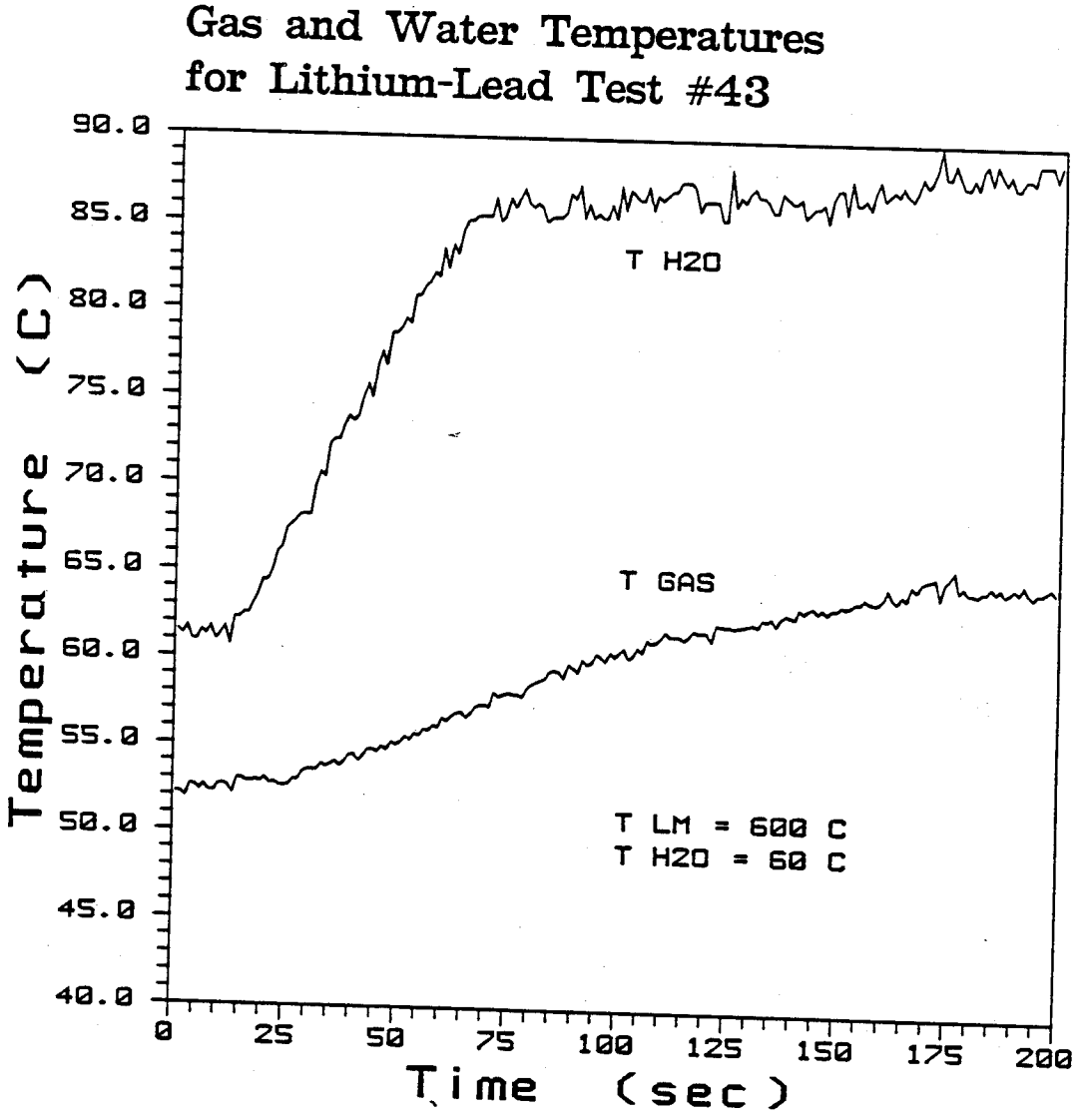
Gas and Water Temperatures
for Lithium-Lead Test #43
90.0
85.0
80.0
75.0
70.0
65.0
60.0
55.0
50.0
45.0
40.0
Temperature (C)
T H2O
T GAS
T LM = 600 C
T H2O = 60 C
0
25
50
75
100
125
150
175
200
Time (sec)

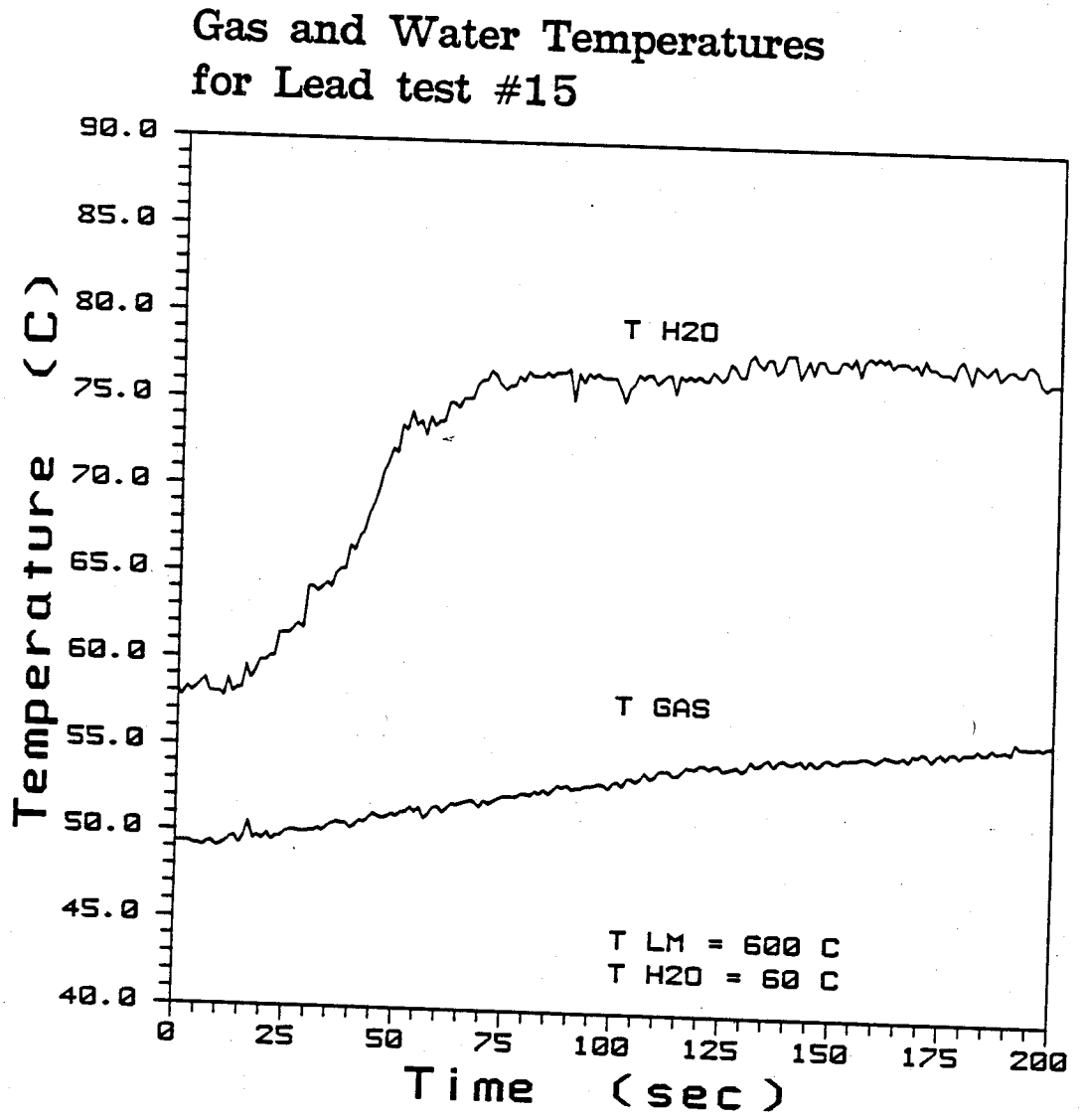
Gas and Water Temperatures
for Lead test #15
90.0
85.0
80.0
75.0
70.0
65.0
60.0
55.0
50.0
45.0
40.0
Temperature (C)
T H2O
T GAS
T LM = 600 C
T H2O = 60 C
0
25
50
75
100
125
150
175
200
Time (sec)

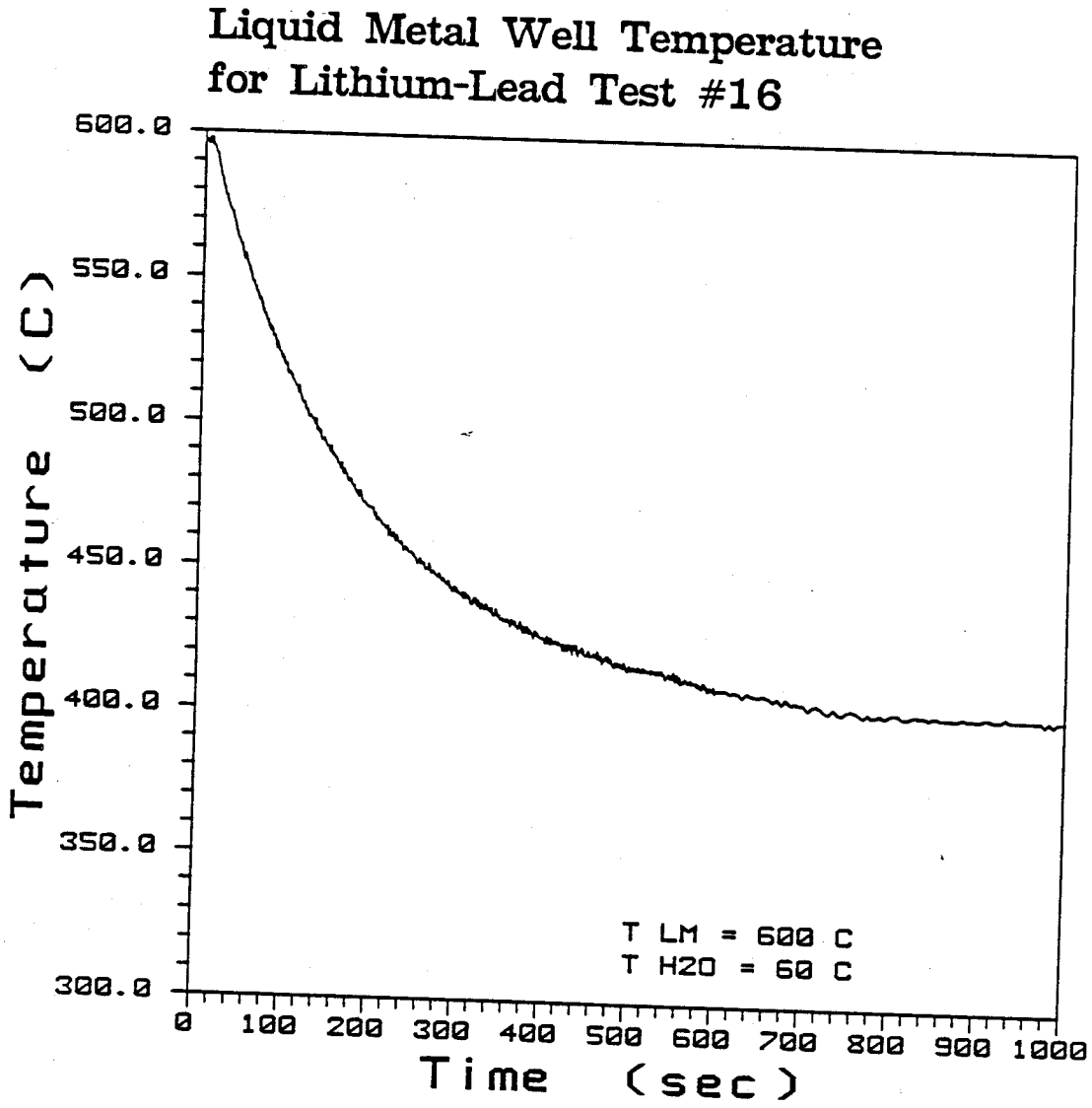
Liquid Metal Well Temperature
for Lithium-Lead Test #16
600.0
550.0
500.0
450.0
400.0
350.0
300.0
Temperature (C)
T LM = 600 C
T H2O = 60 C
0
100
200
300
400
500
600
700
800
900
1000
Time (sec)

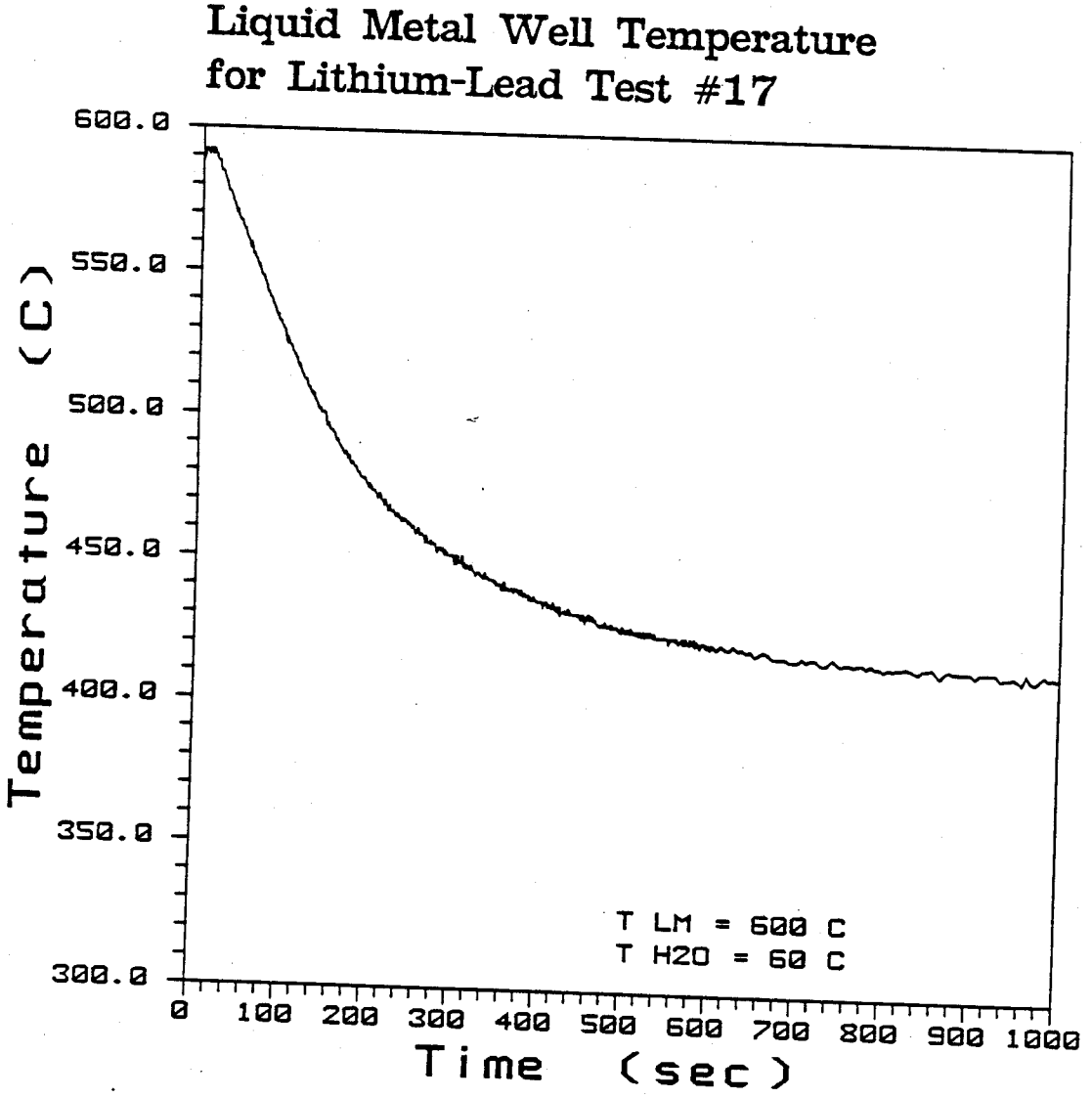
Liquid Metal Well Temperature
for Lithium-Lead Test #17
600.0
550.0
500.0
450.0
400.0
350.0
300.0
Temperature (C)
T LM = 600 C
T H2O = 60 C
0
100
200
300
400
500
600
700
800
900
1000
Time (sec)

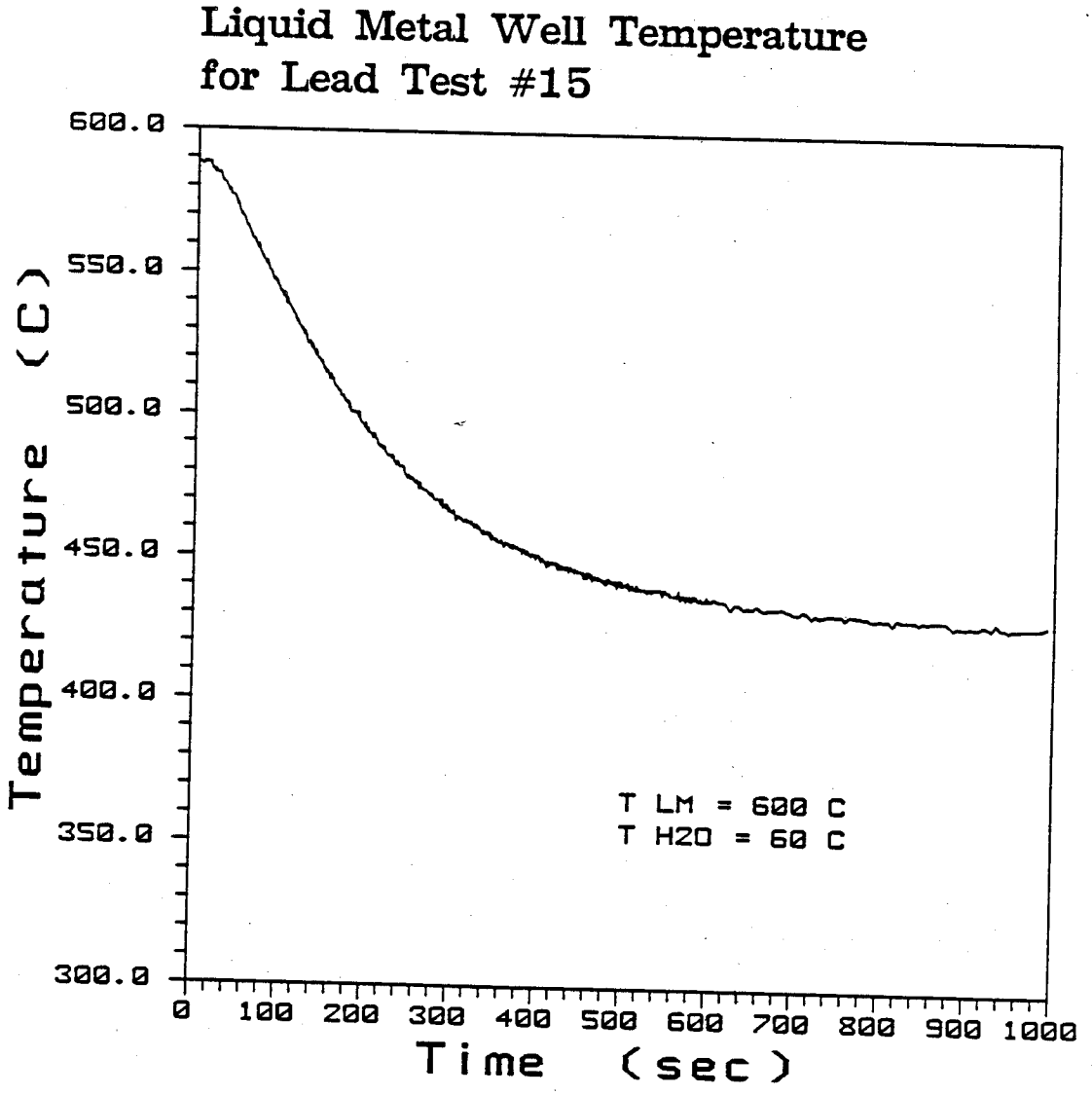
Liquid Metal Well Temperature
for Lead Test #15
600.0
550.0
500.0
450.0
400.0
350.0
300.0
Temperature (C)
0
100
200
300
400
500
600
700
800
900
1000
Time (sec)
T LM = 600 C
T H2O = 60 C

References

[1] R. Buxbaum, "A Chemical Theory Analysis of the Solution Thermodynamics of Oxygen, Nitrogen, and Hydrogen in Lead-Rich Li-Pb Mixtures," Journal of the Less-Common Metals 97 (1984): p. 27-38.

[2] D. W. Jeppson, L. D. Muhlstein, and S. Cohen, "Fusion Reactor Breeder Safety Compatibility Studies," Nuclear Technology/Fusion (Sept. 1983): p. 278-287.

[3] D. K. Sze, R. Clemmer, and E.T. Cheng, "LiPb, A Novel Material for Fusion Applications," University of Wisconsin Fusion Technology Institute Report UWFDM-378 (Oct. 1980).

[4] B. G. Logan, et. al., "Mirror Advanced Reactor Study Interim Report," Lawrence Livermore National Laboratory Report UCRL-5333 (1983).

[5] J. P. Herzog, M. L. Corradini, "Modeling of Lithium-Lead/Water Interactions in a Fusion Reactor Design," University of Wisconsin Fusion Technology Institute Report UWFDN-559 (Sept. 1984).

[6] J. P. Herzog, M. L. Corradini, "Modeling of Lithium-Lead/Water Interactions in a Fusion Reactor Design: Part II. Modeling Improvements," University of Wisconsin Fusion Technology Institute Report UWFDM-649 (August 1985).

[7] D. W. Jeppson, J. L. Ballif, W. W. Yuan, and B. E. Chou, "Lithium Literature Review," Hanford Engineering Development Laboratory Report HEDL-TME 78-15 (April 1978).

[8] F. Van Zeggeren and S. H. Storey, The Computation of Chemical Equilibria, (Cambridge: Cambridge Press, 1970).

[9] B. E. Deal and H. J. Svec, "Metal-Water Reactions. II. Kinetics of the Reaction between Lithium and Water Vapor," Jour. of the Amer. Chem. Soc. 75, (Dec. 20, 1953): p. 6173-6175.

[10] W. R. Irvine and J. A. Lund, "The Reaction of Lithium with Water Vapor," Jour. of the Electrochemical Soc. 110, No. 2, (Feb. 1963): p. 141-144.

[11] L. F. Epstein, "Recent Developments in the Study of Metal-Water Reactions," Progress in Nuclear Energy 4th Ser. 4 (1961): p. 477.

12 L. Baker, Jr. and L. C. Just, "Studies of Metal-Water Reactions at High Temperatures: III. Experimental and Theoretical Studies of the Zirconium-Water Reaction," Argonne National Laboratory Report ANL-6548 (May 1962).

13 J. H. Brophy, R. M. Rose, and J. Wulff, The Structure and Properties of Materials, 2 vols. (New York: J. Wiley and Sons, 1964) vol. 2: p. 63.

14 P. A. Finn, R. G. Clemmer, D. R. Armstrong, N. E. Parker, and L. Bova, "The Reactions of Li-Pb Alloys with Water," Transactions of the American Nuclear Society 34, (1984): p. 55.

15 G. Kuhlborsch, H. Dietz, and D. Droste, The Chemical Behaviour of Eutectic Lithium-Lead Alloy $Li_{17}Pb_{83}$ in Comparison with Pure Lithium," Commission of the European Communities Joint Research Center Report, Ispra, Italy, (Oct. 1984).

16 G. Kuhlborsch and F. Reiter, "Physical Properties of $Li_{17}Pb_{83}$ Related to its Use as a Fusion Reactor Blanket Material," Nuclear Engineering Design/Fusion 1, (1984): p. 195-203.

17 V Coen, "Lithium-Lead Eutectic as Breeding Material in Fusion Reactors," Journal of Nuclear Materials 133 and 134, (1985): p. 46-51.

18 H. M. Kottowski and G. Grossi, "Investigation of Eutectic PbLi-Water Interactions in Constraint Geometry at Variable System Pressures," Commission of the European Communities Joint Research Center Report, Ispra Italy, (Oct. 1983).

19 H. M. Kottowski, Joint Research Center, ISPRA, Private Communication (Aug. 1986).

20 D. W. Jeppson and L. D. Muhlstein, "Safety Considerations of Lithium Lead Alloy as a Fusion Reactor Breeding Material," Hanford Engineering Development Laboratory Report HEDL-SA 3223-FP, (1985).

21 E. M. Larsen, University of Wisconsin-Madison, Private Communication, (Dec. 1987)

22 D. W. Jeppson, et al., November-December 1984 Fusion Safety Studies Progress Report letter to J. G. Crocker (Fusion Safety Program, EG&G Idaho) (Jan. 30, 1985).

23 M. L. Corradini, University of Wisconsin-Madison, Private Communication (Dec. 1987).

24 V.K.Dihr, G. P. Purohit, "Subcooled Film-Boiling Heat Transfer from Spheres," Nucl. Eng. and Design 47 (1978): 49-66.

25 W. Masterton, E. Slowinski, Chemical Principles (Philadelphia: W. B. Saunders Co., 1977) p. 292.

26 M. M. El-Wakil, Nuclear Heat Transport (Chicago: American Nuclear Society, 1978) p. 105.

27 R. Bird, W. Stewart, E. Lightfoot, Transport Phenomena (New York: J. Wiley & Sons, 1964) p. 413.

28 Omega Temperature Handbook, (Stamford: Omega Engineering, 1985).

29 M. M. El-Wakil, Nuclear Heat Transport (Chicago: American Nuclear Society, 1978) p. 201.

30 Harry Saxton and Oleg Sherby, "Viscosity and Atomic Mobility in Liquid Metals," Trans. of the Amer. Soc. for Metals 55 (1962): p. 826-841.

31 Norbert A. Lange, Lange's Handbook of Chemistry, Editor: John A. Dean, 12th ed. (New York: McGraw-Hill, 1979) p. 10-13.

32 Glenn F. Knoll, Radiation Detection and Measurement (New York: J. Wiley & Sons, 1979): p. 105-147.

33 R. Bird, W. Stewart, E. Lightfoot, Transport Phenomena (New York: J. Wiley & Sons, 1964) p. 519-522.

34 Ibid., p. 560-562.

35 Adrian Bejan, Convection Heat Transfer (New York: J. Wiley & Sons, 1984) p. 12.

36 John Collier, Convective Boiling and Condensation (New York: McGraw-Hill, 1972) p. 124-133.

37 S. Glasstone, K. J. Laidler, and Henry Eyring, The Theory of Rate Processes (New York: McGraw-Hill, 1941).

38 A. D. Pasternak and D. R. Olander, "Diffusion in Liquid Metals," AIChE Journal 13 (Nov. 1967): p. 1052-1057.

[39] G. Thomaes and J. Van Itterbeek, "Application of the Principle of Corresponding States to the Viscosity and Diffusion of Pure Liquids and Mixtures," Jour. of Molecular Physics 2, (1959): p. 372-378

[40] Thomas W. Chapman, "The Viscosity of Liquid Metals," AIChE Journal 12, (March 1966): p. 395-400.

[41] Thomas Chapman, University of Wisconsin-Madison, Private Communication (Dec. 1987).

[42] Omesh Chopra, Argonne National Laboratory, Private Communication (Dec. 1987).

[43] Glen Meyers, Analytical Methods in Conduction Heat Transfer (New York: McGraw-Hill, 1978).

[44] Adrian Bejan, Convection Heat Transfer (New York: John Wiley, 1984).